PART I: THE STRUCTURE DETERMINATION OF MANGANESE TETRAPHENYLPORPHYRIN

PART II: THE REDETERMINATION OF THE STRUCTURE OF PORPHINE

Thesis for the Degree of Ph. D.
MICHIGAN STATE UNIVERSITY
BETTY MEI-HORNG LEE CHEN
1970





This is to certify that the

thesis entitled

Part I: The Structure Determination of Manganese

Tetraphenylporphyrin.

Part II: The Redetermination of the Structure

of Porphine.

presented by

Betty Mei-horng Lee Chen

has been accepted towards fulfillment of the requirements for

Ph.D. degree in Cham: stry

Major professor

Date 4 1971.

O-7639

0-14

JUL 2 7 1000

550







ABSTRACT

PART I: THE STRUCTURE DETERMINATION OF MANGANESE TETRAPHENYLPORPHYRIN

PART II: THE REDETERMINATION OF THE STRUCTURE OF PORPHINE

By

Betty Mei-Horng Lee Chen

The structures of manganese tetraphenylporphyrin and porphine were determined by means of three dimensional X-ray crystallographic techniques. Both molecules crystallize in the monoclinic space group $P2_1/c$ with four molecules in the unit cell. The unit cell dimensions for manganese tetraphenylporphyrin are $a=14.56~\text{Å},\ b=21.77~\text{Å},\ c=17.02~\text{Å},\ and\ \beta=135.6^{\circ},\ those for porphine are <math>a=10.27~\text{Å},\ b=12.09~\text{Å},\ c=12.36~\text{Å},\ and\ \beta=102.2^{\circ}.$

Manganese tetraphenylporphyrin was shown to coordinate with an axial chlorine ion. The locations of the manganese and chlorine atoms were determined by the heavy atom method; the remaining atoms, including all the hydrogens, were located from difference syntheses. All atomic parameters were refined by the least squares method. The porphyrin molecules in the crystal were stacked approximately perpendicular to the crystal were stacked approximately perpendicular to the crystallization, with an acetone molecule from crystallization trapped between adjacent porphyrin molecules.

The Mn(III) ion in an approximately square-pyramidal geometry is displaced 0.27 Å from the mean plane of the four basal nitrogen atoms toward the axial chlorine ligand. The chlorine atom is slightly tilted ($\sim 5^{\circ}$) from the apical position to keep a reasonable contact distance (3.45 Å) to a carbon atom belonging to the phenyl group of an adjacent porphyrin molecule. The bond distances of Mn-Cl (2.36 Å) and Mn-N (2.01 A), which are slightly shorter than expected, may be responsible for the high stability of this porphyrin. The porphyrin skeleton is ruffled since one pair of diagonal pyrrole groups is displaced below the NLS plane while the other pair is above it with apparent deviations of 0.3 - 0.5 Å for the peripheral carbon atoms. The porphyrin nucleus and phenyl groups were shown to be aromatic; the former was electronically separated from the latter by single bonds which join the phenyl rings to the porphyrin nucleus. The dihedral angles between individual phenyl groups and the NLS plane are 54.2° , 123.5° , 49.7° and 77.4° respectively.

The structure of porphine was determined previously by Webb and Fleischer, with an alleged copper impurity and a postulated "four half-hydrogen" structure for the central hydrogen atoms. Since the peak heights of the half-hydrogens were only slightly greater than background, and since the exact nature of these half-hydrogens with respect to van der Waals contacts was not reported, a redetermination



of the porphine structure was undertaken. In addition to collecting a complete set of all independent reflections, additional and more elaborate counting techniques were applied to those reflections which might contain a significant contribution to the hydrogen atom structure. The results indicated only two central hydrogen atoms bonded to one pair of diagonal nitrogen atoms. The central hydrogen atoms are coplanar to the porphine nucleus with N-H distances of 0.89 Å and 0.92 Å, respectively. The locations of H22 and H24 are inclined toward N21 and N23 at angles of 5.80 and 4.50 relative to the line joining the two opposite nitrogen atoms (N22-N24), respectively.



PART I: THE STRUCTURE DETERMINATION OF MANGANESE TETRAPHENYLPORPHYRIN

PART II: THE REDETERMINATION OF THE STRUCTURE OF PORPHINE

Ву

Betty Mei-Horng Lee Chen

A THESIS

Submitted to
Michigan State University
in partial fulfillment of the requirements
for the degree of

DOCTOR OF PHILOSOPHY

Department of Chemistry

1970



1-70293

ACKNOWLEDGMENT

The author wishes to express her appreciation to Professor Alexander Tulinsky for his guidance throughout the course of this study.

Appreciation is extended to Mr. Richard Vandlen and to Dr. N. V. Mani for their assistance.

Appreciation is also extended to Dr. Alan Adler for furnishing the samples of porphine and manganese tetraphenylporphyrin.

Appreciation is also extended to the Molecular Biology Section of the National Science Foundation for providing financial support.

Thanks are particularly due to her husband, Jingshyong, for his constant encouragement and assistance.



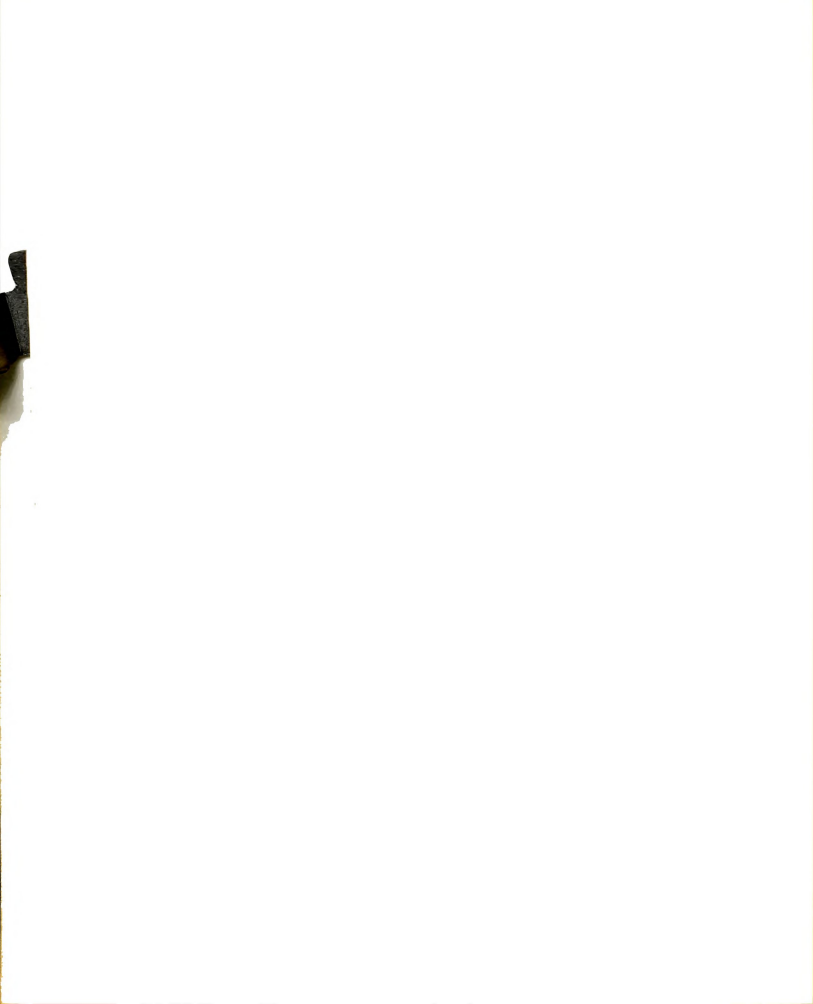
TABLE OF CONTENTS

																		Page
DEFINI:	TION	S OF	SYMBOI	LS (JSED													ix
GENERA	L IN	TRODU	CTION															1
PART I	: T	HE ST	RUCTUE	RE I	DETER	MIN	ΙAΤ	IOI	v C	F	MAN	IGA	NE	SE	:			
	T	ETRAP	HENYLI	PORI	PHYRI	N	•	•		•	•	•	•	•	•	•	•	5
I.	INT	RODUC	TION															6
	1.	Meta	llopoi	rphy	rins													6
	2.	Revi	ew of	Por	phyr	ins	a	nd	Ме	ta	110	ppc	orp	hy	ri	ns		7
	3.	Mang	anese	Por	phyr	ins		•										12
II.	EXP	ERIME	NTAL															15
	1.	Phot	ograph	nic	Stud	lies												15
	2.	Diff	ractor	nete	er Ir	ter	si	tу	Da	ta	C	11	lec	ti	on	ı		18
III.	STR	UCTUR:	E DETE	ERMI	[NAT]	ON												24
	1.	Intr	oduct:	ion														24
	2.	Loca	tion o	of t	the M	lang	an	es	e A	to	m							25
	3.	Elec	tron I	Dens	sity													31
	4.	Diff	erence	e De	ensit	У												33
	5.	Refi:	nement	t .														37
		(1)	Weigh	ntir	ng So	hen	ie											38
		(2)	The M	Metl	nod o	of I	ea	st	Sq	[ua	res	3						39
		(3)	Phil:	lips	s' Ak	sor	pt	io	n C	or	red	cti	ion	ı				40
		(4)	Find:	ing	the	Ace	to	ne	Mo	le	cu.	Le						46
		(5)	Find:	ing	the	Нус	lro	gei	n A	to	ms							46
IV.	STR	UCTUR.	AL RES	SUL.	rs .													49
**	DTG	arra a r	017															co



TABLE OF CONTENTS (Continued)

			Page
PART	II:	THE REDETERMINATION OF THE STRUCTURE OF PORPHINE	83
VI	· INT	PRODUCTION	84
	1.	General	84
	2.	Visible Spectroscopy	86
	3.	Infrared Studies	88
	4.	Nuclear Magnetic Resonance	91
	5.	X-Ray Studies	92
VII	. EXI	PERIMENTAL	95
	1.	The Problem of the Hydrogen Atoms	95
	2.	Preliminary X-ray Examination	101
	3.	Techniques for Measuring Intensities	105
		(1) Stationary Crystal-Stationary Counter Technique	106
		(2) Moving Crystal-Stationary Counter Technique	107
		a. The X-ray Detector	110
		b. Constant-time Step Scan Technique.	110
		c. Constant-count Step Scan Technique	113
		(3) Moving Crystal-Moving Counter Technique	116
	4.	Data Collection	116
	5.	Calibration Between Measuring Techniques .	118
VIII.	. STF	RUCTURE DETERMINATION	119
	1.	Isotropic Refinement	119
	2.	Anisotropic Refinement	121
	3.	Extinction Correction	121
	4.	Weighting Scheme	125
IX.	. RES	SULTS	132
X	. DIS	Scussion	144
	REE	PERENCES	157
	API	PENDICES	
	1.	General Review of X-ray Diffraction	161
	2.	Observed and Calculated Structure Ampli- tudes of ClMnTPP and Porphine	172



LIST OF TABLES

TABL	E P	age
1.	Crystallographic Data for MnTPP	19
2.	Boundary Planes and Their Distances from the Center of the Crystal	44
3.	Maximum Observed and Calculated Absorption Factors	45
4.	Scale Constants for Each Reciprocal Level	45
5.	Final Atomic Coordinates, Thermal Parameters and Peak Heights for ClMnTPP	50
6.	Coordinates, Isotropic Temperature Factors and Peak Heights of Hydrogen Atoms	54
7.	Atomic Parameters of the Acetone Molecule	55
8.	Parameters for the Equation, $\texttt{m}_1 \texttt{x} + \texttt{m}_2 \texttt{y} + \texttt{m}_3 \texttt{z} = \texttt{d}$, Selected to Fit Planes	56
9.	Dihedral Angles between NLS Plane and the Individua Phenyl Plane and Angle between NLS Plane and Mn-Cl Line	1 56
10.	Atomic Deviations from Least-Squares Planes of Individual Pyrrole and Phenyl Rings	58
11.	Atomic Deviation from the Least-Squares Plane of Four Nitrogen Atoms	59
12.	Average Stereochemical Parameters of Porphine Skeleton in Some Five Coordination Metallotetraphenylporphyrins	81
13.	Intensities of (241) Reflection Measured by CTST and SX Techniques	112
14.	Step Scan Measurement	114
15.	Intensities of Reflection (412) Measured by CCST	115



LIST OF TABLES (Continued)

TABL	E	Page
16.	Atomic Coordinates and Isotropic Temperature Factors for Porphine (from Webb & Fleischer)	120
17.	The Reflections Corrected for Extinction $\ \ .\ \ .\ \ \ .$	124
18.	Error for Intensity Less than $400 \dots \dots \dots$	130
19.	Final Atomic Parameters and Peak Heights of Carbon and Nitrogen Atoms of Porphine	133
20.	Final Coordinates, Isotropic Temperature Factors, and Peak Heights of Hydrogen Atoms of Porphine .	135
21.	Atomic Deviations from the Least-Squares Planes of Individual Pyrrole, Inner Eight Atoms and Four Nitrogen Atoms	136
22.	Average Pyrrole Bond Lengths in Some Free Base Porphyrins and Porphine	149
23.	Average Pyrrole Bond Angles in tri-TPP and the Porphine of This Work	150
24.	Fractional Coordinates and Peak Heights of Central Hydrogen Atoms from Two Porphine Structure Analysis	155



LIST OF FIGURES

FIGU	RE Pa	age
1.	(a) Manganese tetraphenylporphyrin, (b) Porphine	2
2.	Geometry of metals in metalloporphyrins	9
3.	Flow chart for data collection procedure	22
4.	Harker section of ClMnTPP	29
5.	Harker Line of ClMnTPP	30
6.	Approximate crystal geometry for computing absorption factors	43
7.	Porphine skeleton nomenclature	47
8.	Atomic deviations $(\stackrel{Q}{A})$ from NLS plane	60
9.	Atomic deviations from least-squares plane based on inner sixteen atoms of ClMnTPP	61
10.	(a) Bond distances (in $\overset{\circ}{A}$)	62
	(b) Intramolecular distances and dihedral angles	63
	(c) Bond angles for ClMnTPP	64
11.	A diagram in perspective of MnTPP molecule (ORTEP).	66
12.	Crystal structure of ClMnTPP viewed in the projection along a	68
13.	<pre>Intermolecular distances from chlorine atom</pre>	70
14.	Bond distances and bond angles of acetone molecule of crystallization	72
15.	The geometry and the dimensions of square pyramidal coordination in ClMnTPP molecule	78
16.	Possible central hydrogen models	85

LIST OF FIGURES (Continued)

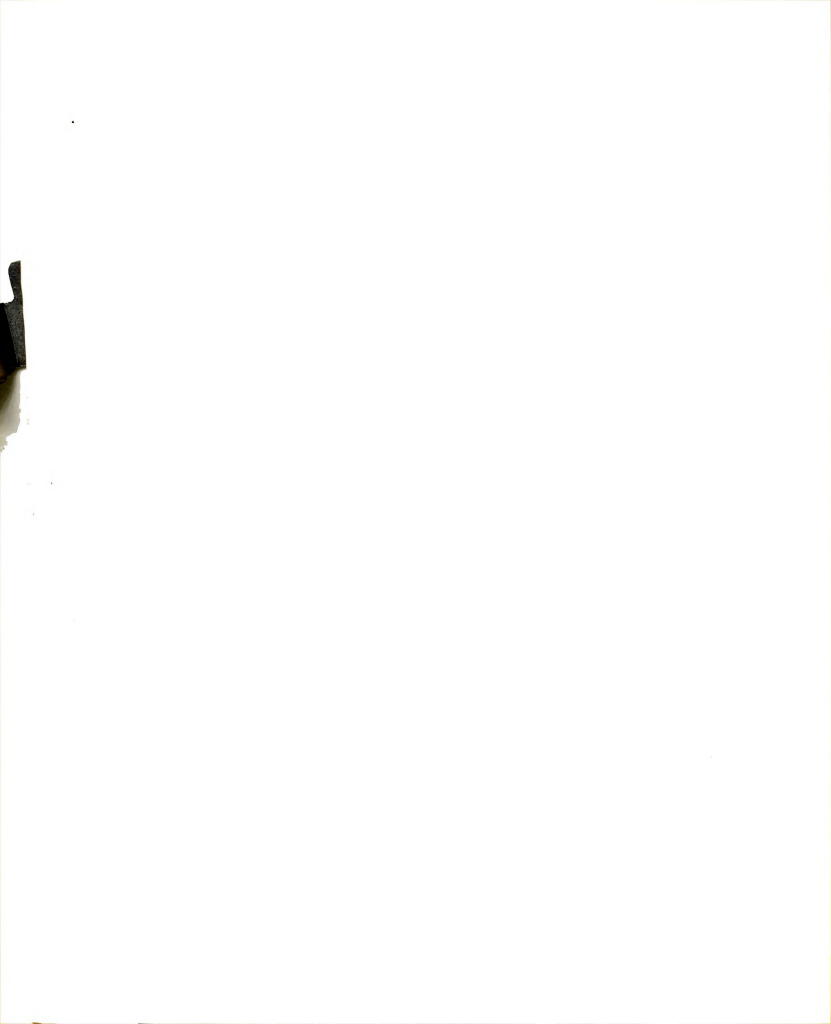
FIGU	RE	Page
17.	Mason's intramolecular hydrogen-bonded models for porphine	90
18.	Coproporphyrin	90
19.	Porphine numbering scheme	97
20.	Number of reflections $(F_c \ge 1.0)$ vs scattering angle (2θ)	100
21.	Dimensions of porphine crystals	102
22.	Errors (%) vs. intensity	128
23.	Atomic deviations $(\overset{\circ}{A})$ from nuclear least squares plane	137
24.	Porphine bond distances (\mathring{A})	138
25.	Porphine bond angles (degrees)	13 9
26.	Composite electron density of the hydrogen atoms perpendicular to the ac plane	141
27.	The difference electron density in the vicinity of the four nitrogen atoms	142
28.	The interatomic distances and angles of the nitrogen and hydrogen atoms	143
29.	Deviations of porphyrin skeleton from planarity .	146
30.	Porphine resonance forms	152
31.	Polar coordinates of a reciprocal lattice point $(hk l)$ for orthorhombic crystal system	163
32.	Maximum absorption factor \underline{vs} 2 θ	166
33.	Schematic representation of a four-circle diffraction	170



DEFINITIONS OF SYMBOLS USED

a, b, c	Primitive translations or unit cell axes of the crystal lattice, and their magnitudes.
β.	Angle between $\overline{c}^{>}$ and $\overline{a}^{>}$.
a*, b*, c*	Primitive translations of the reciprocal lattice.
h, k, &	Set of three integers with ranges from $-\infty$ to $-\infty$.
\vec{h} , \vec{k} , $\vec{\ell}$	Negative of the above set
(h,k, l)	Parallel lattice planes which intersect \overline{a} , \overline{b} , and \overline{c} at intervals of a/h, b/k, and c/ ℓ respectively.
fj	Atom j's scattering factor or ability relative to a classical electron to scatter X -rays.
тj	= exp - B $_{\rm j}(\sin\theta/\lambda)^2$ isotropic temperature factor of atom $$ j
	= exp - $(\beta_{11}h^2 + \beta_{22}k^2 + \beta_{33}l^2 + 2\beta_{12}hk + 2\beta_{13}hl + 2\beta_{23}kl)$ anisotropic temperature factor of atom j.
z_{i}	Number of electrons belonging to atom i.
r_{j} $f(hk\ell)$	$ = x_j \overline{a}^{\flat} + y_j \overline{b}^{\flat} + z_j \overline{c}^{\flat}. \text{Position vector for atom } j. $ $ = \sum_{j=1}^{N} f_j \left(hk_{\ell} \right) \exp 2\pi i \left(hx_j + ky_j + \ell z_j \right) \text{struc-} $
	ture factor for the reflection from (h,k,ℓ) planes. N atoms per unit cell.
I(hkl)	Intensity of the reflection from the (h,k,ℓ) planes.

$ F_0(hk l) $	Observed structure amplitude, whose square is proportional to $\text{I}(hk\ell)\text{.}$
2 0	Scattering angle.
Φ, χ, 2θ, ω	Angular settings for the diffractometer.
λ	Wavelength of X-ray radiation.
A (hk ½)	Absorption correction for the reflection from the (h,k,ℓ) planes.
μ	Linear absorption coefficient.
Poi	Electron density calculated with structure factors whose phases, S, are those of ith set of F (hk_{ℓ}) and whose amplitudes are $ F_0 (\text{hk}_{\ell}) $.
$\Delta ho_{ exttt{i}}$	Difference synthesis calculated with coefficients $ F_0 - F_c $ and phases, S_c .
R	$= \frac{\sum \mathbf{F_0} - \mathbf{F_c} }{\sum \mathbf{F_0} }$ Residual index.



GENERAL INTRODUCTION

Porphyrins (Fig. 1a) are derivatives of porphine (Fig. 1b), a system in which four pyrrole rings are linked by four methine carbon atoms to give a sixteen-membered macrocyclic ring. The porphyrins are found to be essential for certain biological functions such as: (i) oxygen storage and transport, as in myoglobin and hemoglobin; (ii) cellular respiration involving electron transport, as in the cytochromes; and (iii) photosynthesis, as in the chlorophyll-containing chloroplasts. All these biologically active substances consist of three distinct parts: the porphyrin, a central metal atom, and a complicated molecular environment.

Recently, manganese porphyrins have been considered to be important in chloroplasts, since manganese is essential in the energy converting unit of the plant. There is evidence that the plant can restore its ability to reduce carbon dioxide and evolve oxygen by adding manganese ions back to the energy system. Although there is little evidence to indicate the function and environment of manganese, it has been suggested that manganese is complexed with ligands of biological interest such as porphyrins. Thus, the structural properties of manganese-containing porphyrins may be of importance and biological interest.

(a) Manganese tetraphenylporphyrin, $MnC_{44}H_{28}N_4$.

(b) Porphine, $C_{20}H_{14}N_4$ Figure 1.

Manganese tetraphenylporphyrin (Fig. 1a, hereafter referred to as MnTPP) is a synthetic porphyrin. Single crystals of MnTPP form in the monoclinic crystal system and contain four molecules in the unit cell. Since space group requirements dictate that each asymmetric unit contains one complete molecule, the molecular structure of MnTPP is not affected in any obvious way by crystal symmetry. For this reason and others already mentioned, an X-ray crystallographic study of the structure of MnTPP was undertaken in anticipation of perhaps providing information of biological interest and utility, as well as adding to the general understanding of metalloporphyrins.

In the other portion of this work, a redetermination of the structure of porphine was carried out. As the parent compound of the porphyrin series, the structure of porphine is particularly important because any understanding of the porphyrins must rest intimately upon the understanding of porphine.

The central hydrogen atoms of the free base of porphine and of porphyrins are known to influence the detailed structure of the porphyrin skeleton. Various techniques have been used to probe properties of these central hydrogen atoms. Low temperature visible spectroscopy suggested the existence of cis and trans isomers, i.e., hydrogen atoms on adjacent and on opposite pyrrole nitrogen atoms, respectively. Attempts to detect hydrogen bonding between hydrogens and neighboring nitrogen atoms by infrared spectroscopy

were inconclusive. Nuclear magnetic resonance spectroscopy suggested the rapid exchange of the inner hydrogen atoms. On the other hand, the X-ray diffraction analysis of the triclinic form of tetraphenylporphyrin (tri-TPP) showed that the two inner hydrogen atoms were localized and located on opposite nitrogen atoms, whereas the results of a similar study of the tetragonal form of TPP indicated a disordered structure for the molecule (two equally probable positions in the plane of the molecule 90° apart). From the X-ray diffraction work of Webb and Fleischer, the porphine molecule was reported to be essentially planar with an average symmetry close to $D_{4h}(4/mmm)$ and to contain four inner half-hydrogen atoms. The latter were suggested to be due to a rapid interconversion of N-H tautomers. However, since the crystals were also reported to contain a 5-10% impurity of copper porphine and since the electron densities of the half-hydrogen atoms were only slightly above background, the situation of the central hydrogen atoms remained unceratin. For these reasons and others to be elaborated upon later, an X-ray crystallographic re-examination of the structure of porphine was undertaken.

PART I

THE STRUCTURE OF MANGANESE TETRAPHENYLPORPHYRIN

I. INTRODUCTION

1. Metalloporphyrins

The porphine skeleton with four pyrrole rings and four methine carbon atom bridges is shown in Figure 1b. There are fourteen replaceable hydrogen atoms, eight pyrrole hydrogens, four methine hydrogens, and two central hydrogen atoms bonded to nitrogen atoms. Derivatives which are produced by the replacement of inner hydrogen atoms by metals are the metalloporphines, while those whose outer hydrogens are replaced by other groups are called porphyrins. The four methine carbon atoms can also be replaced by azanitrogen atoms forming azaporphines which, in turn, are related to the phthalocyanines by fusion of a benzene ring to each pyrrole. The two inner hydrogens of phthalocyanine are also replaceable by a wide variety of metals.

Porphine is a planar molecule, made up of eleven conjugate double bonds, with considerable flexibility to fold as demanded by environmental stresses and strains. Some forces which can affect the conformation of the porphyrin moiety are: (1) a central metal atom, (2) side-chain substitutions on the porphyrin ring, and (3) intermolecular forces from the environment of the molecule. Of greatest

concern in this work is the coordination of the central metal atom and its effect on the porphyrin system.

2. Review of Porphyrins and Metalloporphyrins

Extensive reviews of structural studies of porphyrins and metalloporphyrins have been written by Hoard¹ and Fleischer.² The following on the geometry of metals in metalloporphyrins is intended as a brief summary of these reviews (see Fig. 2).

Since porphyrins consist of large conjugated systems which can serve as tetradentate ligands, metallic cations are able to be accommodated at the center of the system with the four nitrogen atoms serving as ligands. The metals of metalloporphyrins have been found in a variety of coordinations. Four coordinate compounds formed by central metal atoms bonded with the four pyrrole nitrogen atoms have approximate square planar geometry. Although the porphine skeleton of these porphyrins is a conjugated system and is usually assumed to be planar, some of the metalloporphyrins, such as CuTPP3 and nickel etio-I porphyrin4 have been found to possess nonplanar porphyrin rings. Furthermore, there are small variations of metal-nitrogen (M-N) distances from one porphyrin to another. The reasons for the nonplanarity and the variation in M-N bond distances are as yet not well understood.

Five coordinate metalloporphyrins are found to have square pyramidal geometry. In general, the metal is



- Figure 2. Geometry of metals in metalloporphyrins.
 - (1) four-coordinate with a square planar geometry.
 - (2) tetragonal pyramid coordination of five-coordinate metalloporphyrins.
 - (3) six-coordinate metalloporphyrins.
 - (4) possible seven-coordinate metalloporphyrins.
 - (5) square antiprism of the eight-coordinate tin phthalocyanine complex.
 - (6) manganese(III) phthalocyanine dimer.
 - (7) μ -oxo-bis(porphyriniron(III) dimer.





Figure 2.

displaced from the mean plane of the pyrrole nitrogen atoms toward the apical ligand. For example, iron in high spin ClFeTPP5 shows an out-of-plane displacement of about 0.4 %, and vanadium in vanadyl-substituted etioporphyrin6 is 0.48 % out of the plane. In some of these porphyrins, there is a significant shortening of the axial bond between the apical ligand and the metal. For example, the axial length of Fe-Cl in ClFeTPP is 2.19 %, while the corresponding value listed in International Tables for X-Ray Crystallography is 2.38 %. Similar shortening effects are also observed in the 0-Mg (2.07 A) bond of (%20)MgTPP7.

Six coordinate compounds display distorted octahedral geometry; eight coordination is found as a square-antiprism sandwich in the tin phthalocyanine complex, 8 and higher coordinate metalloporphyrins do not seem to form. On the other hand, dimeric metalloporphyrins such as $\mu\text{-oxo-bis}(\text{por-phyriniron}(\text{III}))^9$ are known. Here, the iron atom has five coordination and is about 0.5 % out of the nitrogen plane in the direction toward the oxygen bridge, with the Fe-O-Fe angle being about 170° .

In general, the bond distances of the porphine core as determined from X-ray studies do not correspond to an average of single and double bond distances nor a single-bond-double-bond array of a conjugated double bond system. The average carbon-nitrogen distance of most metalloporphyrins is about 1.37 $\mathring{\rm A}$, which is shorter than the 1.42 $\mathring{\rm A}$ distance expected for a trigonally hybridized C-N \circ -bond,

but longer than the 1.27 $\mbox{\mbox{$\mathring{\Lambda}$}}$ distance observed for the C=N double bond. In the pyrrole ring, the average $\mbox{\mbox{$C_a$}}-\mbox{\mbox{$C_b$}}$ bond length (where $\mbox{\mbox{$C_a$}}$ is the carbon atom adjacent to the pyrrole nitrogen while $\mbox{\mbox{$C_b$}}$ is the carbon adjacent to $\mbox{\mbox{$C_a$}}$) is about 1.45 $\mbox{\mbox{$\mathring{\Lambda}$}}$, a definitely shorter value than the bond length of 1.49 $\mbox{\mbox{$\mathring{\Lambda}$}}$ expected between trigonally hybridized carbon atoms, while the average $\mbox{\mbox{$C_b$}}-\mbox{\mbox{$C_b$}}$ bond length of 1.35 $\mbox{\mbox{$\mathring{\Lambda}$}}$ indicates a lengthening of the double bond value of 1.33 $\mbox{\mbox{$\mathring{\Lambda}$}}$.

The center-nitrogen distance (Ct-N), which indicates the radius of the central hole of the porphyrin core, has been observed in most cases to be smaller in metalloporphyrins than that of the corresponding free base porphyrins. The bond distances of the metal-nitrogen (M-N) of metalloporphyrins have been observed to vary from 2.05 Å in ferric porphyrin to 1.95 Å in nickel etio-I porphyrin. There seems to be no direct relationship between the M-N bond length and the size of metal atom. Furthermore, the metal atom can be in or out of the mean plane of the four nitrogen atoms. This effect has been carefully examined in iron porphyrins by Hoard, 10 who predicted that a low-spin iron porphyrin would have iron in the nitrogen plane while the metal in high-spin iron porphyrin would be 0.5 % out of the mean plane. Indeed, this prediction has been verified by the structure analysis of bisimidazoleiron(III) tetraphenylporphyrin. 11

3. Manganese Porphyrins

Porphyrin complexes of Mg, Co, and Fe are known to occupy central roles in chlorophyll, vitamin B_{12} , and hemeproteins. Recently, manganese porphyrins have received a great deal of attention because of their possible link to chloroplasts. Two reasons for this interest are: (1) the relationship of manganese porphyrins in photosynthesis, and (2) the coordination chemistry of this transition metal in a porphyrin environment.

The chloroplast, which is the most essential component in photosynthesis, contains protein, lipid, chlorophyll, inorganic ions and carotenoids. Among these components, chlorophylls and inorganic ions, such as manganese ions, have been considered to be most important in the energy transfer process. 12,13 Chloroplasts can be broken down into subunits, with the smallest subunit, a quantasome, being about 200 A in diameter. For each quantasome, there are precisely two manganese atoms per 300 chlorophyll molecules. In addition, there is evidence that manganese is an essential element for the oxygen evolving step of photosynthesis. When manganese ions are re-added to the plant's environment, its ability to evolve oxygen is restored, and the plant can perform its normal function of reducing CO, and evolving oxygen. All the evidence indicates that the presence of manganese is a functional requirement of the chloroplasts. However, the manganese is difficult to remove from chloroplasts, and its physical properties as such are not easily observed.

Calvin¹⁴ has suggested that the manganese atoms in the chloroplast are bound to porphyrin type ligands. He has demonstrated that manganese porphyrin can undergo reversible oxidation-reduction changes between Mn(II)-Mn(III) and Mn(III)-Mn(IV), with the Mn(III) species being unusually stable. This initial work supported the relevance of manganese porphyrin as a possible photosynthetic model compound.

The physical and chemical properties of manganese porphyrins have been studied by Boucher, 15,16 Magnetic susceptibility measurements in the solid and in solution, at a number of different temperatures, yield an effective magnetic moment in the range of 4.5 to 5.0 B.M. The expected value for a spin-free d4 manganese(III) complex is 4.9 B.M. These measurements suggest that there is no spin pairing. The far infrared spectra show metal-anion stretching absorptions in the region of 160 to 500 cm -1, consistent with the strong binding of an additional ligand in the axial coordinate position of the metal. In solution, electronic spectra showed that six-coordinated manganese porphyrins were present with various ligands. From these spectra it was concluded that manganese porphyrins have significant metal-porphyrin π -bonding; however, the porphyrin-metal d-orbital π interaction is difficult to describe quantitatively. Two possible geometries of the molecule have been predicted. One possibility is that of tetragonal geometry with the metal ion in the plane of four pyrrole

nitrogen atoms, with an axial anion and a solvent molecule at somewhat larger distances from the metal. The other possibility is that the metal atom is out of the plane of the porphyrin (about 0.5 Å), coming closer to the axial anion. The latter geometry can be rationalized by saying that because of the large size of the metal ion, it cannot fit into the nitrogen cavity. In any case, the exact molecular structure of manganese porphyrins was still in question. For such reasons, it seemed particularly appropriate to carry out a detailed structural determination of a manganese porphyrin.

II. EXPERIMENTAL

1. Photographic Studies

Photographic methods provide a quick and easy way to obtain a general view of the geometry of a diffraction pattern, the symmetry of the reciprocal lattice, and the relative intensity distribution of a large number of reflections. Methods available to obtain such information are oscillation and moving film photography (Weissenberg and precession methods).

In the oscillation method, the crystal is mounted in a manner such that some principle axis coincides with the oscillation axis and the crystal is oscillated through a small angle, i.e., 5-10°, around this axis by means of some threaded gear or other mechanism. The photographic film is placed in a cylindrical camera around the oscillation axis. A small number of planes will come into a reflecting position with this oscillating motion and will produce spots on a film in the form of a series of separated layer lines. The diffraction pattern recorded in this way can provide useful information regarding the symmetry of the crystal lattice and the spacing of the lattice along the oscillation axis.

Single crystals of MnTPP were grown by slow evaporation of an acetone solution. The dark purple crystals exhibited polyhedral morphology with many well-defined faces. A crystal of suitable size (approximately $0.4 \times 0.2 \times 0.3$ mm) and with good morphological quality was chosen for photographic examination. A 10° oscillation photograph of a crystal mounted with its largest dimension perpendicular to the spindle oscillation axis showed that the intensity distribution of the upper and lower halves of the photograph were symmetrical with respect to the zero layer line. This distribution indicated the presence of a mirror plane of symmetry in the direct lattice perpendicular to the oscillation axis and either a monoclinic lattice or one with higher crystal symmetry (i.e., orthorhombic or higher).

In the Weissenberg film method, a single layer line normal to the oscillation axis is selected for observation by means of a slotted screen which allows only the reflections in that layer to be recorded on the photographic film. As the crystal rotates, the film moves past the screen slot in a synchronous way and reflections which occur at different times are recorded at different translational positions on the film. The moving film photograph displays the reciprocal lattice plane which is perpendicular to the oscillation axis and can be used to determine the symmetry of these planes and to index reflections. Photographs of several successive layers of the MnTPP crystal were taken. The lack of any further symmetry elements showed that MnTPP crystallized in a monoclinic lattice. The unique b axis of the

monoclinic crystal system coincided with the oscillation axis and the a* and c* reciprocal axes were selected so that the zero layer photograph showed the reflections $(h0 \ell)$ absent when the ℓ index was odd. This characteristic extinction is due to a c-axis glide plane, and corresponds to a reflection across a plane accompanied by a translation of c/2 parallel to the plane along the c axis.

In the precession method, the crystal oscillates about an axis with the latter also undergoing an oscillation. The net motion closely resembles a precession motion. During these motions, the film always remains parallel to the reciprocal lattice plane which is perpendicular to the X-ray beam in the absence of a precession angle, and thus records the true, undistorted, geometry of the reciprocal lattice plane. Precession photographs of MnTPP taken of the reciprocal planes parallel to the b-axis (hk0 and $0k \, \ell$) showed that 0k0 reflections were absent whenever k was odd. This absence indicates the presence of a 2-fold screw axis along the b axis of the crystal (i.e., 2-fold rotation plus b/2 translation along the rotational axis).

Thus, the preliminary studies of the crystal MnTPP showed that the crystal belongs to a monoclinic system with a space group possessing the following conditions for systematically absent reflections:

0k0 reflections, k = (2n + 1) = odd

h0 l reflections, l = (2n + 1) = odd.

From these conditions, the space group was uniquely

determined as $P2_1/c$, space group No. 14, subgroup number 2, as tabulated by the <u>International Tables for X-ray Crystal</u>-lography.

2. Diffractometer Intensity Data Collection

A second crystal, which was slightly smaller than the one used for photographic studies, with dimensions of about 0.25 x 0.15 x 0.15 mm (see Fig. 6) was used for intensity measurements. The crystal was mounted on a goniometer head whose axis was coincident with the o circle of a guarter circle crystal orienter (see Fig. 31 given in Appendix 1). The orientation of the crystal with respect to the diffractometer axis was such that the unique b axis of the crystal was also coincident to the o axis of the diffractometer. The a* c* plane was thus located in the equatorial plane $(\gamma = 0)$. The unit cell dimensions of the crystal were determined by measuring the angular orientation which centered the intensity of 12 moderately intense reflections well-distributed in reciprocal space and with large 2θ angles. The angular coordinates were used with the method of least squares to obtain the best unit cell parameters and least squares orientation of the crystal. The results are listed in Table 1.

The density of a single crystal of MnTPP was measured by flotation in an aqueous silver nitrate solution and indicated that there were four molecules in the unit cell. The observed density of the crystal was 1.30 g/cm³; however, the calculated density based on four MnTPP molecules in the unit cell was only 1.17 g/cm³. The high observed molecular weight (738 instead of 667) suggested the presence of additional material in the unit cell. This material could have been introduced at the time of preparation(ions) or crystallization(solvent). The discrepancy was resolved later during the structure determination.

Table 1. Crystallographic Data for MnTPP

Space Group	Monoclinic P2 $_{1}/\mathrm{c}$	Z* = 4
a	14.588 ± 0.005 Å	Empirical formula MnC44H28N4
b	$21.765 \ \pm \ 0.006$	M.W. = 667
С	$\textbf{17.023} \pm \textbf{0.006}$	$D_{\rm obs} = 1.30 \pm 0.01 \text{ g cm}^{-3}$
β	135.62 ± 0.04 degree	$D_{cal} = 1.17 \text{ g cm}^{-3}$
Volume	3773.8 ± 3.4 Å3	

^{*}Number of molecules in the unit cell.

The quality of the crystal chosen and the best quadrant for data collection can be ascertained by measurement of the mosaic spreads of the crystal, essentially a measurement of the degree of misalignment of the mosaic blocks (minute perfect crystal blocks) which make up the real crystal. For MnTPP, the reflections (080), (300), $(\overline{3}00)$, (006) and $(00\overline{6})$ were chosen to measure the mosaic spreads. The mosaic spreads of $(\overline{3}00)$, (300), (006), and $(00\overline{6})$

reflections (at $\chi = 0^{\circ}$) were measured by: (1) presetting 2θ at the center of the reflection as determined by use of a left/right device which allows either the left half or the right half of the diffracted beam to be selectively examined, (2) off-setting the open angular setting to the background level of the peak, and recording the intensity. I. of the diffracted beam as a function of the angle of in increments of 0.05° from background to background. The mosaic spreads of the (080) reflection (at $\chi = 90^{\circ}$) were measured by: (1) presetting $2\theta_{max}$, (2) presetting ϕ at the value of the a^* , c^* , $-a^*$, and $-c^*$ axes, (3) offsetting the ω angle to the background level and recording the intensity, I, as a function of the ω angle in increments of 0.050 from background to background. The mosaic spread of $(00\overline{6})$ was found to have the maximum basal peak width which was 0.45°. All the remaining mosaic spreads were about 0.30 in width and symmetrical in shape. The data collection was thus restricted to the quadrant defined by the -a* axis (0 = 298.5°), and a* axis ($\phi = 118.5^{\circ}$) and including the c* axis at $\phi = 38.9^{\circ}$.

A set of intensity data was collected with a Picker 4-Circle Automatic Diffractometer using the moving crystal-moving counter technique (2θ scan). In this technique, the reflection was scanned and counted with the radiation filtered through a nickel filter (β filter) in order to remove Cu K β radiation. A second scan was then made with a balanced cobalt filter (α filter), i.e., one whose

absorption edge is at a wavelength just longer than the Ka radiation being used. A flow chart of the data collection procedure is shown in Figure 3. Within a 20 limit of 100°, the total number of reflections measured was 3978. In order to ascertain which reflections should be considered as unobserved, the lower limit of intensity corresponding to the average background intensity fluctuation was determined as follows. Any measured intensity of reflections which are systematically absent, i.e., (h0%) and (0k0) reflections k or & odd, should be mainly due to the effects of background radiation. Using this assumption, an average intensity of 7 counts/10 sec was obtained by measuring 93 systematically absent reflections. Thus the minimum observable intensity for reflection was set to be slightly larger than this average background value. Eliminating the unobserved reflections, systematically absent reflections, and all redundant reflection (± hk0 reflections), a total of 2977 unique and observable reflections remained for the structure determination of MnTPP.

If during the course of data collection procedure the intensity of any of the monitor reflections (004), ($\overline{7}00$) and (080) was outside the expected counting statistic error, approximately the square-root of the original intensity ($\sqrt{1}$), the crystal was realigned and data collection was resumed. Throughout the data collection the intensity of the monitors did not fluctuate by more than 10% of their original value. Since there was no systematic

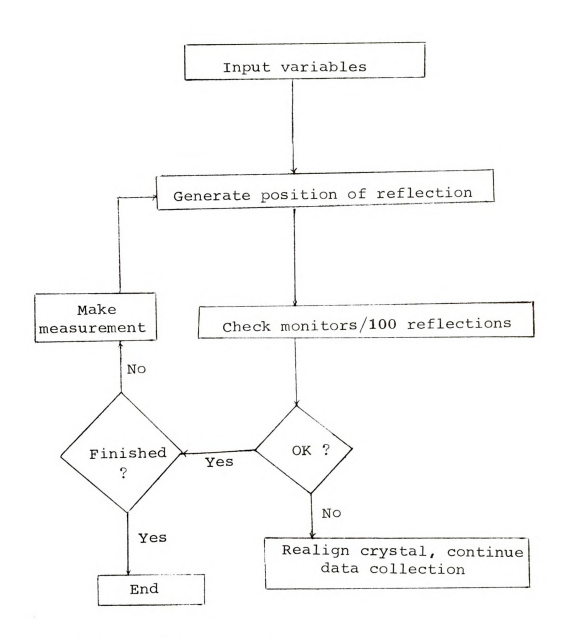


Figure 3. Flow chart for data collection procedure.

intensity decrease a decay correction was not considered necessary.

The absorption of X-rays by the crystal (see Appendix 1) showed a functional dependence on both 2θ and ϕ . Although initially only an approximate absorption correction was applied to the data in terms of both these angles, a more accurate correction was applied later.

The intensities of all the independent reflections were subsequently corrected for Lorentz and polarization effects, and converted to a set of relative structure amplitudes (|F|).

TII. STRUCTURE DETERMINATION

1. Introduction

It is well known that an X-ray wave scattered by the atoms of a crystal can be characterized by a quantity F(hk) called the structure factor. This quantity is a complex number whose magnitude is the amplitude of the scattered wave and whose orientation in the complex plane is determined by the phase of the scattered wave. The structure factors depend on the arrangement of atoms in the crystal. If the magnitudes and phases of the structure factors are known, the electron density distribution in the unit cell can be calculated; conversely if the electron density is known, structure factors can be obtained. The fundamental difficulty encountered in crystallography is that the magnitudes of the structure factors are obtainable from measured intensities, but the phases cannot be measured directly. Determination of the phases of the structure factors is known as the phase problem.

There is no general solution for the phase problem. However, it has been found that structures in which one or a few atoms are markedly heavier than the remainder are usually more easily solved than those in which all the atoms

are alike. The reasons for this are: (1) it is possible to locate the heavy atoms in the crystal by methods which do not require knowledge of the phases, and (2) once the heavy atoms have been found they can serve as a trial phase model from which the remaining atoms can be found.

2. Location of the Manganese Atom

The Patterson function is a Fourier series whose coefficients are the squares of the structure amplitudes, $|F(hk\ell)|^2. \label{eq:final_pattern}$ The structure amplitudes are directly derivable from X-ray intensities. The Patterson function is related to the electron density function, both of which can be expressed mathematically as the following Fourier series

electron density:

$$\rho(xyz) = \frac{1}{V} \sum_{hk\ell} F(hk\ell) \exp -2\pi i (hx + ky + \ell z)$$
 (1)

Patterson function:

$$P(uvw) = \frac{1}{V^2} \sum_{\substack{n \ge 1 \\ k \nmid \ell}} |F(hk\ell)|^2 \cos 2\pi (hu + kv + \ell w) (2)$$

Then, (1) has a peak at each atom location, while (2) has peaks corresponding to the end of the vectors between atom locations. The coordinates of the r^{th} peak in (2) are related to those of i^{th} and j^{th} peaks in (1) by

$$u_r = x_j - x_i$$
, $v_r = y_j - y_i$, and $w_r = z_j - z_i$.

Thus for every pair of peaks in (1), there is a specific peak in (2).

Harker $(1936)^{17}$ pointed out that in some cases much useful information is concentrated in certain planes of the three-dimensional Patterson function. For space group $P2_1/c$, there are four equivalent positions:

- (a) x_i , y_i , z_i
- (b) \bar{x}_i , \bar{y}_i , \bar{z}_i
- (c) \bar{x}_i , $1/2 + y_i$, $1/2 z_i$
- (d) x_i , $1/2 y_i$, $1/2 + z_i$.

For atoms which are related by equivalent positions (a) and (c), there is a corresponding peak in the section v=1/2, $(u=2\bar{x}_i,\,w=1/2-2z_i)$. This section (v=1/2) is called a Harker section. The same reasoning applies to atoms related by (b) and (c), with the corresponding vector occurring on the Harker line with coordinates, (u=0, v=1/2+2y, w=1/2).

If the crystal contains only a few heavy atoms in the unit cell, the locations of these atoms can be solved by the use of the Patterson function. The Patterson peaks are approximately proportional to the product of atomic number of the atoms giving rise to them $(\mathbf{Z_i}\mathbf{Z_j})$, thus the peaks due to the heavy atoms stand out against the background of other smaller peaks. The overlapping of peaks which is caused by finite widths can be reduced by a process known as sharpening. Thus, the Patterson coefficients can be modified to make the heavy-atom vectors appear approximately as vectors between point atoms. Normally the scattering



power of an atom decreases as a function of ($\sin \theta/\lambda$), but sharpening can remove this fall-off characteristic by making the scattering power equal to atomic number Z for all ($\sin \theta/\lambda$). A common expression used for sharpening 18 is

$$|F_{point}| = |F_0|/\bar{f}$$
, where $\bar{f} = \sum_{i=1}^{\infty} (f_m)_i / \sum_{i=1}^{\infty} (Z_m)_i$

 $\mathbf{Z}_{\mathbf{m}}$ is the number of electrons in an atom of $\,\mathbf{m}\,$ type. $\,\mathbf{f}_{\mathbf{m}}$ is atomic scattering factor of atom $\,\mathbf{m}\,.$

Once the $|F_{\mathrm{point}}|'$ s are obtained from the observable $|F_0|s'$, they can be squared and used as the coefficients for a sharpened Patterson function. The effect of sharpening enhances the heavy-atom vectors and makes peaks more resolved.

MnTPP contains four Mn atoms in the unit cell and their positions were found by the use of Patterson function. The Patterson coefficients were sharpened with the Mn atomic scattering factor

$$|\mathbf{F}_{point}| = (\mathbf{z}_{Mn}/\mathbf{f}_{Mn}) |\mathbf{F}_{0}|$$
,

where Z_{Mn} is the number of electrons of the Mn atom (25), and the denominator is the atomic scattering factor of Mn atom, as obtained from the f-curve tabulated in <u>International Tables for X-ray Crystallography</u>. The vector peak due to Mn-Mn interactions showed clearly in the Harker section of the Patterson map (shown in Fig. 4). The coordinates of Mn atoms from the Harker section and Harker line (Fig. 5) are



Figure 4. Harker section of ClMnTPP. Peak 1 is Mn-Mn vector, peak 2 is Cl-Cl vector.

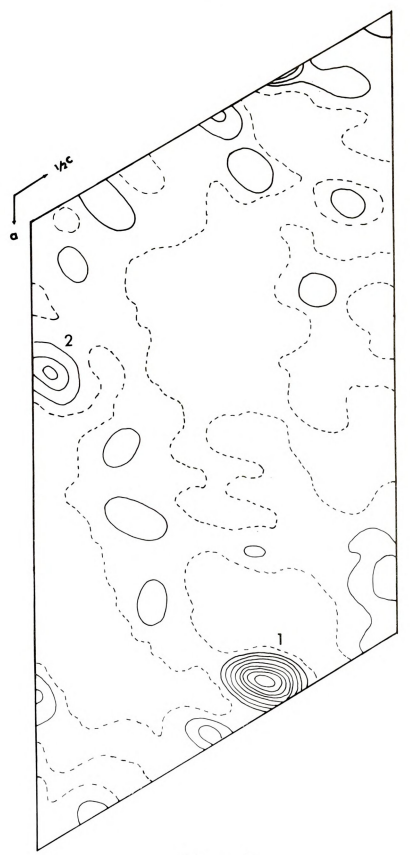
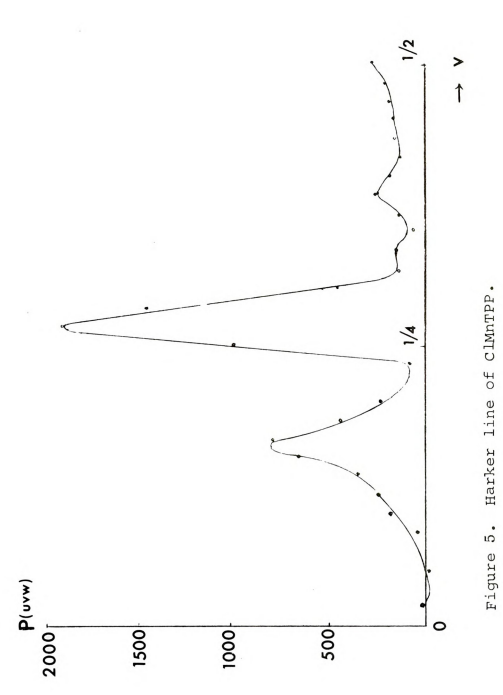
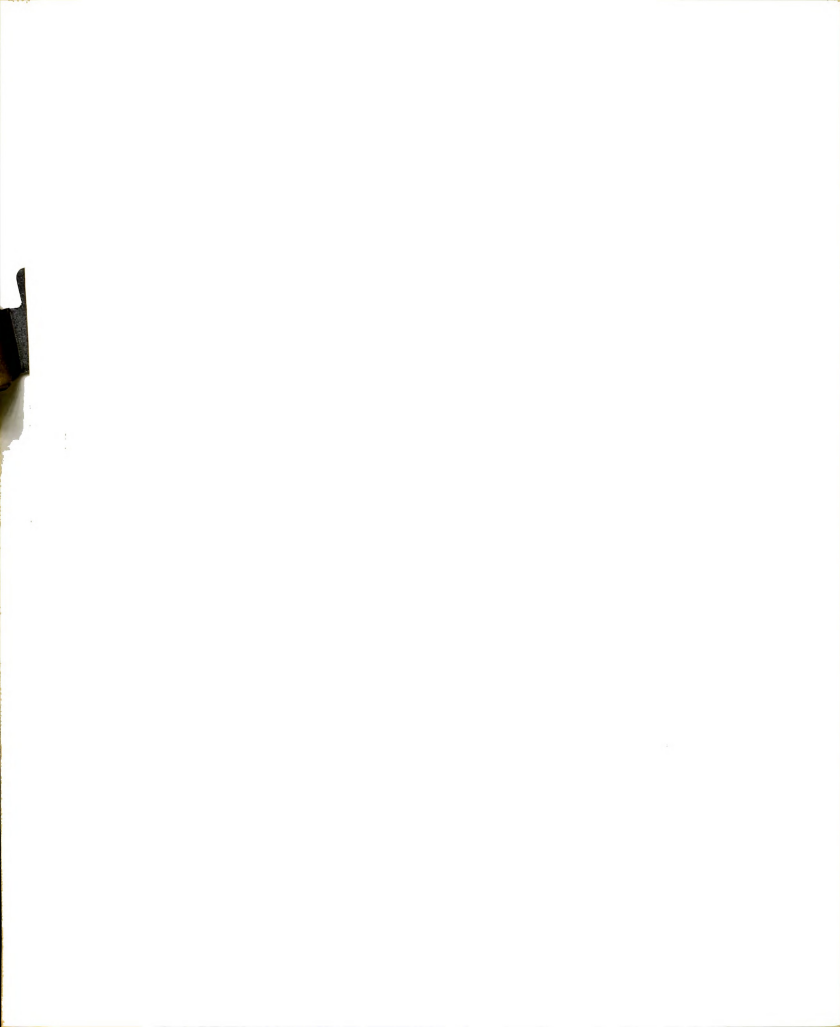


Figure 4.



)





(in fractions of a unit cell):

x = -0.4766

y = 0.1142

z = 0.0875.

The remaining atoms in the unit cell were found by using electron density methods.

3. Electron Density

The structure factor with one heavy atom in the unit cell can be written as

$$\begin{split} \mathbf{F}(\mathbf{h}\mathbf{k}\ell) &= \mathbf{f}_{\mathbf{H}} &= \mathbf{exp} \ 2\pi \mathbf{i} \left(\mathbf{h}\mathbf{x}_{\mathbf{H}} + \mathbf{k}\mathbf{y}_{\mathbf{H}} + \ell\mathbf{z}_{\mathbf{H}}\right) + \\ &= \sum_{\mathbf{n}} \mathbf{f}_{\mathbf{n}} &= \mathbf{exp} \ 2\pi \mathbf{i} \left(\mathbf{h}\mathbf{x}_{\mathbf{n}} + \mathbf{k}\mathbf{y}_{\mathbf{n}} + \ell\mathbf{z}_{\mathbf{n}}\right) \end{split} \tag{3}$$

where f_H is the scattering factor of the heavy atom, whose positional parameters are x_H , y_H , z_H . If f_H is much greater than f_n , then the first term will tend to dominate the scattering factor expression. To a first approximation, the structure factor can then be represented as

$$F_C \cong f_H \exp 2\pi i (hx_H + ky_H + \ell z_H)$$

or in centrosymmetrical case

$$F_C \cong |F(hk_{\ell})| \cdot S_C(hk_{\ell})$$
 (3a)

where $S_{_{\mathbf{C}}}$ is the sign of the calculated structure factor, $F_{_{\mathbf{C}}}$, and $|F(hk \ell)|$ is the observed structure amplitude. By use of equation (3a), an electron density can be computed from the calculated heavy atom phases and the magnitudes

of the Fost

$$\rho_{(xyz)} = \frac{1}{v} \sum_{hk \ell} |F_0(hk\ell)| S_c(hk\ell) \cos 2\pi (hx + ky + \ell z) (4)$$

where $|F_0|$ is observed structure amplitude. Light atoms found in this approximate electron density can then be used to generate a new set of better phases. By continuing this "bootstrapping" procedure, all atoms except the very light ones can usually be found.

In the present work, an electron density was calculated on the basis of the manganese atomic position derived from the Patterson function. In this calculation some small and phase undetermined reflections ($|F_0| < 10$) were excluded. Many peaks which were ascribed as light atoms appeared in an approximate plane in the unit cell. However, at this stage it was impossible to discern the expected molecular geometry, probably because the phases based on just the Mn atom contained considerable errors and introduced many spurious peaks in the density along with the correct ones. However, one strong peak was found approximately 2.5 A away from the manganese atom and approximately perpendicular to mean plane of peaks. The Harker section was re-examined, and indeed, there was a vector due to an atom with approximately fourteen electrons. Anions that could possibly be coordinated with manganese, introduced either during preparation or crystallization, were considered.

Manganese porphyrin can be synthesized 15 from a mixture of divalent manganese acetate and free base porphyrin in a



reaction medium such as glacial acetic acid or N,N¹-dimethylformamide.¹9 Dilute sodium halide solution is used to extract and to purify the product. In the presence of air, Mn(II) porphyrin is rapidly oxidized to the very stable Mn(III) porphyrin, for which a halide complex has been reported under these prepartory conditions.

Among possible anions, it was decided from the above that chloride was the most likely anion bound to the manganese atom; moreover, it also corresponded to about the correct number of electrons. Thus, the peak from Harker section and Harker line with coordinates,

x = 0.6350

y = 0.1667

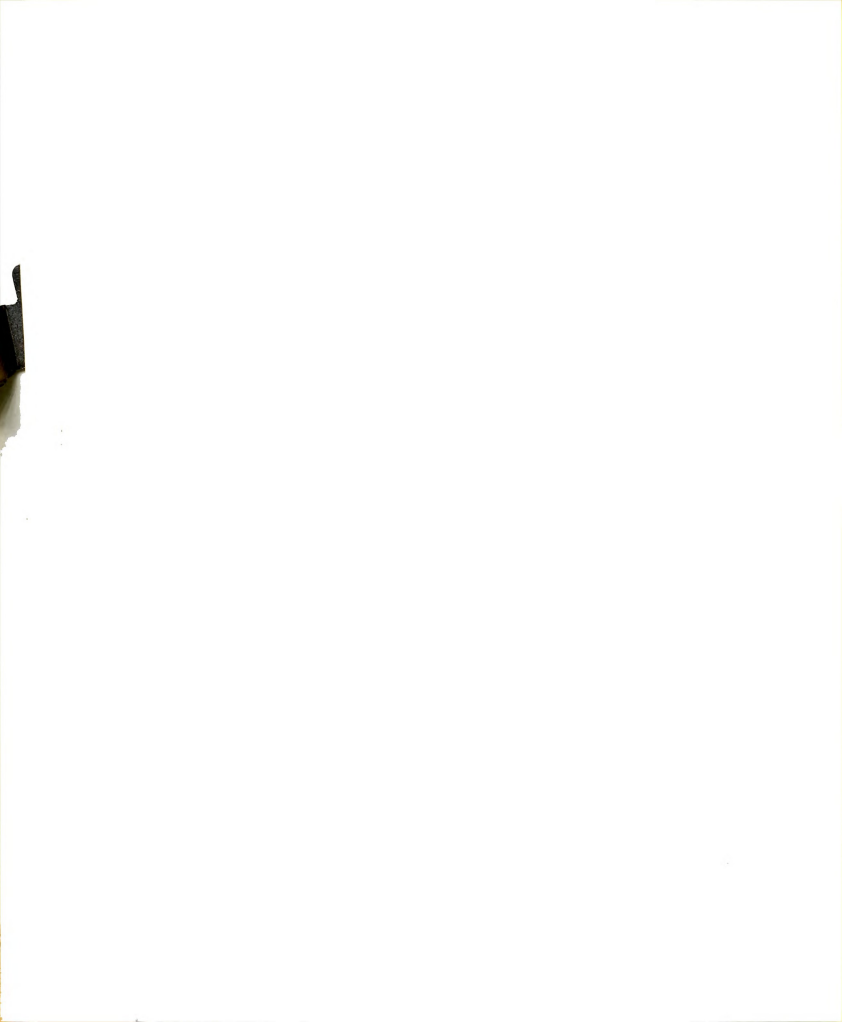
z = 0.2467

was assigned as chlorine. This increased the expected molecular weight to 702 a.m.u. and the calculated crystal density based on four ClMnTPP molecules was 1.23 g/cm³ ($D_{\rm obs}=1.30~{\rm g/cm^3}$).

Another electron density phased with the Mn and Cl contributions was calculated. This new map showed little improvement of the light atom structure over the original one except for the appearance of the chlorine atom.

4. Difference Synthesis

The difference synthesis is a Fourier series whose coefficients are the quantities F_0 - F_c , $\triangle F$,



$$\Delta \rho = \frac{1}{V} \sum_{hk \ell} \left(|F_0| - |F_c| \right) \cdot S_c \cos 2\pi (hx + ky + \ell z)$$
 (5)

where S_{C} is the sign of the calculated structure amplitudes $|F_c|$. In the early stages of a structure determination, when the exact phases of $|F_0|$ are not known well, a trial structure can sometimes be arrived at by calculating a difference synthesis where dominating heavy atom contributions are removed. Three criteria should be considered in selecting the coefficients. In the first case, when $|{
m F_0}|$ is approximately equal to $|{
m F_C}|(|{
m F_0}|pprox |{
m F_C}|)$, the calculated phase is probably close to the true phase. The second case is then $|F_0|$ is much larger than $|F_C|(|F_0|>>|F_C|)$. Here, because F_{c} is small, the calculated phase is fairly uncertain due to the fact that small changes could cause fairly large changes in F_c . Thus, use of the calculated phase for $|F_0|$ becomes very unreliable and can introduce large errors. In the third case, where $|\mathbf{F}_{_{\mathbf{C}}}|$ is much larger than $|F_0|(|F_c| >> |F_0|)$, even though the discrepancy is large the sign of the difference is correct. Therefore, the reflections used in a difference synthesis should be mostly those satisfying the first and third cases.

Because an unambiguous location of the light atoms could not be obtained from the $|F_0|$ synthesis due to the many spurious peaks, a difference synthesis was computed. Since the difference synthesis is very sensitive to the scale constant between $|F_0|$ and $|F_C|$, an accurate scale constant must be applied to either the $|F_C|$ or $|F_0|$ (if $|F_0|$)

is not on the absolute scale). The scale constant $\,k\,$ can be obtained from a Wilson plot of the data. A Wilson plot is based on the equation 20 , 21

$$\ln(\langle |F_0|^2 \rangle / \sum_{i=1}^{N} f_{0i}^2) = \ln k - 2B(\sin \theta / \lambda)^2$$
 (6)

where $\langle | \mathbf{F_0} |^2 \rangle$ is related to the average intensity, $\mathbf{f_0}$ is the scattering factor of ith atom, N is the total number of atoms in the unit cell and B is an average thermal parameter. By plotting the quantity $\ln(\langle |F_0|^2 \rangle / \sum_{i=1}^{N} f_{0i}^2) \underline{vs}$ $(\sin \theta/\lambda)^2$, a straight line can be obtained from which the intercept is ln k and the slope is 2B. In applying the Wilson plot to the intensity data of MnTPP, the reflections were separated into 12 ranges of 2θ , where each range contained about the same number of reflections (approximately 250). Values for $\langle |F_0|^2 \rangle$ and (sin θ/λ) were calculated for each range. The quantity for was taken from f-curves at the average ($\sin \theta/\lambda$) for each range. The result of this plot gave for B the value of approximately 4.0 Å^2 . The value of the isotropic thermal parameter obtained was about that expected for organic compounds (between 3 to 5 $\stackrel{\text{O}}{A}{}^2)^{2.2}_{\bullet}$ The summation of observed and calculated structure factors suggested for the scale constant a value of approximately 0.82. Since the value of k obtained from the Wilson plot seemed unreasonable this latter value was used in the structure factor calculations.

Initially, isotropic temperature factors of $3.5~^{\hat{\chi}^2}$ and $4.5~^{\hat{\chi}^2}$ were assigned to Mn and Cl atoms, respectively. The

R-factor of the calculation, where R is defined as $\Sigma \mid \left| F_0 \right| - \left| F_C \right| \left| \Sigma \right| \right| = \left| F_0 \right|, \text{ based on the Mn atom alone was 0.69,}$ while the R-factor including both Mn and Cl atoms was 0.52. The observed and difference syntheses calculated were based on the latter structure.

The structure determination can be divided into three stages. In the first stage, a difference, $\Delta\rho_1$, and observed electron density, ρ_{01} , were computed using 1266 reflections whose calculated structure factors were greater than 14 electrons (on an absolute scale). By considering only those peaks which occurred in both densities as possible atoms, four nitrogen atoms and thirteen carbon atoms were located with reasonable bond distances in the approximately expected geometry. The structure factor calculation with these seventeen atoms had an R-factor of 0.458. The same structure factor calculation excluding the chlorine atom from the calculation increased the R-factor to 0.507. Thus, at this stage, it was decided that Cl atom was truly in the crystal.

In the second stage, new observed and difference syntheses, ρ_{02} , and $\Delta\rho_2$ were calculated with 2037 terms whose magnitudes were greater than 8 electrons (based on the structure factor calculation with R = 0.458). Twelve additional carbon atoms were located. The observed electron and difference densities were plotted in the vicinity of each atom to obtain better coordinates and to approximate individual temperature factors. The heights of two peaks from ρ_{01}

decreased in $\rho_{0.2}$, with two new peaks forming near the original peaks. Furthermore, the distances between the new peaks and their adjacent peaks were closer to acceptable bond lengths. Thus, the coordinates assigned to the old peaks were replaced by those of the two new peaks for the next calculation. A structure factor calculation using a new scale constant of 0.75, including the Mn atom, the Cl atom, four nitrogen atoms, and 23 carbon atoms had an R-factor of 0.385.

In the third stage of the structure determination, new difference and observed electron density maps, $\Delta \rho_3$ and ρ_{03} , including 2725 terms, were calculated from which the remaining 21 carbon atoms were found. Individual isotropic temperature factors were then assigned to each atom by comparing the peak heights and shapes in the observed and calculated density maps. A structure factor calculation including the complete molecule, except hydrogen atoms, had an R-factor of 0.235.

5. Refinement by the Method of Least Squares

Once a model of a trial structure has been proposed, it is usual to improve the preliminary coordinates of the atoms. This process is known as refinement. Of the several methods of refinement which can be used in crystal structure analysis, that of least squares was used for ClMnTPP.

The principle of least squares, applied to a structure refinement, is that the best values for a set of parameters are those which minimize the sum of the squares of the properly weighted differences between the observed and calculated structure amplitudes for all independent reflections. The quantity to be minimized can be written

$$R = \sum_{i=1}^{N} w_i (|F_0| - |F_C|)^2,$$

where N is the total number of the independent reflections, and \mathbf{w}_i is the individual weight of the observed structure factor. The weight of the reflection is defined to be the inverse of the square of the standard deviation of the corresponding observation

$$w_{i} = \frac{1}{\sigma_{i}^{2}} .$$

Usually, only relative weights can be estimated easily.

(1) Weighting Scheme

In order for the method of least squares to work best, it is necessary to have a reasonable weighting scheme applied to the observed structure factors. The weighting scheme, similar to that described by Hughes, 47 which was chosen for the refinement of ClMnTPP structure was

when
$$|F_0| \leq 15.0$$
, $\sigma = 2.0$ and when $|F_0| > 15.0$, $\sigma = 0.1 \times |F_0|$.

Thus, when $|F_0|$ was greater than 15.0, the standard deviation

of the reflection was assumed to be directly related to the magnitude of the observed structure amplitude; when less than 15.0, the error was assumed constant.

(2) The Method of Least Squares

In the least squares refinement, the parameters which are varied are the three coordinates of each atom, the overall scale constant, and the individual temperature factors. For the latter, each atom can be assumed to have an isotropic temperature correction of the form of $\exp(-B \sin^2 \theta/\lambda^2)$, or an anisotropic temperature correction in terms of six parameters which describe a thermal ellipsoid as:

$$T(hk\ell) = \exp - (\beta_{11}h^2 + \beta_{22}k^2 + \mu_{33}\ell^2 + 2\beta_{12}hk + 2\beta_{13}h\ell + 2\beta_{23}k\ell) .$$

Individual isotropic temperature factors can be converted to the anisotropic form by the relationships

$$\beta_{11} = Ba^{*2}/4$$
 , $\beta_{12} = Ba^{*} \cdot b^{*}/4$, etc

where $\ a^{*}$, b^{*} , etc are reciprocal cell constants.

The isotropic thermal parameters of the last structure factor calculation, which had an R-factor of 0.235, were converted into anisotropic parameters, and the weighting scheme described above was applied before a least squares calculation was performed using the program ORFLS.²³ After completion of one complete cycle of refinement in which

atomic coordinates and anisotropic temperature factors were varied, (atomic parameters of the 24 inner atoms were allowed to vary first followed by the atomic parameters of the outer atoms) the residual index, R, decreased to 0.173. By readjusting the scale constant from 0.75 to 0.72, the R-factor decreased further to 0.157. After another cycle of refinement in which the anisotropic temperature factors of only the Mn and Cl atoms were varied, the R-factor was 0.149. One further cycle of refinement on all parameters brought the R-factor to 0.125. At this time the bond distances and angles of the model were calculated, and were found to deviate in a significant way from those expected on the basis of other porphyrin structures.

Because of the manner in which the crystal was mounted (long direction perpendicular to the \$\phi\$-axis), the data were affected by serious absorption problem. Since this effect was only corrected in an approximate way, it was decided to apply a more nearly accurate absorption correction at this time based on a method proposed by Phillips.²⁴

(3) Phillips Absorption Correction

Generally, as a crystal rotates about the goniometer axis at the angular setting $\chi=90^{\circ}$, the intensities of an axial reflection vary as a function of the azimuthal angular setting, ϕ , for the corresponding reciprocal lattice level. By measuring the intensities of an axial reflection as a function of ϕ , a relative transmission T

(or absorption, A) curve can be obtained. The transmission and absorption coefficients of the axial reflections have the relationship:

$$A = 1/T = I_{max}(\phi_0)/I(\phi)$$

where ϕ_0 is the particular angular setting which gives the maximum intensity.

In the Phillips' absorption correction, the trans-mission coefficients for any general reflection (hk ℓ) are given approximately by the expression

$$T(hk \ell) = [T(\phi_{inc}) + T(\phi_{ref})]/2$$

where $\phi_{\mbox{inc}}$ and $\phi_{\mbox{ref}}$ are the azimuthal angles of the incident and reflected beams. Both $\phi_{\mbox{inc}}$ and $\phi_{\mbox{ref}}$ can be expressed in terms of $\phi_{\mbox{hk}\,\ell}$, the crystal setting at which the reflection plane (hk ℓ) is parallel to the incident X-ray beam, more explicitly

$$\phi_{\text{inc}} = (\phi_{\text{hk}\ell} - \epsilon_{\text{hk}\ell})$$
 , and $\phi_{\text{ref}} = (\phi_{\text{hk}\ell} + \delta_{\text{hk}\ell})$

where $\epsilon_{hk\ell}$ and $\delta_{hk\ell}$ are the angular differences between $\phi_{hk\ell}$ and the angles of the incident and diffracted beams projected on the equatorial plane. For a four-circle diffractometer, $\epsilon_{hk\ell}$ and $\delta_{hk\ell}$ are given as

$$\epsilon_{hk\ell} = \delta_{hk\ell} = \sin^{-1} (\sin \theta \cos \chi)$$

It should be pointed out that this semi-empirical method can give only the relative values for each absorption correction; the additional scale constants corresponding to

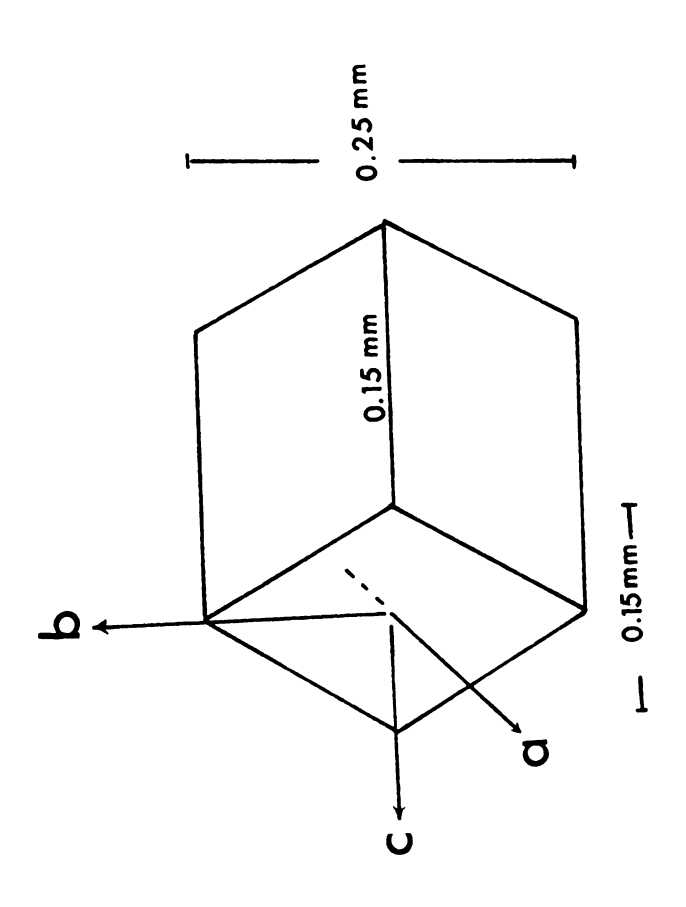
the reciprocal lattice levels must be obtained from other sources.

The absorption factor A can be obtained either by experimental observation or by calculation by evaluating the integral

$$A = \int_{V} \frac{1}{V} \exp \left[-\mu(\gamma_{\alpha} + \gamma_{\beta})\right] d\bar{V}$$

where V is the volume of the crystal, μ is its linear absorption coefficient, γ_{α} the path length along the primary beam direction, and γ_{β} that along the diffracted beam direction. This integral can be solved by numerical methods (computer program, ORABS)²⁵. Input to ORABS consists of the unit cell dimensions, the linear absorption coefficient, and the distances from the surface boundary planes to an internal reference point. The absorption curve can then be computed as a function of azimuthal angles ϕ and reciprocal lattice levels. The relative scale constants between the corresponding reciprocal lattice levels can be evaluated by considering the direction of least absorption from each absorption curve.

The dimensions of an idealized ClMnTPP crystal and the orientation of the three axes of the unit cell within the crystal are shown in Figure 6. The linear absorption coefficient of ClMnTPP is 41.0 cm⁻¹, and the six boundary planes and their distances from the center of the crystal are listed in Table 2. The calculated absorption curves were in good agreement with the observed ones in both shape



Approximate crystal geometry for computing absorption factors. Figure 6.

and magnitude, in Table 3 are listed the maximum absorption factors obtained from these observed and calculated absorption curves. The scale constants obtained on the basis of the least absorption in each absorption curve are also presented in Table 4.

Table 2. Boundary Planes and Their Distances from the Center of the Crystal.

Planes	<u>Distances (cm)</u>
100	0.0100
1 00	0.0100
111	0.0075
Ī11	0.0078
111	0.0076
īī1	0.0075

A new data reduction was computed using this new absorption correction, but no significant improvement resulted in the R-factor of the last cycle of refinement. At this stage it became increasingly more evident that the discrepancy between the observed and calculated crystal densities was probably an important factor affecting the residual index. After substracting the contribution to the crystal density due to ClMnTPP, there still remained approximately 40 a.m.u. of additional mass.

Table 3. Maximum Calculated and Observed Absorption Factors.

(A _{max}) _{ob}	(A _{max}) _{cal}
1.70	1.70
1.73	1.69
1.68	1.65
1.60	1.57
1.54	1.55
1.47	1.52
1.43	1.43
1.33	1.36
1.26	1.29
1.17	1.22
	1.70 1.73 1.68 1.60 1.54 1.47 1.43 1.33

Table 4. Scale Constants for each Reciprocal Level

Reciprocal Levels	Scale Constant
020	1.00
040	1.00
060	1.01
080	1.01
0,10,0	1.02
0,12,0	1 .03
0,14,0	1.04
0,16,0	1.06
0,18,0	1.08
0,20,0	1.11

(4) Finding the Acetone Molecule

A difference electron density (at R = 0.125) was computed and four relatively large peaks (~ 3 electron/A3) were found in the vicinity of the Cl atom and the porphyrin molecule. From an examination of the distances between peaks, the corresponding angles, and the peak electron densities, they were found to display the geometry expected of an acetone molecule. By including Mn, Cl, the TPP molecule, and an acetone molecule into the next structure factor calculation, the R-factor was 0.129. After one cycle of refinement on coordinates and anisotropic temperature factors of all the atoms, the R-factor decreased to 0.085. After one more cycle on the coordinates and the anisotropic temperature factors of Mn, Cl, and the acetone molecule, the R-factor decreased to 0.078. Since the Rfactor had improved significantly, the convergence of the least squares calculation was assumed. An attempt was now made to locate the hydrogen atoms.

(5) Finding the Hydrogen Atoms

The nomenclature of the atoms in the porphyrin molecule is shown in Figure 7. Hydrogen atoms are named corresponding to the carbon atoms to which they are bonded. A difference electron density based on the structure at an R-factor of 0.078 was calculated to see if hydrogen atoms would be observable. All hydrogen atoms were found at

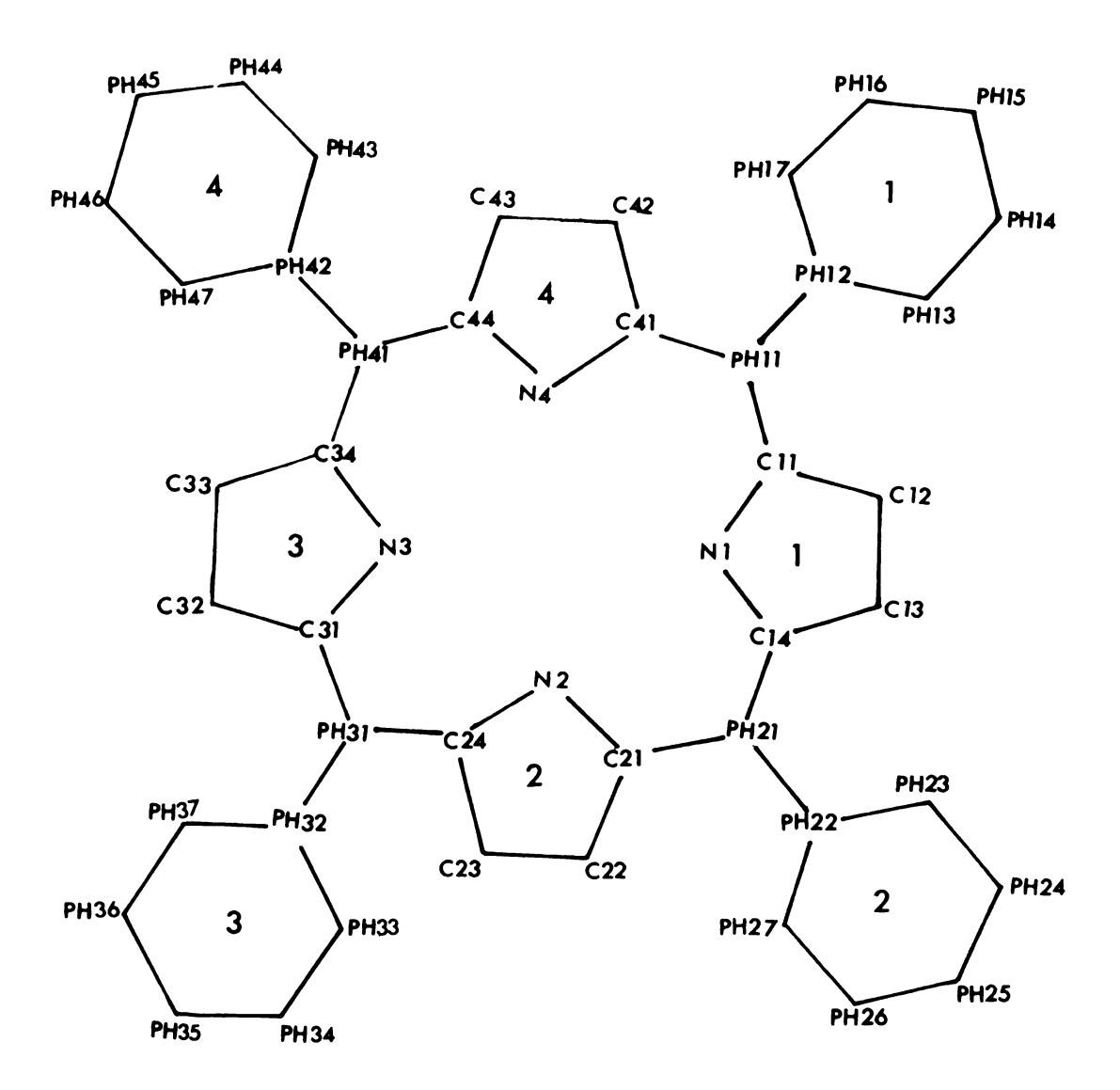


Figure 7. Porphyrin skeleton nomenclature. Numbering of phenyl and pyrrole groups is also indicated.

approximately the correct locations, but only 13 hydrogen atoms which had the better peak heights and shapes were selected to be included in the next structure factor calculation. The isotropic temperature factors of the hydrogen atoms were assumed to be approximately 20% greater than those of their adjacent carbon atoms before the former had been converted to anisotropic values. One cycle of least squares refinement in which the coordinates of all the atoms (including H) and the anisotropic temperature factors of all the atoms except the 13 hydrogen atoms were varied, decreased the R-factor to 0.072. Another difference map was calculated and it showed the remaining hydrogens much improved in peak heights and positions. These were included in calculations and the R-factor became 0.067 after one more cycle of refinement on all the coordinates and anisotropic temperature factors. Since the acetone molecule seemed to occupy the crystal lattice incompletely, a weight of 75% was applied to all of its atoms. The final structure factor calculation gave R = 0.069 and the least squares refinement was terminated at this point.

The calculated crystal density based on ClMnTPP and including a 0.75 occupancy of acetone is 1.31 $\rm g/cm^3$, while the observed density is 1.30 $\rm g/cm^3$.

IV. STRUCTURAL RESULTS

The final coordinates, anisotropic temperature factors, the mean square atomic displacement (\vec{u}^2) in the direction of each principal axis, and peak heights of all the atoms in ClMnTPP are listed in Table 5. The labeling of the atoms has already been shown in Figure 7. The coordinates, the peak heights, and the isotropic temperature factors of the hydrogen atoms are shown in Table 6. The atomic parameters of the acetone molecule are listed in Table 7.

The procedure for fitting a set of points to a plane or a line by a least squares method was described by Schomaker. The equation of a plane can be denoted as $m_1x + m_2y + m_3z = d$, where d is the distance from an origin to the fitting plane. The parameters m_1 , m_2 , m_3 , and d for the equations which best describe the individual pyrrole rings, the phenyl groups, the four inner nitrogen atoms, the sixteen-inner atoms of the porphyrin and the nuclear least squares plane (NLS) which encompasses the four pyrrole rings and four bridge carbon atoms are listed in Table 8. The dihedral angles (in degrees) between the NLS plane and those of each individual phenyl ring and the angle between the NLS plane and the line between the Mn and Cl atom are given in Table 9.

Table 5. The Final Atomic Coordinates, Thermal Parameters,

Coordinates inFractions				Anisot	ropic Te	mperature
Atom	х	У	z	۴11	^β 22	β 33
Mn	-0.4773	0.1150	0.0900	0.0067	0.0011	0.0056
Cl	0.6276	0.1673	0.2585	0.0010	0.0019	0.0061
N1	0.4000	0.0619	0.0756	0.0052	0.0013	0.0054
C11	0.2801	0.0789	0.0336	0.0093	0.0015	0.0074
C12	0.2413	0.0356	0.0695	0.0103	0.0016	0.0077
C13	0.6626	0.4926	0.3672	0.0078	0.0016	0.0081
C14	0.4342	0.0077	0.1351	0.0068	0.0015	0.0054
N2	0.6437	0.0427	0.1493	0.0067	0.0011	0.0064
C21	0.3663	0.4865	0.3183	0.0074	0.0013	0.0056
C22	0.2666	0.4461	0.2867	0.0079	0.0014	0.0065
C23	0.1951	0.4777	0.2963	0.0095	0.0013	0.0066
C24	0.7512	0.0381	0.1666	0.00 63	0.0012	0.0058
N3	0.6266	0.1595	0.0721	0.0067	0.0012	0.0053
c31	0.7493	0.1448	0.1195	0.0063	0.0016	0.0057
C32	0.7238	0.2445	0.0747	0.0089	0.0021	0.0092
C33	0.8108	0.1974	0.1222	0.0111	0.0014	0.0092
C34	0.6085	0.2211	0.0415	0.0092	0.0016	0.0066
N4	0.3738	0.3243	0.4839	0 ° 006 3	0.0013	0.0063
C41	0.2497	0.3269	0.4387	0.0069	0.0013	0.0063
C42	0.1744	0.2749	0.3665	0.0073	0.0019	0.0072
C43	0.2549	0.2397	0.3722	0.0088	0.0018	0.0060
C44	0.3810	0.2695	0.4464	0.0081	0.0014	0.0065
PH11	0.2046	0.3704	0.4644	0.0078	0.0014	0.0065
PH12	0.0727	0.3606	0.4201	0.0057	0.0017	0.0074
PH13	0.9734	0.4045	0.3491	0.0087	0.0034	0.0105
PH14	0.8479	0.3964	0.3065	0.0090	0.0052	0.0127
PH15	0.8246	0.3440	0.3352	0.0117	0.0040	0.0160
PH16	0.9247	0.3004	0.4079	0.0157	0.0037	0.0190
PH17	0.0475	0.3099	0.4512	0.0123	0.0023	0.0125
PH21	0.4586	0.4712	0.3179	0.0083	0.0009	0.0057
PH22	0.4388	0.4128	0.2605	0.0073	0.0015	0.0047
PH23	0.5304	0.3659	0.3225	0.0117	0.0012	0.0085
PH24	0.5125	0.3112	0.2694	0.0131	0.0016	0.0111
PH25	0.4037	0.3038	0.1563	0.0127	0.0019	0.0091
PH26	0.3123	0.3498	0.0952	0.0126	0.0023	0.0095
PH27	0.3307	0.4052	0.1470	0.0119	0.0022	0.0065
PH31	0.8071	0.0864	0.1575	0.0061	0.0015	0.0053
PH32	0.9326	0.0772	0.1929	0.0074	0.0013	0.0072
PH33	0.0460	0.0598	0.3016	0.0064	0.0023	0.0076
PH34	0.1642	0.0541	0.3320	0.0070	0.0028	0.0122
PH35	0.1730	0.0664	0.2579	0.0114	0.0024	0.0140
PH36	0.0611	0.0846	0.1509	0.0117	0.0021	0.0145
PH37	0.9406	0.0895	0. 1173	0.0114	0.0021	0.0093

and Peak Heights of MnClTPP.

$\begin{array}{c ccccccccccccccccccccccccccccccccccc$	Parame	ters		Displa	quare A cements	\star (\mathbf{A}^2)	Peak Height (e/X3)
0.0003 0.0057 -0.0004 2.59 3.89 4.59 19.9 0.0006 0.0037 0.0003 1.57 2.82 3.25 7.1 0.0002 0.0071 0.0002 2.91 3.03 4.54 5.5 -0.0000 0.0062 -0.0000 2.53 3.13 4.54 5.5 -0.0003 0.0049 -0.0001 1.97 2.73 3.22 5.5 -0.0004 0.0051 -0.0007 1.87 2.56 3.62 5.9 -0.0004 0.0051 -0.0007 1.87 2.56 3.62 5.9 -0.0007 0.0059 -0.0007 1.87 2.56 3.62 5.9 -0.0004 0.0061 -0.0003 2.39 3.09 4.07 5.3 0.0002 0.0044 -0.0002 2.05 2.67 3.45 6.2 0.0003 0.0046 0.0004 1.97 2.26 3.25 7.6 0.0003 0.0048 -0	β12	β13	β23	$8\pi^2\bar{\mathbf{u}_1^2}$	$8\pi^2\bar{\mathbf{u}}_{2}^2$	$8\pi^2\bar{\mathbf{u}}_3^2$	ρο
0.0006 0.0039 0.0003 1.57 2.82 3.25 7.1 0.0000 0.0071 0.0002 2.91 3.03 4.54 5.5 -0.0000 0.0062 -0.0000 2.53 3.13 4.54 5.3 -0.0003 0.0049 -0.0001 1.97 2.73 3.22 5.5 -0.0004 0.0051 -0.0001 1.85 2.12 3.68 7.0 -0.0007 0.0059 -0.0002 1.72 3.03 3.89 5.4 -0.0004 0.0061 -0.0003 2.39 3.09 4.07 5.3 -0.0004 0.0061 -0.0002 2.05 2.67 3.45 6.2 0.0003 0.0044 -0.0002 2.05 2.67 3.45 6.2 0.0003 0.0048 -0.0000 1.92 2.94 3.25 6.0 0.0004 0.0071 0.0082 2.00 3.65 5.76 5.3 0.0003 0.0081 0.0							
0.0000 0.0070 0.0001 2.25 2.85 4.36 6.1 0.0002 0.0071 0.0002 2.91 3.03 4.54 5.5 -0.0000 0.0062 -0.0000 2.53 3.13 4.54 5.5 -0.0000 0.0051 -0.0001 1.87 2.73 3.22 5.5 -0.0007 0.0051 -0.0007 1.87 2.56 3.68 7.0 -0.0007 0.0059 -0.0002 1.72 3.03 3.89 5.4 -0.0004 0.0051 -0.0003 2.39 3.09 4.07 5.3 0.0002 0.0044 -0.0002 2.05 2.67 3.45 6.2 0.0003 0.0046 -0.0002 2.05 2.67 3.45 6.2 0.0000 0.0048 -0.0000 1.92 2.94 3.25 6.0 0.0004 0.0071 0.0008 2.70 3.65 5.76 5.3 -0.0005 0.0062 0.0							
0.0002 0.0071 0.0002 2.91 3.03 4.54 5.5 -0.0000 0.0062 -0.0000 2.53 3.13 4.54 5.3 -0.0000 0.0051 -0.0001 1.87 2.73 3.22 5.5 -0.0004 0.0051 -0.0007 1.87 2.56 3.62 5.9 -0.0004 0.0061 -0.0002 1.72 3.03 3.89 5.4 -0.0004 0.0061 -0.0003 2.99 3.09 4.07 5.3 0.0002 0.0044 -0.0002 2.05 2.67 3.45 6.2 0.0003 0.0046 0.0004 1.97 2.26 3.25 7.6 0.0004 0.0071 0.0008 2.70 3.65 5.76 5.3 0.0004 0.0071 0.0008 2.70 3.65 5.76 5.3 0.0005 0.0062 0.0005 2.59 2.85 4.18 5.8 0.0004 0.0049 -0.000							
$\begin{array}{cccccccccccccccccccccccccccccccccccc$							
$\begin{array}{cccccccccccccccccccccccccccccccccccc$							
$\begin{array}{cccccccccccccccccccccccccccccccccccc$							
-0.0004							
-0.0007 0.0059 -0.0002 1.72 3.03 3.89 5.4 -0.0004 0.0061 -0.0003 2.39 3.09 4.07 5.3 0.0002 0.0044 -0.0002 2.05 2.67 3.45 6.2 0.0003 0.0046 0.0004 1.97 2.26 3.25 7.6 0.0000 0.0048 -0.0000 1.92 2.94 3.25 6.0 0.0004 0.0071 0.0008 2.70 3.65 5.76 5.3 -0.0003 0.0081 0.0004 2.10 3.82 5.30 5.5 0.0005 0.0062 0.0005 2.59 2.85 4.18 5.8 -0.0004 0.0079 -0.0002 1.87 2.70 3.68 6.6 -0.0004 0.0050 0.0061 1.78 3.10 3.65 5.7 -0.0009 0.0049 -0.0009 2.39 3.75 5.01 5.2 -0.0007 0.0055 -0.0006 2.82 3.00 4.18 5.5 -0.0009 0.0059 -0.0006 1.94 2.56 4.10 5.8 0.0001 0.0055 0.0003 2.31 2.97 4.25 6.6 -0.0008 0.0046 -0.0011 1.92 2.79 5.34 5.7 -0.0009 0.0072 0.0003 3.00 6.37 6.59 4.7 -0.0002 0.0072 0.0000 3.00 6.37 6.59 4.7 -0.0002 0.0077 -0.0001 3.16 8.19 9.78 4.1 -0.0022 0.0111 -0.0005 2.33 8.55 9.73 4.1 -0.0017 0.0154 -0.0006 2.23 7.44 10.87 4.1 -0.0007 0.0154 -0.0006 2.23 7.44 10.87 4.1 -0.0007 0.0154 -0.0006 2.23 7.44 10.87 4.1 -0.0002 0.0054 -0.0001 1.75 2.53 3.51 6.3 -0.0004 0.0045 -0.0002 2.97 5.01 7.11 4.8 -0.0002 0.0054 -0.0001 1.75 2.53 3.51 6.3 -0.0004 0.0045 -0.0002 2.97 5.01 7.11 4.8 -0.0002 0.0082 -0.0003 2.20 3.00 5.17 6.5 -0.0000 0.0100 -0.0002 2.94 3.42 6.41 5.3 -0.0000 0.0100 -0.0002 2.94 3.42 6.41 5.3 -0.0000 0.0000 0.0000 2.53 4.44 5.01 5.2 -0.0000 0.0000 0.0000 2.53 4.44 5.01 5.2 -0.0000 0.0000 0.0000 2.53 4.44 5.01 5.2 -0.0000 0.0000 0.0000 2.53 4.44 5.01 5.2 -0.0000 0.0000 0.0000 2.53 4.44 5.01 5.2 -0.0000 0.0000 0.0000 2.50 5.17 6.5 -0.0000 0.0000 0.0000 2.50 5.34 5.38 6.64 4.7 -0.0000 0.0000 0.0000 2.50 5.34 5.38 6.64 4.7 -0.0000 0.0000 0.0000 2.50 5.34 5.38 6.64 4.7 -0.0000 0.0000 0.0000 2.50 5.34 5.38 6.64 -0.0000 0.0000 0.0000 2.50 5.34 5.38 6.64 -0.0000 0.0000 0.0000 2.50 5.34 5.38 6.64 -0.0000 0.0000 0.0000 2.50 5.34 5.38 6.64 -0.0000 0.0000 0.0000 2.50 5.34 5.38 6.64 -0.0000 0.0000 0.0000 2.50 5.34 5.34 5.38 -0.0000 0.0000 0.0000 0.0000 2.50 5.34 5.34 5.38 -0.00000 0.0000 0.0000 2.50 5.34 5.34 5.38 -0.00000 0.0000 0.0000 0							
-0.0004							
0.0002 0.0044 -0.0002 2.05 2.67 3.45 6.2 0.0003 0.0046 0.0004 1.97 2.26 3.25 7.6 0.0004 0.0071 0.0008 2.70 3.65 5.76 5.3 -0.0003 0.0081 0.0004 2.10 3.82 5.30 5.5 0.0005 0.0062 0.0005 2.59 2.85 4.18 5.8 -0.0004 0.0049 -0.0002 1.87 2.70 3.68 6.6 -0.0004 0.0050 0.0001 1.78 3.10 3.65 5.7 -0.0009 0.0049 -0.0009 2.39 3.75 5.01 5.2 -0.0007 0.0055 -0.0006 2.82 3.00 4.18 5.5 -0.0009 0.0059 -0.0006 1.94 2.56 4.10 5.8 0.0001 0.0055 0.0003 2.31 2.97 5.34 5.7 0.0002 0.0072 0.0000							
0.0003 0.0046 0.0004 1.97 2.26 3.25 7.6 0.0000 0.0048 -0.0000 1.92 2.94 3.25 6.0 0.0004 0.0071 0.0008 2.70 3.65 5.76 5.3 -0.0003 0.0081 0.0004 2.10 3.82 5.30 5.5 0.0005 0.0062 0.0005 2.59 2.85 4.18 5.8 -0.0004 0.0050 0.0001 1.78 3.10 3.65 5.7 -0.0004 0.0050 0.0001 1.78 3.10 3.65 5.7 -0.0007 0.0055 -0.0006 2.82 3.00 4.18 5.5 -0.0009 0.0059 -0.0006 2.82 3.00 4.18 5.5 -0.0009 0.0059 -0.0006 1.94 2.56 4.10 5.8 0.0001 0.0055 0.0003 2.31 2.97 4.25 6.6 -0.0008 0.0072 0.0000							
$\begin{array}{cccccccccccccccccccccccccccccccccccc$							
$\begin{array}{cccccccccccccccccccccccccccccccccccc$							
-0.0003							
0.0005 0.0062 0.0005 2.59 2.85 4.18 5.8 -0.0004 0.0049 -0.0002 1.87 2.70 3.68 6.6 -0.0004 0.0050 0.0001 1.78 3.10 3.65 5.7 -0.0009 0.0049 -0.0009 2.39 3.75 5.01 5.2 -0.0007 0.0055 -0.0006 2.82 3.00 4.18 5.5 -0.0009 0.0059 -0.0006 1.94 2.56 4.10 5.8 0.0001 0.0055 0.0003 2.31 2.97 4.25 6.6 -0.0008 0.0046 -0.0011 1.92 2.79 5.34 5.7 0.0002 0.0072 0.0000 3.00 6.37 6.59 4.7 -0.0003 0.0077 -0.0001 3.16 8.19 9.78 4.1 -0.0017 0.0154 -0.0006 2.23 7.44 10.87 4.1 -0.0007 0.0100 -0.0000 2.97 5.01 7.11 4.8 -0.0004 0.0045							
-0.0004 0.0049 -0.0002 1.87 2.70 3.68 6.6 -0.0004 0.0050 0.0001 1.78 3.10 3.65 5.7 -0.0009 0.0049 -0.0009 2.39 3.75 5.01 5.2 -0.0007 0.0055 -0.0006 2.82 3.00 4.18 5.5 -0.0009 0.0059 -0.0006 1.94 2.56 4.10 5.8 0.0001 0.0055 0.0003 2.31 2.97 4.25 6.6 -0.0008 0.0046 -0.0011 1.92 2.79 5.34 5.7 0.0002 0.0072 0.0000 3.00 6.37 6.59 4.7 -0.0003 0.0077 -0.0001 3.16 8.19 9.78 4.1 -0.0022 0.0111 -0.0005 2.33 8.55 9.73 4.1 -0.0017 0.0154 -0.0006 2.23 7.44 10.87 4.1 -0.0007 0.0100 -0.0000 2.97 5.01 7.11 4.8 -0.0002 0.0054 -0.0001 1.75 2.53 3.51 6.3 -0.0004 0.0045 -0.0002 2.23 2.61 3.35 6.3 -0.0004 0.0045 -0.0002 2.23 2.61 3.35 6.3 -0.0002 0.0082 -0.0003 2.20 3.00 5.17 6.5 -0.0000 0.0100 -0.0002 2.94 3.42 6.41 5.3 -0.0005 0.0082 -0.0003 2.20 3.00 5.17 6.5 -0.0006 0.0075 -0.0013 3.45 5.38 6.64 4.7 -0.0003 0.0070 -0.0006 2.53 4.44 5.01 5.2 0.0002 0.0044 0.0045 -0.0002 2.94 3.42 6.41 5.3 -0.0005 0.0082 -0.0008 3.13 4.55 5.63 5.2 -0.0006 0.0075 -0.0013 3.45 5.38 6.64 4.7 -0.0003 0.0070 -0.0006 2.53 4.44 5.01 5.2 0.0002 0.0044 0.0002 2.10 2.76 3.19 6.2 0.0001 0.0059 -0.0000 2.10 2.56 5.18 5.8 0.0007 0.0042 0.0004 2.42 4.55 5.76 5.1 0.0007 0.0042 0.0004 2.42 4.55 5.76 5.1 0.0007 0.0058 0.0001 2.56 5.34 9.13 4.7 -0.0000 0.0101 -0.0001 3.38 4.55 8.24 4.7 -0.0000 0.0101 -0.0001 2.56 5.34 9.13 4.7 -0.0000 0.0101 -0.0001 2.56 5.34 9.13 4.7							
-0.0004 0.0050 0.0001 1.78 3.10 3.65 5.7 -0.0009 0.0049 -0.0009 2.39 3.75 5.01 5.2 -0.0007 0.0055 -0.0006 2.82 3.00 4.18 5.5 -0.0009 0.0059 -0.0006 1.94 2.56 4.10 5.8 0.0001 0.0055 0.0003 2.31 2.97 4.25 6.6 -0.0008 0.0046 -0.0011 1.92 2.79 5.34 5.7 0.0002 0.0072 0.0000 3.00 6.37 6.59 4.7 -0.0003 0.0077 -0.0001 3.16 8.19 9.78 4.1 -0.0022 0.0111 -0.0005 2.33 8.55 9.73 4.1 -0.0017 0.0154 -0.0006 2.23 7.44 10.87 4.1 -0.0007 0.0100 -0.0000 2.97 5.01 7.11 4.8 -0.0002 0.0054 -0.0001 1.75 2.53 3.51 6.3 -0.0004 0.0045 -0.0002 2.23 2.61 3.35 6.3 -0.0004 0.0045 -0.0002 2.23 2.61 3.35 6.3 -0.0002 0.0082 -0.0003 2.20 3.00 5.17 6.5 -0.0000 0.0100 -0.0002 2.94 3.42 6.41 5.3 -0.0005 0.0082 -0.0003 3.13 4.55 5.63 5.2 -0.0006 0.0075 -0.0013 3.45 5.38 6.64 4.7 -0.0003 0.0070 -0.0006 2.53 4.44 5.01 5.2 0.0002 0.0044 0.0002 2.10 2.76 3.19 6.2 0.0001 0.0059 -0.0000 2.10 2.56 5.18 5.8 0.0007 0.0042 0.0042 0.0004 2.42 4.55 5.76 5.1 0.0007 0.0058 0.0001 2.56 5.34 9.13 4.7 -0.0000 0.0101 -0.0001 3.38 4.55 8.24 4.7 -0.0000 0.0101 -0.0001 3.38 4.55 8.24 4.7 -0.0000 0.0101 -0.0001 3.38 4.55 8.24 4.7 -0.0000 0.0101 -0.0001 3.38 4.55 8.24 4.7 -0.0001 0.0110 -0.0004 2.76 4.03 8.39 4.9							
-0.0009							
-0.0007 0.0055 -0.0006 2.82 3.00 4.18 5.5 -0.0009 0.0059 -0.0006 1.94 2.56 4.10 5.8 0.0001 0.0055 0.0003 2.31 2.97 4.25 6.6 -0.0008 0.0046 -0.0011 1.92 2.79 5.34 5.7 0.0002 0.0072 0.0000 3.00 6.37 6.59 4.7 -0.0003 0.0077 -0.0001 3.16 8.19 9.78 4.1 -0.0022 0.0111 -0.0005 2.33 8.55 9.73 4.1 -0.0017 0.0154 -0.0006 2.23 7.44 10.87 4.1 -0.0007 0.0100 -0.0000 2.97 5.01 7.11 4.8 -0.0002 0.0054 -0.0001 1.75 2.53 3.51 6.3 -0.0004 0.0045 -0.0002 2.23 2.61 3.35 6.3 -0.0005 0.0082 -0.0002 2.94 3.42 6.41 5.3 -0.0005 0.0							
-0.0009 0.0059 -0.0006 1.94 2.56 4.10 5.8 0.0001 0.0055 0.0003 2.31 2.97 4.25 6.6 -0.0008 0.0046 -0.0011 1.92 2.79 5.34 5.7 0.0002 0.0072 0.0000 3.00 6.37 6.59 4.7 -0.0003 0.0077 -0.0001 3.16 8.19 9.78 4.1 -0.0022 0.0111 -0.0005 2.33 8.55 9.73 4.1 -0.0017 0.0154 -0.0006 2.23 7.44 10.87 4.1 -0.0007 0.0100 -0.0000 2.97 5.01 7.11 4.8 -0.0002 0.0054 -0.0001 1.75 2.53 3.51 6.3 -0.0004 0.0045 -0.0002 2.23 2.61 3.35 6.3 -0.0002 0.0082 -0.0003 2.20 3.00 5.17 6.5 -0.0005 0.0082 -0.0008 3.13 4.55 5.63 5.2 -0.0006 0.0							
$\begin{array}{cccccccccccccccccccccccccccccccccccc$							
-0.0008 0.0046 -0.0011 1.92 2.79 5.34 5.7 0.0002 0.0072 0.0000 3.00 6.37 6.59 4.7 -0.0003 0.0077 -0.0001 3.16 8.19 9.78 4.1 -0.0022 0.0111 -0.0005 2.33 8.55 9.73 4.1 -0.0017 0.0154 -0.0006 2.23 7.44 10.87 4.1 -0.0007 0.0100 -0.0000 2.97 5.01 7.11 4.8 -0.0002 0.0054 -0.0001 1.75 2.53 3.51 6.3 -0.0004 0.0045 -0.0002 2.23 2.61 3.35 6.3 -0.0002 0.0082 -0.0003 2.20 3.00 5.17 6.5 -0.0005 0.0082 -0.0008 3.13 4.55 5.63 5.2 -0.0006 0.0075 -0.0013 3.45 5.38 6.64 4.7 -0.0003 0.0070 -0.0006 2.53 4.44 5.01 5.2 0.0007 0.							
$\begin{array}{cccccccccccccccccccccccccccccccccccc$							
$\begin{array}{cccccccccccccccccccccccccccccccccccc$							
-0.0022 0.0111 -0.0005 2.33 8.55 9.73 4.1 -0.0017 0.0154 -0.0006 2.23 7.44 10.87 4.1 -0.0007 0.0100 -0.0000 2.97 5.01 7.11 4.8 -0.0002 0.0054 -0.0001 1.75 2.53 3.51 6.3 -0.0004 0.0045 -0.0002 2.23 2.61 3.35 6.3 -0.0002 0.0082 -0.0003 2.20 3.00 5.17 6.5 -0.0000 0.0100 -0.0002 2.94 3.42 6.41 5.3 -0.0005 0.0082 -0.0008 3.13 4.55 5.63 5.2 -0.0006 0.0075 -0.0013 3.45 5.38 6.64 4.7 -0.0003 0.0070 -0.0006 2.53 4.44 5.01 5.2 0.0002 0.0044 0.0002 2.10 2.76 3.19 6.2 0.0001 0.0059 -0.0000 2.10 2.56 5.18 5.8 0.0007 0.0042 0.0004 2.42 4.55 5.76 5.1 0.0007 0.0058 0.0001 2.56 5.34 9.13 4.7 -0.0000 0.0101 -0.0001 3.38 4.55 8.24 4.7 -0.0001 0.0110 -0.0004 2.76 4.03 8.39 4.9							
-0.0017 0.0154 -0.0006 2.23 7.44 10.87 4.1 -0.0007 0.0100 -0.0000 2.97 5.01 7.11 4.8 -0.0002 0.0054 -0.0001 1.75 2.53 3.51 6.3 -0.0004 0.0045 -0.0002 2.23 2.61 3.35 6.3 -0.0002 0.0082 -0.0003 2.20 3.00 5.17 6.5 -0.0000 0.0100 -0.0002 2.94 3.42 6.41 5.3 -0.0005 0.0082 -0.0008 3.13 4.55 5.63 5.2 -0.0006 0.0075 -0.0013 3.45 5.38 6.64 4.7 -0.0003 0.0070 -0.0006 2.53 4.44 5.01 5.2 0.0002 0.0044 0.0002 2.10 2.76 3.19 6.2 0.0001 0.0059 -0.0000 2.10 2.56 5.18 5.8 0.0007 0.0042 0.0004 2.42 4.55 5.76 5.1 0.0007 0.0058 0.0001 2.56 5.34 9.13 4.7 -0.0000 0.0101 -0.0001 3.38 4.55 8.24 4.7 -0.0001 0.0110 -0.0004 2.76 4.03 8.39 4.9							
-0.0007 0.0100 -0.0000 2.97 5.01 7.11 4.8 -0.0002 0.0054 -0.0001 1.75 2.53 3.51 6.3 -0.0004 0.0045 -0.0002 2.23 2.61 3.35 6.3 -0.0002 0.0082 -0.0003 2.20 3.00 5.17 6.5 -0.0000 0.0100 -0.0002 2.94 3.42 6.41 5.3 -0.0005 0.0082 -0.0008 3.13 4.55 5.63 5.2 -0.0006 0.0075 -0.0013 3.45 5.38 6.64 4.7 -0.0003 0.0070 -0.0006 2.53 4.44 5.01 5.2 0.0002 0.0044 0.0002 2.10 2.76 3.19 6.2 0.0007 0.0042 0.0004 2.42 4.55 5.76 5.1 0.0007 0.0058 0.0001 2.56 5.34 9.13 4.7 -0.0000 0.0101 -0.0001 3.38 4.55 8.24 4.7 -0.0001 0.0110							
-0.0002 0.0054 -0.0001 1.75 2.53 3.51 6.3 -0.0004 0.0045 -0.0002 2.23 2.61 3.35 6.3 -0.0002 0.0082 -0.0003 2.20 3.00 5.17 6.5 -0.0000 0.0100 -0.0002 2.94 3.42 6.41 5.3 -0.0005 0.0082 -0.0008 3.13 4.55 5.63 5.2 -0.0006 0.0075 -0.0013 3.45 5.38 6.64 4.7 -0.0003 0.0070 -0.0006 2.53 4.44 5.01 5.2 0.0002 0.0044 0.0002 2.10 2.76 3.19 6.2 0.0007 0.0042 0.0004 2.42 4.55 5.76 5.1 0.0007 0.0058 0.0001 2.56 5.34 9.13 4.7 -0.0000 0.0101 -0.0001 3.38 4.55 8.24 4.7 -0.0001 0.0110 -0.0004 2.76 4.03 8.39 4.9							
-0.0004 0.0045 -0.0002 2.23 2.61 3.35 6.3 -0.0002 0.0082 -0.0003 2.20 3.00 5.17 6.5 -0.0000 0.0100 -0.0002 2.94 3.42 6.41 5.3 -0.0005 0.0082 -0.0008 3.13 4.55 5.63 5.2 -0.0006 0.0075 -0.0013 3.45 5.38 6.64 4.7 -0.0003 0.0070 -0.0006 2.53 4.44 5.01 5.2 0.0002 0.0044 0.0002 2.10 2.76 3.19 6.2 0.0001 0.0059 -0.0000 2.10 2.56 5.18 5.8 0.0007 0.0042 0.0004 2.42 4.55 5.76 5.1 0.0007 0.0058 0.0001 2.56 5.34 9.13 4.7 -0.0000 0.0101 -0.0001 3.38 4.55 8.24 4.7 -0.0001 0.0110 -0.0004 2.76 4.03 8.39 4.9							
-0.0002 0.0082 -0.0003 2.20 3.00 5.17 6.5 -0.0000 0.0100 -0.0002 2.94 3.42 6.41 5.3 -0.0005 0.0082 -0.0008 3.13 4.55 5.63 5.2 -0.0006 0.0075 -0.0013 3.45 5.38 6.64 4.7 -0.0003 0.0070 -0.0006 2.53 4.44 5.01 5.2 0.0002 0.0044 0.0002 2.10 2.76 3.19 6.2 0.0001 0.0059 -0.0000 2.10 2.56 5.18 5.8 0.0007 0.0042 0.0004 2.42 4.55 5.76 5.1 0.0007 0.0058 0.0001 2.56 5.34 9.13 4.7 -0.0000 0.0101 -0.0001 3.38 4.55 8.24 4.7 -0.0001 0.0110 -0.0004 2.76 4.03 8.39 4.9							
-0.0000 0.0100 -0.0002 2.94 3.42 6.41 5.3 -0.0005 0.0082 -0.0008 3.13 4.55 5.63 5.2 -0.0006 0.0075 -0.0013 3.45 5.38 6.64 4.7 -0.0003 0.0070 -0.0006 2.53 4.44 5.01 5.2 0.0002 0.0044 0.0002 2.10 2.76 3.19 6.2 0.0001 0.0059 -0.0000 2.10 2.56 5.18 5.8 0.0007 0.0042 0.0004 2.42 4.55 5.76 5.1 0.0007 0.0058 0.0001 2.56 5.34 9.13 4.7 -0.0000 0.0101 -0.0001 3.38 4.55 8.24 4.7 -0.0001 0.0110 -0.0004 2.76 4.03 8.39 4.9							
-0.0005 0.0082 -0.0008 3.13 4.55 5.63 5.2 -0.0006 0.0075 -0.0013 3.45 5.38 6.64 4.7 -0.0003 0.0070 -0.0006 2.53 4.44 5.01 5.2 0.0002 0.0044 0.0002 2.10 2.76 3.19 6.2 0.0001 0.0059 -0.0000 2.10 2.56 5.18 5.8 0.0007 0.0042 0.0004 2.42 4.55 5.76 5.1 0.0007 0.0058 0.0001 2.56 5.34 9.13 4.7 -0.0000 0.0101 -0.0001 3.38 4.55 8.24 4.7 -0.0001 0.0110 -0.0004 2.76 4.03 8.39 4.9							
-0.0006 0.0075 -0.0013 3.45 5.38 6.64 4.7 -0.0003 0.0070 -0.0006 2.53 4.44 5.01 5.2 0.0002 0.0044 0.0002 2.10 2.76 3.19 6.2 0.0001 0.0059 -0.0000 2.10 2.56 5.18 5.8 0.0007 0.0042 0.0004 2.42 4.55 5.76 5.1 0.0007 0.0058 0.0001 2.56 5.34 9.13 4.7 -0.0000 0.0101 -0.0001 3.38 4.55 8.24 4.7 -0.0001 0.0110 -0.0004 2.76 4.03 8.39 4.9							
-0.0003 0.0070 -0.0006 2.53 4.44 5.01 5.2 0.0002 0.0044 0.0002 2.10 2.76 3.19 6.2 0.0001 0.0059 -0.0000 2.10 2.56 5.18 5.8 0.0007 0.0042 0.0004 2.42 4.55 5.76 5.1 0.0007 0.0058 0.0001 2.56 5.34 9.13 4.7 -0.0000 0.0101 -0.0001 3.38 4.55 8.24 4.7 -0.0001 0.0110 -0.0004 2.76 4.03 8.39 4.9							
0.0002 0.0044 0.0002 2.10 2.76 3.19 6.2 0.0001 0.0059 -0.0000 2.10 2.56 5.18 5.8 0.0007 0.0042 0.0004 2.42 4.55 5.76 5.1 0.0007 0.0058 0.0001 2.56 5.34 9.13 4.7 -0.0000 0.0101 -0.0001 3.38 4.55 8.24 4.7 -0.0001 0.0110 -0.0004 2.76 4.03 8.39 4.9							
0.0001 0.0059 -0.0000 2.10 2.56 5.18 5.8 0.0007 0.0042 0.0004 2.42 4.55 5.76 5.1 0.0007 0.0058 0.0001 2.56 5.34 9.13 4.7 -0.0000 0.0101 -0.0001 3.38 4.55 8.24 4.7 -0.0001 0.0110 -0.0004 2.76 4.03 8.39 4.9							
0.0007 0.0042 0.0004 2.42 4.55 5.76 5.1 0.0007 0.0058 0.0001 2.56 5.34 9.13 4.7 -0.0000 0.0101 -0.0001 3.38 4.55 8.24 4.7 -0.0001 0.0110 -0.0004 2.76 4.03 8.39 4.9							
0.0007 0.0058 0.0001 2.56 5.34 9.13 4.7 -0.0000 0.0101 -0.0001 3.38 4.55 8.24 4.7 -0.0001 0.0110 -0.0004 2.76 4.03 8.39 4.9							
$\begin{array}{cccccccccccccccccccccccccccccccccccc$							
-0.0001 0.0110 -0.0004 2.76 4.03 8.39 4.9							
	-0.0001	0.0110	-0.0004	2.88	3.96	5.59	4.7

Table 5. Continued.

	Coordinates in Fractions			Anisot	ropic Te	emperature
Atom	х	У	Z	β11	β22	β33
PH41 PH42 PH43 PH44 PH45 PH46 PH47	0.4927 0.4930 0.4717 0.4901 0.5244 0.5412 0.5238	0.2457 0.1810 0.1680 0.1085 0.0636 0.4254 0.3650	0.4808 0.4509 0.3612 0.3432 0.4146 0.0041 0.0233	0.0095 0.0091 0.0250 0.0232 0.0089 0.0198 0.0184	0.0015 0.0017 0.0021 0.0034 0.0046 0.0025 0.0011	0.0080 0.0090 0.0158 0.0161 0.0152 0.0128 0.0089
$\sigma x 10^4$	0.9-10	0.3-5	9-8 .0	0.3 - 64	1 - 9	1 - 45

 $^{^{*}}$ In the direction of each principal axis.

Parame	ters			quare A		Peak Height <u>(e/A³)</u>
β12	β13	β 23	$8\pi^2 \bar{u}_{1}^2$	$8\pi^2\bar{u}_2^2$	$8\pi^2\bar{u}_3^2$	ρo
-0.0007 -0.0015 -0.0036 -0.0044 -0.0002 -0.0013 -0.0013	0.0075 0.0073 0.0175 0.0168 0.0083 0.0068 0.0070	-0.0006 -0.0019 -0.0040 -0.0032 -0.0037 0.0003 -0.0002	2.02 1.92 1.38 3.72 2.45 4.36 1.82	2.70 2.67 4.97 4.62 4.86 6.41 5.05	4.90 6.37 12.50 12.70 14.80 15.99 11.28	5.9 5.5 4.6 4.4 4.5 3.7 4.9
	= '	_			-	

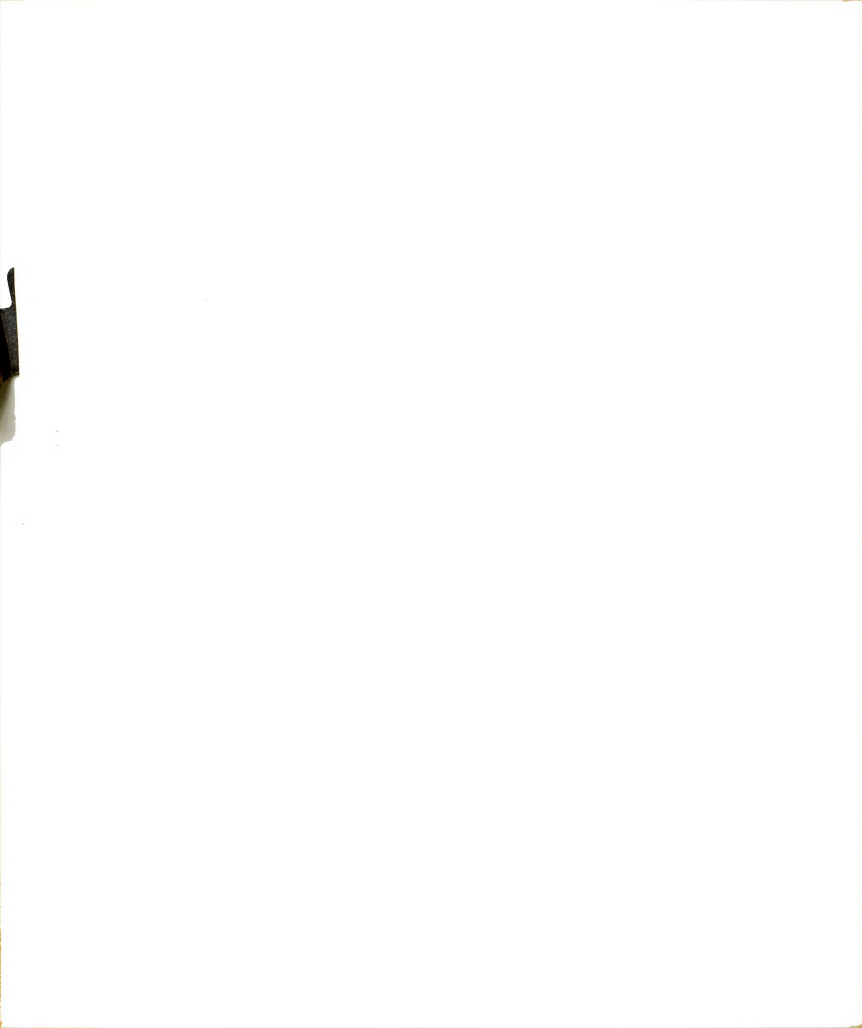


Table 6. Coordinates, Isotropic Temperature Factors, and Peak Heights of the Hydrogen Atoms.

Atom	×	У	z	В	Peak Heights e/A ³
HC12	0.1460	0.0419	0.0461	5.0	0.4
HC13	0.6644	0.4472	0.3372	4 。6	0.4
HC22	0.2521	0.4055	0.2724	4.1	0.5
HC23	0.1339	0.4528	0.2940	4.3	0.4
HC32	0.8952	0.1971	0.1435	5.4	0.5
HC33	0 .73 06	0.2926	0.0662	5.4	0.4
HC42	0.0663	0.2663	0.3201	4.2	0.5
HC43	0.2319	0.1957	0.3274	4.3	0.5
HPH13	0.9900	0.4520	0.3388	6.3	0.4
HPH14	0.7801	0.4309	0.2810	7.7	0.3
HPH15	0.7495	0.3310	0.3030	7.3	0.3
HPH16	0.9145	0.2574	0.4471	10.4	0.5
HPH17	0.1045	0.2772	0.4941	6.8	0.5
HPH23	0.6089	0.3745	0.3935	5 . 2	0.4
HPH24	0.5867	0.2796	0.3119	6.4	0.4
нрн25	0.4036	0.2602	0.1263	8.3	0.5
нрн26	0.2275	0.3440	0.0002	6.0	0 $^{\circ}4$
HPH27	0.2656	0.4466	0.0937	5 .3	0.5
HPH33	0.0347	0.0476	0.3632	4 。2	0.6
HPH34	0.2588	0.0500	0.4203	5 . 7	0.5
нрн35	0.2658	0.0548	0.2839	7.2	0.3
нрн36	0.0577	0.1032	0.0888	7.4	0 。5
HPH37	0.8660	0.0994	0.0365	5.9	0.5
нрн43	0.4000	0.2000	0.2830	10.6	0.3
нрн44	0.4332	0.1167	0.2667	10.9	0.3
нрн45	0.5373	0.0242	0.3870	8.0	0.3
нрн46	0.5297	0.3564	0.0944	8.4	0.4
HPH47	0.5827	0.4534	0.0673	5.8	0.3

Table 7. Atomic Parameters of the Acetone Molecule.

Atom	×	У	z	β11	β22	βзз	β12
01	0.8601	0.0380	0.5021	0.0285	0.0050	0.0212	0.0015
C2	0.9001	0.0860	0.5075	0.0152	0.0020	0.0105	0.0025
C3	0.9576	0.1030	0.4626	0.0192	0.0092	0.0113	0.0054
C4	0.9120	0.3621	0.0686	0.0320	0.0067	0.0110	-0.0096
σx10⁴	18-54	8 - 30	3 - 30	8 - 14	1 - 27	11-16	1 - 16

Atom	β13	β 23	$8\pi^2 \overline{\mathrm{u}}_{1}^2$	$8\pi^2\bar{\mathbf{u}}_{2}^2$	$8\pi^2\bar{\mathrm{u}}_3^2$	Peak Height e/83
01	0.0139	0.0016	8.44	11.95	18.27	3.0
C2	-0.0013	0.0027	0.81	6.28	23.89	3.3
C3	0.0133	0.0028	2.02	6.41	19.43	2.8
C4	0.0121	-0.0013	3.65	5.97	25.83	2.6
0×104	3 - 40	4 - 16				

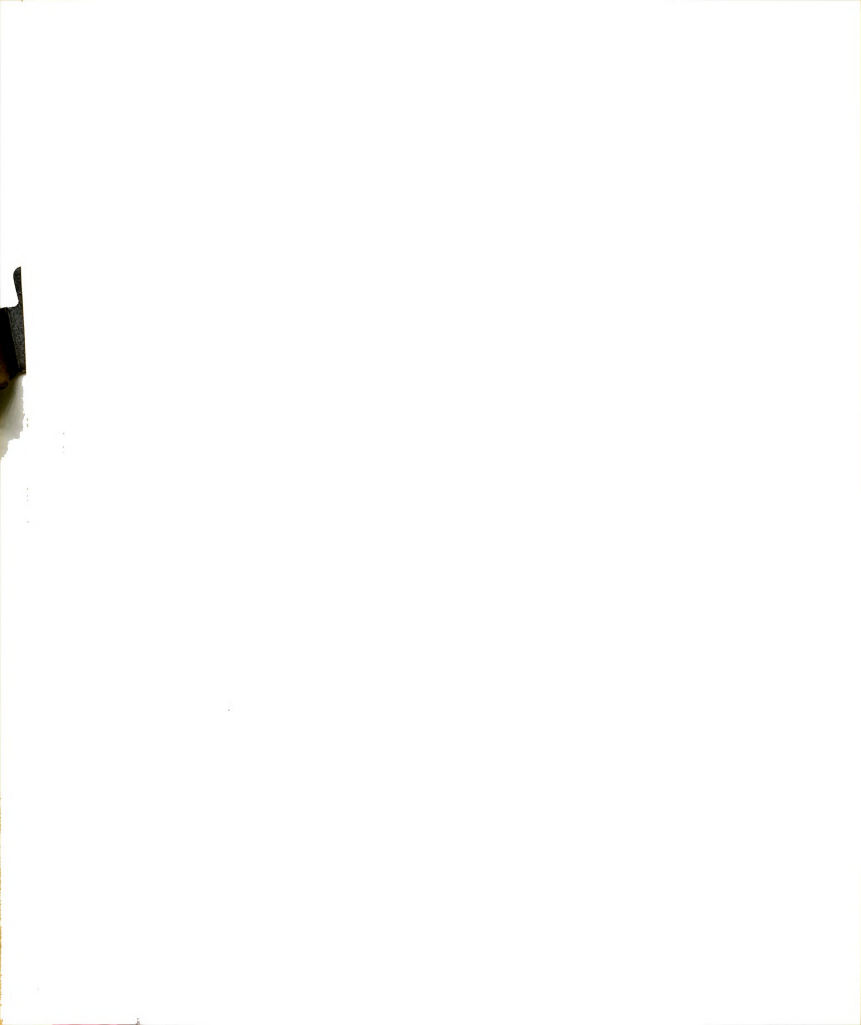


Table 8. Parameters for the Equation, $m_1x + m_2y + m_3z = d$ Selected to Fit Planes.

Planes	m ₁	m ₂	m ₃	đ
1st Pyrrole	2.321	11.87	11.76	0.682
2nd Pyrrole	-1.338	6.826	12.39	1.298
3rd Pyrrole	-5.342	5.542	15.14	-1.385
4th Pyrrole	-5.590	10.781	13.97	-0.404
1st Phenyl	-5.536	-10.58	14.01	-2.980
2nd Phenyl	1.319	- 8.341	-13.22	4.960
3rd Phenyl	-0.008	20.86	3.433	2.280
4th Phenyl	11.60	- 4.116	- 2.852	4.521
NLS	-3.7 57	8.992	1.356	0.021
Inner 16 Atoms	-3.727	9.049	13.53	0.047
Inner 4 Nitrogen	-3.753	9.190	13.50	0.041

Table 9. Dihedral Angles between the NLS Plane and the Individual Phenyl Planes and the Angle between NLS Plane and Mn-Cl Line.

Plane	Dihedral Angle (degrees)
1st Phenyl	54.2
2nd Phenyl	123.5
3rd Phenyl	49.7
4th Phenyl	77.4

Angle between NLS plane and Mn-Cl line* -- 85.30

^{*}The equations for the line between Mn and Cl atoms are: x = 0.575 + 0.004 t, y = 0.141 + 0.022 t, and z = 0.174 + 0.071 t, where t is a parameter with real values.

The atomic deviations from the calculated least squares planes on the basis of different groups of atoms are listed in Tables 10 and 11. The atomic deviation for each atom in the porphyrin skeleton from the NLS plane is shown in Figure 8, and the atomic deviation for each atom from the least squares plane of the inner sixteen atoms is shown in Figure 9. The various bond distances of the porhyrin skeleton are presented in Figure 10a, and Figure 10b, with the corresponding bond angles in Figure 10c. The MnTPP molecule drawn in perspective in terms of its vibration ellipsoids is shown in Figure 11 (ORTEP).²⁶

The structure of ClMnTPP crystal viewed on the bc plane is shown in Figure 12. There are four molecules packed in each unit cell, with the molecules stacking nearly perpendicular to the \dot{c}^* direction. The molecules in the unit cell are related by the following symmetry operations: molecule II can be generated by rotating molecule I about a 2-fold axis at z=1/4 and x=1/2, followed by a translation of 1/2 along the b axis; the same rotation and translation generate molecule IV from molecule III; the pair of molecules I and IV and the pair II and III are related by a center of symmetry.

Table 10. The Atomic Deviations from the Least-Squares Planes of the Individual Pyrrole and Phenyl Rings.

Atom	\underline{d} , (\underline{A})	Atom	d,(A)	
First Pyrrole		Second	Second Pyrrole	
N-1 C-11 C-12 C-13 C-14	0.011 -0.005 -0.003 0.010 -0.013	N-2 C-21 C-22 C-23 C-24	-0.018 0.012 -0.002 -0.009 0.016	
s.d*	0.011	s.d	0.014	
Third Pyrrole		Fourth	Fourth Pyrrole	
N-3 C-31 C-32 C-33 C-34	0.012 -0.008 0.006 0.001 -0.011	N-4 C-41 C-42 C-43 C-44	-0.017 0.017 -0.010 0.000 0.010	
s.d	0.010	s.d	0.014	
First Phenyl		Second	Phenyl	
PH12 PH13 PH14 PH15 PH16 PH17	-0.017 0.001 0.013 -0.011 -0.006 0.020	PH22 PH23 PH24 PH25 PH26 PH27	0.002 0.005 -0.005 -0.004 0.011 -0.010	
s.d	0.014	s.d	0.008	
Third	Phenyl	Fourth	Phenyl	
РН32 РН33 РН34 РН35 РН36 РН37	-0.002 0.008 -0.005 -0.003 0.009 -0.006	PH42 PH43 PH44 PH45 PH46 PH47	0.026 -0.019 0.001 0.011 -0.013 -0.005	
s.d	0.007	s.d	0.016	

^{*} Standard deviation.

Table 11. Atomic Deviations from the Least Squares Plane of Four Nitrogen Atoms.

Atoms	d(X)
N1	0.047
N2	-0.047
и3	0.047
N4	-0.047
s.d	0.054



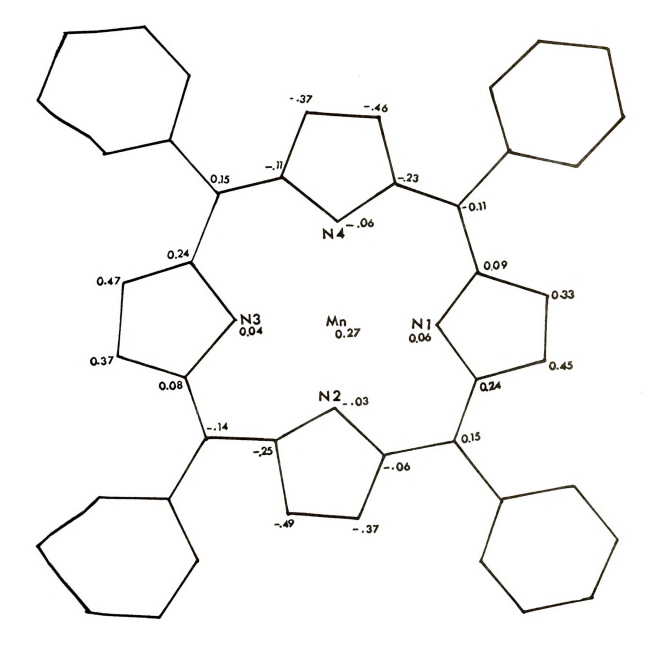
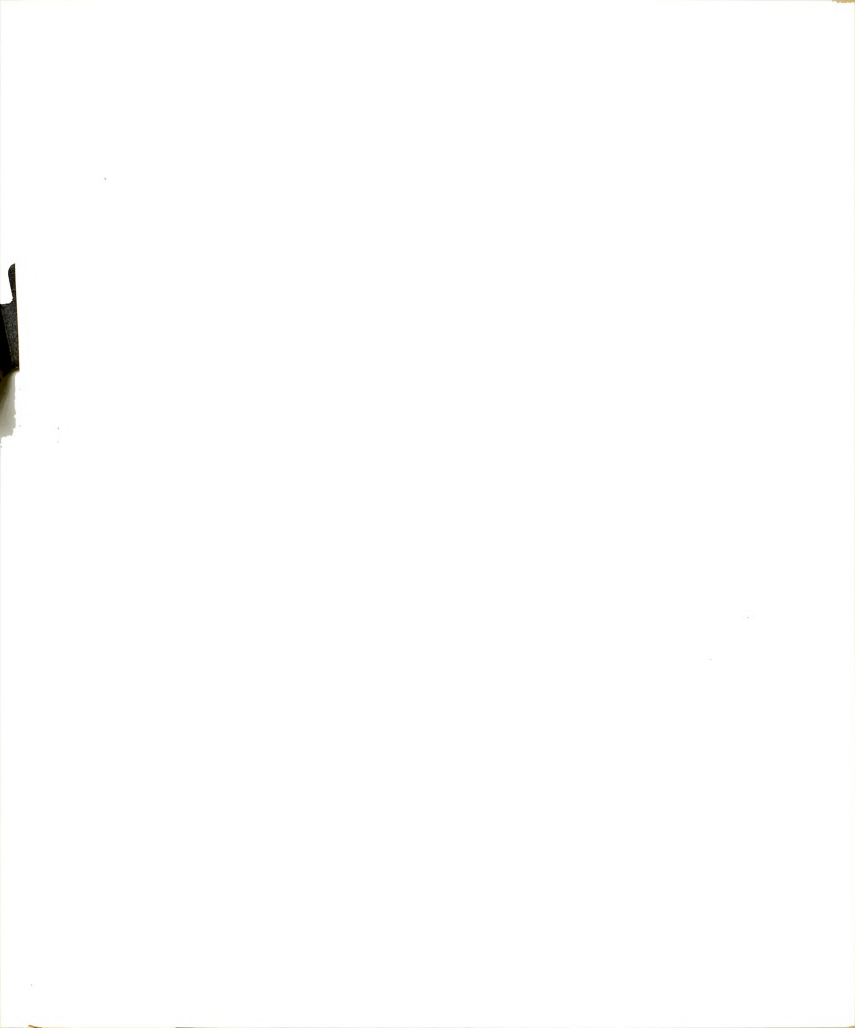


Figure 8. Atomic deviations in (Å) from the nuclear least squares plane (NLS).



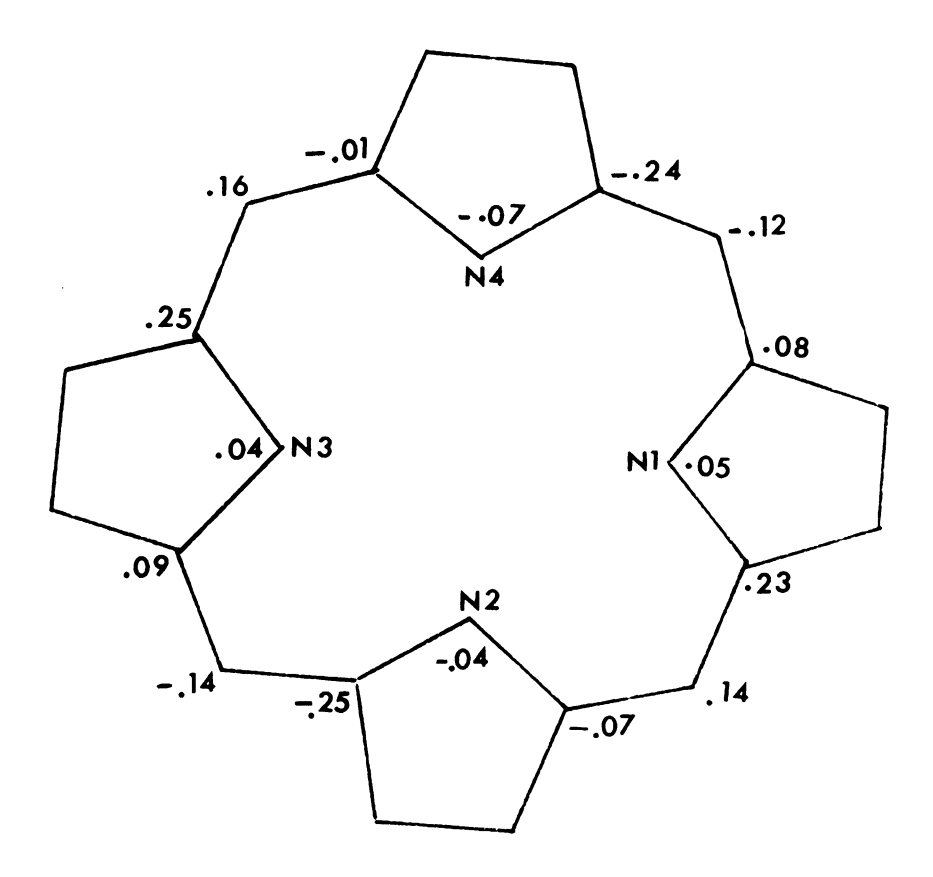
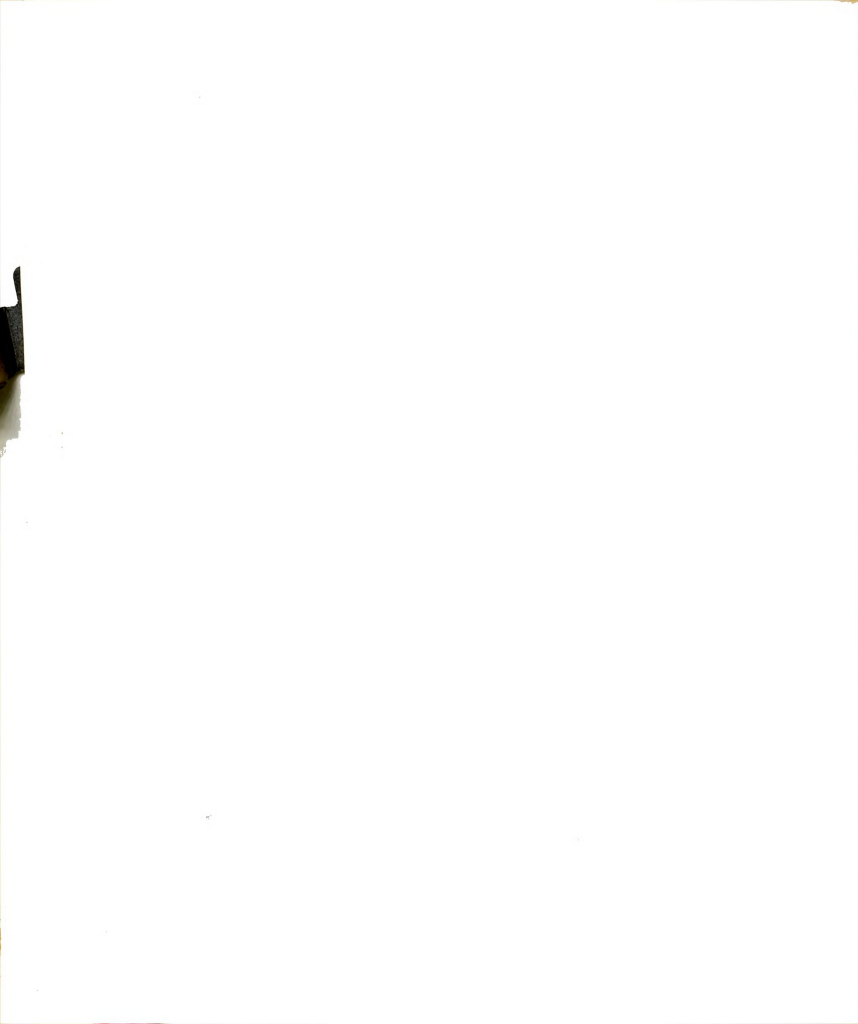


Figure 9. Atomic deviations in (\mathring{A}) from the least squares plane based on the inner sixteen atoms of ClMnTPP.



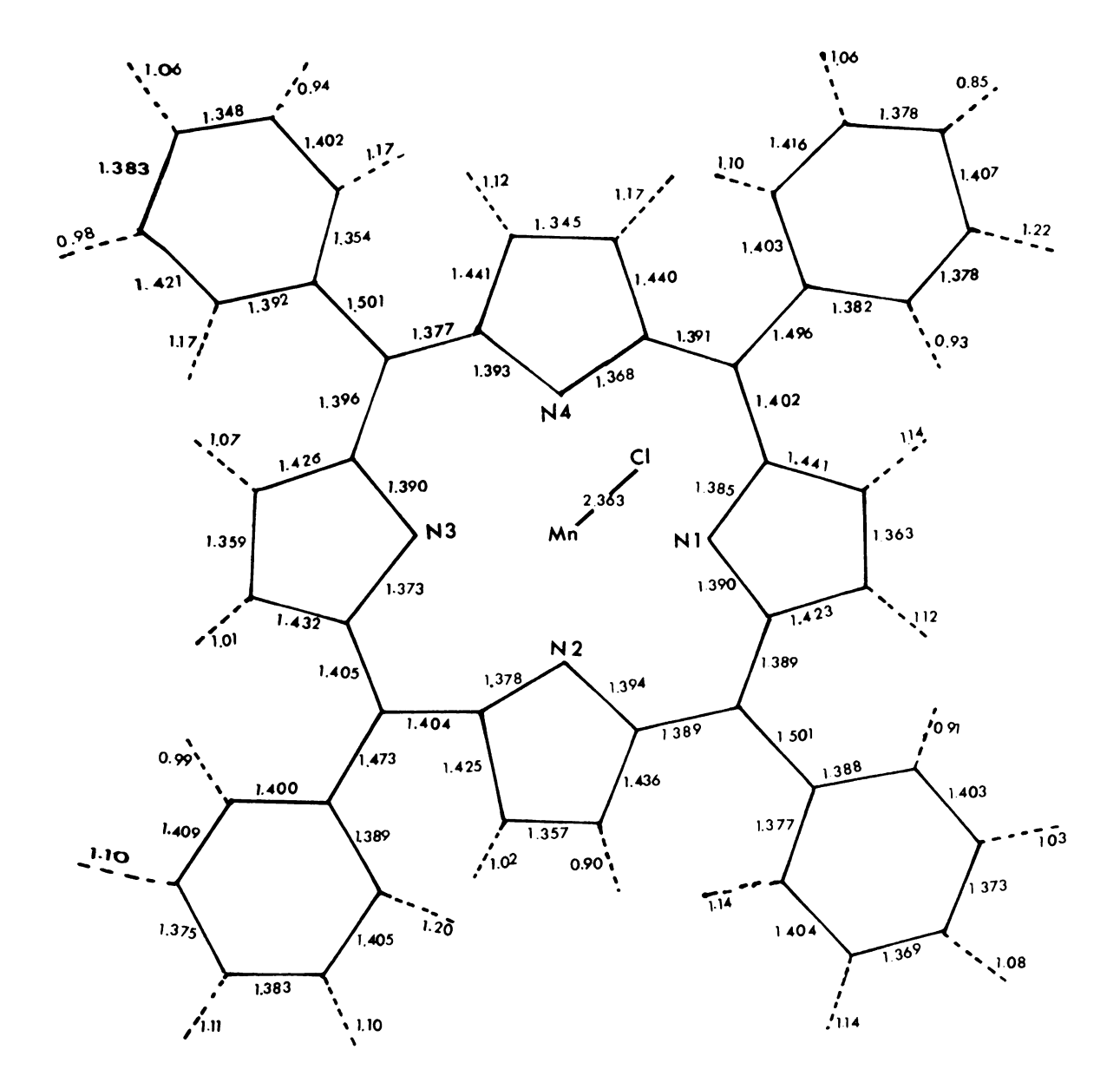
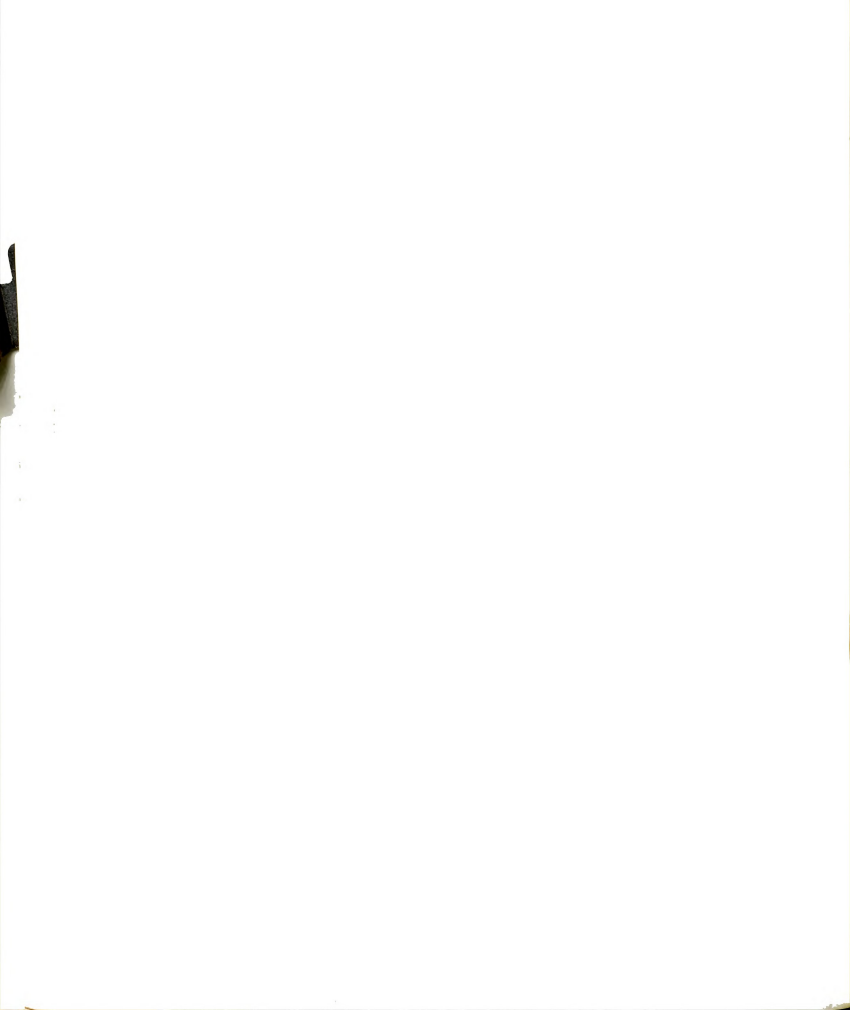


Figure 10a. Bond distances (in $\overset{\circ}{A}$). Broken lines indicate C-H bond distances.



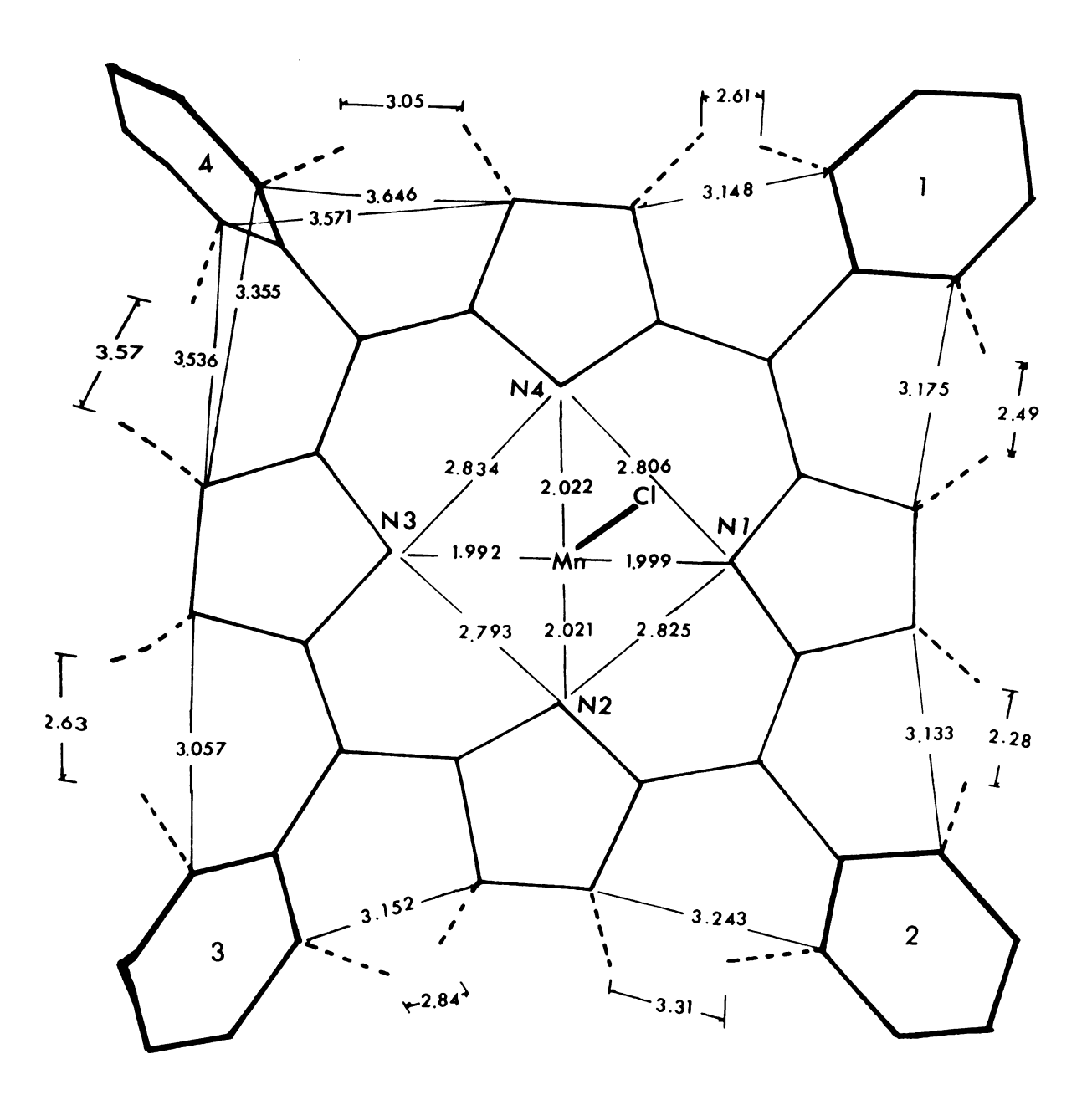


Figure 10b. Intramolecular distances. The numbering of the phenyl groups is indicated in the figure. The dihedral angles from phenyl groups 1,2,3, and 4 to the NLS plane are 54.2°, 123.5°, 49.7°, and 77.4°, respectively.



Figure 10c. ClMnTPP bond angles (degrees). Angle between line Mn-Cl and NLS plane is $85.5^{\,0}_{\,\,\circ}$

 $\angle N1,Mn,N3 = 166.90$

 $\angle N2,Mn,N4 = 161.70$

 $\angle N1,Mn,C1 = 100.0^{\circ}$

 $\angle N2,Mn,C1 = 101.0^{\circ}$

 $\angle N3,Mn,Cl = 93.10$

 $\angle N4,Mn,C1 = 97.20$

the standard deviation of the angles of the carbon-carbon and carbon-nitrogen bonds is approximately $0.6\sim1.0$ degree.

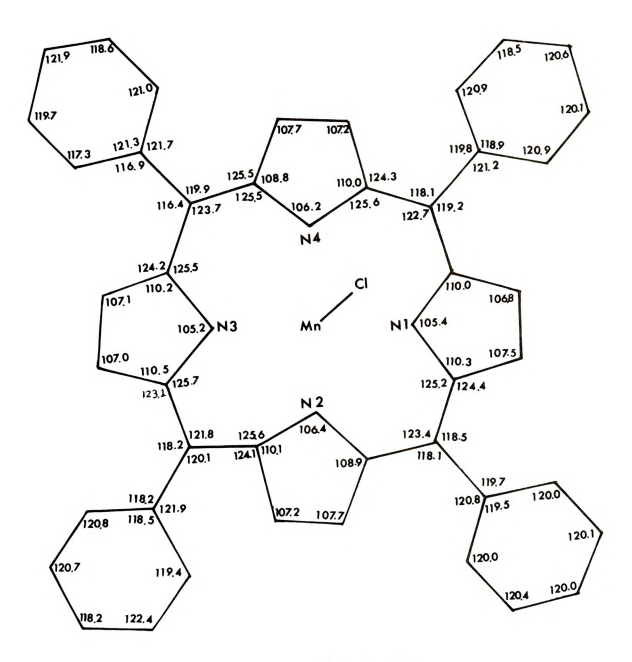
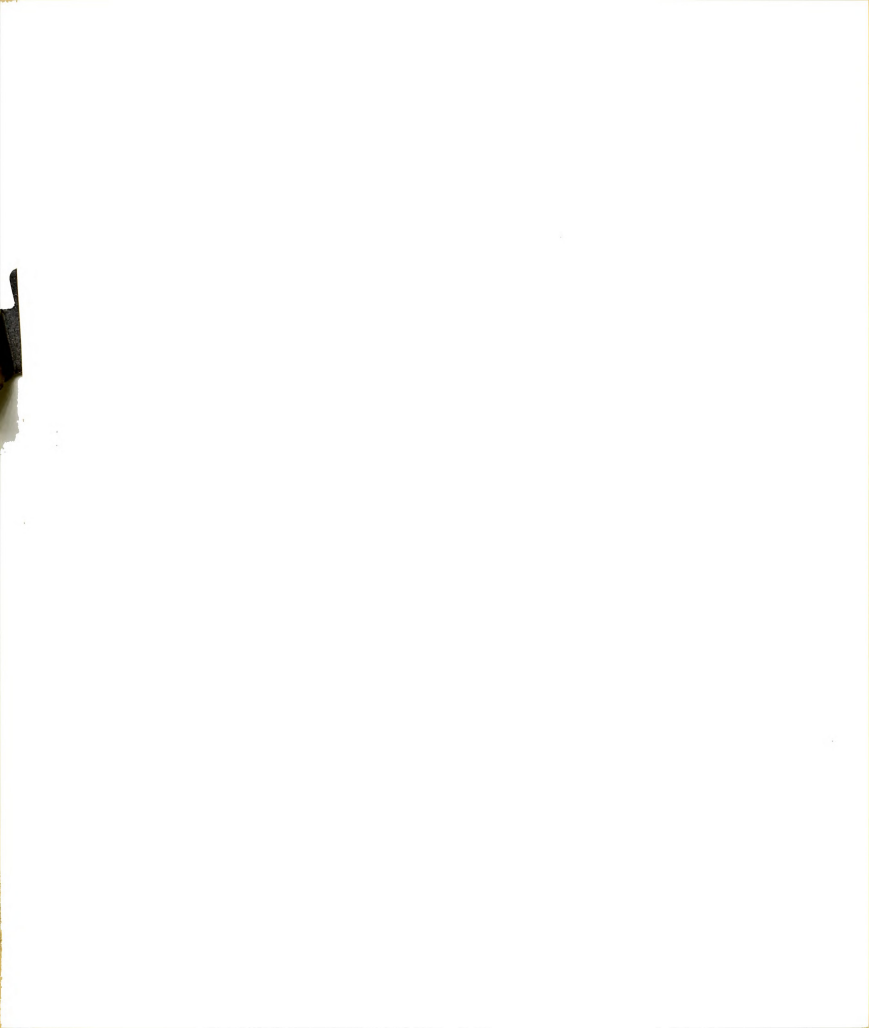


Figure 10c.



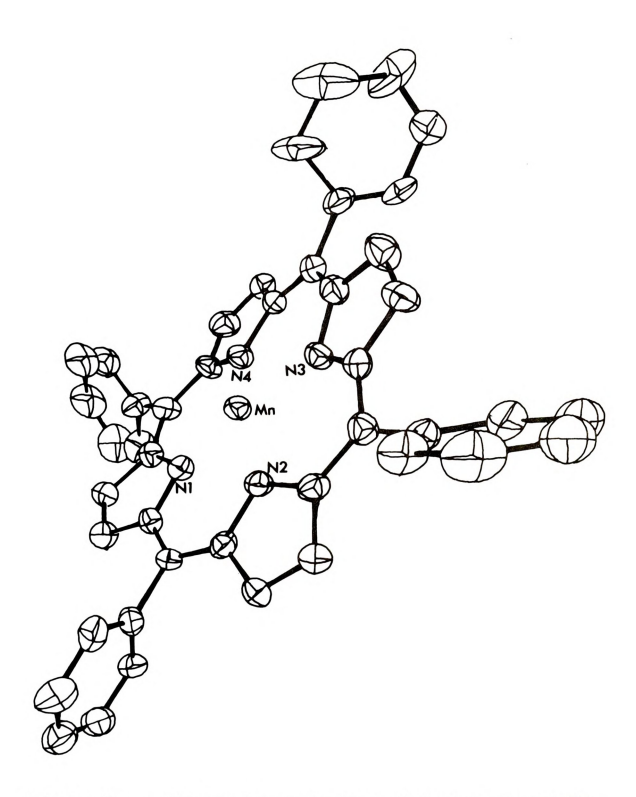


Figure 11. A diagram in perspective of the MnTPP molecule (ORTEP).

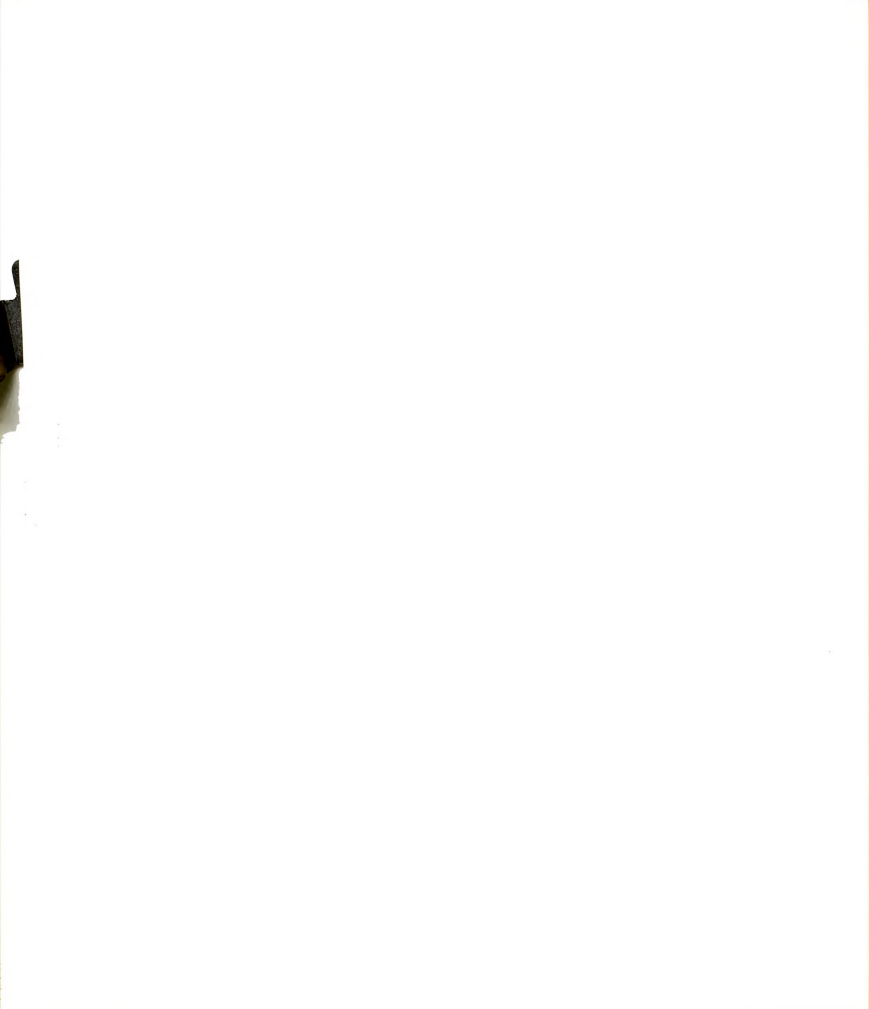
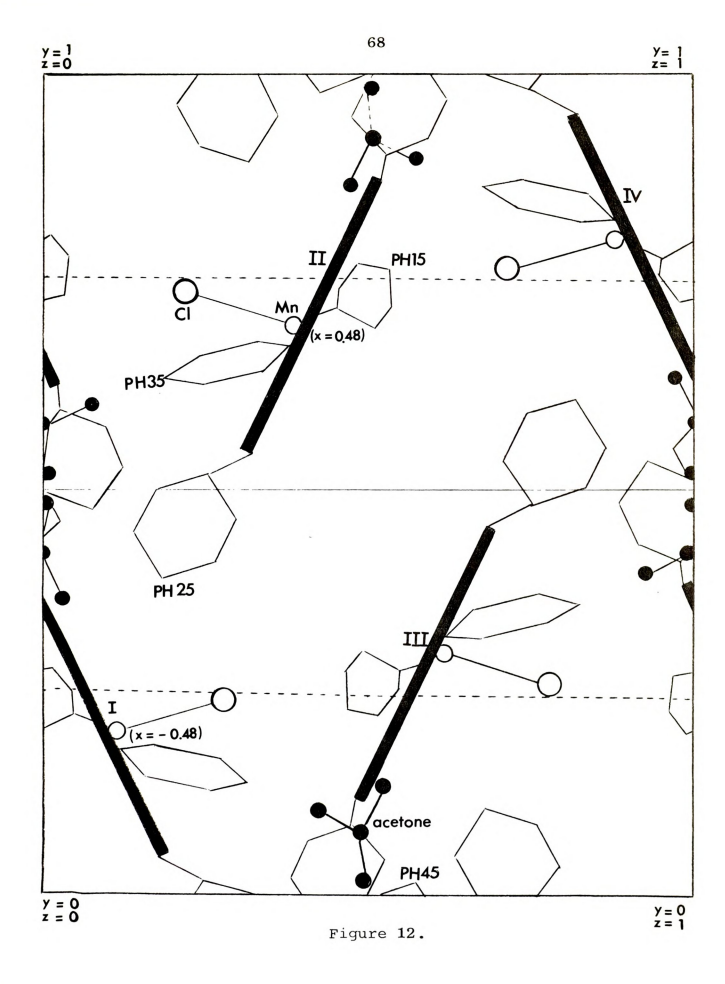
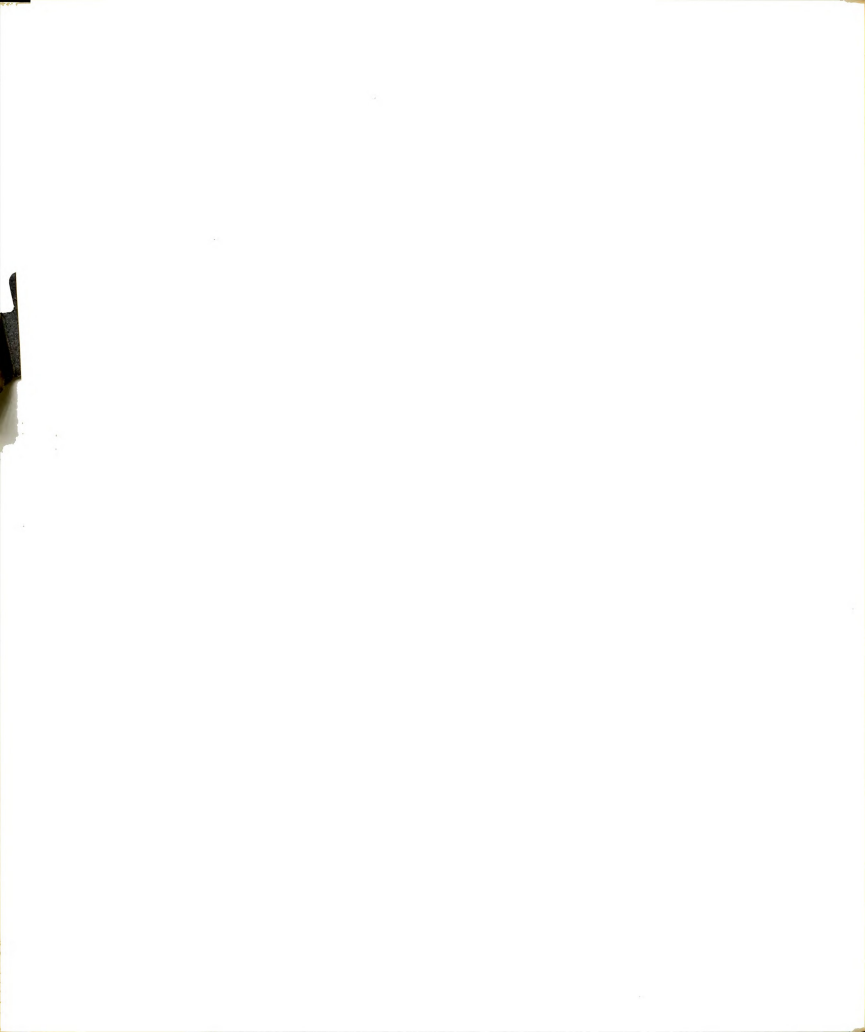




Figure 12. Crystal structure of ClMnTPP as viewed in the projection along \$\delta\$. The solid bar represents the approximate least squares plane of the porphine core.

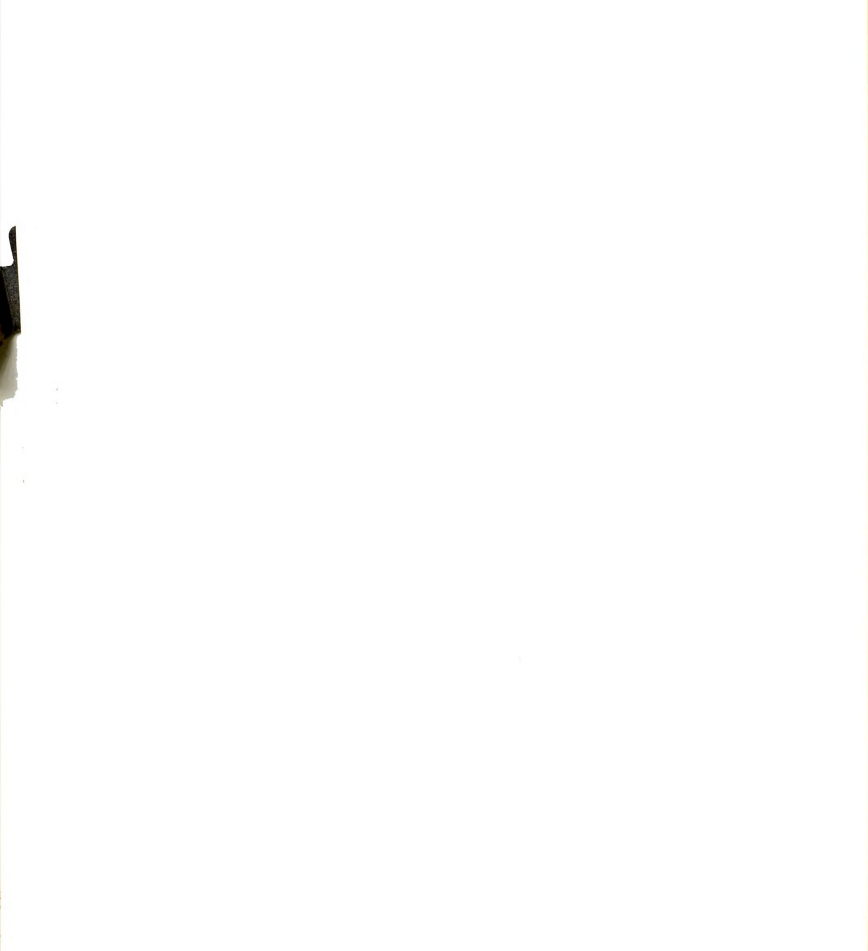




V. DISCUSSION

The data presented in Table 5 indicate that the anisotropic temperature factors of the carbon atoms generally increase as the distance of the atoms increases from the center of the molecule. Hence the peripheral carbon atoms have decreased peak heights and increased standard deviations in atomic coordinates. Such characteristics have also been observed in the $Mg(H_2O)\mbox{TPP}$ and free base tri-TPP structures. These observations are assumed to be due to the contribution of quasi-rigid body angular oscillations.

An acetone molecule of crystallization was found between adjacent ClMnTPP molecules. The closest approach of the molecule to the porphyrin is through the central carbon atom of the acetone to the chlorine atom of ClMnTPP; the interatomic distance of 3.58% does not indicate that any particularly significant interaction is occurring (see Fig. 13). As is typical of solvent molecules trapped in a crystal lattice, the large temperature factors of the acetone molecule indicate that it is either disordered with respect to the acetone molecules in neighboring unit cells or that the acetone lattice site is only partially occupied. A somewhat related case in which a solvent molecule of pyridine was included in the phthalocyanine complex of manganese(III)²⁷ was observed. Two planar and parallel manganese phthalocyanine-ring systems which are joined by an oxygen atom midway between the two



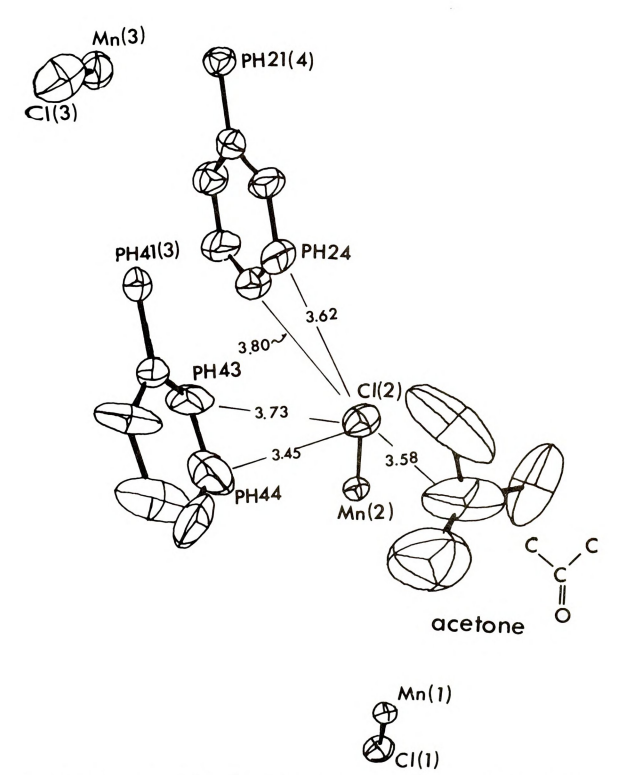
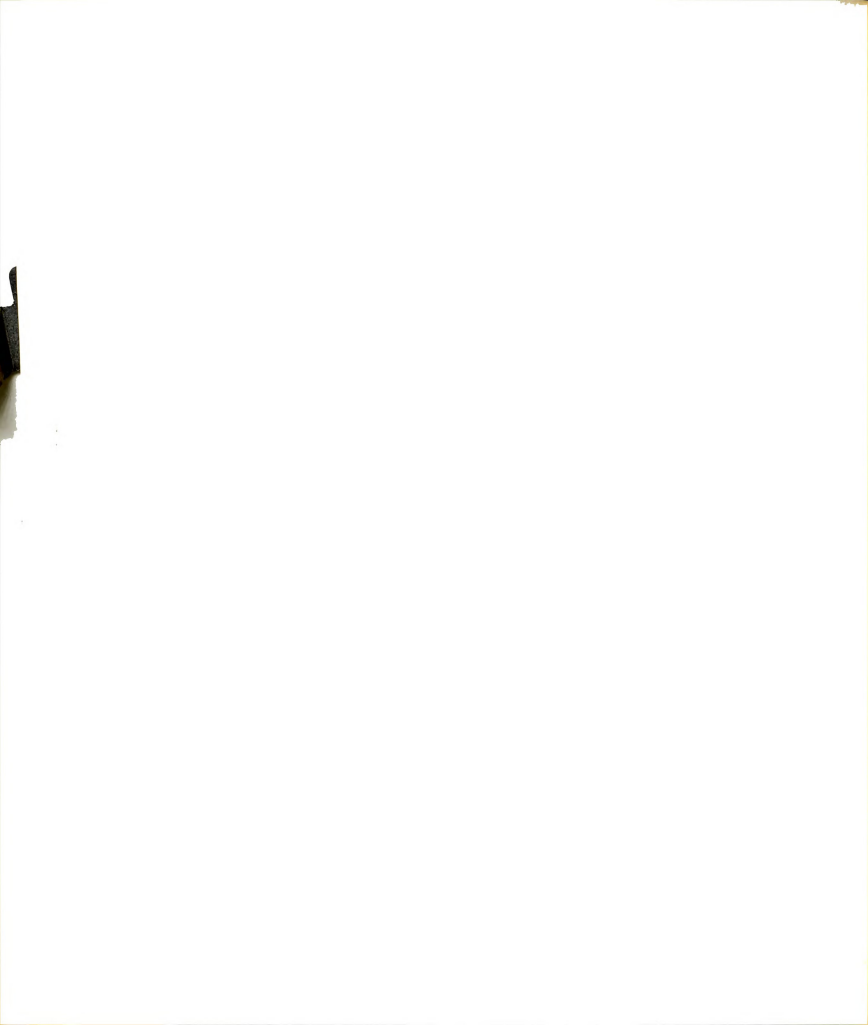


Figure 13. Intermolecular distances from the chlorine atom.



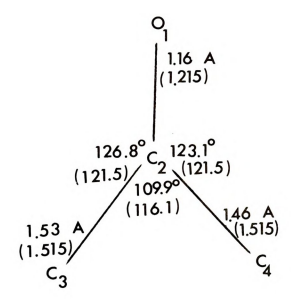
manganese atoms have two pyridine molecules coordinated to the manganese atoms on either side of Mn-O-Mn bridge (see Fig. 2).

The bond distances and bond angles of the acetone of crystallization are shown in Figure 14. The numbers in parentheses are those reported for an acetone molecule in the gas phase. 28 Although large discrepancies exist between the two, there is sufficient correlation between the bond lengths, angles and planarity of the molecule to state confidently that it is an acetone molecule of crystallization.

The residual densities in the final difference electron density map were in the range of 0.11 to 0.18 e/ \mathbb{A}^3 in the region of the clMnTpp molecule. Due to the large thermal motion of the atoms in the acetone molecule, the peak heights of its carbon atoms were much lower than those in the ClMnTPP molecule. Either thermal motion or disorder prevented location of the hydrogen atoms in the acetone molecule. The random residual electron density in the vicinity of the acetone molecule was of the order of 0.65 e/ \mathbb{A}^3 , somewhat greater than the average peak height for the hydrogen atoms of the ClMnTPP molecule.

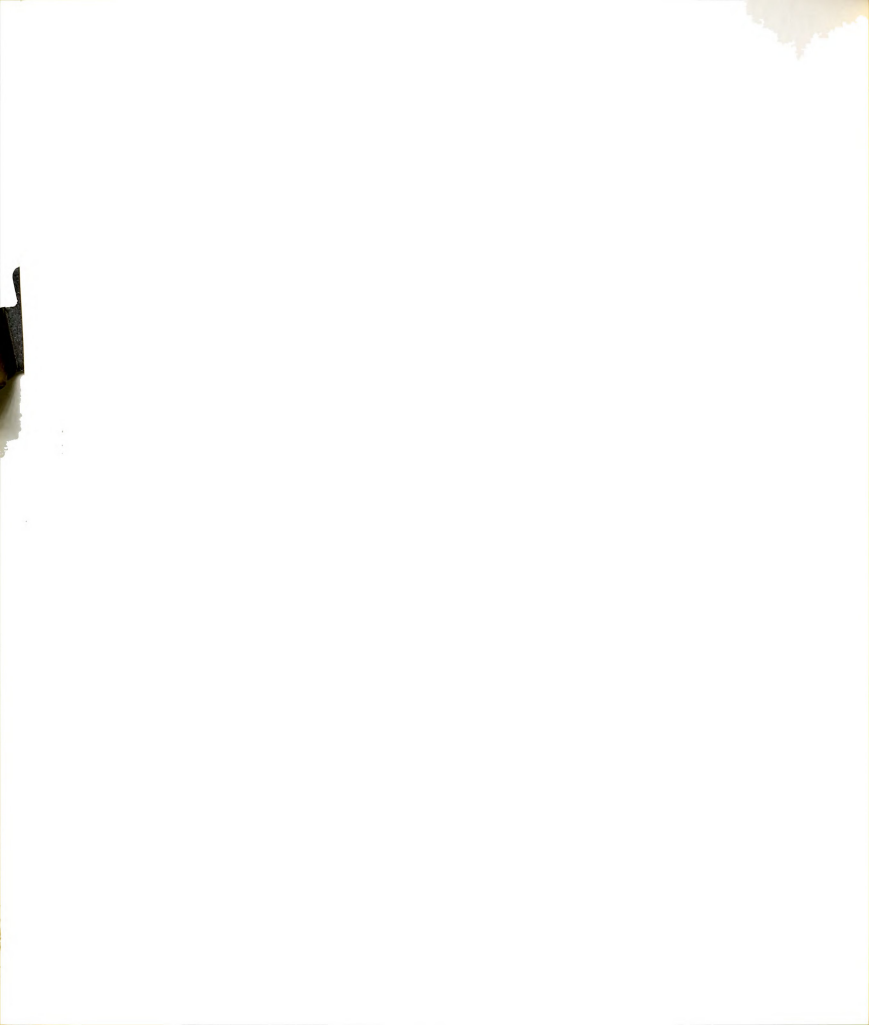
The bond distances of the porphyrin skeleton as listed in Figure 10a have an average C-N bond distance of 1.384 \pm 0.009 Å, an average $\rm C_a$ -C_m bond distance of 1.394 \pm 0.009 Å (where $\rm C_a$ is the carbon atom adjacent to the pyrrole nitrogen, and $\rm C_m$ is the methine carbon atom), and an average C-H bond distance of 1.07 \pm 0.09 Å. The reported values of bond distances in an aromatic system (such as benzene) listed in Volume III of the International Tables for X-ray Crystallography are C-C bond of





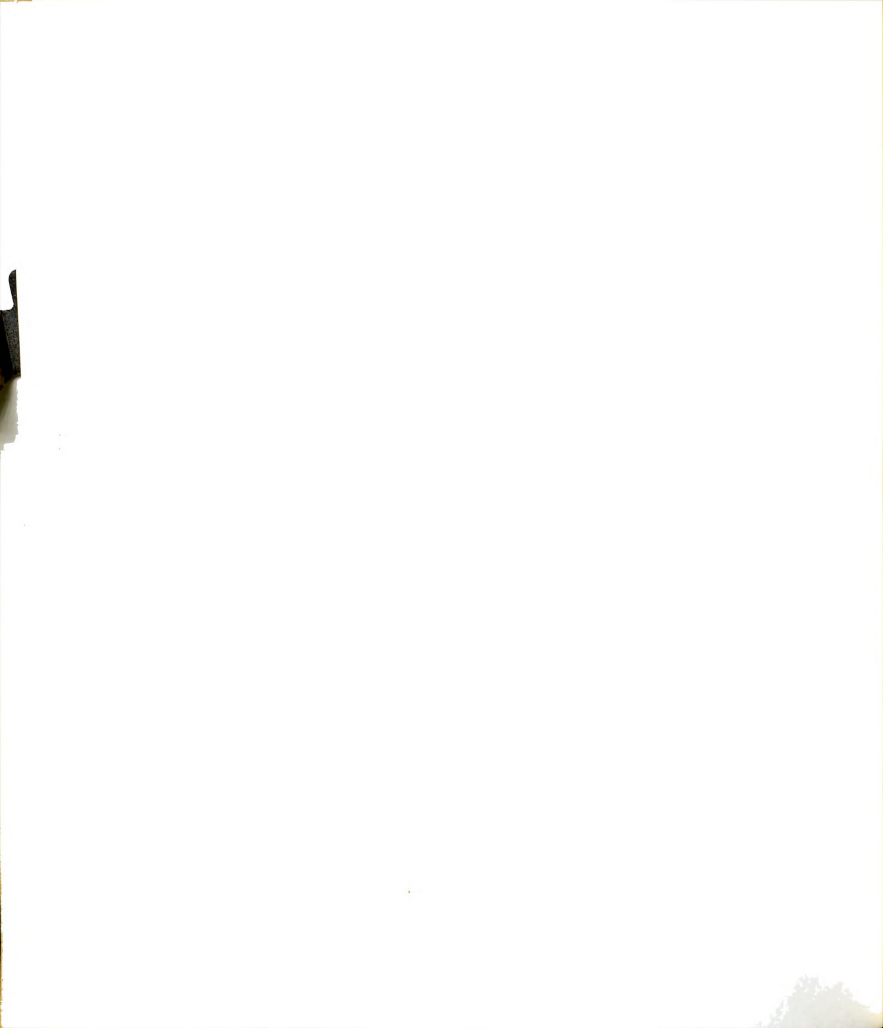
ACETONE

Figure 14. Bond distances and bond angles of the acetone molecule of crystallization.



1.395 \pm 0.003 Å, and C-H bond of 1.084 \pm 0.006 Å. The comparison of the bond distances reported in literature with those determined in this structure analysis shows that the average $\rm C_a$ -C_m and C-H is close to the expected value.

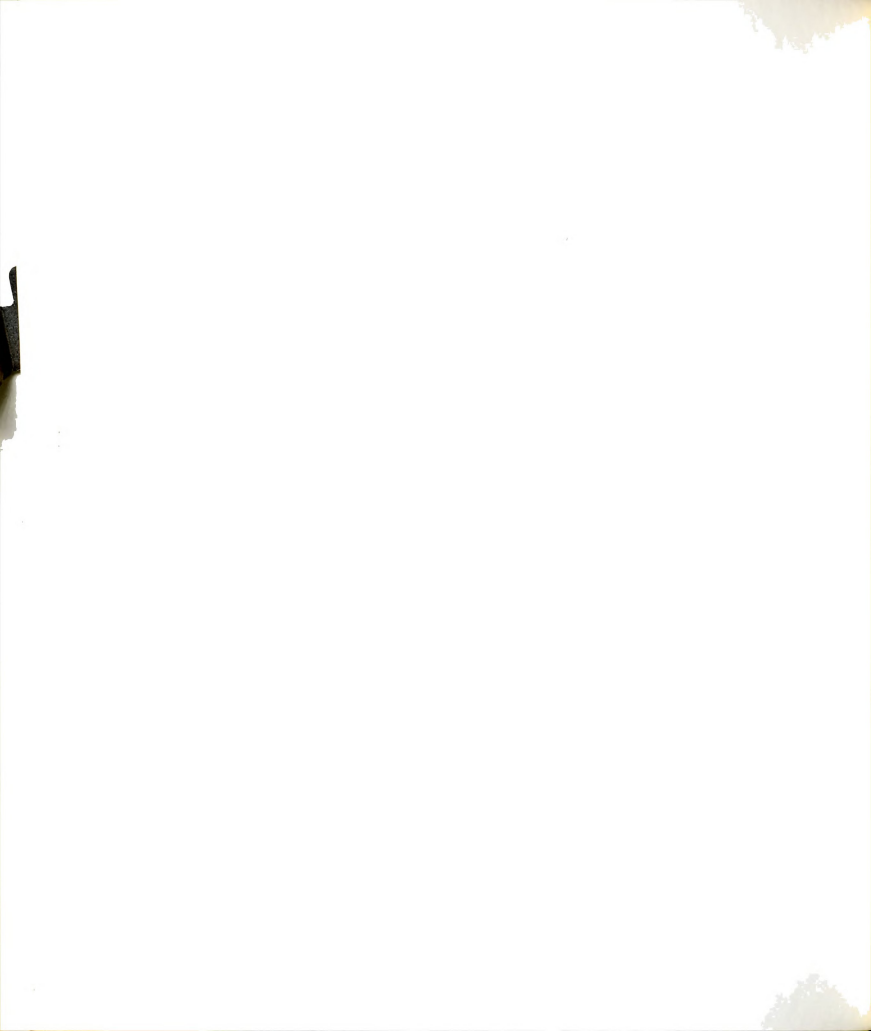
From Figure 10a, the average bond distance on the basis of different groups of atoms in CLMnTPP has a somewhat different meaning. The average $c_a^{}$ - $c_b^{}$ bond distance is 1.433 ± 0.007 Å and the average $c_{\rm b}^{-}c_{\rm b}^{-}$ is $1.356 \pm$ 0.008 Å (where $\, c_{_{\! h}} \,$ is the carbon atom adjacent to $\, c_{_{\! a}}) \, .$ The former bond length is shorter than the o bond length of 1.49~Å between $~\mathrm{sp^2}~$ hybridized carbon atoms, while the latter is longer than the expected double bond value of 1.33 A. This behavior is commonly observed in most of the porphyrins. The other C-C bond distance joining the bridge carbon atom and the terminal carbon atom of the phenyl group has an average value of 1.493~Å, typical of a \circ bond in trigonally hybridized carbon atoms. Because of possible steric interference between phenyl hydrogen atoms and pyrrole hydrogen atoms if the phenyl groups were coplanar to the porphyrin core, the phenyl groups are rotated out of the NLS plane. Thus, the π electron systems of the phenyl rings are isolated from the corresponding system in the porphyrin core by pseudo-single bonds. As is indicated in Table 10, the phenyl and pyrrole rings are essentially planar as individual entities. The dihedral angles between the individual rotated phenyl groups and the



NLS plane are 54.2° , 123.5° , 49.7° , and 77.4° . The large variation in the angles shows indirectly the crystal packing forces.

The standard deviations of the molecular parameters are in the range between 0.007 and 0.009 Å for $\rm c_a^- \rm c_b^-$, $\rm c_b^- \rm c_b^-$, $\rm c_a^- \rm c_m^-$ and C-N bonds. The standard deviations of the crystallographic structure parameters from the last cycle of the least squares structure factor calculation based on the errors of carbon and nitrogen coordinates are in the range between 0.006 and 0.013 Å for C-C and C-N bonds. According to Cruickshank's statistical significance tests 52 , 53 comparing the errors of the molecular parameters to those of the crystallographic structure parameters, the errors in the molecular parameters are insignificant, since they fall within the value of three standard deviations of the crystallographic structure parameters.

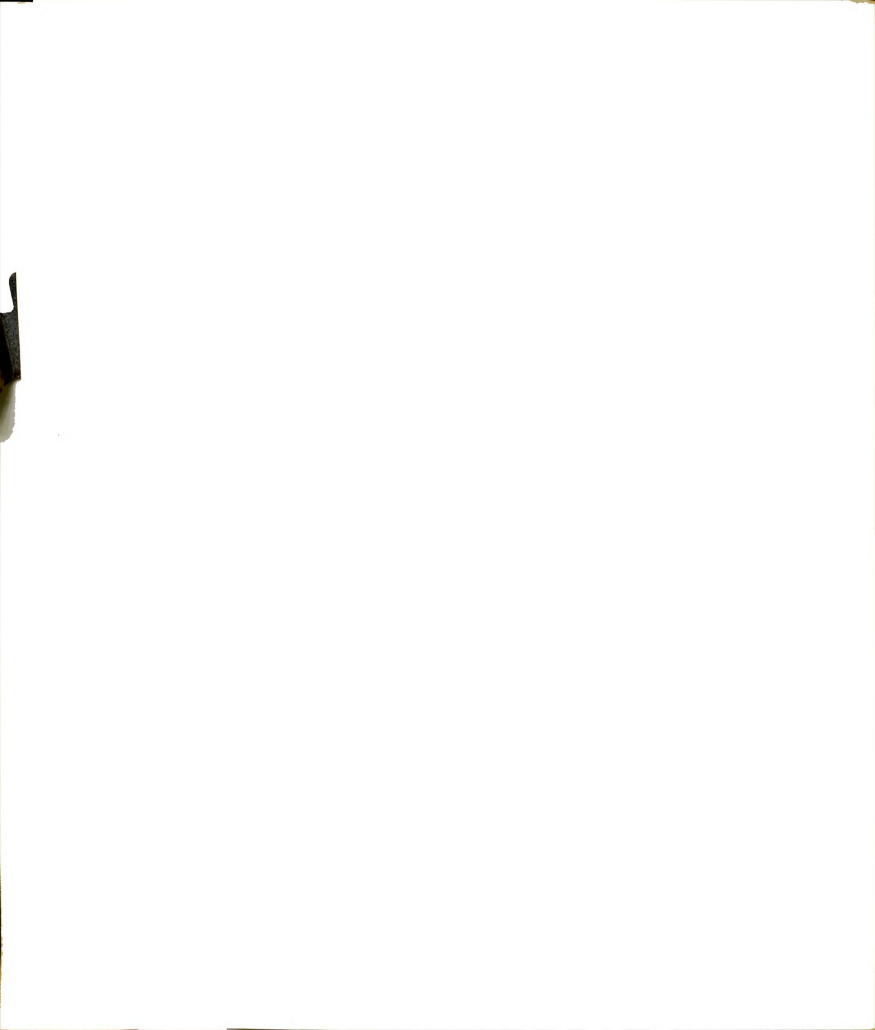
The atomic deviations from the least squares plane based on the inner sixteen atoms of the porphine core are given in Figure 9. Although the atomic deviations of the nitrogen atoms, which range from 0.04 to 0.07 %, are probably not significant, every other pyrrole atom (<u>i.e.</u>, C14, C24, C34, and C41) shows an appreciable atomic deviation of approximately 0.25 %, alternating above and below the least squares plane. The bridge carbon atoms, PH11, PH21, PH31, and PH41, deviate approximately 0.1 % from the mean plane. One can conclude from these atomic deviations



that the inner sixteen-membered ring is decidedly nonplanar, in contrast to the sixteen-membered ring found in tri-TPP whose carbon atoms are approximately within the plane.

From the many porphyrins whose structures have been determined, it is obvious that deviations from the planarity of the NLS plane vary uniquely from one porphyrin to another, depending on the particular molecular structure and various crystallographic packing forces. In the pre-Sent case of ClMnTPP, the atomic deviations from the individual planes of each pyrrole and phenyl group are within the error of the determination (see Table 10). However, considering the whole porphyrin skeleton, one pair of diagonally opposite nitrogen atoms, N1 and N3, is displaced about 0.05 Å slightly above the mean plane of the nitrogen quartet, while the other pair is displaced about the same distance below the plane (see Table 11). The peripheral carbons of the pyrroles have an apparent (0.3-0.5 A) deviation from the NLS plane in the same direction as their corresponding nitrogen atoms (see Fig. 8). Because of this alternating arrangement, the porphine core of ClMnTPP is ruffled in a puckered way. Furthermore, the atomic deviations show approximate $\bar{4}$ symmetry.

In the structure of free base tri-TPP, each individual pyrrole was found to be planar, but the departure from the planarity of the porphine core differs in a significant way from CLMnTPP. In tri-TPP, one pair of pyrroles carrying



the central hydrogen atoms is inclined away from NLS plane, while the other pair is approximately in the plane. In addition, the atomic deviations from the NLS plane of C lMnTPP are substantially more pronounced than those observed in tri-TPP.

Figure 15 shows the details of the central part of the CIMnTPP molecule. It can be seen that the four nitrocaen-nitrogen distances are similar, and the nitrogen-Chlorine distances are not equivalent. The difference of O.22 A between N2-Cl and N3-Cl corresponds to a difference of 7.90 between the angles /N2, Mn. Cl and /N3, Mn. Cl. In other words, the apical chlorine atom is slightly inclined toward the N3 atom. Calculations show that the chlorine atom is inclined about 4.7° from the normal of the plane of basal nitrogen atoms. Thus, the square pyramid coordination of the manganese by the four nitrogens and one chlorine is somewhat distorted. Examination of the geometry around the chlorine atom shows an acetone molecule and two phenyl groups belonging to two different adjacent molecules to be the close neighbors (see Fig. 13). If the chlorine atom were at the apical position of the square pyramid, the contact between Cl atom and PH44 atom of the other ClMnTPP molecule would be much shorter than 3.45 A, about the minimum van der Waals contact distance. Therefore, the chlorine atom, by tipping itself away from the apical of the square pyramid, is able to keep a reasonable

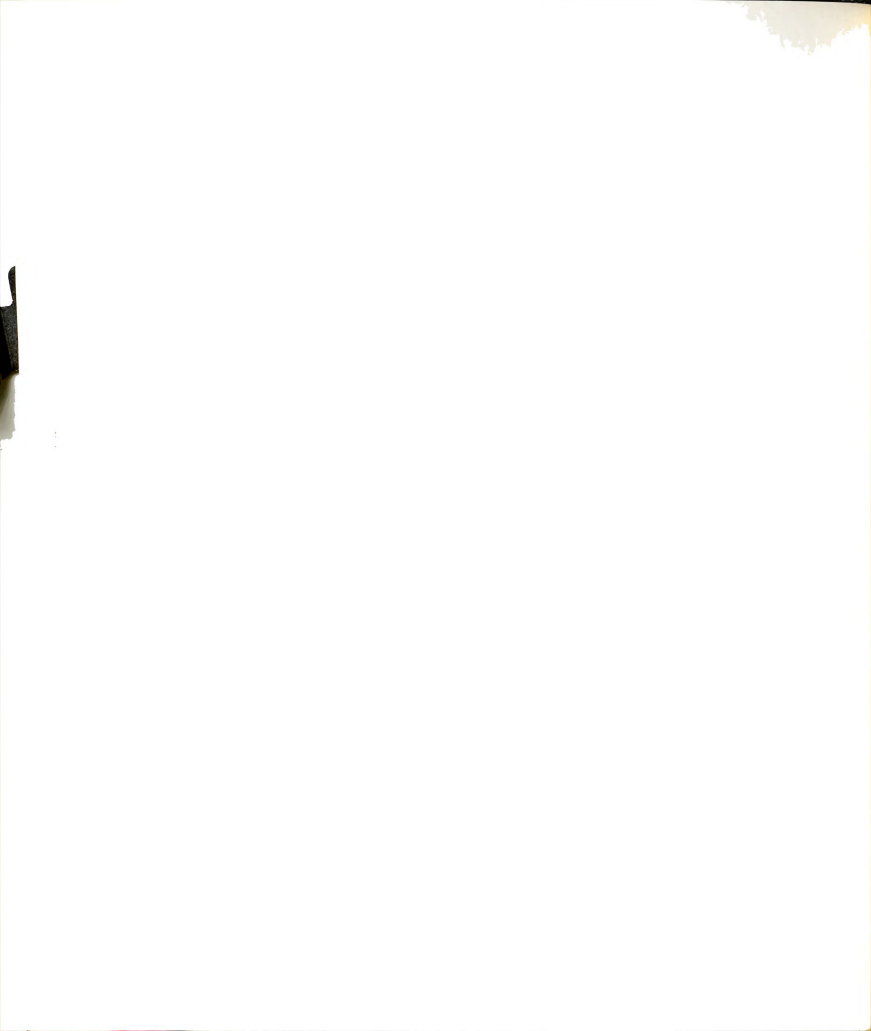




Figure 15. The geometry and the dimensions of square pyramidal coordination in ClMnTPP molecule.

3.346 8 1.999 8 N1-Cl Mn-N1 /N1,Mn,C1 =99.980 2.021 / N2,Mn,Cl = N2-C1 3.392 Mn-N2 101.04 / N3,Mn,Cl = 3.171 1.992 N3-C1 Mn-N3 93.12 3.297 2.022 \angle N4,Mn,Cl = N4-C1 Mn-N4 97.21

Average Mn-N distance 2.008 $^{\circ}_{A}$

Average center-nitrogen, Ct-N, 1.9

Out-of-plane displacement, Mn-Ct, 0.273

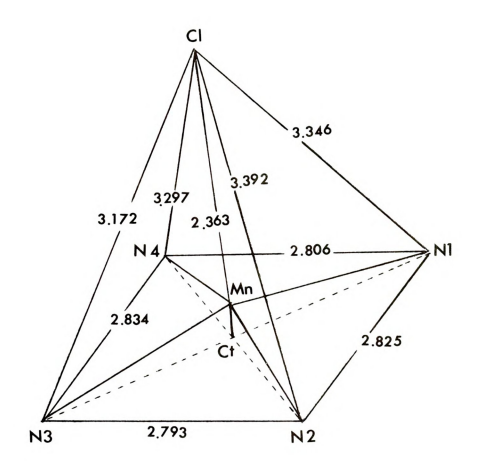
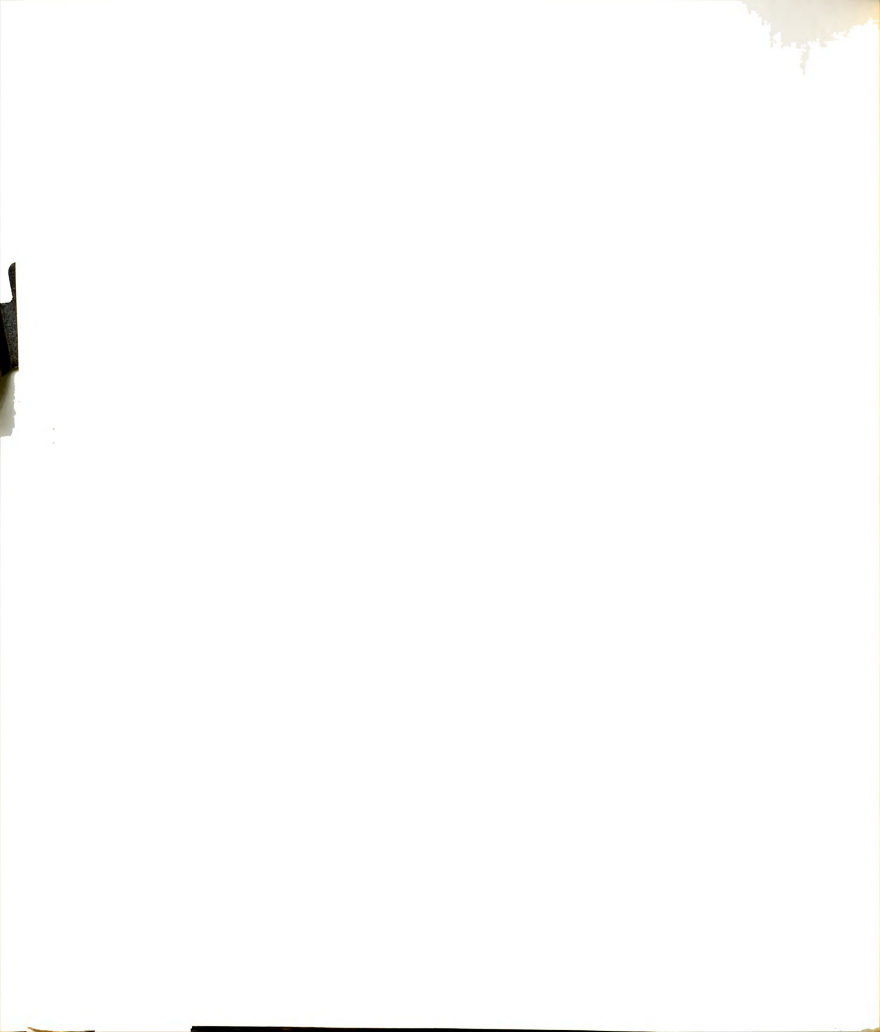
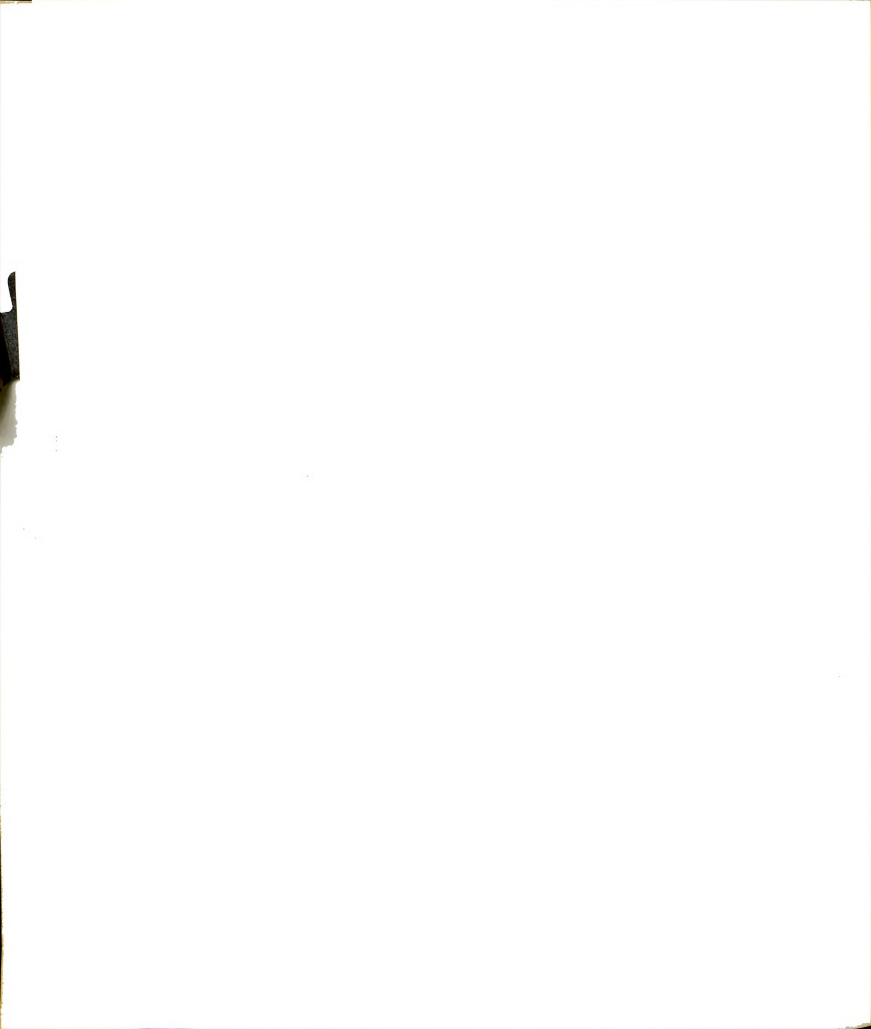


Figure 15.



contact distance to the surrounding atoms. In a similar manner, the phenyl group with the PH44 atom has also adjusted its angular rotation so as to avoid other close constraints and contacts with adjacent molecules due to the crystal packing arrangement.

Of other interest is the fact that the Mn atom is displaced 0.27 A from the mean nitrogen plane, and the bond length of Mn-Cl of 2.363 Å is somewhat shorter than expected. Although there are no other convincing axial bond length data available for five coordinate compounds, general references to Mn-Cl bond distances in a variety of compounds can be found for comparison. The Mn-Cl bond distance in manganous chloride dihydrate29 (MnCl2 ·2H2O) is 2.57 Å, while Mn-Cl distance in the complex of hexamethylenetetramine with manganous chloride30 (abbreviated HMT, MnCl₂·2(CH₂)₆N₄·2H₂O) is approximately 2.47 Å. It can be said that the longer bond distance in MnCl, '2H,O is expected due to the ionic character, while the shorter length in HMT corresponds to some covalent bond character. Consequently, the Mn-Cl distance of 2.363 A in CLMnTPP suggests that there is significant covalent bond character. In addition, the average Mn-N distance of 2.008 A is also somewhat shorter than that expected by covalent radii estimates (2.04 Å). The shortening of both the Mn-Cl and Mn-N distances might be responsible for the relative high stability of this unique porphyrin.



The shortening of axial ligand distance of square pyramid geometry is also found in ClFeTPP. A qualitative consideration by molecular orbital studies suggested that the $3\ {\rm d_z}^2$ orbital of the metal combined with an appropriate studies orbital of axial ligand to give a strong bonding and a weakly antibonding orbital. Also, the 4s and 4 p₂ orbitals of the metal can further contribute to the bonding.

The structural parameters of some five-coordinate metallotetraphenylporphyrins are listed in Table 12. Because Mq(H2O)TPP, ClFeTPP, and (H2O)ZnTPP31 crystallize in the same disordered structure type, the precision of parameter determination is not so good as desired. However, it can be seen that the radius of the central hole of the porphine core Ct-N of ClMnTPP is the shortest of all these tetraphenylporphyrins. There appears to be a contraction of about 0.05 Å in going from the Ct-N value of 2.043 Å of porphine to that of 1.989 A of CLMnTPP. This contraction might be the cause of the ruffling of the porphyrin core upon metal and side-chain substitutions. In addition to the shortening of Ct-N distance, the Mn-N bond distance of $2.008~{\rm \AA}$ is somewhat shorter than that of $2.04~{\rm \AA}$ estimated from covalent radii. The other bond length Ca-N, Ca-Cb and Cb-Cb: are approximately the same as those of other tetraphenylporphyrins. A comparison of the bond lengths of ClMnTPP and porphine indicates a slight expansion of the Ca-N bond, and a slight contraction of the Ca-Cb

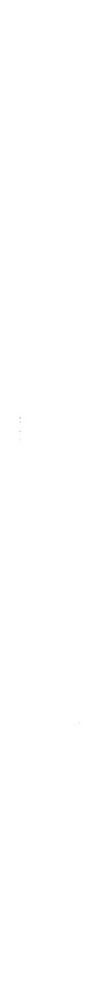


Table 12. Average Stereochemical Parameters of the Porphine Skeleton in Some Five Coordination Metallotetraphenylporphyrins (two free base molecules are given for comparison).

	ClMnTPP	$Mg(H_2O)TPP$	ClFeTPP	(H ₂ O)ZnTPP	tri-TPP	Porphine*
a _{M-N}	2.008	2.072	2.049	2.05		
bCt-N	1.989	2.054	2.012	2.04	2.065	2.043
c _a -N	1.384	1.376	1.384	1.38	1.369	1.379
c_a-c_b	1.433	1.431	1.446	1.430	1.442	1.442
$^{d}c_{b}-c_{b}$	1.356	1.360	1.380	1.37	1.351	1.355
c_a - c_m^e	1.394	1.415	1.395	1.42	1.398	1.382
f $_{\triangle}$	0.273	0.27	0 . 383	0.20		

^aMetal-nitrogen distance.

bCenter-nitrogen distance.

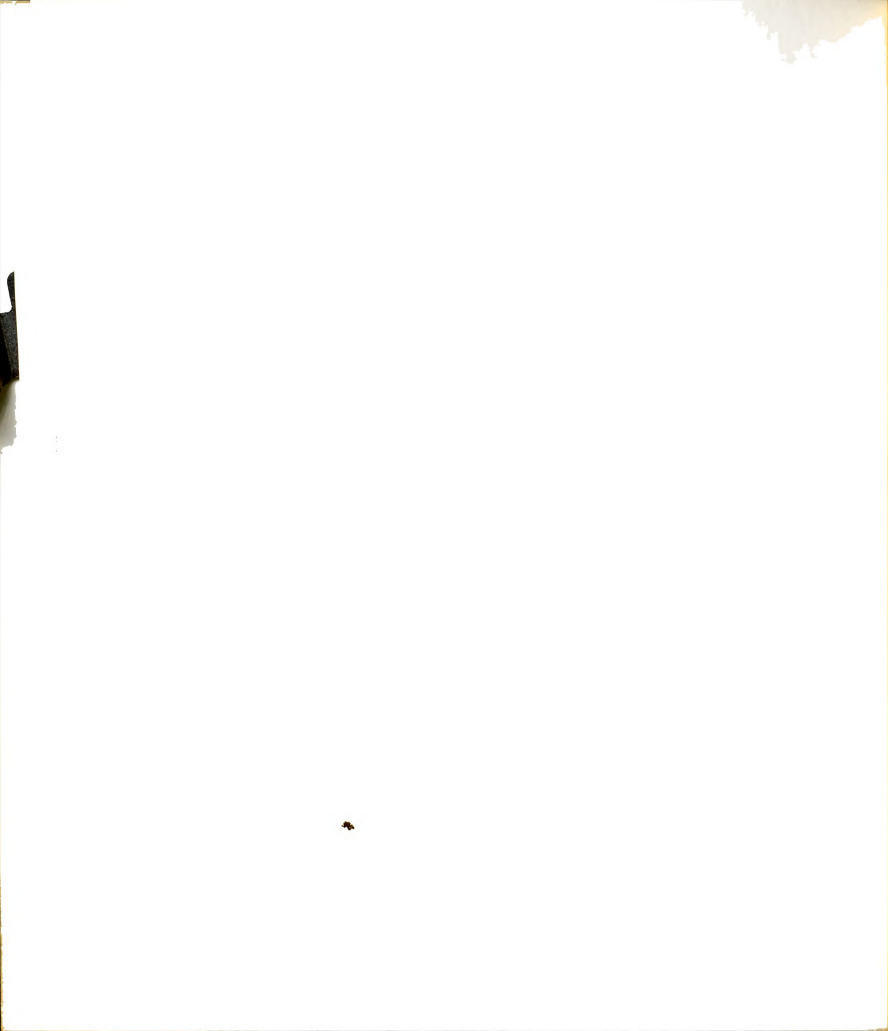
 $^{^{\}mathrm{c}}\mathrm{c}_{\mathrm{a}}$ is the carbon atom adjacent to pyrrole nitrogen.

 $^{{}^{}d}c_{b}^{}$ is the carbon atom adjacent to $c_{a}^{}$.

 $^{^{\}mathrm{e}}\mathrm{C}_{\mathrm{m}}$ is the methine carbon atom.

 $^{^{\}mathbf{f}}$ Δ is the out-of-plane displacement of the central metal atom.

 $^{^\}star$ From the structure determination in Part II.

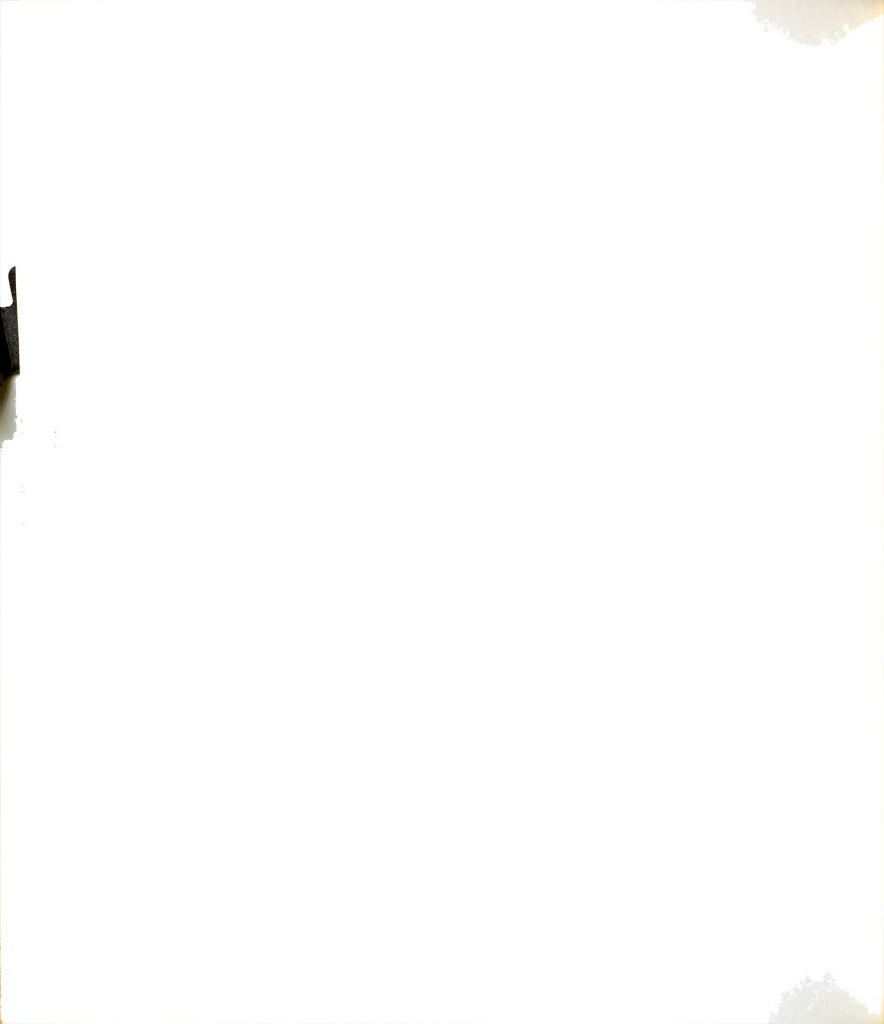


bond, but the $\mathbf{C_b^- C_{b^+}}$ bond, as in general, is relatively insensitive to metal substitution.



PART II

THE REDETERMINATION OF THE STRUCTURE OF PORPHINE

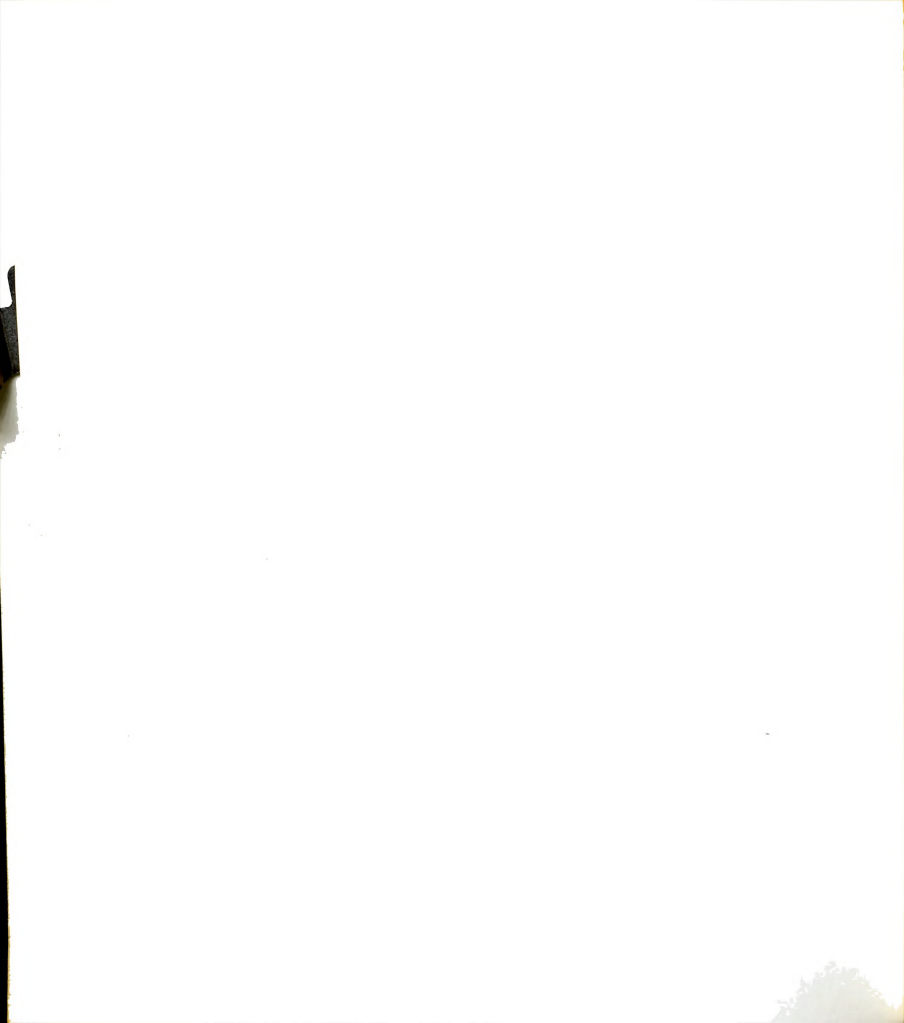


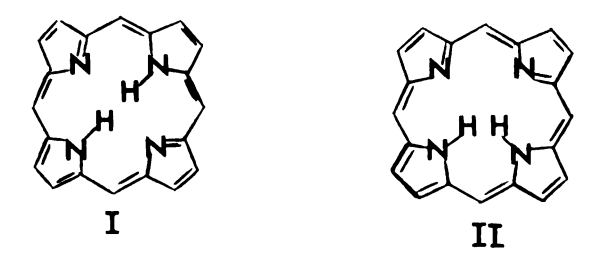
VI. INTRODUCTION

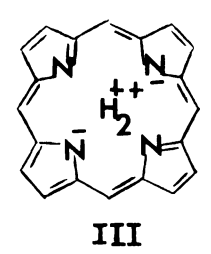
1. General

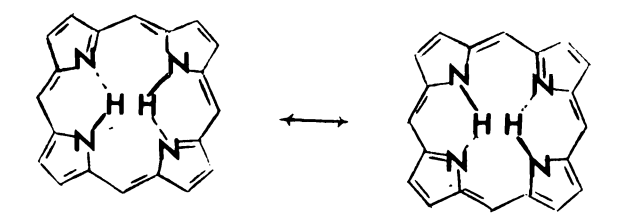
Porphine (Fig. 1b) is the parent compound of all the porphyrins. The bond distances, the bond angles and the planarity of this molecule form the basis of all comparisons among the porphyrins. Porphine crystallizes with a monoclinic space group in which each asymmetric unit contains one complete molecule. With such an arrangement, the structure of porphine can be expected to be relatively free from any crystalline imposed symmetry or distortion and to approximate the molecule in its free state. Therefore, accurate structural parameters, which are important for the discussion of the general characteristics of porphyrins, are particularly important for this molecule.

Since porphine is a conjugated system, its carbonnitrogen skeleton can be represented in terms of several
resonance forms. The usual structural assignments to the
free base of porphine lead to several possible configurations for the center imino hydrogen atoms: 32 1) hydrogen
atoms on opposite nitrogen atoms (Fig. 16, I), 2) hydrogen atoms on adjacent nitrogen atoms, (II), 3) hydrogens
in an ionic form, (III), and 4) hydrogen atoms occupying









IV (Resonance structures)

Figure 16. Possible central hydrogen models $(\text{from Dorough \& Shen } (1950))^{32}$

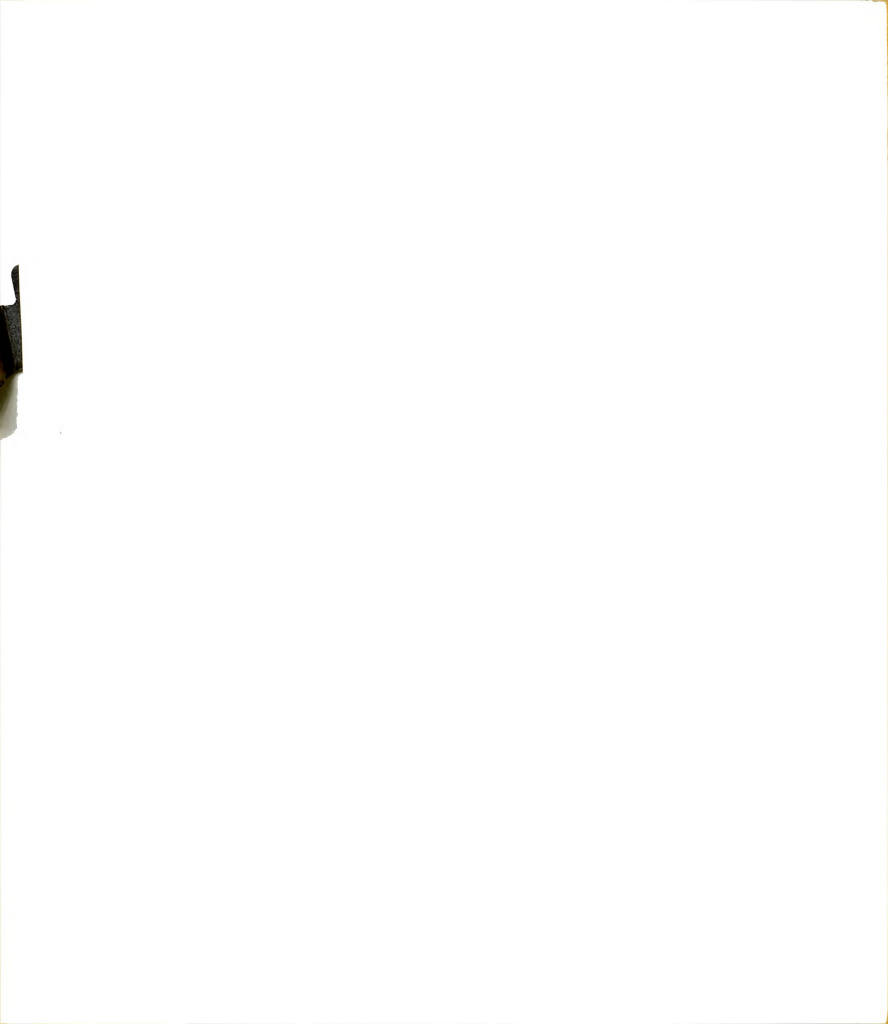


equivalent bridging positions between two nitrogen atoms, (IV). In early studies, neither isomer I nor isomer II could be conclusively isolated, even though a great number of free base porphyrin compounds had been investigated.

It was thus concluded that the structure of porphine was that of either an inseparable equilibrium mixture of isomers I and II or some other species (III or IV), in which the hydrogen atoms were bonded in an entirely different manner. The inner-hydrogen structure of the free base porphine and other porphyrins has been studied by infrared and visible spectroscopy, nuclear magnetic resonance, and X-ray diffraction. These studies will be discussed briefly.

2. Visible Spectroscopy

Studies of the visible absorption spectra of porphine and some derivatives of it were carried out by Erdman and Corwin.³³ They observed that the absorption spectrum of a porphine in which one of the two inner hydrogens had been replaced by a methyl group was identical with the absorption spectrum of the corresponding unmethylated free base. These results were interpreted to mean that the replaced hydrogen was bonded covalently since the methyl group was certainly bonded covalently, and the ionic and the resonance hydrogen bridge structures (see Fig. 16, III and IV) were precluded. However, the covalent character of inner hydrogens implied that porphine could exist as structural isomers.



Subsequently, the visible spectrum of the free base of a tetraphenyl porphyrin (TPP) was studied by Dorough et al.32 The free base dissolved in E.P.A. (which is a mixture of ether, isopentane and alcohol) forms a clear glass without crystallizing at low temperature. The absorption spectrum of the solution was observed at room temperature and the glass at liquid-air temperature. The low temperature spectrum exhibited a blue shift for the long wavelength absorption band, and a red shift for the short wavelength band, the relative heights of these bands were interchanged, and at the low temperature the fine structure of some small bands was resolved. However, the spectra of the metalloporphyrins of Sn(II) and Aq(II) showed no shifting of bands at the two different temperatures. Since divalent metals are presumably bonded equivalently to all nitrogens, the metallo-spectra led to the interpretation that isomeric metallo-structures were impossible. Hence, the behavior of the free base suggested that more than one species was present.

Emission spectra provide an experimental method for obtaining information concerning whether or not a given set of absorption bands is due to one or more absorbing species. A fluorescence spectrum is physically and absolutely characteristic of a given substance and results from an electronic transition from the lowest vibrational level of the first excited state to the ground state. If a sample contains two different species it will exhibit two absorption

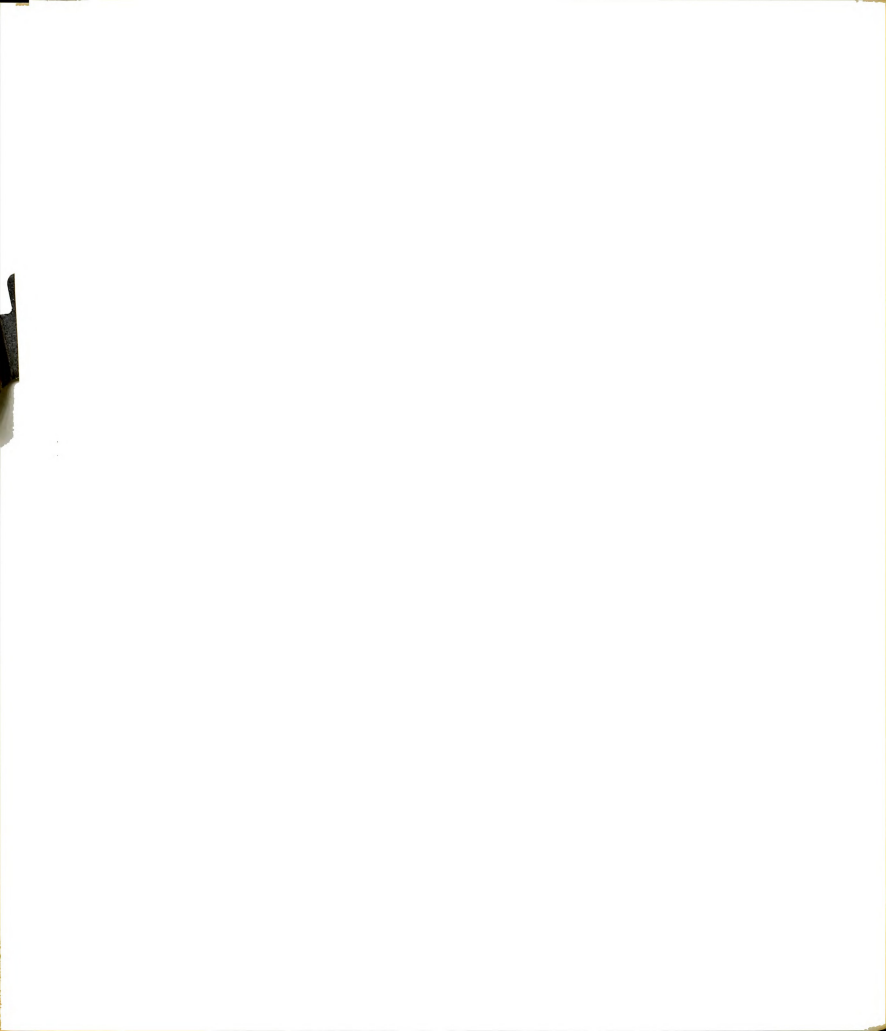


bands which can be excited by a particular wavelength of light and thus two different fluorescence spectra will be obtained. Fluorescence spectra which could corroborate the conclusions drawn from visible absorption spectra have been carried out³², but they contained so many overlapping bands they could not be interpreted easily. However, they appeared to support the proposition that the free base existed as an equilibrium mixture which resulted from the tautomerism of the imino hydrogen atoms.

Theories have been developed which attempt to predict the structural properties of some free base porphyrins and metalloporphyrins. Molecular orbital calculations of porphine by Gouterman³⁴ predicted that the spectrum of the structure with the two central hydrogens on adjacent nitrogens would resemble closely that of the "opposite" tautomer, since the energy of each of four B and Q bands was predicated to fall within 500 cm⁻¹ of its counterpart. Thus the calculation suggested that any "adjacent" tautomer present in solution would be very difficult to detect spectroscopically.

3. Infrared Studies

In the first systematic study of the infrared spectra of porphyrins (in Nujol), Falk and Willis³⁵ found that the N-H stretching vibration appeared as a weak band at 3280-3300 cm⁻¹. In dilute carbon tetrachloride solution, porphyrins gave N-H stretching bands around 3320 cm⁻¹.



A comparison of the N-H stretching bands of pyrrole and indole in dilute solution led to the conclusion that intermolecular hydrogen bonding had to be present, but, the exact nature of this bonding was not suggested.

Subsequently, from solid state infrared spectroscopic studies of porphine and many of its derivatives, Mason36 concluded that the nitrogen atoms of the porphine nucleus were extensively hydrogen bonded. To account for the observations he proposed three possible intramolecular hydrogen-bonding schemes for the free base porphyrin (see Fig. 17). In the first model, the hydrogen atoms were attached to adjacent nitrogen atoms and hydrogen bonded to the remaining nitrogen atoms (Fig. 17a). In the second. the hydrogen atoms were bonded to opposite nitrogen atoms and were hydrogen bonded to the adjacent nitrogen atoms (Fig. 17b). In the third, the hydrogen atoms were symmetrically located between each pair of nitrogen atoms (Fig. 17c). At the time the dimensions of the porphine nucleus were not known, so these models were examined on the assumption that the dimensions of the porphine core were very close to those of phthalocyanine37 (an azaporphine), whose approximate structural parameters were available. From the latter, Mason concluded that the first model would be less stable than the others due to the penetration of each hydrogen atom into the van der Waals sphere of the other. Using similar assumptions and scale models of the porphine core, Badger, et al., 38 excluded the third

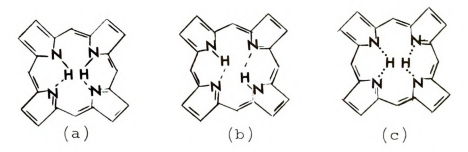


Figure 17. Mason's intramolecular hydrogen-bonded models for porphine.

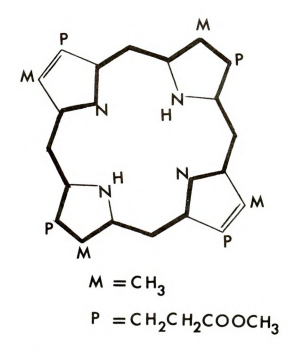


Figure 18. Coproporphyrin.



model, which had symmetrical hydrogen bonds, because the N...N distances of 2.65 and 2.76 $^\circ$ A found for phthalocyanine would clearly cause the N...H bonds to be unsymmetrical. Thus through the process of elimination, the second model was considered the most reasonable.

4. Nuclear Magnetic Resonance

High resolution proton nuclear magnetic resonance spectra of free base porphyrins have been reported by Becker, Bradley, and Watson. 39 The spectra were interpreted in terms of a "ring current" in the # conjugated system as indicated by the heavy line in the porphine skeleton of coproporphyrin I (as shown in Fig. 18). In coproporphyrin I, the methyl groups attached to the two types of pyrrole rings are at different distances from the π electron distribution and should thus experience a different local electrical field. However, the single sharp CH2 line observed in the nmr spectrum indicated the methyl groups were magnetically equivalent. Furthermore, at the freezing temperature of solvent, CDCl2 (-63°C), no broadening of the CH3 line was observed. Thus rapid tautomerism, which would average the properties of the pyrrole rings, was suggested as the only possible interpretation of the CH, magnetic equivalence. Calculations showed that the rate of the tautomerism of NH proton should be much greater than 200 sec-1.

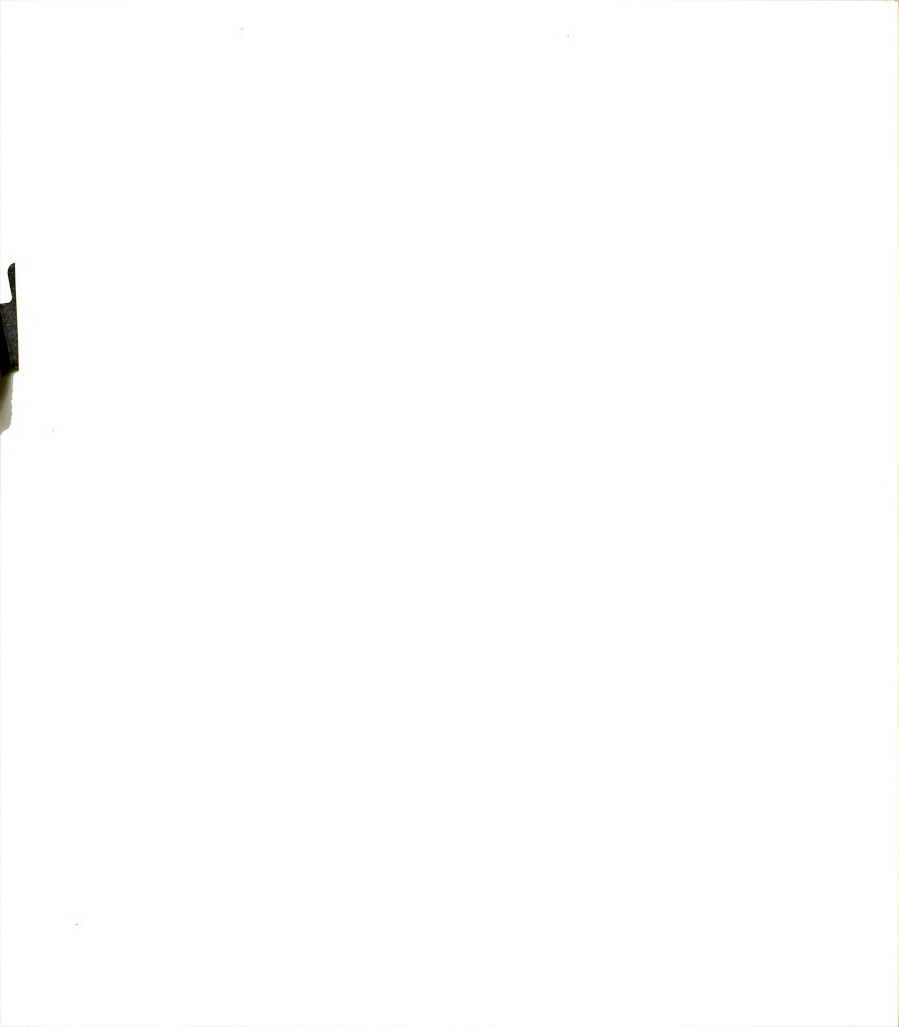


5. X-ray Studies

Several conflicting models of the inner hydrogen atom structure of porphine emerged from the visible, infrared and nuclear magnetic resonance spectroscopic studies. However, the X-ray diffraction crystal structure studies of tri-TPP⁴⁰, tetragonal TPP⁴¹ and porphine⁴² suggest that the central hydrogen atoms are bonded to diagonal nitrogen atoms.

The structure determination of tri-TPP shows two independent pyrroles and phenyl groups. Although the individual pyrrole and phenyl groups are planar, the porphyrin core is nonplanar, as indicated by the fact that one pair of the centrosymmetrical pyrroles is essentially coplanar to the nuclear least squares plane (NLS) of the porphyrin ring, while the other pair, carrying the central hydrogen atoms, is inclined approximately $\pm 6.6^{\circ}$ to this plane. The slight deviation of the two central hydrogen atoms from the NLS plane gives H-H contact greater than the in-plane distance. The four bonds which connect the methine carbon atoms to the terminal carbon atoms of the phenyl groups are abnormally long (1.5 Å), and separate the phenyl rings electronically from the porphyrin ring .

The crystal and molecular structure of tetragonal TPP were determined by Hoard, et al. They found that in each molecule the central hydrogen atoms are bonded to opposite nitrogens. The crystal structure achieves the space group symmetry requirement $(S_4-\bar{4})$ statistically by using a stereochemical species in which hydrogen atoms are attached to a



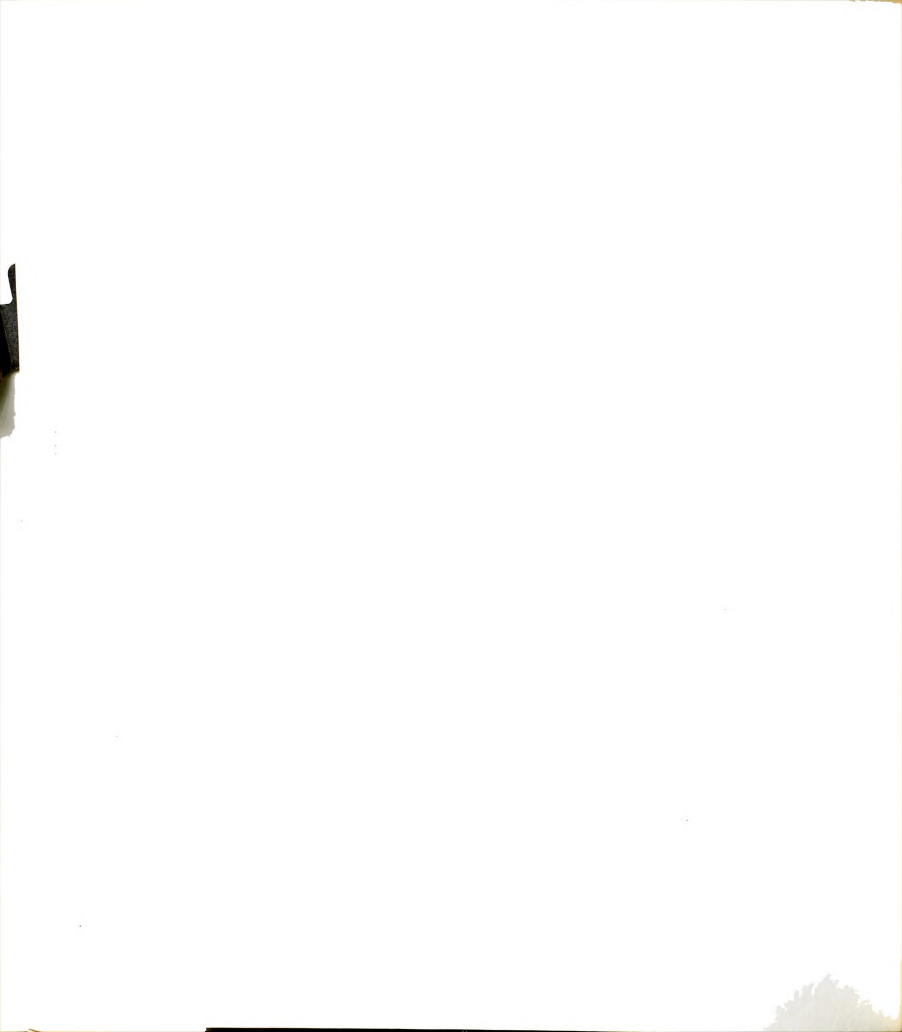
diagonal pair of nitrogen atoms which in turn are in orientations differing by a 90° rotation. The H-H separation is about 2.1 %.

The bond parameters of the pyrrole of tetragonal TPP are almost identical to the average of the two pairs of crystallographically independent pyrroles of tri-TPP. Since tetragonal TPP has the molecular symmetry of a fourfold inversion axis, the four pyrroles are crystallographically equivalent. For this reason, the pyrrole with a central hydrogen is indistinguishable from that without a hydrogen atom. Therefore, a precise determination of the inner hydrogen atom structure in tetragonal TPP is limited.

The structure of porphine was originally determined by Webb and Fleischer. They reported the porphine molecule to be planar, with approximate D_{4h} (4/mmm) symmetry, with four half-hydrogens bonded to the nitrogen atoms. The latter was explained as due to the interconversion of N-H tautomers first suggested by Becker on the basis of nuclear magnetic resonance work. During the structure refinement of the porphine, a peak corresponding to 2-3 electrons was observed at the center of the ring, and it was assumed to be due to a 5-10% impurity of copper porphine. When this electron density at the center of the molecule was removed with a calculated contribution, the four peaks which appeared in the vicinity of the nitrogen atoms were assumed to be half-hydrogen atoms. Since peak heights of the half-hydrogen atoms, 0.31, 0.42, 0.29 and 0.44 e R^{-3} , were only slightly



greater than the background of ± 0.2 e 3 . Their structure determination of the central hydrogens of porphine was at best unreliable. Furthermore, even though the N-H bond distances were reported, the exact nature of the half-hydrogen atoms in relationship to van der Waal's hydrogen contacts was not considered.

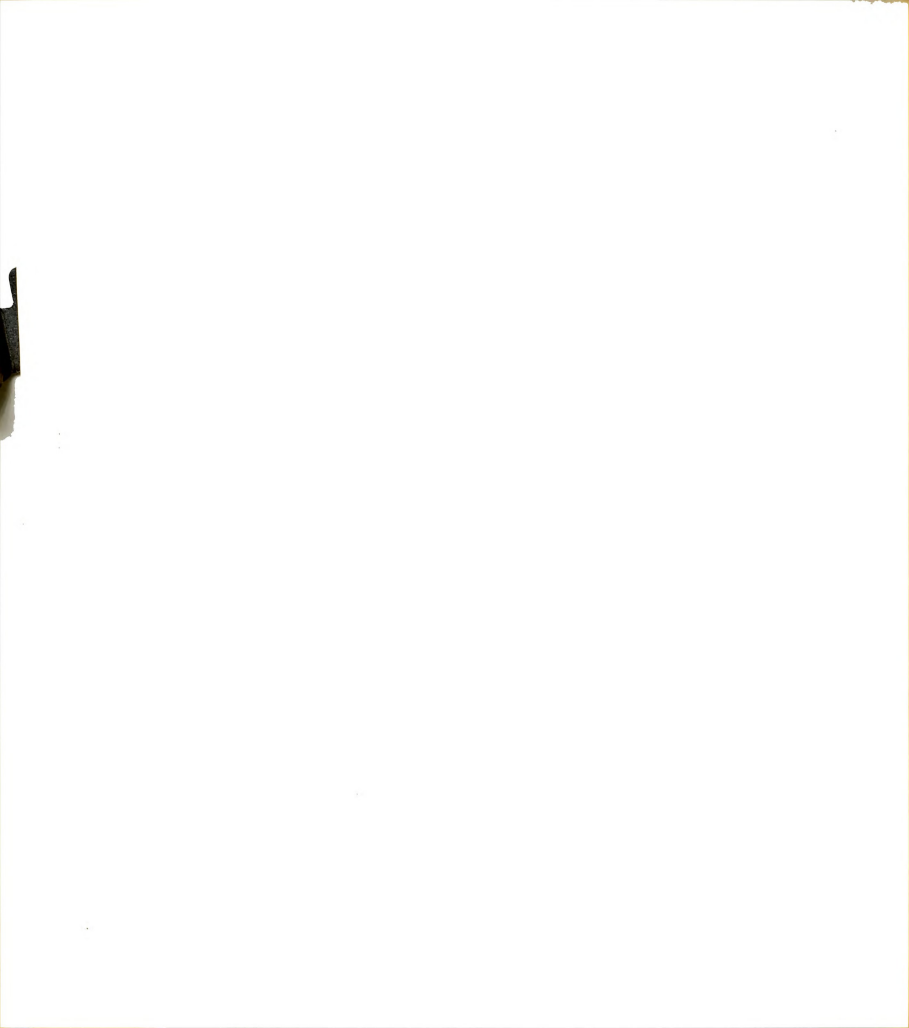


VII. EXPERIMENTAL

1. The Problem of the Hydrogen Atoms

The atomic resolution usually obtainable with $CuK\alpha$ radiation, approximately 0.8 Å, is sufficient to resolve hydrogen atoms bonded to carbon or nitrogen atoms. hydrogen atoms appear only as weak features on the observed electron density of heavier atoms, they are commonly found from a difference synthesis which provides a means for finding hydrogen atoms by subtracting from the observed electron density the density due to the heavier atoms. a difference synthesis is used, the observed structure amplitudes ($|F_0|$), the calculated structure amplitudes ($|F_c|$), the phases, and the scale constant between $|F_0|$ and $|F_c|$ are important factors in determining the hydrogen locations. To locate hydrogen atoms with certainty, accurate structural parameters of the nonhydrogen atoms, which relate to the $|\mathbf{F}_{_{\mathbf{C}}}|^{'}\!\mathbf{s}$, and accurate intensity data, which relate to $|F_0|$'s, are required.

Since the hydrogen atom structure of the porphine molecule, particularly the central hydrogens, was the principal interest in redetermining the structure, it was desirable to know which reflections had a substantial hydrogen atom contribution before intensity data collection



was undertaken. In addition to collecting a complete set of intensities for all independent reflections, additional and more elaborate counting techniques could be applied to those reflections with an expected significantly measurable hydrogen atom contribution, thus minimizing counting errors, and adding more significance to the hydrogen atom locations as revealed in a difference synthesis. The reflections which were to be examined in greater detail were ascertained via a structure factor calculation in which were required the approximate atomic parameters of the hydrogen atoms and the cell parameters of porphine. The necessary structural parameters were obtained from the structure determination of porphine by Webb and Fleischer. 42

The numbering scheme for the carbon and nitrogen atoms in porphine is given in Figure 19. The hydrogen atoms are numbered corresponding to the atoms to which they are bonded. The hydrogen atom structure factor calculations included the methine and central hydrogen atoms, the latter in three different combinations. These combinations arise from the fact that the central hydrogen atoms might be associated with different sets of pyrrole nitrogen atoms. The four structure factor calculations which were computed were based on the following structures:

- (1) H22, H24 structure
- (2) H21, H23 structure
- (3) Four one-half hydrogen structure
- (4) Four methine hydrogen structure (H5,H10,H15, and H20).

.

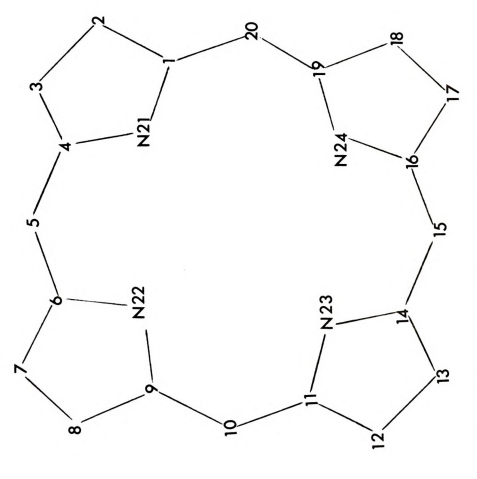
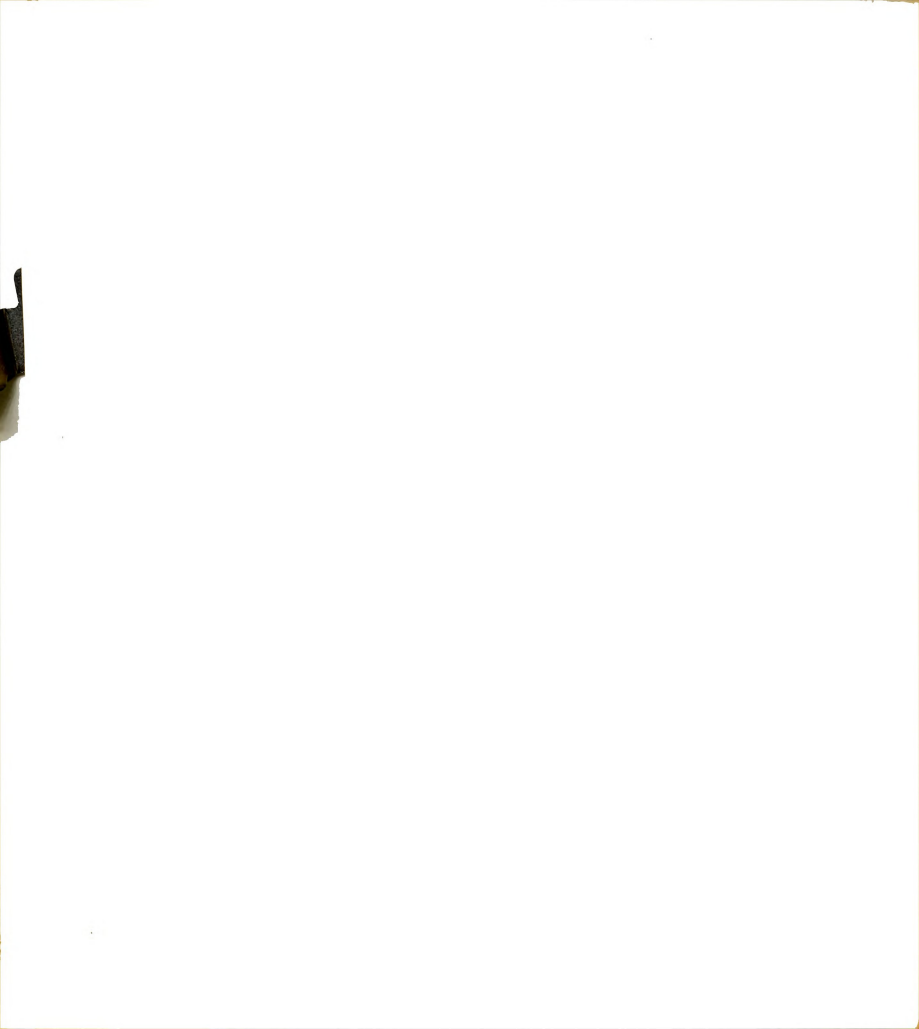
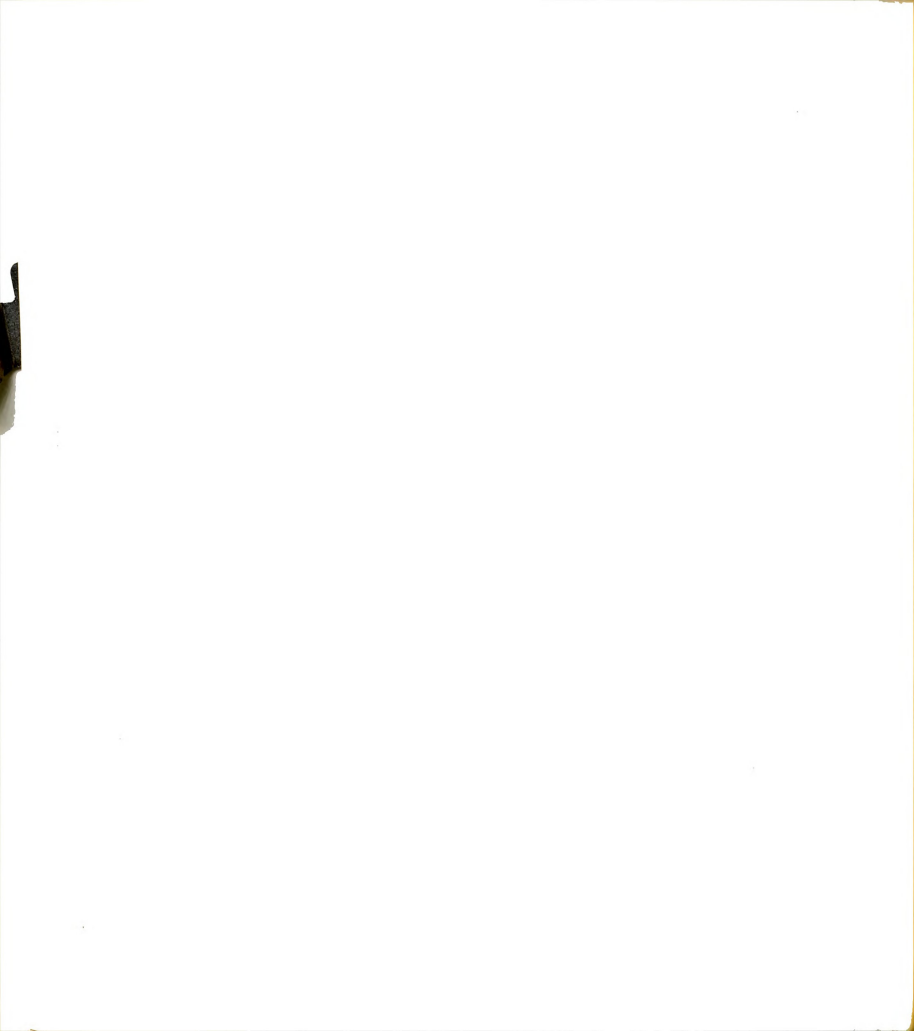


Figure 19. Porphine numbering scheme.



In (1), a structure factor calculation was based on a set of two opposite inner central hydrogen atoms bonded to two pyrrole nitrogen atoms. The second calculation (2) was computed using the other set of two opposite central hydrogen atoms. In (3), half weights were applied to each of four central hydrogen atoms, H21, H22, H23, and H24. This central hydrogen atom structure was the one reported by Webb and Fleischer, which is said to be due to rapid exchange between N-H tautomers. Structure calculation (4) included those hydrogen atoms which are bonded to the bridge carbon atoms of porphine, since these hydrogens were considered important for certain crystal packing properties which might be associated with tri-TPP. All structure factor calculations were confined to the scattering angle of 20 less than or equal to 50° , since the mean scattering factor for a hydrogen atom is less than 0.2 electron beyond this region.

The magnitudes of the four sets of structure factors based on the different models of hydrogen locations were compared. Reflections which might contain significant hydrogen atom contributions were then grouped according to the following scheme: (1) $|F_c| > 2.0$ in any of the structure factor calculations, and (2) $1.0 < |F_c| \le 2.0$ in all the different calculations ($|F_c|_{(\max X)} = 8.0$ for central and 16.0 for methine hydrogen atom calculations). The former included about 10% of all the reflections considered and the latter

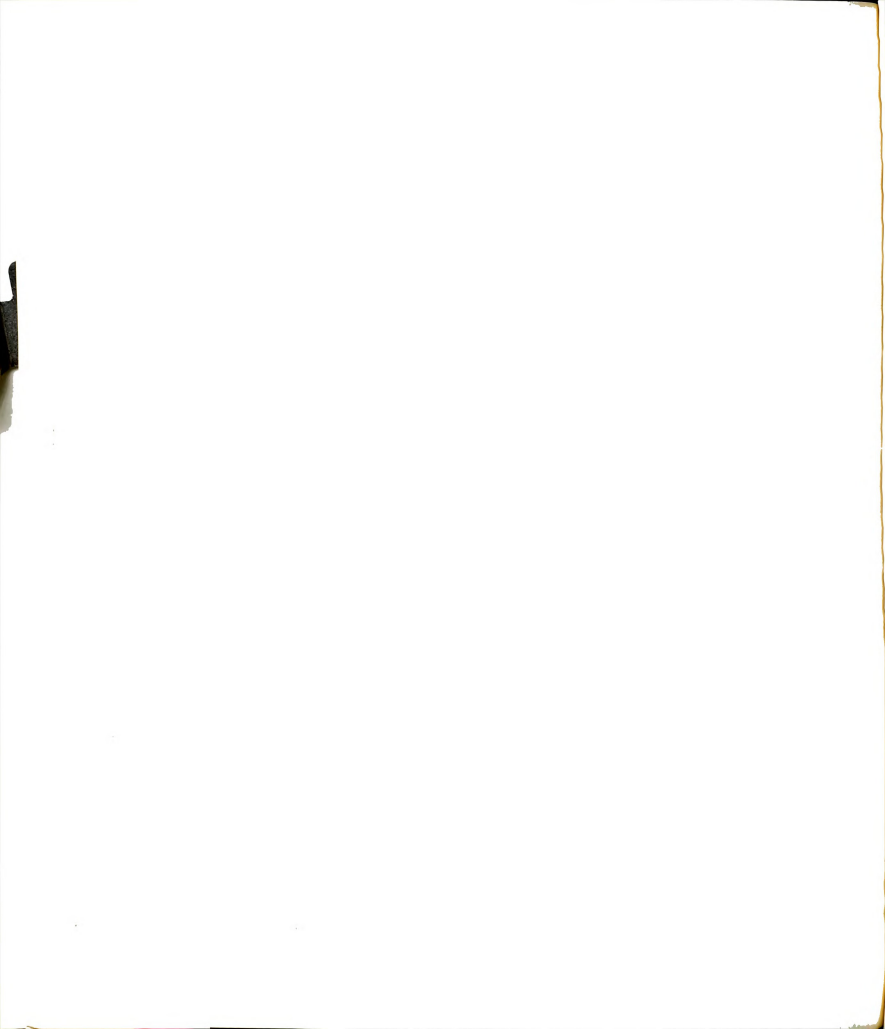


about 20%. The calculated ${\rm F_C}$ for two reflections $(\bar{5}23)$ and $(\bar{5}00)$ are given as examples.

Reflections	Four 1/2H Structure	H21, H23 Structure	H22, H24 Structure	Four Methine H	
(523)	< 1.0	< 1.0	< 1.0	2.3	
(500)	1.2	1.1	1.3	1.6	

After such a process of elimination, eighty reflections considered to be most sensitive to the atomic parameters of the hydrogen atoms were chosen for measurement with more elaborate counting techniques to minimize counting errors. The details of these techniques will be discussed in a later section.

The distribution of structure factors of the central and methine hydrogen atoms of porphine in relationship to the scattering angle (2θ) was also investigated using the four sets of structure factor calculations. A graph of the number of reflections whose calculated structure amplitudes had a value $|\mathbf{F}_{\mathbf{C}}| \geq 1.0$ is shown as a function of the scattering angle in Figure 20. Hence, the reflections which occur at medium scattering angles $(30^0$ to 45^0 of $2\theta)$ may contain significant hydrogen atom contributions and are important for an accurate determination of the hydrogen atom structure.



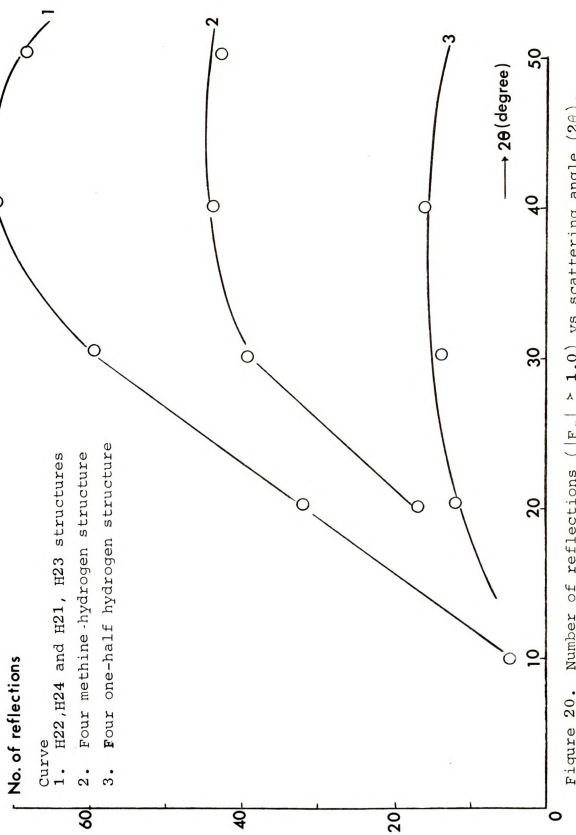
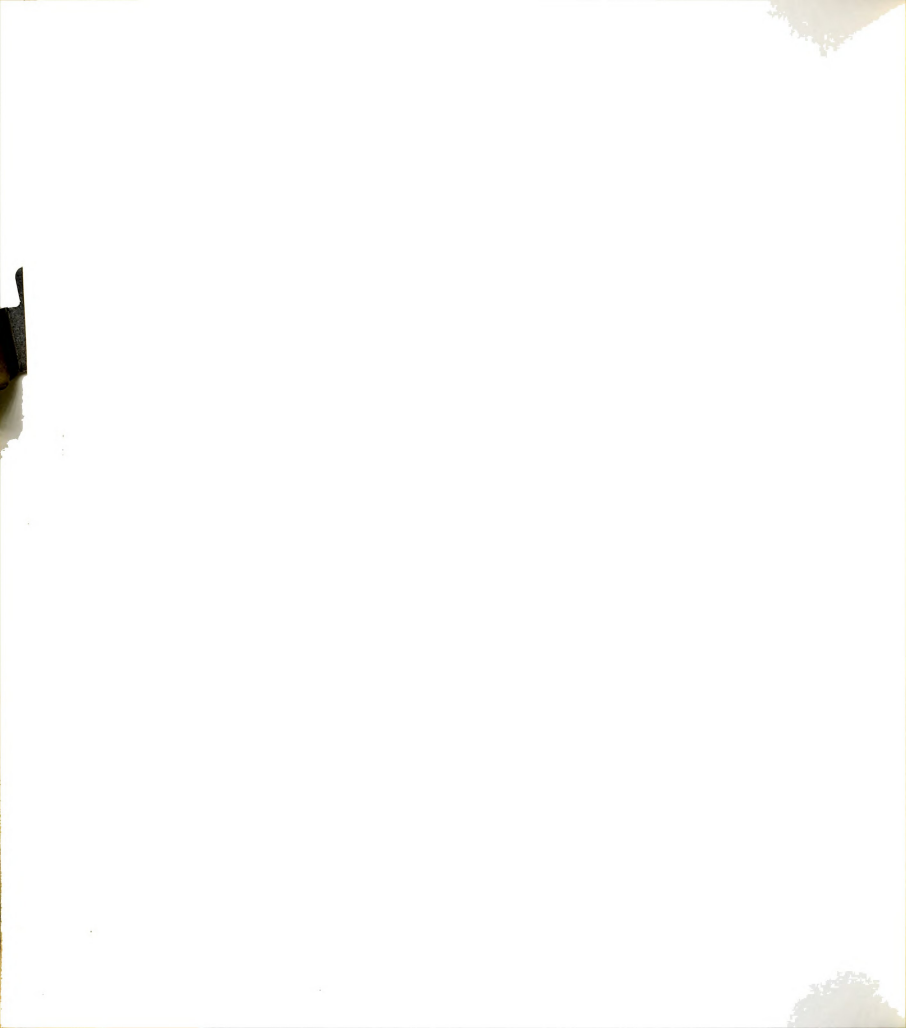


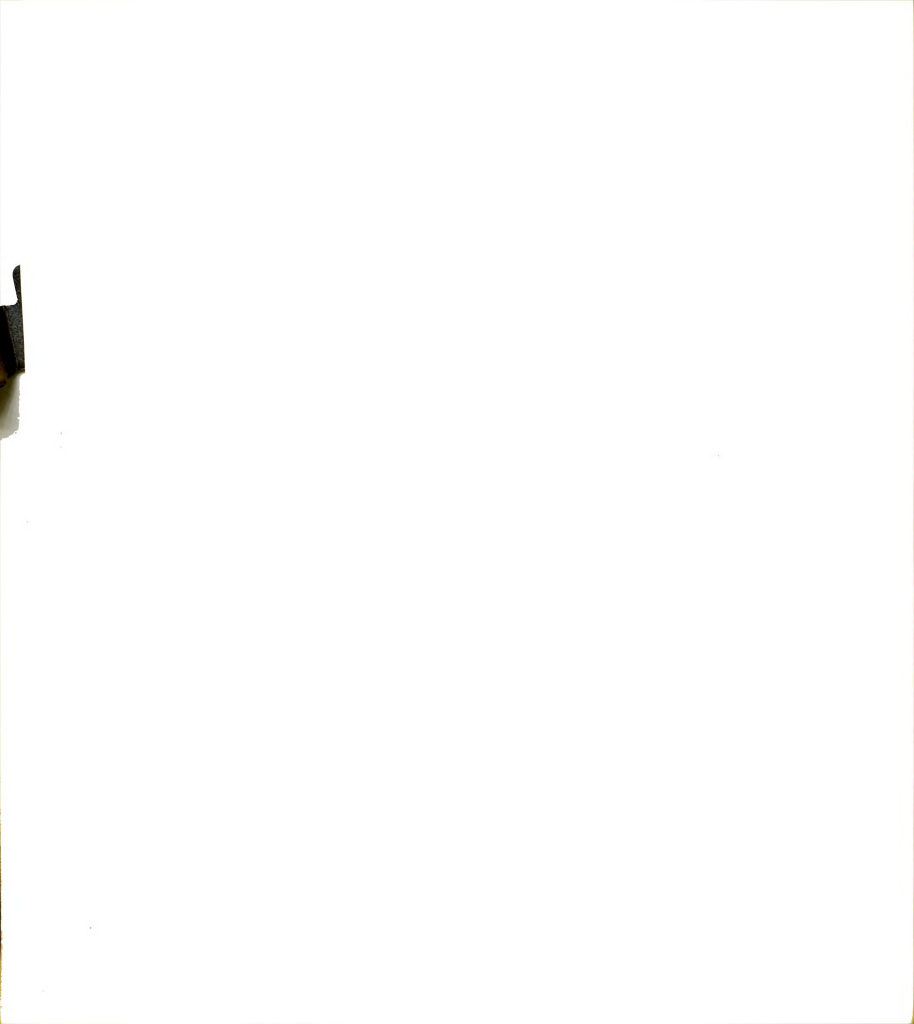
Figure 20. Number of reflections ($|F_{\text{c}}| \succeq 1.0)$ vs scattering angle (20).

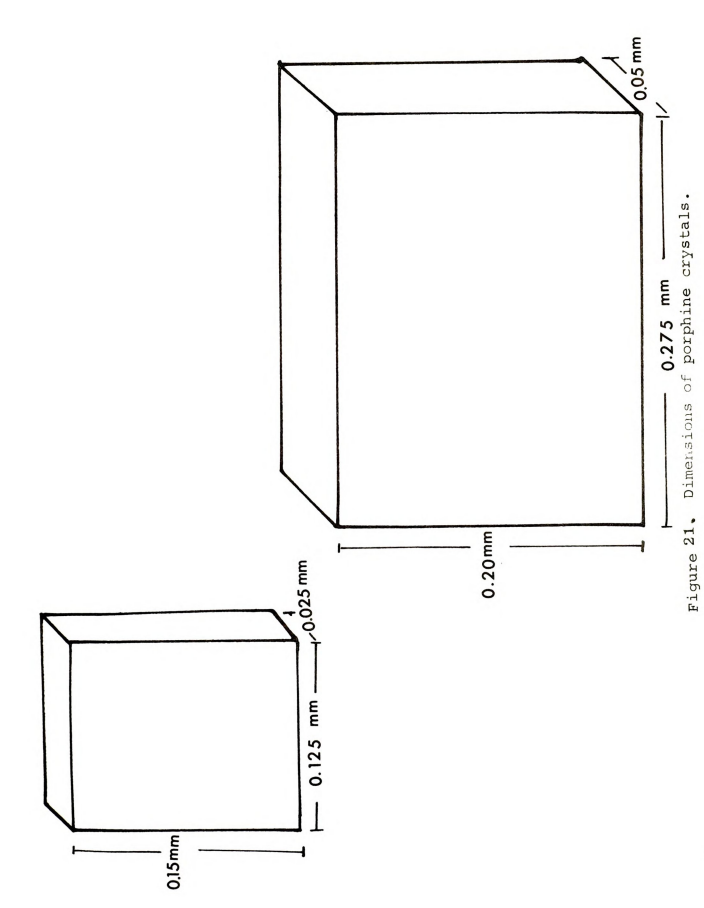


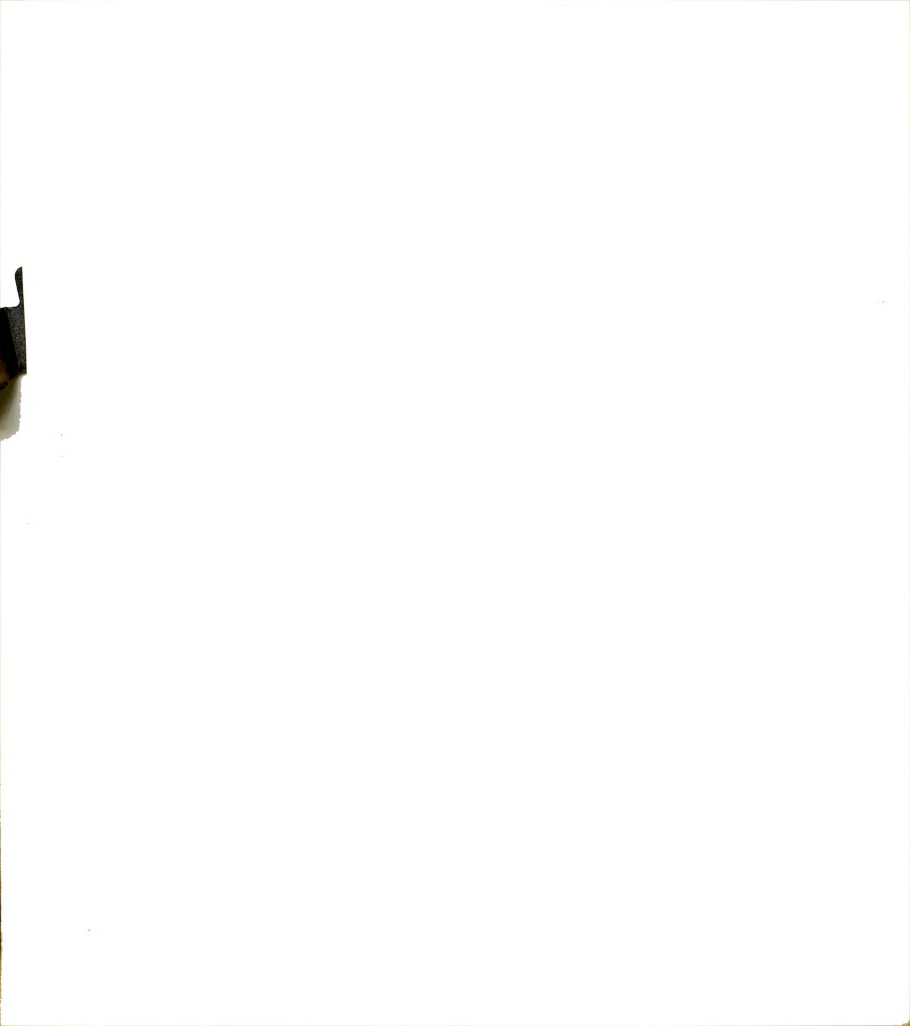
2. Preliminary X-ray Examination

Single crystals of porphine in the form of dark-red square platelets were grown by slow evaporation from a benzene solution. The space group was known to be $P2_1/c$ with the unique b axis located along one of the diagonals of the plate. If the b axis is mounted precisely along the spindle axis of the Weissenberg camera, mirror symmetry perpendicular to the spindle will be seen in an oscillation photograph. Therefore, oscillation photographs were used to find the b axis of the crystal and for preliminary alignment of the crystal.

A crystal with the approximate dimensions of 0.2 x 0.275 x 0.05 mm (shown in Fig. 21) was used for the X-ray (CuK α) data collection which was carried out on a General Electric XRD-5 Diffractometer equipped with a quarter circle single crystal orienter. The porphine crystal was mounted with the unique b axis along the ϕ axis with the a*c* plane in the equatorial plane of the diffractometer when the angular χ setting of the diffractometer is at zero degrees. The angular settings of twelve reflections, which were well-distributed in reciprocal space were carefully measured and subjected to a least squares analysis from which the best orientation and the unit cell dimensions were obtained. The unit cell dimensions and their estimated standard deviations are:







a 10.271 ± 0.003 €

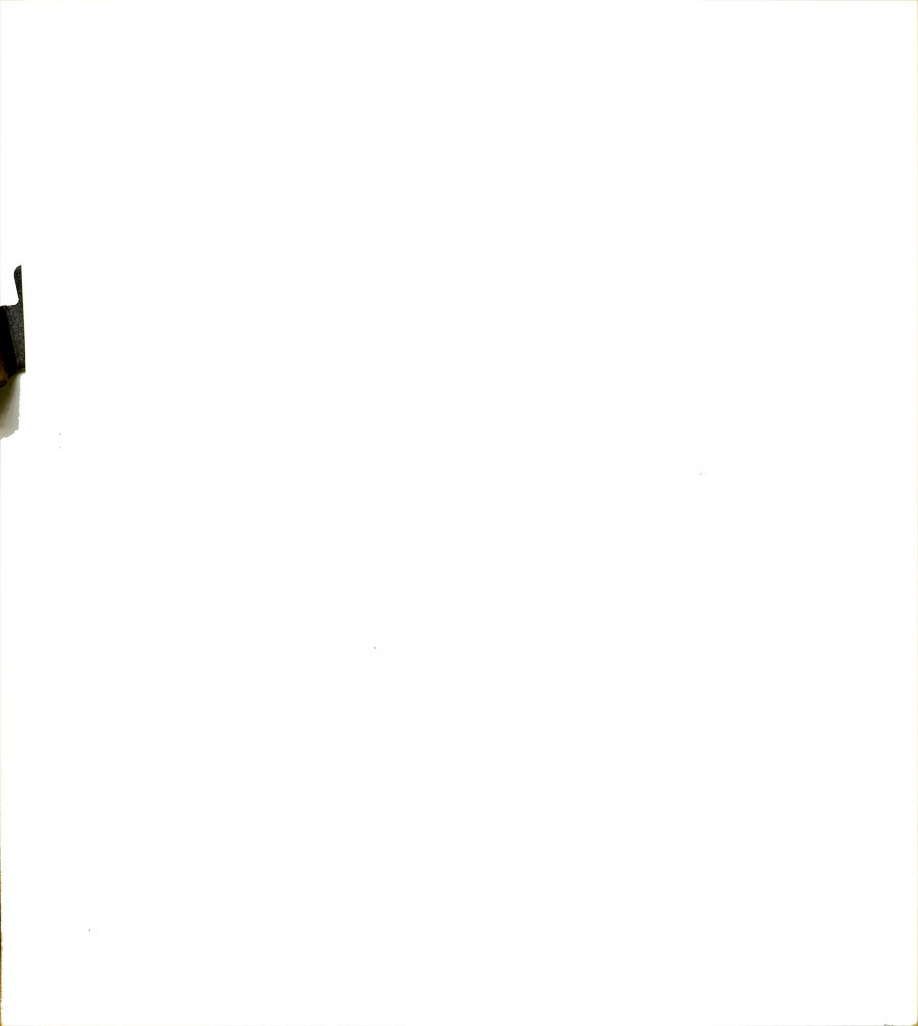
b 12.089 ± 0.003

c 12.362 ± 0.004

B 102.17 + 0.020

Mosaic spreads, which among other things are used for determining the quality of a crystal, were measured on certain reflections by offsetting the azimuthal angle of the reflection to background level and then recording the intensity in 0.05° steps across the peak until the background was encountered again. Since the peak shapes of these mosaic spreads were symmetrical with a maximum peak width of about 0.3° close to the base of the peak, the crystal was judged to be of sufficient quality to allow intensity data to be collected in any quadrant. For convenience, data were collected in the quadrant which was bounded by $\pm a^*$ through $\pm c^*$.

The reflections (040) and (0,12,0) were the only observable reflections along the b* axis. However, (0,12,0) was weak and not suitable for accurate measurements. Therefore, an absorption correction was based on the (040) reflection and was measured before and after data collection with the average of the two measurements serving as the correction. The maximum absorption occurred at the ϕ values corresponding to the -a* axis with a value of 1.07 (Amax(-a*)), and the a* axis (Amax(a*)) with a value of 1.14. The ratio Amax(a*)/ Amax(-a*) = 1.06 indicates the discrepancy in the intensity measurements along the a* and -a* directions. Anomalous absorption effects by a crystal can cause such disagreement between the intensities of equivalent reflections along the a*



direction, namely I(hk0), and those along $-a^*$ direction, I(\$\bar{h}k0\$). The average ratio obtained between the reflections of these two zones (hk0, \$\bar{h}k0\$) was 1.03, obtained from the expression

$$\left\langle \frac{I(\bar{h}k0)}{I(hk0)} \right\rangle_{n=53} = 1.03 \pm 0.02$$

n is number of unique reflections.

The average ratio of 1.03 based on 53 measurements was considered more reliable than the ratio of 1.06 obtained from the absorption curve. Therefore, the absorption curve was adjusted slightly in the regions of the -a* and a* directions to have the ratio of 1.03 instead of 1.06. This adjustment gave the maximum absorption correction of 1.09 at the -a* and 1.12 at the a* direction.

The empirical absorption curve was used with Phillips' method (see Part I) to correct for the absorption of X-rays by the crystal. Basically, the procedure for evaluating the absorption factor as given by Phillips is: (1) calculate the azimuthal angles of incident and diffracted beams,

$$\phi_{\text{inc}} = (\phi_{\text{hk}\ell} - \epsilon_{\text{hk}\ell}) ; \phi_{\text{ref}} = (\phi_{\text{hk}\ell} + \delta_{\text{hk}\ell})$$

where

$$\epsilon_{hk\ell} = \delta_{hk\ell} = \sin^{-1}(\sin\theta\cos\chi),$$

 $^{\varphi}_{hk\,\ell}$ is the $^{\varphi}$ value of the reflection,

and (2) obtain the absorption factors $A(\phi_{inc})$ and $A(\phi_{ref})$

.

from the absorption curve. Then, the absorption factor is given by

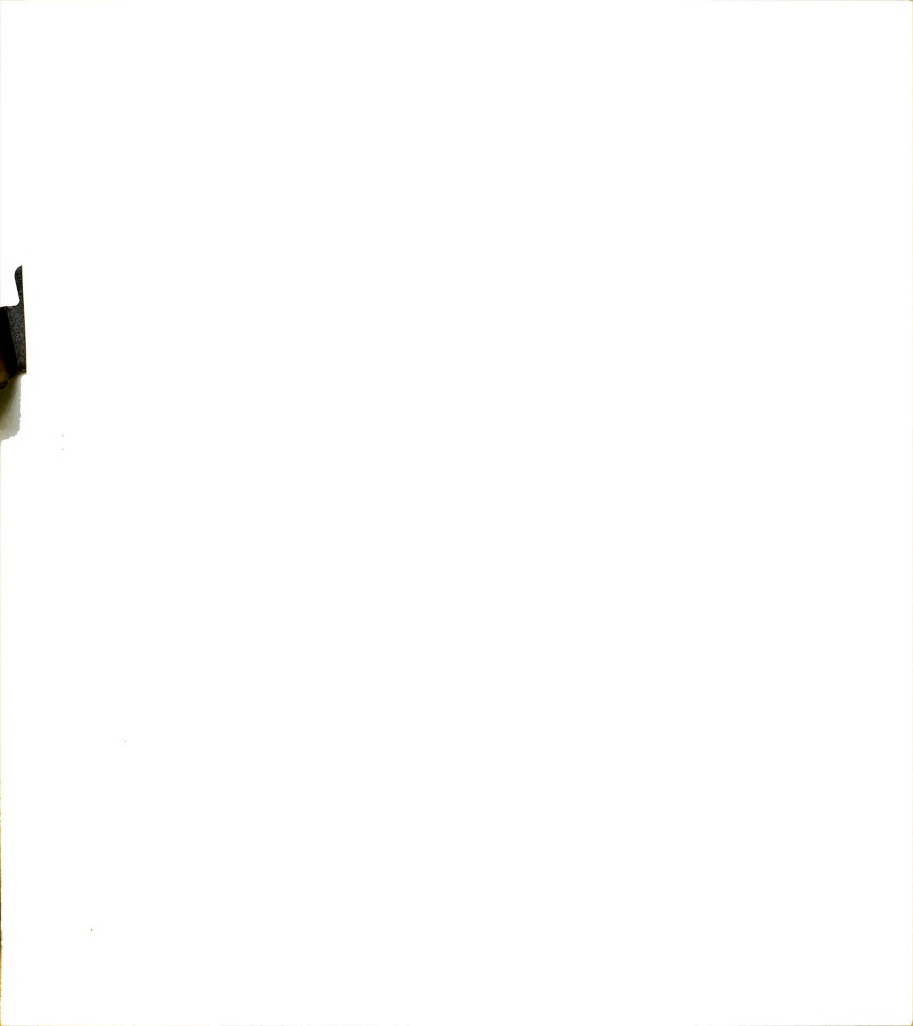
$$\begin{array}{ll} {\rm A}\left({\rm hk}\,\ell\right) & = & 1/{\rm T}\left({\rm hk}\,\ell\right) & = & \frac{1}{\left({\rm T}\left({^{\scriptsize \diamondsuit}}_{\hbox{inc}}\right) \right. + {\rm T}\left({^{\scriptsize \diamondsuit}}_{\hbox{ref}}\right)\right)/2} \\ \\ & = & \frac{2}{1/{\rm A}\left({^{\scriptsize \diamondsuit}}_{\hbox{inc}}\right) + 1/{\rm A}\left({^{\scriptsize \diamondsuit}}_{\hbox{ref}}\right)} \end{array}$$

3. Techniques for Measuring Intensities

In a crystal structure determination, the intensities of all the reflections obtained from intensity-data measurements form a set of relative integrated intensities; from these intensities a set of structure amplitudes can be derived by applying various geometrical and other correction factors. The integrated intensity, I, can be expressed as (see Appendix 1)

$$I = \frac{E \omega_V}{I_0}$$

where $\mathbf{I_0}$ is the uniform intensity of the incident beam, $\boldsymbol{\omega}_{\mathbf{V}}$ is the angular velocity of the crystal, and \mathbf{E} is the total energy of the diffracted beam. The equation indicates that the integrated intensity of a reflection is proportional to the total energy reflected by the crystal at a reflecting position. The measurement of the integrated intensity of a reflection is made by recording the number of quanta entering the detector as the crystal rotates a small angular range about the Bragg position. During this



measuring process, the detector (or a counter) can be either kept stationary or given a small movement relative to that of the crystal. Accordingly, some of the various techniques used for measuring intensities are: (1) stationary crystal - stationary counter, (2) moving crystal - stationary counter, and (3) moving crystal - moving counter.

- (1) Stationary Crystal-Stationary Counter Technique* This technique, as its name implies, involves no mechanical motions whatsoever during the measurement of the intensity. It depends on the apparatus and optics of the experimental arrangement. The conditions required in order to achieve a valid integrated intensity measurement⁴³ are:
 - The intensity distribution across the width of the X-ray source must be uniform.
 - 2) The apparent width of the source must exceed; a) the width of the reflection taken at the base of the mosaic spread curve, b) the dispersion of the spectra range to be measured, and c) the size of the crystal as it must be completely bathed in the X-ray beam.
 - 3) The width of the aperture at the counter must be greater than the apparent width of the source.
 - The response of the counter must be uniform across the entire aperture used, and
 - 5) If the source intensity varies with time, monitor reflections measured at definite intervals must be used to record the fluctuation of X-ray intensity.

^{*}Hereafter, referred to as SX.

The SX technique offers speed and simplicity in data collection, but cannot be used to measure high-order reflections whose spectral components, $K\alpha_1$ and $K\alpha_2$, have angular separations greater than the width of the counter.

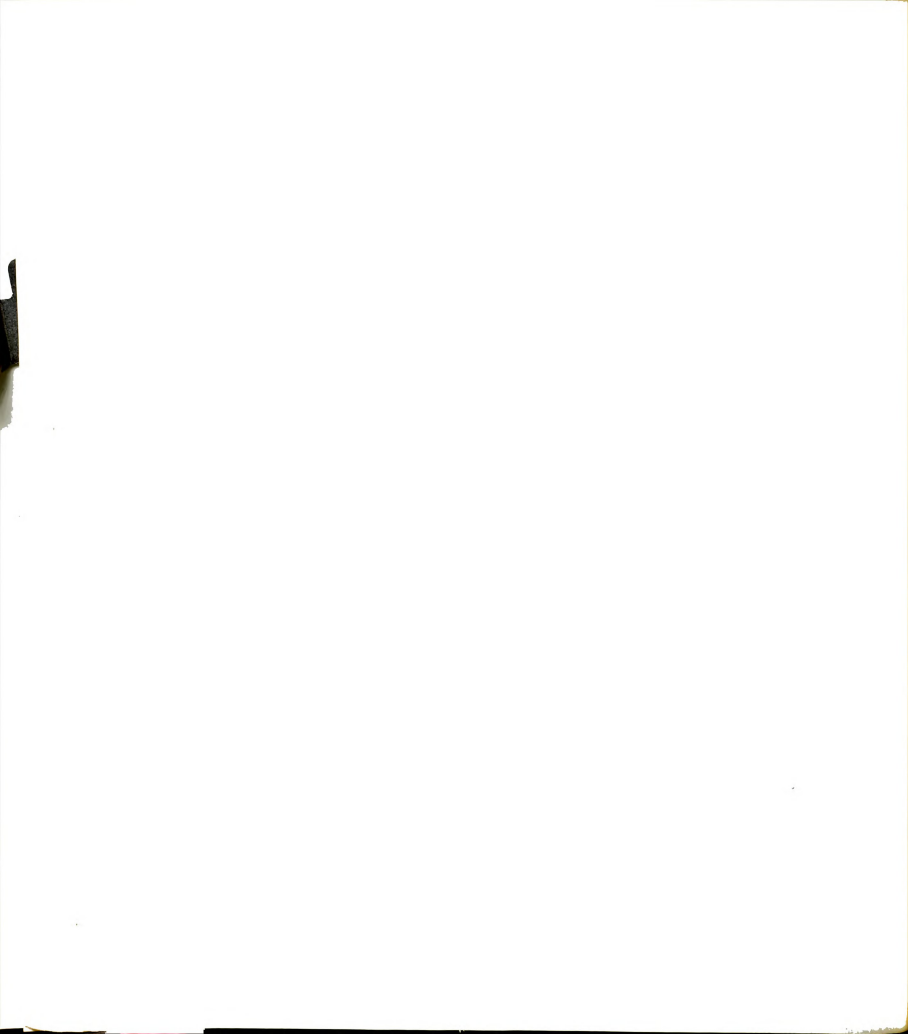
In this work, the SX technique was used to measure the intensities of all reflections within a limiting sphere defined by $2\theta \le 100^{\circ}$. A crystal of appropriate size was chosen so that it was totally immersed in the X-ray beam. Before the intensity of each reflection was measured, the angular settings of the reflection were adjusted so that the diffracted intensity was maximized. The intensity was measured at the adjusted angular settings for a ten second period with a nickel filter and then with a cobalt filter (see balanced filter discussion in Appendix 1). The integrated intensity of a reflection was taken to be the difference between the intensity recorded with the nickel filter and that recorded with the cobalt filter.

(2) Moving Crystal - Stationary Counter Technique*

In this measuring technique, the detector is fixed at the Bragg angle, 2θ , of the reflection and the crystal is rotated with respect to the omega, ω , angle (see Appendix 1). The conditions for a valid integrated-intensity measurement are:

 The crystal must be rotated through an angle large enough to cause every volume element to diffract

^{*} Hereafter referred to as MX.



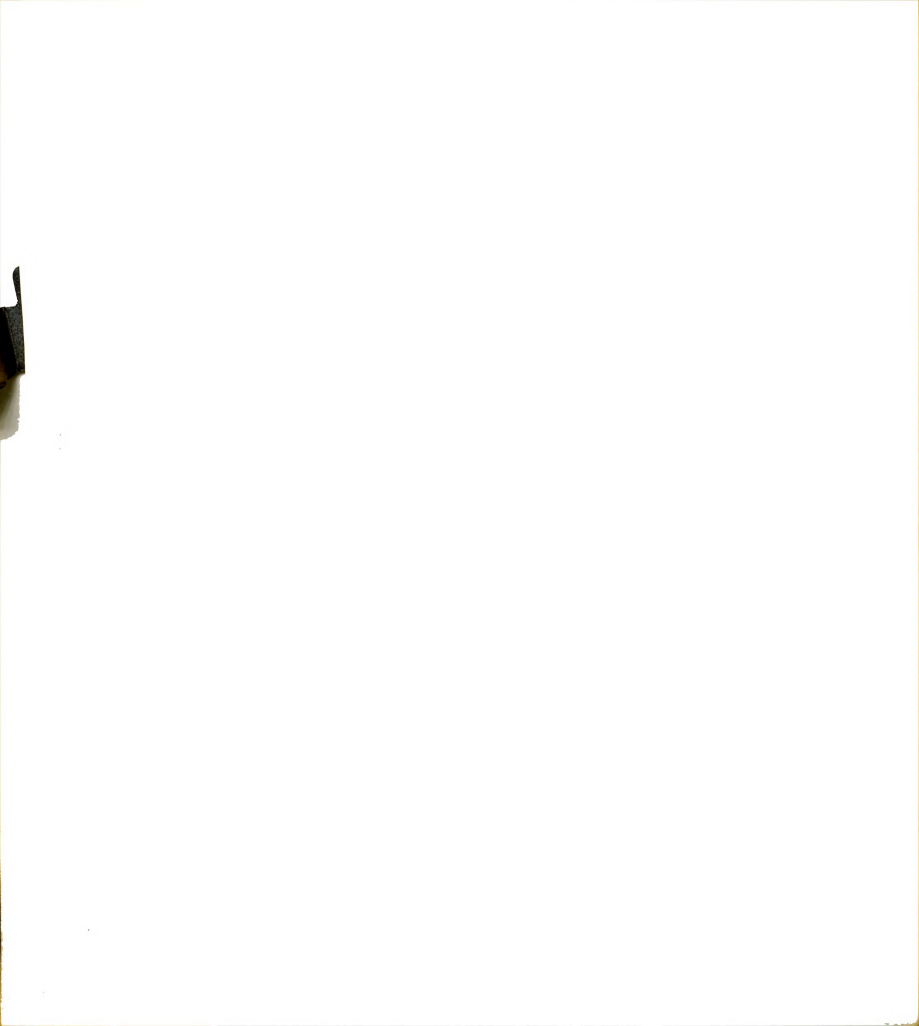
from the full width of the source.

- 2) The counter aperture must be large enough to accept all the radiation of the desired spectral range which is diffracted during the rotation of the crystal.
- The response of the counter must be uniform across the full aperture.
- Each and every increment of the angular position of the crystal rotation carries the same weight in the summation of the diffracted intensity.

The MX technique can be executed either by a continuous scanning motion in angular rotation or by a step-by-step motion. In the present work, a manual step-scan method was used in the intensity collection of the eighty reflections which had been considered to have an important contribution to the structure of the inner and methine hydrogen atoms of the porphine molecule.

The step scan of the MX technique consisted basically of using a count-six-drop-two omega (ω) scan procedure (Wyckoff, 1967).44 The intensity is measured at each of six steps of the most sensitive angular position (ω) and the four largest measurements are used to compute the intensity of the reflection. The reasons for applying this procedure to this work are: (1) to increase the tolerance of the most sensitive angular setting (ω) , and (2) to have the best efficiency of total counting time.

Two methods, constant-count timing and constant-time



counting can be used to record the intensity at each step in the ω scan procedure. The counting rate in the constant-time-counting procedure consists of accumulating counts during a predetermined time $\tau,$ and dividing the count accumulation, N_j , by $\tau.$ The other method, constant-count, is to measure the time t_j required to accumulate the predetermined number of counts, c. The expressions for the counting rate, \mathbf{I}_j , in each method are:

 $I_j = N_j/\tau$ for constant-time counting $I_j = c/t_j$ for constant-count timing.

The corresponding estimated variances of these methods as derived by A. J. C. Wilson 45 are:

and

$$\sigma_{\text{ct}}^{2}(\text{I}_{j}) = \text{I}_{j}/\tau$$
$$\sigma_{\text{cc}}^{2}(\text{I}_{j}) \sim \text{I}_{j}^{2}/c$$

where the subscripts ct and cc denote constant-time and constant-count, respectively. The variance of the intensity for a reflection can be minimized by proper adjustment of the time of measurement for the constant-time method, or by a careful choice of the predetermined count for the constant-count method. The variance of intensities in the constant-time count is directly proportional to the intensity, \mathbf{I}_{j} , while that in constant-count method is proportional to the square of the intensity. Therefore, the magnitude of the intensity of the reflection should also be taken into the consideration to choose which of the measuring techniques should be used for that reflection. In this work, the constant-time step scan technique was used for the intensity measurement of low intensity reflections, i.e., integrated intensity of a reflection less than 200 counts/10 seconds

as determined from SX measurements, and the constant-count step scan technique was used for medium and high intensity reflections. Details of the application of these measuring techniques will be discussed later.

a. The X-ray Detector.

The electronic circuitry in the detection and counting unit of G.E. XRD-5 Diffractometer consists of two main parts, the Electronic Time Register and the Scaler. The Electronic Time Register consists of six glow transfer counter tubes from which time information can be obtained by observing the relative position of the small glow discharge in each of six glow tubes.

The scaler circuits standardize and accumulate the pulses received from the X-ray detector. In addition, various control circuits are available to provide for manual, preset counts and preset time counting. The pulses accumulated by the scaler in one counting cycle, defined as the time necessary to accumulate a specified number of pulses or a specified time interval, are displayed by eight Decimal Counting Units.

b. Constant-time Step Scan Technique*

This method requires the number count, $N_{\dot{1}}$, for each step to be accumulated for a predetermined time interval, T. The predetermined time, T, is selected by a switch on the XRD-5 scaler units, and N; is indicated by visual read-out scalers. The counting rate, N_i/τ , is recorded and calculated.

Hereafter referred to as CTST.



The step-scan was performed with respect to the most sensitive angular position (ω) . The scan extended approximately ± 0.10 from the calculated position and the step scan was carried out in 0.04° increments. The intensity was measured for a preset time of 100 seconds at each of the steps and the four largest measurements were totalled to give the intensity of the reflection (count-six-drop-two, Wyckoff, 1967).44 The crystal was then moved to the wposition displaying the highest intensity and the background was recorded at this position for 100 seconds with a balanced cobalt filter. Intensities measured for the (241) reflection are given as an example of this measuring technique, along with the corresponding SX values (see Table 13). The intensities of the (241) reflection obtained from the two measurement techniques, can be compared on the basis of relative error, ϵ , (Parish, 1965)46 to see which measurement has the least error. The relative error in the constant-time measurement is inversely proportional to the square root of the total number of counts accumulated at the Bragg position, i.e., $\epsilon \propto 1/\sqrt{N}$. The number of counts accumulated by the SX technique is 97, and that by the CTST technique is 3774. Thus the ratio between the two relative errors can be written as,

$$\frac{\varepsilon_{\text{CTST}}}{\varepsilon_{\text{SX}}} \ = \frac{\sqrt{97}}{\sqrt{3774}} \ \sim \ \frac{1}{6} \ .$$

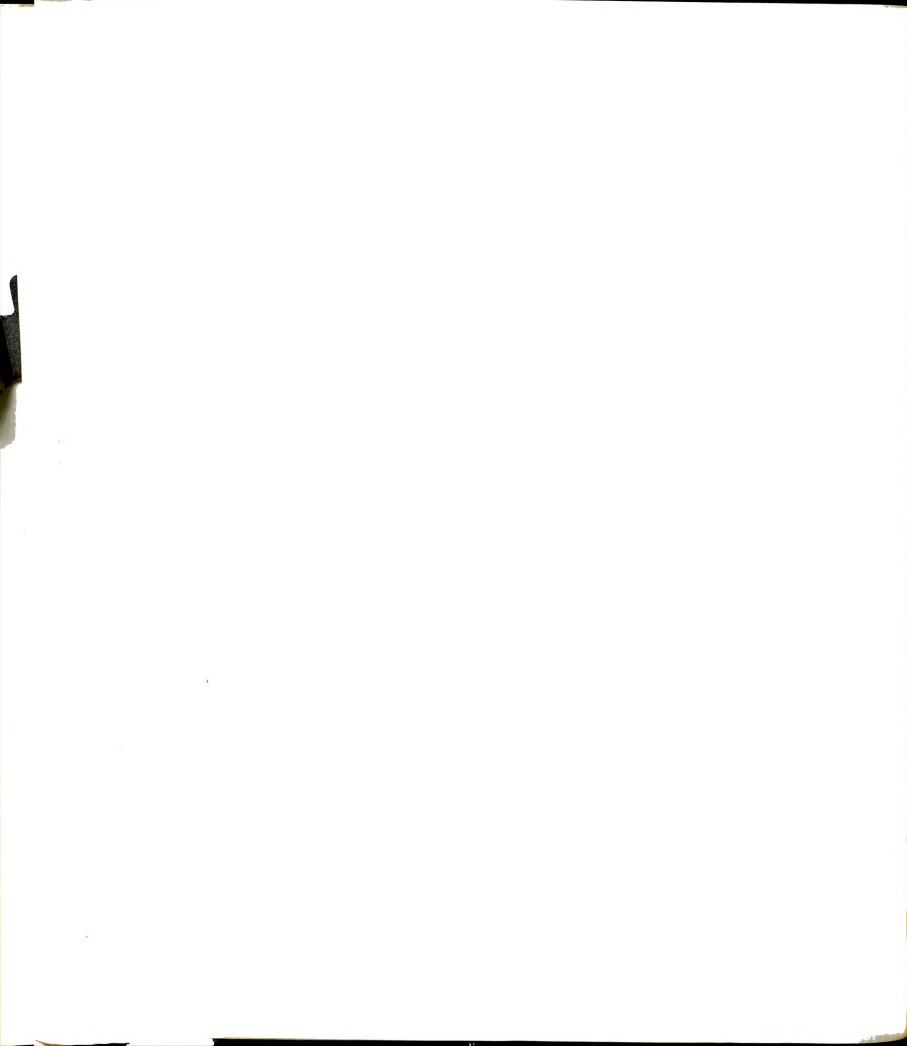
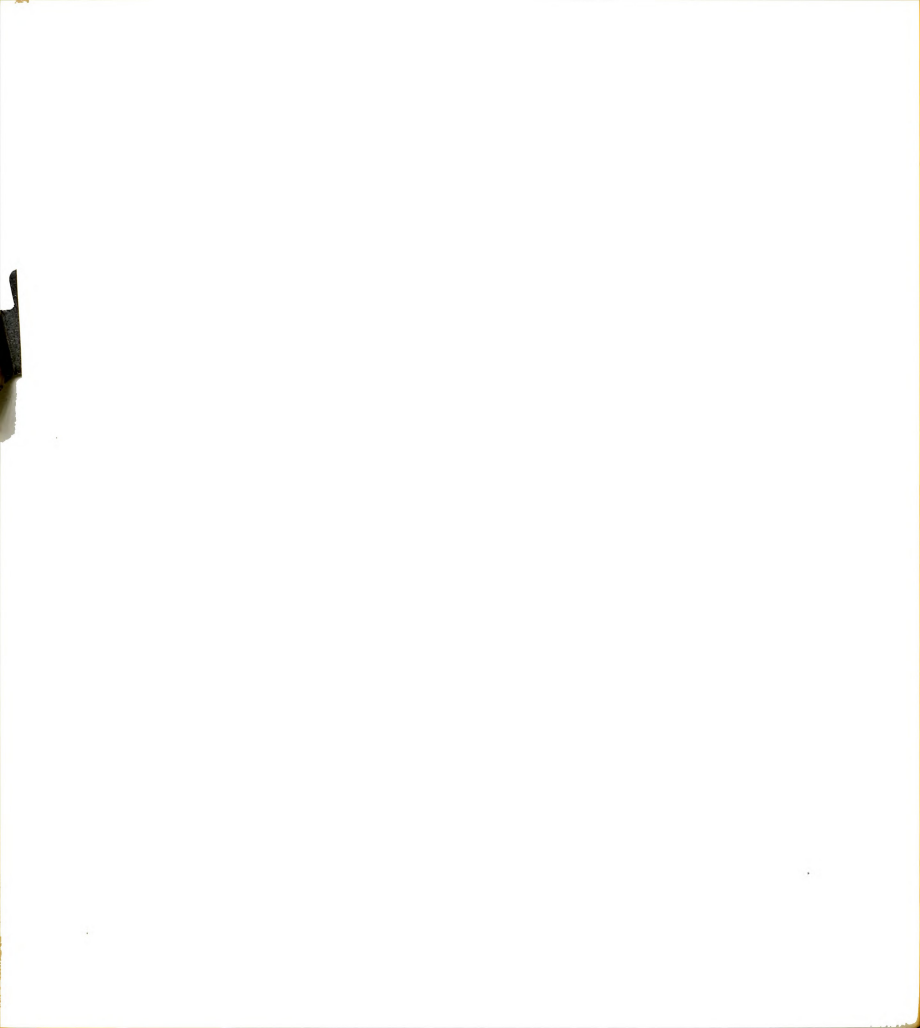


Table 13. Intensities of $(\bar{2}41)$ Reflection Measured by CTST and SX Techniques.

Intensity		CTST		sx
	φ Settings (degree)	Time (sec)	Accumu- lating counts	,
	278.30	100	917	
	278.34	100	939	
	278.38	100	948	
	278.42	100	960	
	278.46	100	927	
	278.50	100	894	
	background at			
	278.42	100	139	
I _{Ni}	94 c/10 sec*			97 c/10 sec
I _{Co}	14			13
Inet	80			84

 $^{^*(}I_{Ni})_{CTST}$ = (939 + 948 + 960 + 927)/400 = 3774/400 = 94 c/10 s

 $⁽I_{CO})_{CTST} = 139/100 = 14 \text{ c/10 s.}$



This calculation indicates that the relative error of (241) reflection obtained from CTST technique is much smaller than that from the SX technique. In addition, the step scan technique across the peak position eliminates slight variations in peak shapes resulting in a better integrated intensity. Therefore, intensities derived by the SX technique were removed by the CTST procedure before conversion to the corresponding structure factors.

c. Constant-Count Step Scan Technique*

This measuring technique is essentially the same as that of CTST technique except that the time, $\mathbf{t_{j}}$, to accumulate a constant number of counts, $\mathbf{c_{i}}$ is recorded. The number of counts to be used at each step was determined according to the intensity scheme listed in Table 14. The reflection ($\overline{4}12$) is used to compare this measuring technique to the SX technique (see Table 15). Based on Wilson's estimated variance, the SX method gives

$$\sigma_{\text{SY}}^2$$
 = $I_{\dot{\gamma}}/\tau$ = $(237 \text{ c}/10\text{s})/10\text{s}$ = 2.4 c/s²

and CCST has a variance of

$$\sigma_{\text{CCST}}^2 = \Gamma_{\text{j}}^2/c = \frac{24 \times 24 (c/s)^2}{4000} = 0.2 c/s^2$$

This estimated variance indicates that the intensity of this reflection as determined by the CCST technique is about an

×

^{*}Abbreviated as CCST.

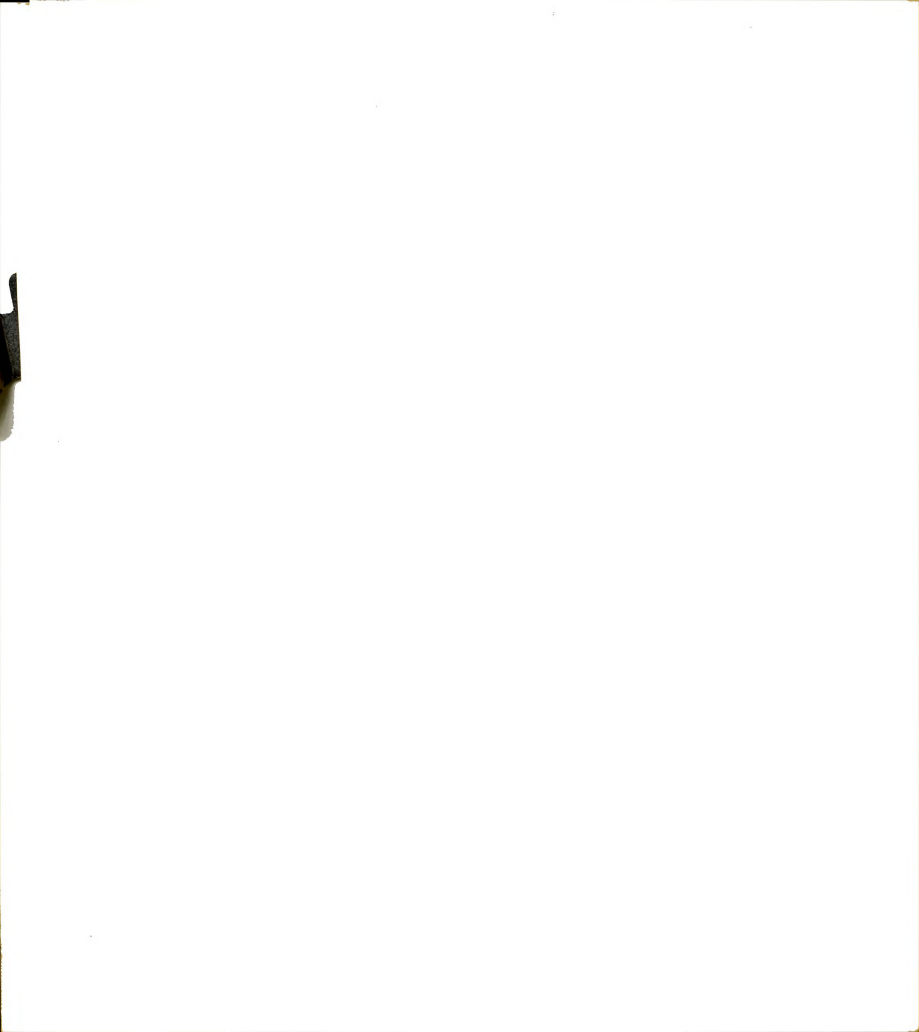


Table 14. Step Scan Measurement.

Intensity Range $(ext{c/10s})$ of SX	Counting Technique	Count at Each Step	Time at Each Step (seconds)	Back- ground at Peak
I < 200	const.		100	100 s.
200 ≤ I < 2000	const.	1000		100 c.
2000 \(\text{\tint{\text{\tint{\text{\tinit}\text{\text{\text{\text{\text{\text{\text{\text{\text{\texi}\text{\texi}\tex{\text{\text{\texi}\text{\text{\text{\text{\text{\text{\text{\te\tin}\text{\text{\texi}}\text{\text{\text{\text{\texi}\text{\tex{\text{\texi}\text{\text{\texit{\texic}\text{\texi}\text{\texit{\texi}\text{\texi}\text{\texitile}}\text{\texitile}}\texiti	const.	10,000		1000 c.
I ~ 10,000	const.	100,000		10,000 c.

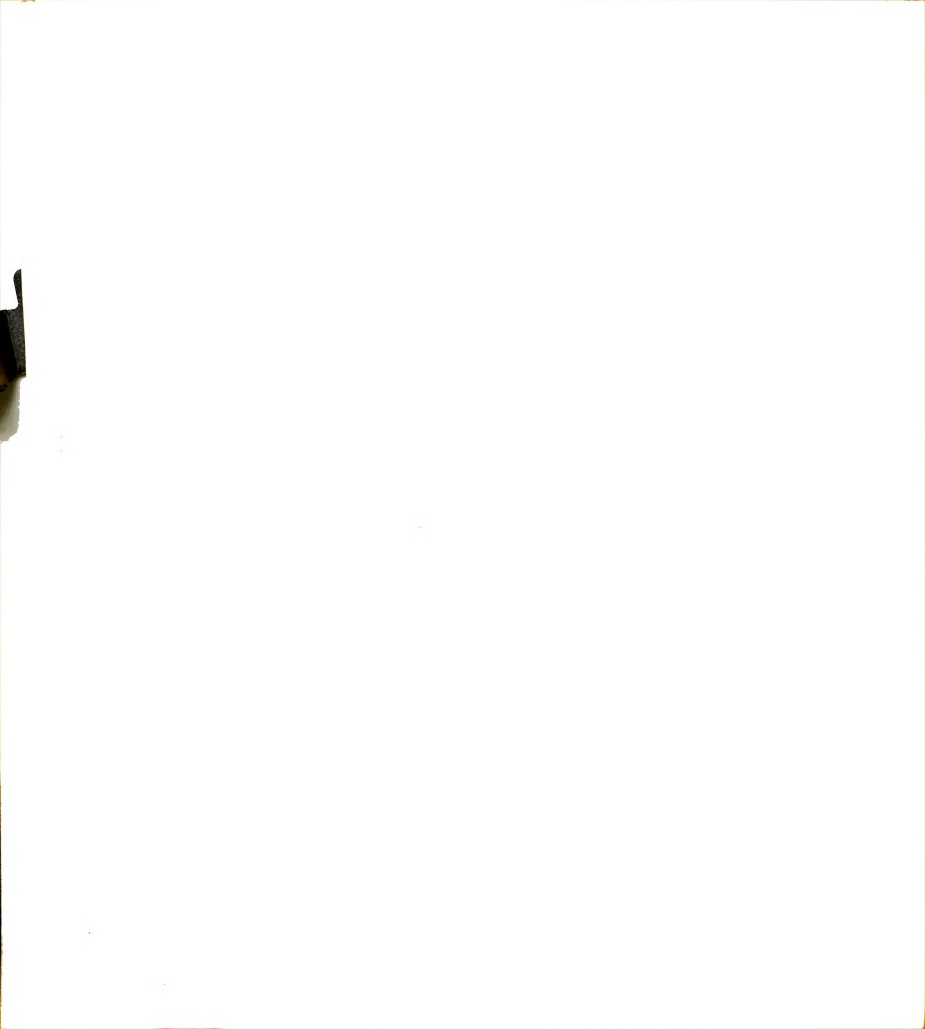


Table 15. Intensities of Reflection $(\overline{4}12)$ Measured by SX and CCST Techniques

Intensity	CCST			sx		
	o Settings (degree)	No. Count for Each Step	Time (sec)			-
	278.24	1000	40.62			
	278.28	1000	38.31			
	278.32	1000	35.97			
	278.36	1000	34.71			
	278.40	1000	35.55			
	278.44	1000	39.22			
	backgrour at	nd				
	278.36	100	25.92			
I _{Ni}		277 counts/1	0 sec*	274 c	ounts/10	sec
I _{Co}		39		37		
Inet		238		237		

 $^{^*(}I_{Ni})_{CCST} = 4000/(38.31 + 35.97 + 34.71 + 35.55) = 277 c/10s$ $(I_{CO})_{CCST} = 100/25.92 = 39 c/10s$



.

order of magnitude better than that measured by the SX technique. Therefore, the latter procedure was replaced by the former for the hydrogen structure determination of porphine.

(3) Moving Crystal-Moving Counter Technique (2θ-scan)*

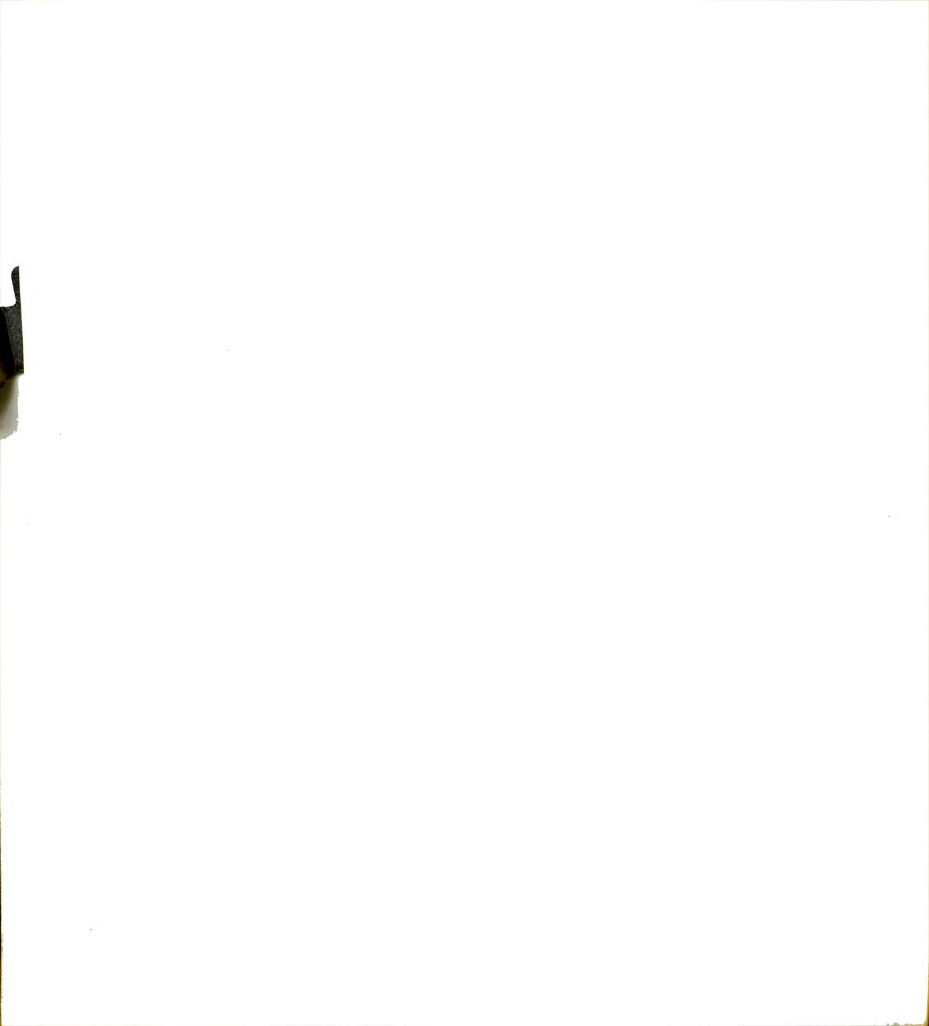
In the MX-MC intensity measurement technique, the counter moves at twice the angular displacement of the crystal. The conditions necessary to obtain a valid integrated intensity are very similar to those for the MX measurement.

4. Data Collection

With the scattering angle limit of 100° a total of 1725 reflection intensities were measured using the SX technique. In order to estimate the intensity limit for unobserved reflections, the systematically absent reflections of the $(h0\,\ell)$ zone and the (0k0) reflections were measured. For these 88 reflections, the average intensity was 5 counts/10 seconds. Therefore, reflections with intensities greater than 5 counts/10 seconds were taken to be observed reflections. After rejecting the unobserved and redundant reflections ($\pm hk0$), 1206 independent reflections remained to compute structure amplitudes.

During the course of the intensity data collection, the reflections (500), (040) at a ϕ value of c^* -axis and (040) at a ϕ value of \overline{a}^* -axis were used to monitor any intensity fluctuation of the X-ray source and/or the

^{*} Abreviated as MX-MC.



alignment of the crystal during each interval of measurement. A total of 32 monitor measurements were taken throughout the data collection. The standard deviations of the intensities of these monitor reflections were 1.2% for the (500), 1.8% for the (040) reflection along the c*-axis, and 1.1% for the (040) along \bar{a}^* direction. These deviations indicate that the intensity fluctuation of X-ray source was insignificant and the crystal remained well-aligned throughout the data collection.

In space group $P2_1/c$ the intensities of the (hk0) and (hk0) reflections are equivalent. A comparison of these equivalent reflections was made in terms of a residual index R_a expressed as

$$R_{e} = \frac{\frac{67}{2} |\text{I}(\bar{h}k0) - \text{kI}(hk0)|}{\frac{67}{2} |\text{I}(\bar{h}k0) + \text{kI}(hk0)|/2}$$

where k is the scale constant of 1.03 obtained from the average ratio of the intensity of $(\bar{h}k0)$ to that of (hk0). Theoretically, the intensity of an (hk0) reflection should be equal to that of an $(\bar{h}k0)$, but discrepancies which are due to absorption and other such experimental causes are found in practice. The R-value obtained with 67 equivalent reflections was 3.8%. The residual index is an indication of the reliability of the data and is certainly acceptable, especially when considered in terms of the $|F|^{\frac{1}{2}}$ s.

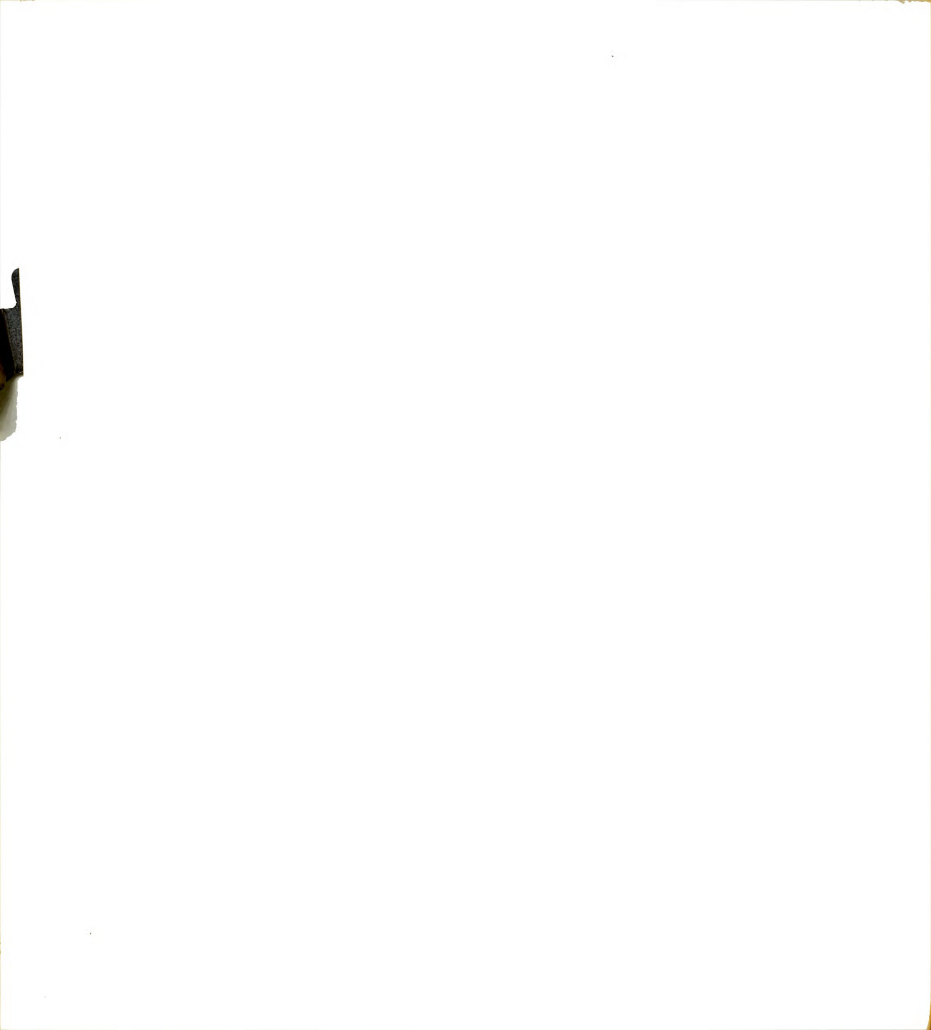
5. Calibration Between Measuring Techniques

Since various intensity measuring techniques were used, systematic errors could arise between different sets of data due to possible scaling errors. Calibration constants between the sets were evaluated by comparing the average ratio of the intensity measured by the SX technique to that measured by the CTST technique, and by comparing the average ratio of intensity measured by the SX method to that determined by the CCST method. They are

$$\left\langle \frac{I_{SX}}{I_{CTST}} \right\rangle_{n=24} = 0.99 \pm 0.06$$

$$\left\langle \frac{I_{SX}}{I_{CCST}} \right\rangle_{n=54}$$
 = 1.00 ± 0.04

where n is the number of the reflections used in the averaging. Since these average ratios were very close to unity, it was not necessary to correct the intensities of the same reflection measured by different techniques, and the intensity measured by the SX technique was directly replaced by that measured by the step-scan method for use in the structure amplitude calculations.



VIII. STRUCTURE DETERMINATION

1. Isotropic Refinement

A trial structure based on the coordinates reported by Webb and Fleischer (abbreviated W&F)42 and isotropic temperature factors for the four nitrogen and twenty carbon atoms (see Table 16) were used to compute a set of initial structure factors. The R-factor for this calculation was 0.142, and decreased to 0.139 after one cycle of least squares refinement of all the parameters (with unit weight), After some small calculated structure factors were eliminated. 1177 (out of 1206) reflections were used to compute the first observed electron density, pol, and the first difference electron density, $\ensuremath{\Delta\rho_1}$. All the hydrogen atoms were located from Δρ1 at approximately the expected positions in the difference density map. The most striking difference from the W&F structure was the presence of only two central hydrogen atoms which were attached to two opposite nitrogen atoms. The peak heights of the two central hydrogen atoms were approximately 0.3 e/A^3 for H22, and 0.4 e/A^3 for H24; these peak heights were somewhat lower than the average peak height (0.5 e/A^3) of the remaining hydrogen atoms. In addition to these features, residual electron

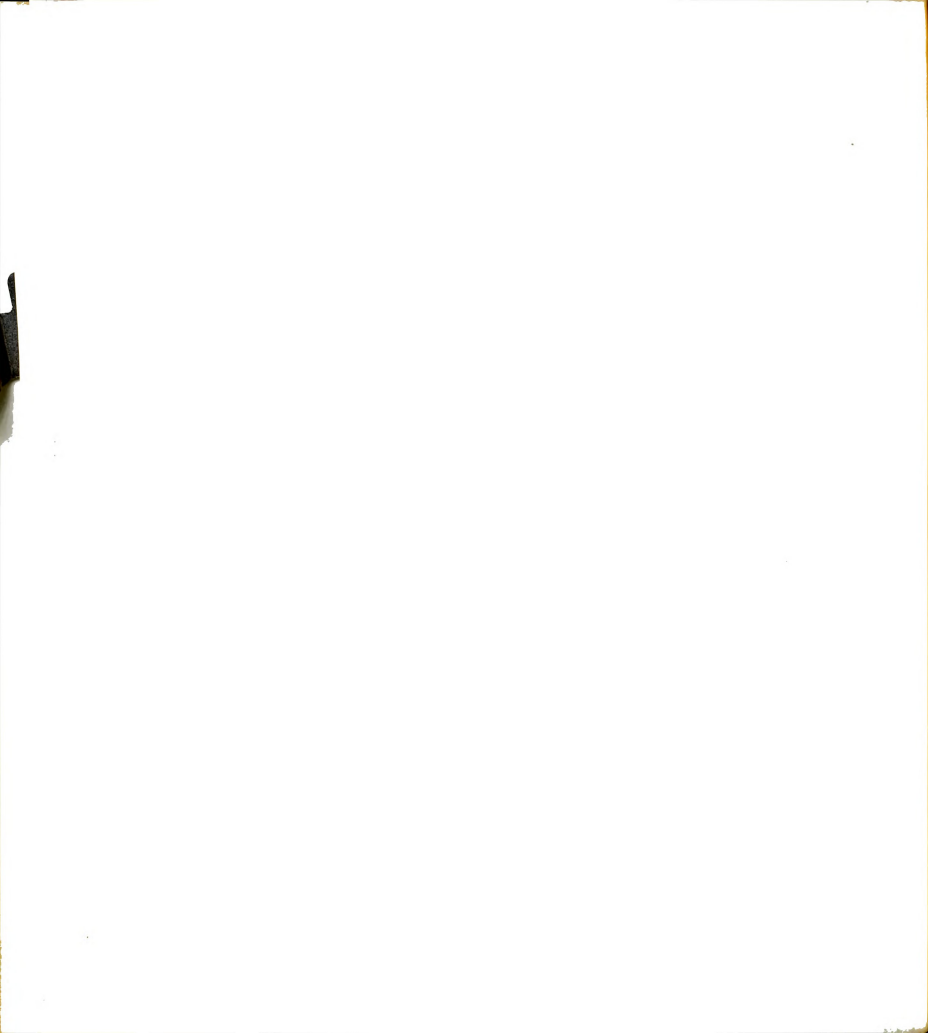
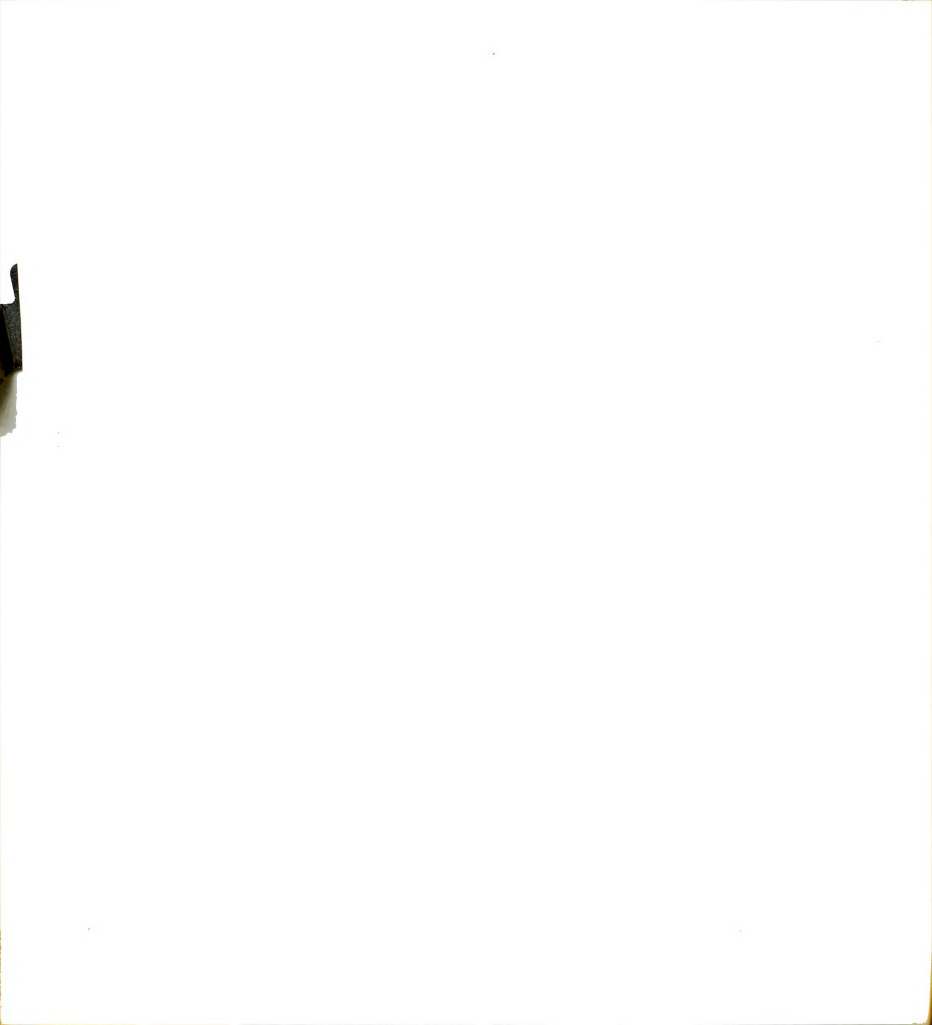


Table 16. Atomic Coordinates and Isotropic Temperature Factors for Porphine (from Webb & Fleischer).

Atom	(Coordina	te ± std. dev.)	a x 10 ⁴ z ± σ _z	в (А2)
cl_{α}	1978 ± 2	4489 ± 2	3114 ± 2	4.2
c2 _β	$\textbf{2661} \ \pm \ \textbf{2}$	5349 ± 2	3825 ± 3	5.1
C3 _P	2884 ± 2	6059 ± 2	$2912 \ \pm \ 3$	5.7
C4	$\textbf{2351} \ \pm \ \textbf{2}$	$5645~\pm~2$	1614 ± 2	4.2
C5 _m	$2396 \ \pm \ 2$	$6123 ~\pm~ 3$	405 ± 3	4.6
C6	1903 ± 2	5735 ± 2	-848 ± 2	4.3
c7 _⊖	$1966~\pm~2$	$6234 ~\pm~ 2$	-2098 ± 3	5.3
c8 _β	$1393 \ \pm \ 2$	5596 ± 2	-3069 ± 3	5.3
C9	949 ± 2	$4684 \; \pm \; 2$	-2449 ± 2	4.2
C10 _m	$292 \ \pm \ 2$	3836 ± 2	-3099 ± 2	4.6
C11	-154 ± 2	2962 ± 2	-2520 ± 2	4.3
C12	-850 ± 2	2097 ± 2	-3221 ± 3	5.6
c13 _β	-1105 ± 2	1407 ± 2	-2309 ± 3	5.4
C14	-566 ± 2	$1829 \ \pm \ 2$	-1016 ± 2	4.5
C15 _m	$-621 ~\pm~ 2$	$1362\ \pm\ 2$	199 ± 3	4.8
C16	-126 ± 2	$\textbf{1756} \ \pm \ \textbf{2}$	1444 ± 3	4.4
c17 ₈	-182 ± 2	$1253\ \pm\ 2$	2697 ± 3	5.3
C18 ₈	$418\ \pm\ 2$	$1870 \ \pm \ 2$	3669 ± 3	5.1
C19	862 ± 2	2780 ± 2	3046 ± 2	4.0
C20 m	1549 ± 2	3604 ± 2	3702 ± 2	4.4
N21	$1811 \; \pm \; 2$	$4682 ~\pm~ 2$	$1782 ~\pm~ 2$	3.9
N22	$1283\ \pm\ 1$	4794 ± 2	-1108 ± 2	3.9
N23	7 ± 1	2770 ± 2	-1188 ± 2	3.9
N24	$\textbf{517} \ \pm \ \textbf{1}$	$2686\ \pm\ 2$	$1698\ \pm\ 2$	3 .8

^aStandard deviations estimated by least squares analysis.

^bThe coordinates x, z are equivalent to z, x of the present work. This Table was taken from L. E. Webb, Ph.D. Thesis, Department of Chemistry, University of Chicago, Chicago, Illinois, 1965.



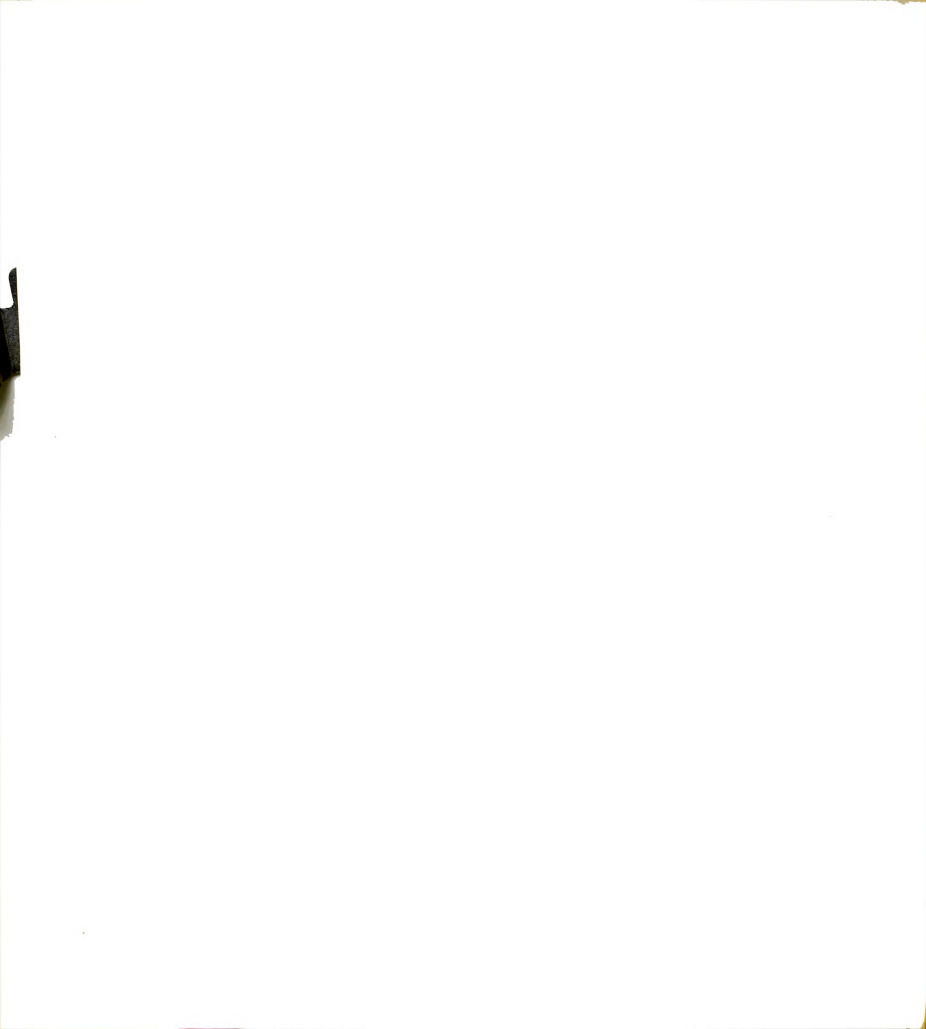
densities found in the vicinity of the outer pyrrole carbon atoms in $\Delta \rho_1$ suggested anisotropic thermal motion for the outer carbon atoms of the porphine molecule. Thus, the individual isotropic temperature factors were converted into the corresponding anisotropic temperature factor form for carbon and nitrogen atoms and the least squares refinement was continued.

2. Anisotropic Refinement

One cycle of least squares refinement in which the coordinates and anisotropic temperature factors of the inner 12 atoms were allowed to vary, followed with another cycle in which the atomic parameters of the outer 12 carbon atoms were allowed to vary, decreased the R-factor about 1% for the first cycle and another 2% in the second cycle to 0.109. Examination of the observed and calculated structure factors indicated the largest discrepancies to be concentrated in some large, low-order reflections, such as (022), $|\mathbf{F_0}| = 137.5 \text{ and } |\mathbf{F_c}| = 161.4. \text{ This observation is characteristic of secondary extinction, and an attempt to correct for extinction was made before proceeding with further refinement.}$

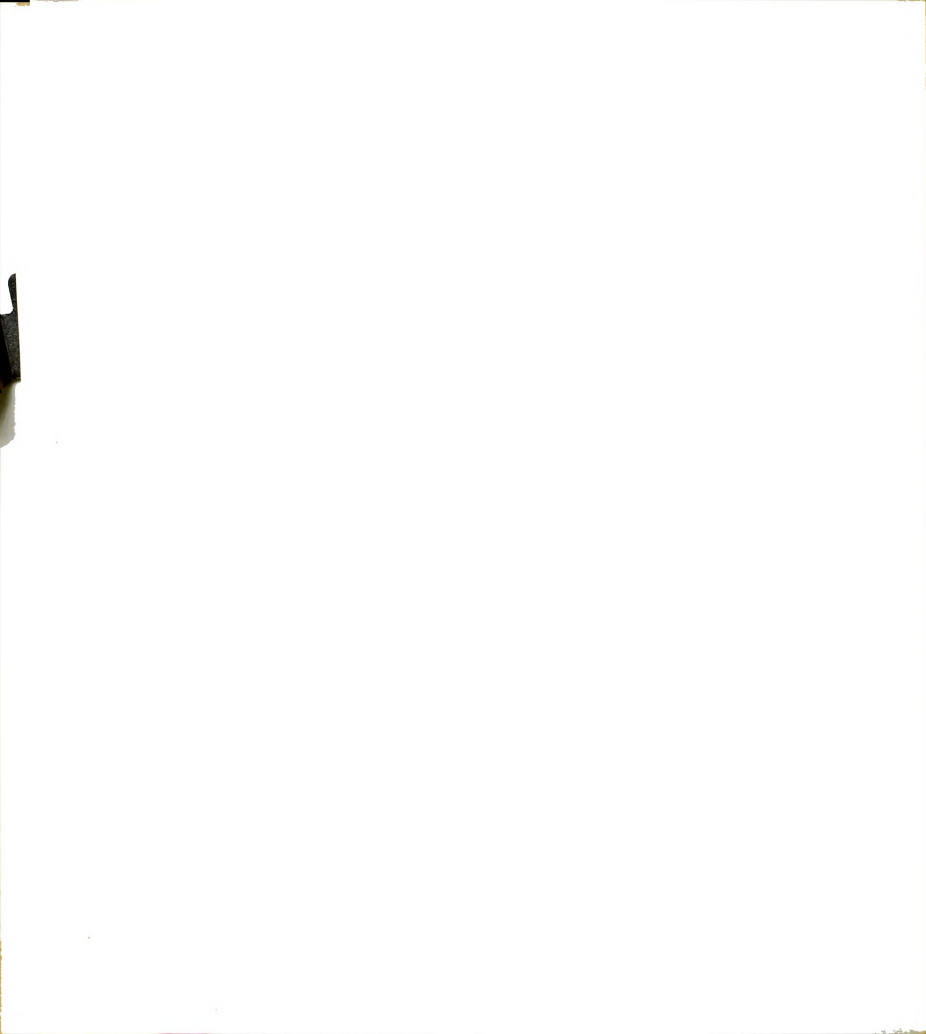
3. Extinction Correction

Secondary extinction is related to the amount of mosaic character of crystals. When the X-ray beam must penetrate deeply into the mosaic crystal before it reaches mosaic



blocks which have parallel reflecting planes as those blocks near the surface, there is an attenuation of the beam reaching the deeper mosaic blocks. This effect is known as secondary extinction and is most pronounced for reflections at low ($\sin \theta/\lambda$) where the intensities are generally large. As a result, the observed values for intense reflections are systematically less than their calculated values. There are several methods by which secondary extinction can be detected and corrected. The extinction correction for the intensity data of porphine was made by remeasuring the low order reflections with a small crystal. The small crystal has fewer planes in the reflecting position at the given time, and thus the attenuation of X-ray beam is less than that for a large crystal.

A small crystal with the dimensions of 0.15 x 0.125 x 0.025 mm (see Fig. 21) was used for intensity measurements of reflections which might be affected by secondary extinction. The volume ratio between the large crystal and the small crystal is 5.88. All reflections distributed in the hemisphere with \pm h \leq 4, k \leq 4 and ℓ \leq 4 were measured by the use of a Picker 4-Circle Automatic Diffractometer. Proper scaling between different instruments as well as crystals was made by using reflections not affected by extinction. The average ratio obtained between structure amplitudes of the small crystal, $|\mathbf{F}_{\rm small}|$, and the structure amplitudes of large crystal, $|\mathbf{F}_{\rm large}|$, was



$$\langle \frac{|F_{large}|}{|F_{small}|} \rangle_{n=30} = 1.61 \pm 0.06$$

where n is the number of reflections.

The residual index in terms of $|F_{\rm Small}|$ and $|F_{\rm large}|$, over extinction-unaffected reflections, was assessed by

$$R_{E} = \frac{\sum ||F_{large}| - 1.6|F_{small}||}{\sum |(|F_{large}| + 1.6|F_{small}|)/2|} = 3.3\%$$

This number indicated that the two sets of structure amplitudes, based on two different sized crystals, measured by different diffractometers and methods were in good agreement. It is of note that the thirty reflections which were used to determine the average ratio of the structure amplitudes had amplitudes ($|F_0|$) ranging from 3 to 74 (absolute scale). The average intensity ratio can be written as the square of average ratio of structure amplitude. The average ratio of intensities had a value of 2.6 which does not correspond to the volume ratio of 5.88. This is probably due to the fact that the automatic diffractometer is more sensitive for X-ray detection.

The structure factor calculation (excluding hydrogen atoms) computed after six strong low-order reflections from the large crystal which showed pronounced secondary extinction were replaced by the new structure amplitudes (see Table 17) and an R-factor of 0.10. A difference electon density was then calculated and examined, from which all the hydrogen coordinates were obtained. Individual

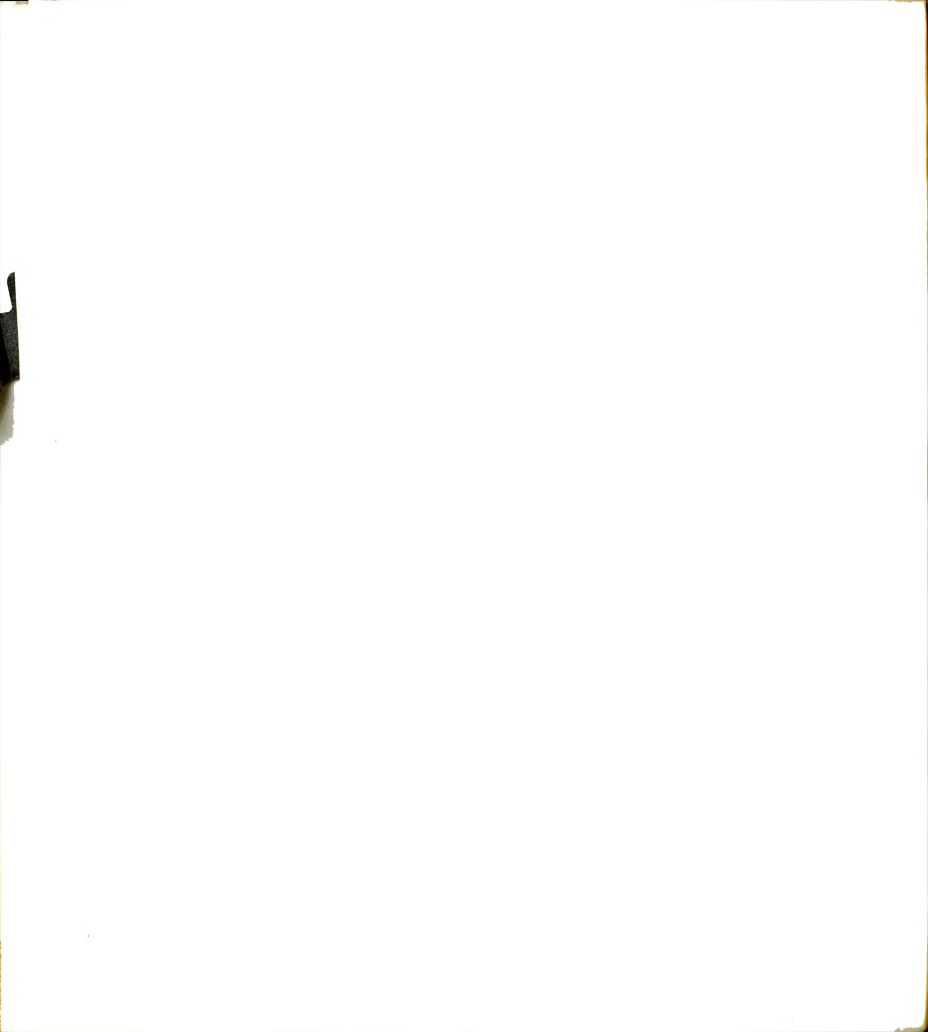
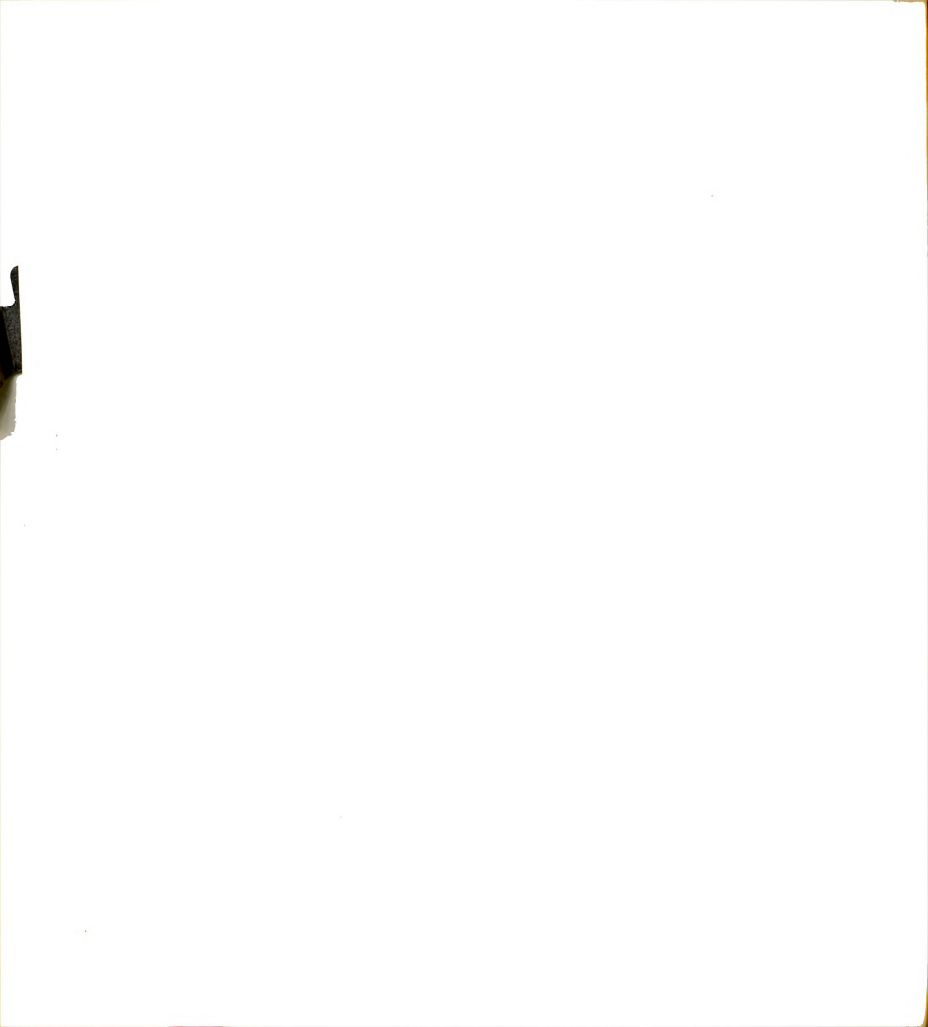


Table 17. The Reflections Corrected for Extinction.

Reflection	Fc	Fo large	Fo small
(022)	161.4	137.5	160.6
(122)	108.8	95.5	111.1
(013)	100.1	89.7	99.8
(023)	122.7	116.3	129.7
(113)	121.4	107.0	122.3
(123)	166.3	155.2	172.8



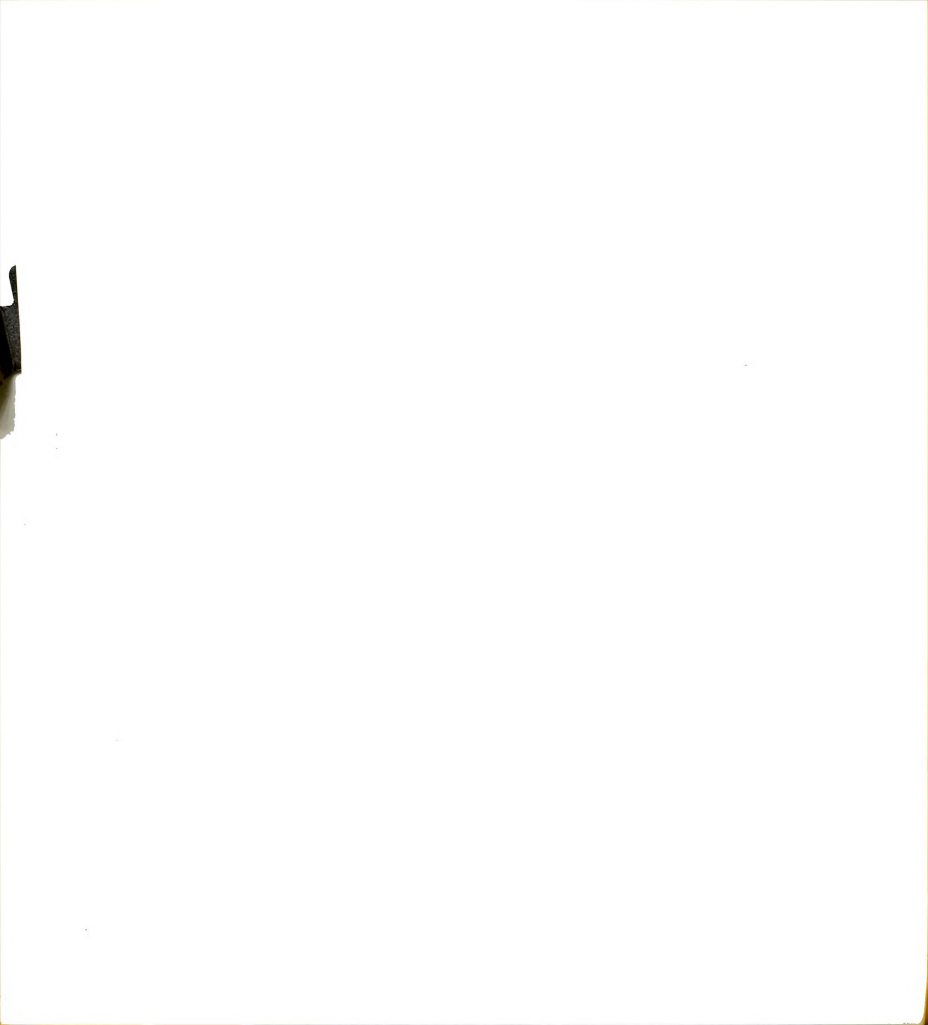
isotropic temperature factor for each hydrogen atom was approximated to be 20% greater than that of its adjacent carbon and nitrogen atom in the porphine molecule. These isotropic values were then converted to anisotropic temperature factor form. The structure factor calculation (hydrogens included) of the porphine molecule had an Rfactor of 0.086, and after one cycle of least squares refinement of all coordinates of carbon and nitrogen atoms, the R-factor decreased to 0.078. With one cycle of least squares refinement of anisotropic temperature factors of the 12 outer atoms followed by another cycle of refining the 12 inner atoms, the R-value went to 0.072 for the former and to 0.068 for the latter. Performing one cycle of least squares on all the hydrogen coordinates, the R-factor improved to 0.067. At this point the refinement by least squares was altered by basing it on a different weighting scheme.

4. Weighting Scheme

As it has been mentioned in Part I, the method of least squares applied to the structure refinement consists in systematically varying the atomic parameters so as to minimize the quantity

$$R = \sum_{i=1}^{n} w_{i}(|\mathbf{F}_{0}| - |\mathbf{F}_{C}|)^{2}$$

where the sum is taken over all independent structure amplitudes and \mathbf{w}_{i} is the weight of an observation. Each

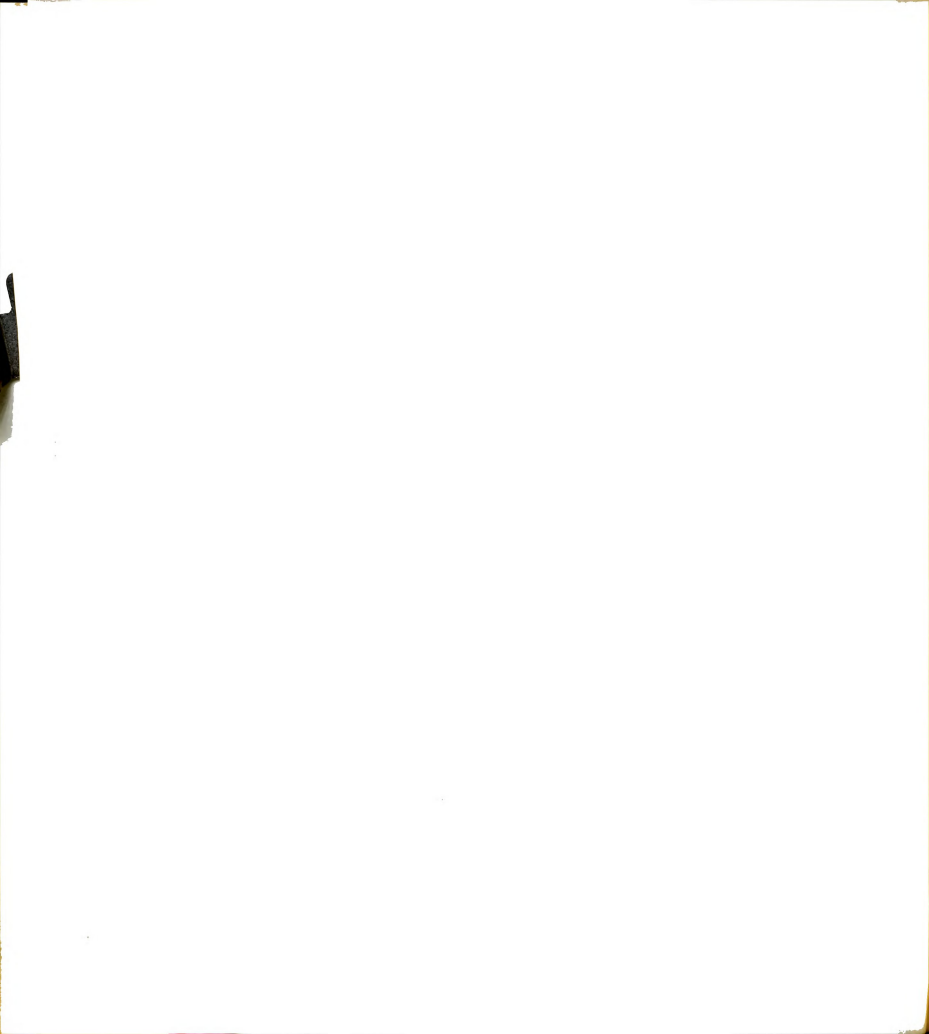


weight w_i is to be taken as the inverse of the square of the standard deviation of the corresponding observation, and may be estimated from the agreement of independent measurements or from considerations of the way the measurement was made. Factors which were taken into consideration for the weighting scheme for the porphine intensity data were counting statistics, the instrumental instability, and the reliability of the measurement. Three different weighting functions were used according to the intensity of the reflection. They were as follows

a) 12,000 > I > 400 (Intensity, I, is counts per 10 sec) $\sigma = 0.04 \times |F_0| \text{ where } \sigma = 1/\sqrt{w}$

or
$$w = 1/\sigma^2 = \frac{1}{(0.04)^2} |F_0|^{-2}$$

Since the weight is inversely proportional to $|F_0|^2$, this weighting scheme is similar to that of Hughes .⁴⁷ The constant of 0.04 (4%) is the error estimated for unit weight observations. Generally, data in this intensity range were very reliable, as evidenced by the small fluctuation observed for the monitors (~2%) throughout the data collection. In addition, the counting statistics, \sqrt{I} , can be expressed in terms of the percentage counting error, \sqrt{I}/I , which is small in this intensity range. The two extreme conditions can be illustrated. For an intensity, I, equal to 12000 counts/10 sec, the counting error is less than 1%; for I equal to 400 counts/10 sec, the counting error is 5%. The latter value corresponds to



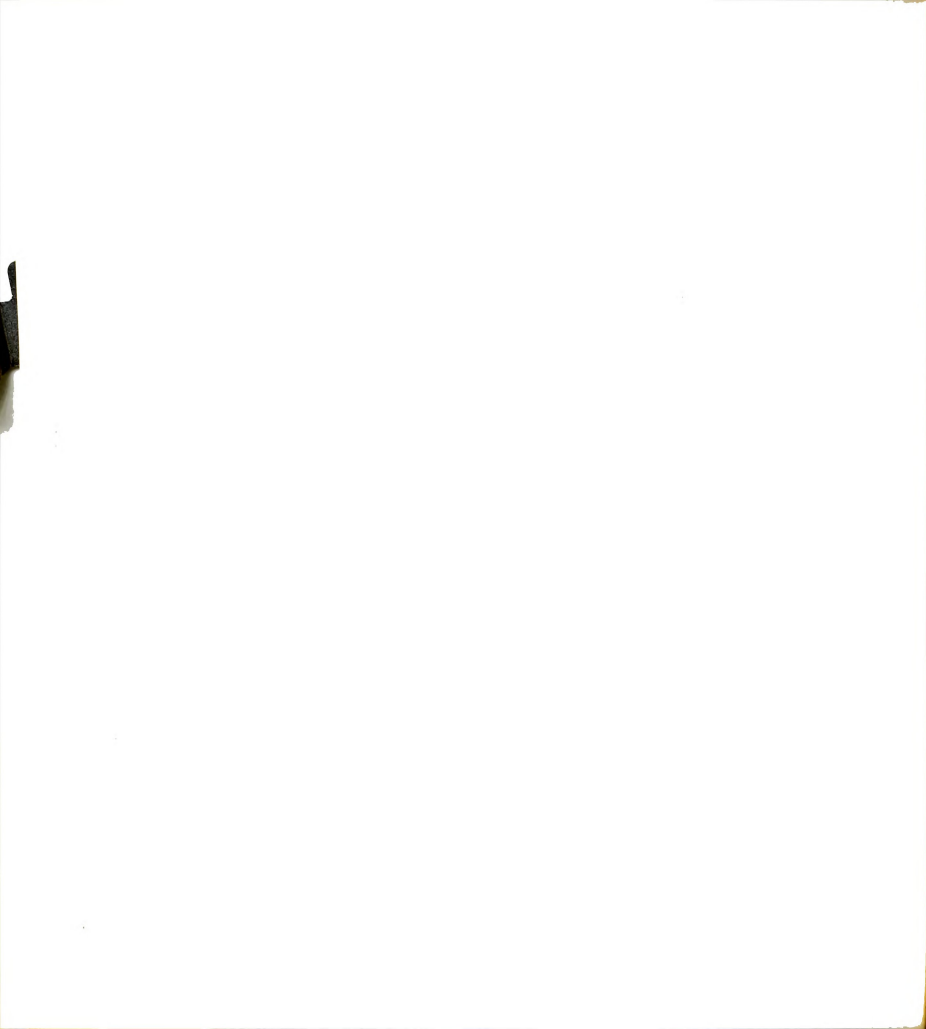
approximately 3% error on structure amplitude, since the standard deviation of |F|, σ_F , is approximately one-half the standard deviation of intensity, σ_I . Thus the average error for an observation in this intensity range was assumed to be slightly greater than 3%, or 4%.

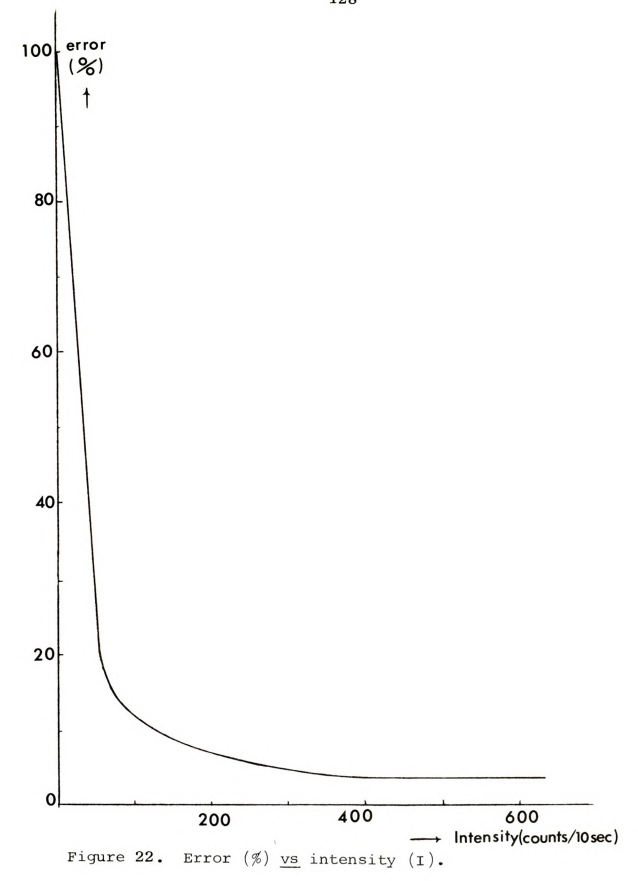
b) I > 12,000
$$\sigma = 0.04 \times I/12000 \times |F_0|.$$

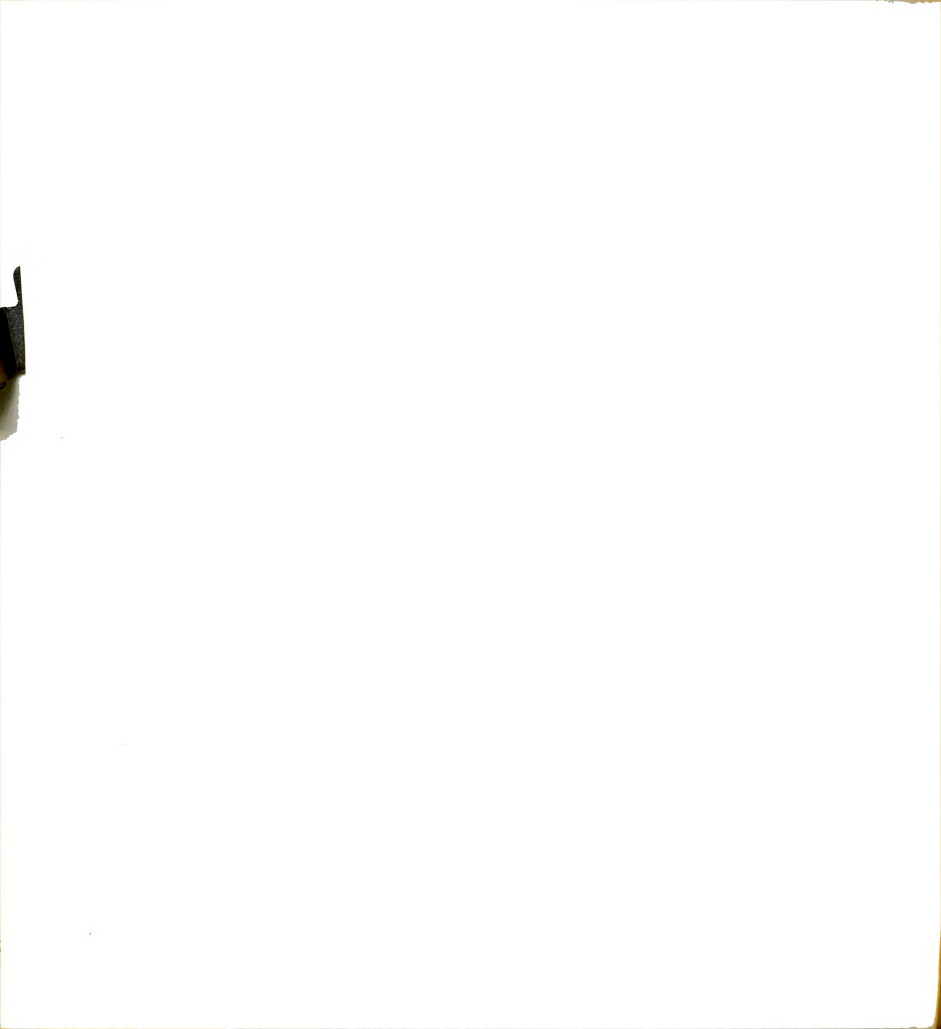
In this intensity range, the error of the observation is assumed to be linearly dependent on the magnitude of the intensity. Because extinction and crystal mis-setting problems are more pronounced for very intense reflections, the errors increase to account for these effects.

The error for an observation in this range was obtained from a curve derived from plotting the error (%) as a function of the intensities (shown in Fig. 22). The boundary conditions, I = 5 and I = 400, were selected so that the relative error was 100% for the former and 4% for the latter. This curve was then constructed by fitting three selected points, determined as follows:

(1) when I = 68, the error is 15%. This error was the maximum counting error for the (306) reflection which was one of the seven reflections selected in the intensity range between 5 and 200 count/10 sec and was measured repeatedly.







- (2) The second point is that when I = 234, the error is 8%. This point was determined from the reflection ($\bar{1}10$) whose counting error of 8% was the largest among five selected reflections in the intensity range from 200 to 300 counts/10 sec.
- (3) The third point is that when I = 300, the error is 5%. This point was obtained from the $(\overline{4}25)$ reflection, as one of the five reflections whose intensities were in the range of 300 to 400 counts/10 sec.

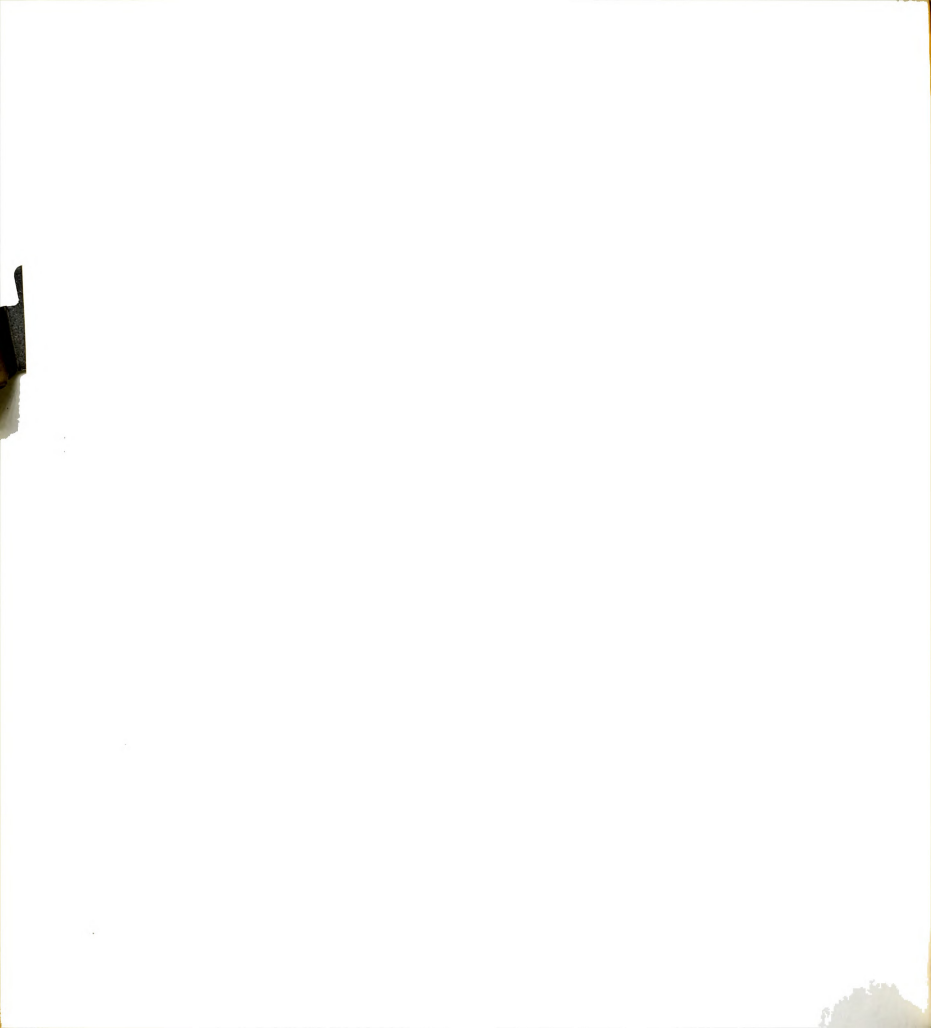
In order to make the calculation of weight easier in this region, the curve was divided into 10 regions and the errors for estimating the standard deviation of a reflection are shown in Table 18.

The weighting scheme was applied to all the reflections except the $(\bar{1}00)$ and $(\bar{2}00)$ reflections. These reflections were not improved by the extinction correction, since the size of the second crystal used was not small enough to correct completely their secondary extinction effects. Zero weight (w = 0) was then applied to these two reflections to exclude them from the refinement.

When the new weights were applied and two cycles of least squares refinement of coordinates and anisotropic temperature factors of all the carbon and nitrogen atoms were performed, the R-factor lowered to 0.059 and the weighted R-factor to 0.041. The difference between the R-factor and the weighted R-factor is

Table 18. Error for Intensity Less than 400.

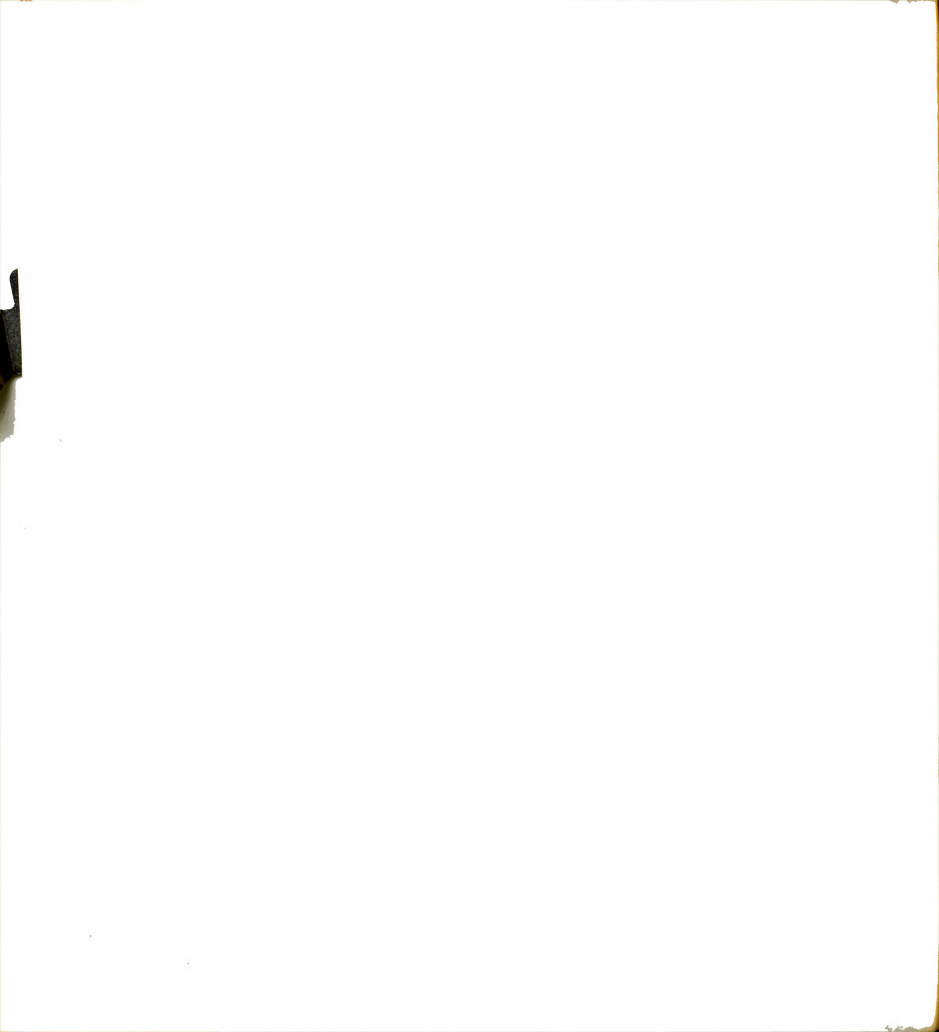
Intensity Range	Error
300 <u><</u> I ~ 400	0.05
250 <u>1 300</u>	0.06
200 i - 250	0.07
150 <u>~</u> I < 200	0.08
125 _ I < 150	0.09
100 <u>~ I < 125</u>	0.11
75 <u>~</u> I ~ 100	0.14
50 <u> </u>	0.23
25 <u>~</u> I < 50	0.53
5 <u>~</u> I ~ 25	1.00



$$R = \frac{\sum ||\mathbf{F_0}| - \mathbf{k}|\mathbf{F_C}||}{\sum ||\mathbf{F_0}||}$$

$$\text{weighted} \quad \text{R = } \quad \frac{\left[\left. \left[\left. \left(\right.\right| \text{F}_{0} \right.\right| \right. - \left. k \left.\right| \text{F}_{C} \right.\right| \right)^{2} \right]^{1/2}}{\left[\left. \left[\left. \left. \left. \right| \right. \right| \text{F}_{0} \right.\right|^{2} \right]^{1/2}}$$

where k is the scale constant between $|F_0|$ and $|F_C|$. Since one additional cycle of least squares on all the hydrogen coordinates had no apparent effect, the refinement of the porphine structure by least squares was terminated with a final R-factor of 0.059 and weighted R-factor of 0.041.



TX. RESHLTS

The final coordinates, anisotropic temperature factors, the mean square atomic displacement (\overline{u}^2) in the direction of each principal axis, and peak heights of all the carbon and nitrogen atoms are listed in Table 19. The final coordinates, isotropic temperature factors and the peak heights of the hydrogen atoms are shown in Table 20. The isotropic temperature factors of the peripheral pyrrole hydrogens were approximated to be 20% greater than the average isotropic temperature factors of their adjacent pyrrole carbons (B = 5.6 %); the isotropic temperature factors of the remaining hydrogen atoms were estimated to be 20% greater than the average isotropic temperature factors of their adjacent atoms (B = 4.6 %).

The atomic deviations from different least squares planes based on the individual pyrrole rings, the plane defined by the four nitrogen atoms, and the plane based on the eight inner pyrrole carbon and nitrogen atoms are given in Table 21. The atomic deviations from the nuclear least squares plane (NLS) of the porphine molecule are shown in Figure 23; the standard deviation (excluding hydrogens) is 0.02 Å. The porphine bond distances and angles are shown in Figure 24 and Figure 25, respectively. The standard

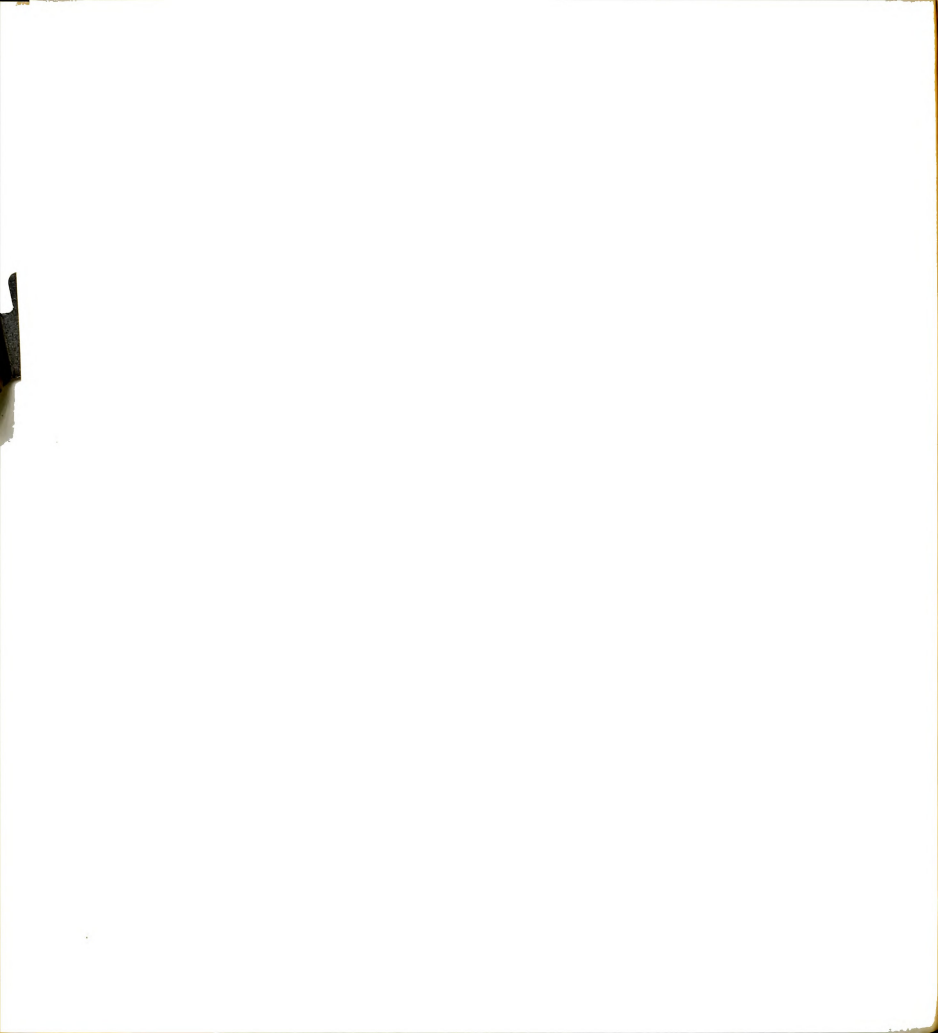




Table 19. Final Atomic Parameters and Peak Heights of

		Coordinates in Fractions			Anisotropic Temperature		
Atom	×	У	z	β11	β22	Взз	
N21	0.1757	0.4670	0.1809	0.0121	0.0066	0.0063	
C1A	0.3113	0.4476	0.1978	0.0112	0.0086	0.0071	
C2B	0.3825	0.5359	0.2657	0.0148	0.0102	0.0072	
C 3 B	0.2904	0.6068	0.2877	0.0177	0.0092	0.0071	
C4A	0.1613	0.5628	0.2353	0.0142	0.0076	0.0061	
С5М	0.0418	0.6121	0.2388	0.0160	0.0067	0.0058	
N22	-0.1116	0.4801	0.1282	0.0113	0.0077	0.0065	
C6A	-0.0846	0.5743	0.1918	0.0151	0.0075	0.0057	
C7B	-0.2088	0.6244	0.1970	0.0186	0.0090	0.0077	
C8B	-0.3077	0.5598	0.1391	0.0135	0.0109	0.0076	
C9A	-0.2475	0.4672	0.0955	0.0091	0.0105	0.0066	
C10M	-0.3120	0.3826	0.0292	0.0102	0.0114	0.0070	
N23	-0.1183	0.2775	0.0014	0.0102	0.0075	0.0069	
C11A	-0.2527	0.2953	-0.0146	0.0133	0.0084	0.0064	
C12B	-0.3260	0.2092	-0.0855	0.0151	0.0097	0.0079	
C13B	-0.2330	0.1407	-0.1097	0.0169	0.0092	0.0082	
C14A	-0.1038	0.1823	-0.0579	0.0151	0.0069	0.0067	
C15M	0.0171	0.1358	-0.0623	0.0154	0.0075	0.0073	
N24	0.1682	0.2671	0.0520	0.0103	0.0065	0.0071	
C16A	0.1425	0.1741	-0.0141	0.0150	0.0149	0.0056	
C17B	0.2661	0.1232	-0.0198	0.0185	0.0083	0.0087	
C18B	0.3661	0.1863	0.0412	0.0157	0.0079	0.0085	
C19A	0.3046	0.2768	0.0861	0.0112	0.0074	0.0068	
C20M	0.3699	0.3598	0.1559	0.0099	0.0092	0.0073	
0×104	0.1- 4	0.1-4	0.1-3	0.1 - 4	0.1 - 2	0.03-2	

 $^{^{*}}$ In the direction of each principal axis.

134

Carbon and Nitrogen Atoms of Porphine.

Parameters			Mean Square Atomic Displacements* (A ²)			Peak Height (e/A ³)
β12	β13	₽23	$8\pi^2\tilde{\mathbf{u}_1^2}$	$8\pi^2\bar{u}_2^2$	$8\pi^2\bar{u}_3^2$	Ро
0.0008	0.0023	-0.0001	3.48	3.82	4.92	7.6
-0.0006	0.0026	0.0014	3.31	4.66	5.54	6.2
-0.0044	0.0015	-0.0002	3.75	4.28	8.23	5.9
-0.0041	0.0019	-0.0014	3.48	4.81	8.43	5.5
-0.0009	0.0017	0.0003	3.48	4.36	5.92	6.0
0.0007	0.0020	0.0006	3.22	4.03	6.54	6.0
0.0026	0.0025	0.0005	3.22	3.65	5.75	7.2
0.0030	0.0029	0.0003	3.06	3.61	6.91	5.9
0.0053	0.0038	0.0012	3.58	4.21	9.17	5.3
0.0047	0.0041	0.0021	3.45	3.89	8.49	5.4
0.0029	0.0021	0.0017	3.00	3.58	6.96	6.2
-0.0004	0.0011	0.0013	3.75	4.32	6.91	5.8
-0.0001	0.0017	0.0013	3.41	4.14	5.09	7.4
-0.0008	0.0022	0.0013	3.25	5.09	5.50	5.9
-0.0037	0.0009	0.0004	4.06	4.54	8.08	5.5
-0.0052	-0.0001	-0.0000	3.51	4.85	9.17	5.2
-0.0023	0.0015	0.0005	3.41	3.99	6.82	5.9
-0.0014	0.0022	-0.0009	3.82	4.70	6.27	5.9
0.0020	0.0025	0.0005	2.97	3.89	5.01	7.9
0.0069	0.0021	0.0034	2.79	3.78	6.45	6.0
0.0053	0.0040	0.0011	3.25	4.89	9.01	5.7
0.0050	0.0043	0.0020	2.91	4.32	8.28	5.6
0.0022	0.0029	0.0024	2.73	3.78	6.01	6.1
0.0001	0.0021	0.0016	3.68	4.03	5.84	5.9
0.1-3	0.1-5	0.1-2				

Table 20. Final Coordinates, Isotropic Temperature Factors, and Peak Heights of Hydrogen Atoms of Porphine.

Atom		Coordinate	Isotropic Temperature Factors	Peak Heights	
-	x*	У	z	В (Д2)	ρ(e Å ⁻³)
H22	-0.0458	0 .4358	0.1183	5.5	0.5
H24	0.1042	0.3167	0.0633	5.5	0.5
н 2 в	0.5058	0.0367	0.2067	6.5	0.5
н 3 в	0.7033	0.1750	0.1650	6.5	0.5
н5м	0.9575	0.1842	0.2117	5.5	0.5
н7в	0.2242	0.1958	0.2700	6.5	0.5
н8в	0.4133	0.0533	0.3783	6.5	0.6
H10M	0.5850	0.3808	0.0192	5.5	0.5
H12B	0.5650	0.2825	0.3958	6.5	0.4
н13в	0.7433	0.4325	0.3400	6.5	0.5
н15м	0.0125	0.4300	0.3875	5.5	0.5
H17B	0.2750	0.4458	0.4342	6.5	0.5
H18B	0.4685	0.1742	0.0542	6.5	0.5
н20м	0.4758	0.3533	0.1708	5.5	0.6

 $^{^{\}star}$ Coordinates of hydrogen atoms were obtained from difference density map.

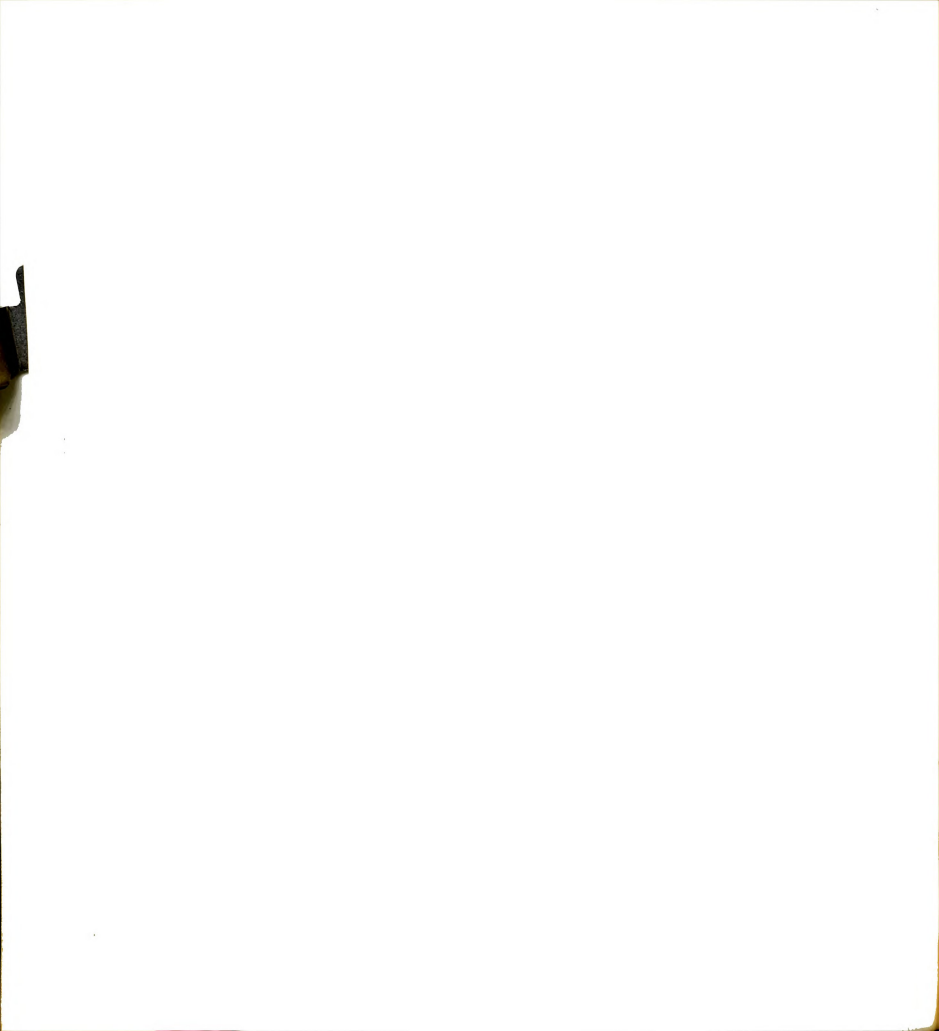
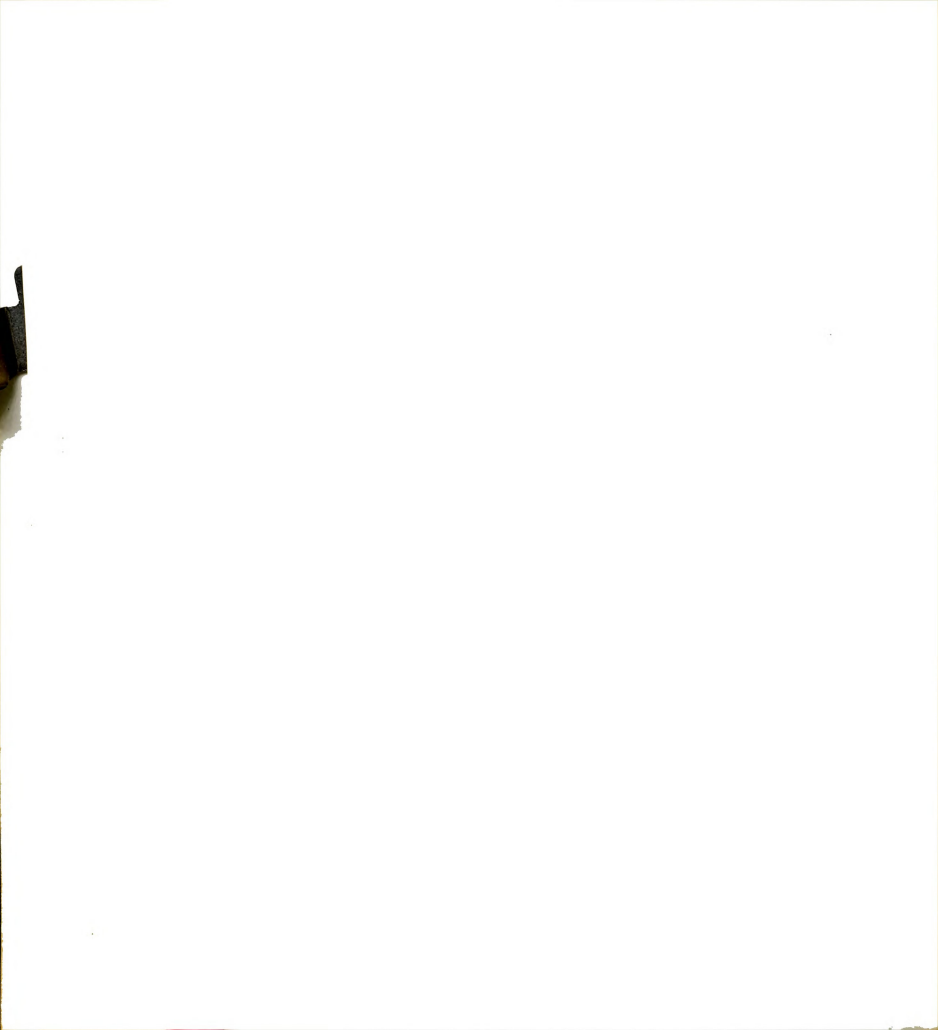


Table 21. Atomic Deviations from the Least Squares Planes of Individual Pyrrole, Inner Eight Atoms, and Four Nitrogen Atoms.

Atom	d (Å)	Atom	d(Å)	Atom	d (Å)
Pyrrole N21		Pyrrole N22		Pyrrole N23	
N21	-0.02	N22	-0.01	N23	0.04
C1	-0.02	С6	0.01	C11	0.00
C2	-0.00	c7	-0.03	C12	-0.01
C3	-0.01	С8	-0.00	C13	0.01
C4	0.00	С9	0.01	C14	-0.01
s.d.*	0.01	s.d.	0.02	s. d.	0.02
Pyrrole N14		Four Nitrogen		Eight Inner Atoms	
N24	0.01	N21	0.01	C1	0.03
C16	-0.01	N22	-0.01	C4	-0.02
C17	0.00	N23	0.01	С6	-0.03
C18	-0.00	N24	-0.01	С9	0.02
C19	0.00	s.d.	0.01	C11	0.02
s.d.	0.01			C14	-0.01
				C16	-0.02
				C19	0.01
				s.d.	0.02

^{*}Standard deviation



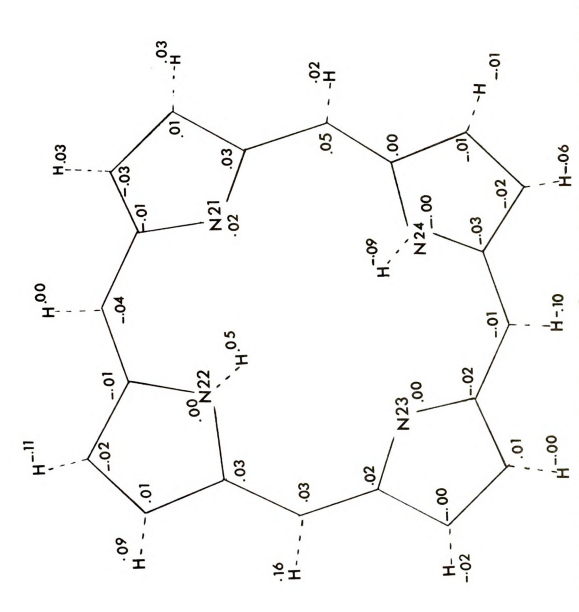
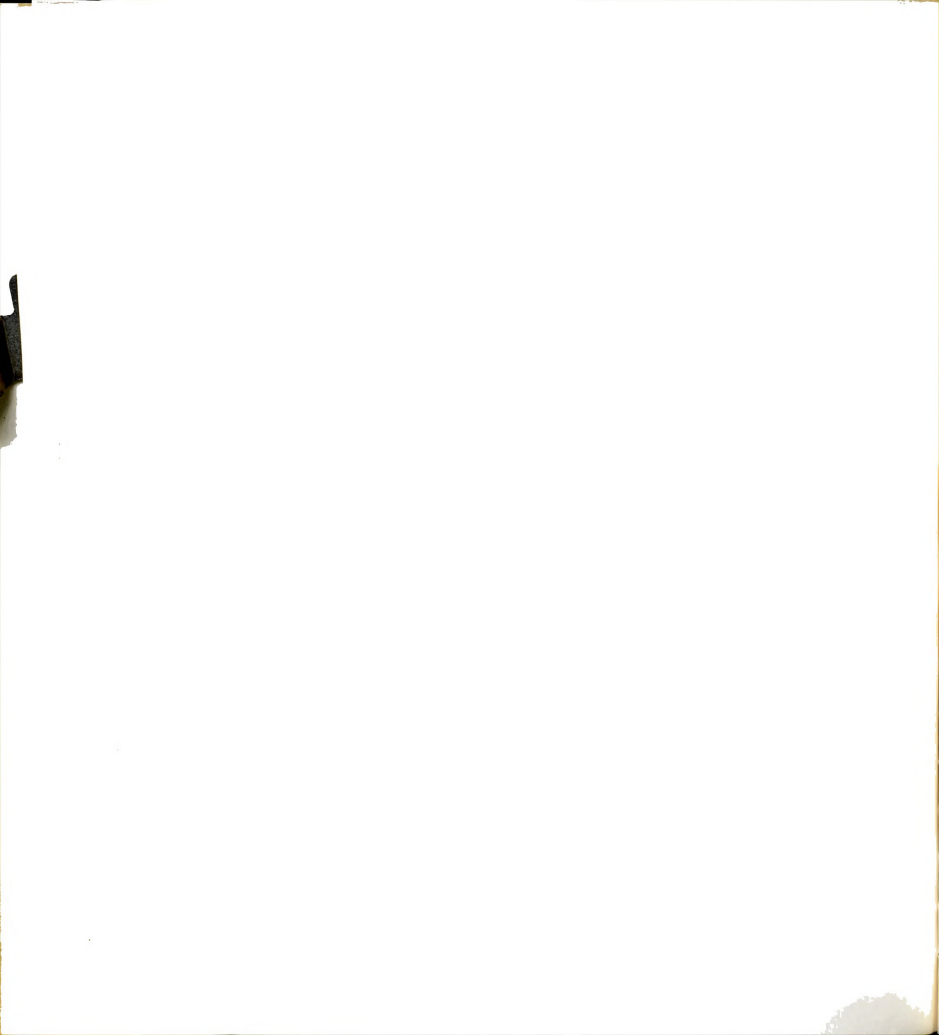


Figure 23. Atomic deviations (A) from nuclear least squares plane.



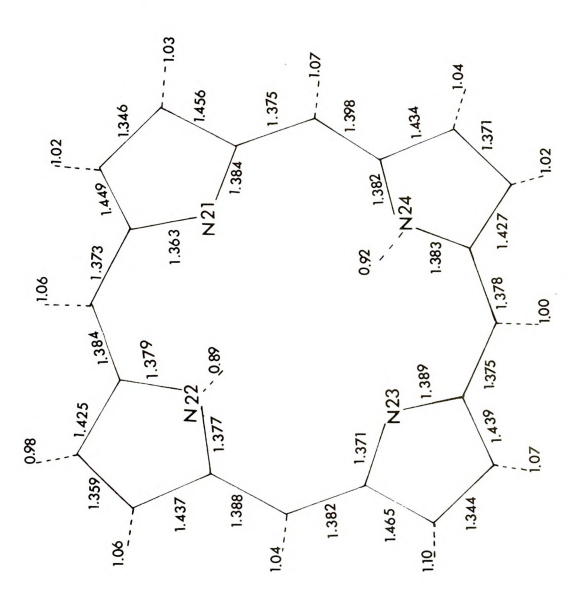


Figure 24. Porphine bond distances (A).



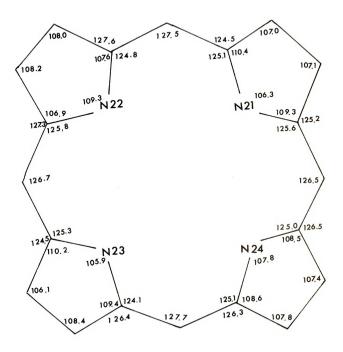
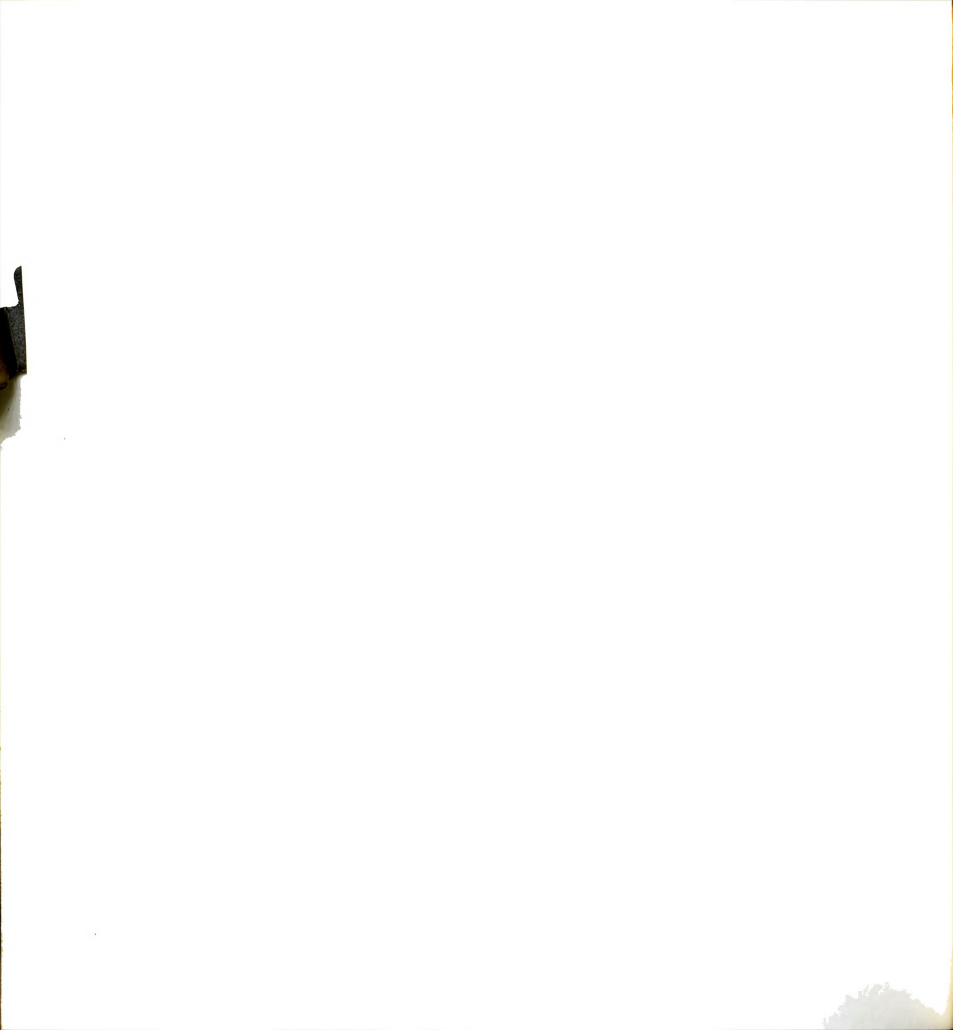


Figure 25. Porphine bond angles (degrees).



deviation of the lengths and angles of carbon-carbon and carbon-nitrogen bonds are approximately 0.004-0.007 % and 0.3-0.50 respectively, based on the standard errors of coordinates of carbon and nitrogen atoms in the last cycle of least squares refinement.

The composite difference electron density (based on the structure factor calculation excluding all hydrogen atoms) projected onto the ac plane is shown in Figure 26. The first contour is drawn at a level of 0.12 e R^{-3} with each additional contour occurring at 0.12 e R^{-3} . In addition, the difference electron-density in the vicinity of four nitrogen atoms is given in Figure 27; the electron densities of hydrogen atoms as well as the residual densities (~ 0.1 e R^{-3}) due to background fluctuation in this region are indicated. Figure 28 shows the interatomic distances and angles of the two central hydrogen atoms with respect to the four nitrogen atoms in porphine molecule.

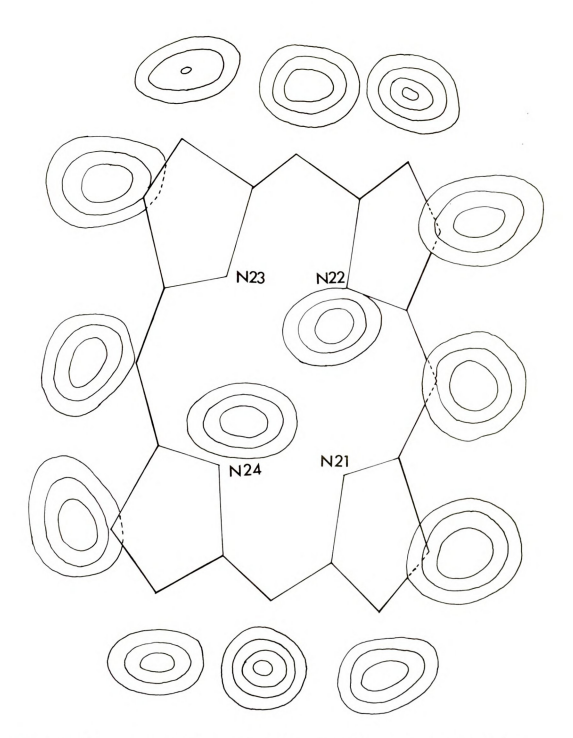
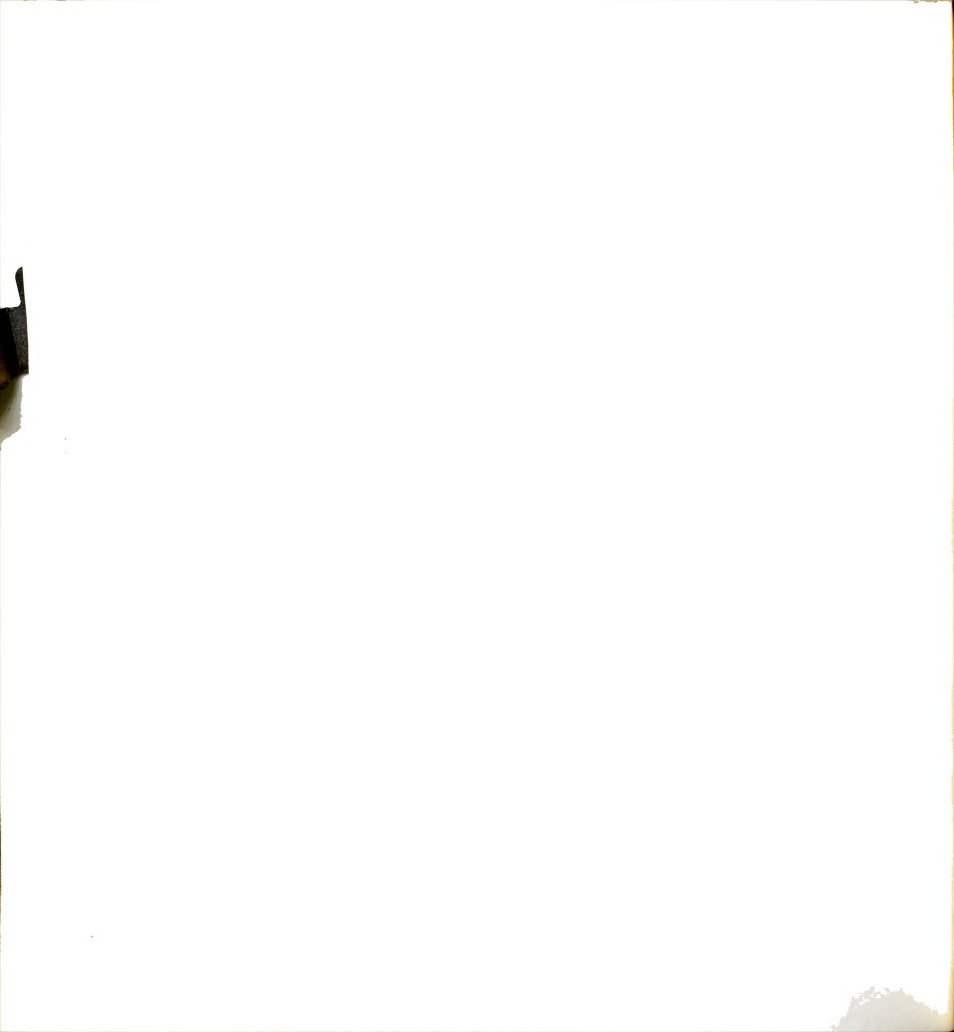


Figure 26. Composite electron density of the hydrogen atoms perpendicular to the ac plane.



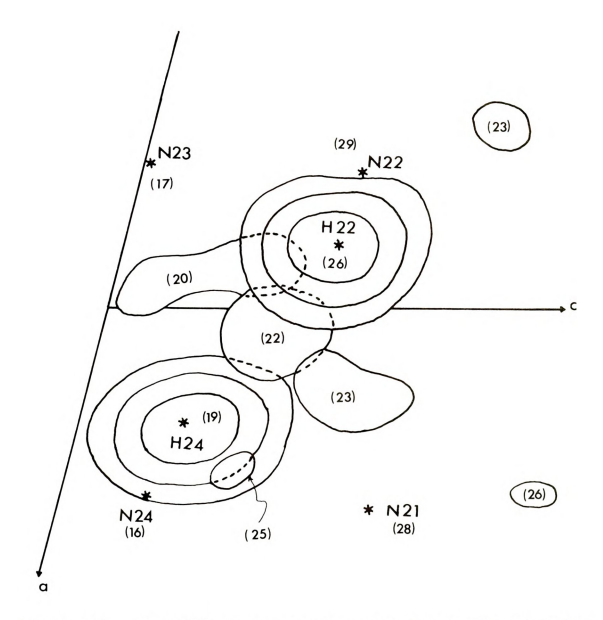
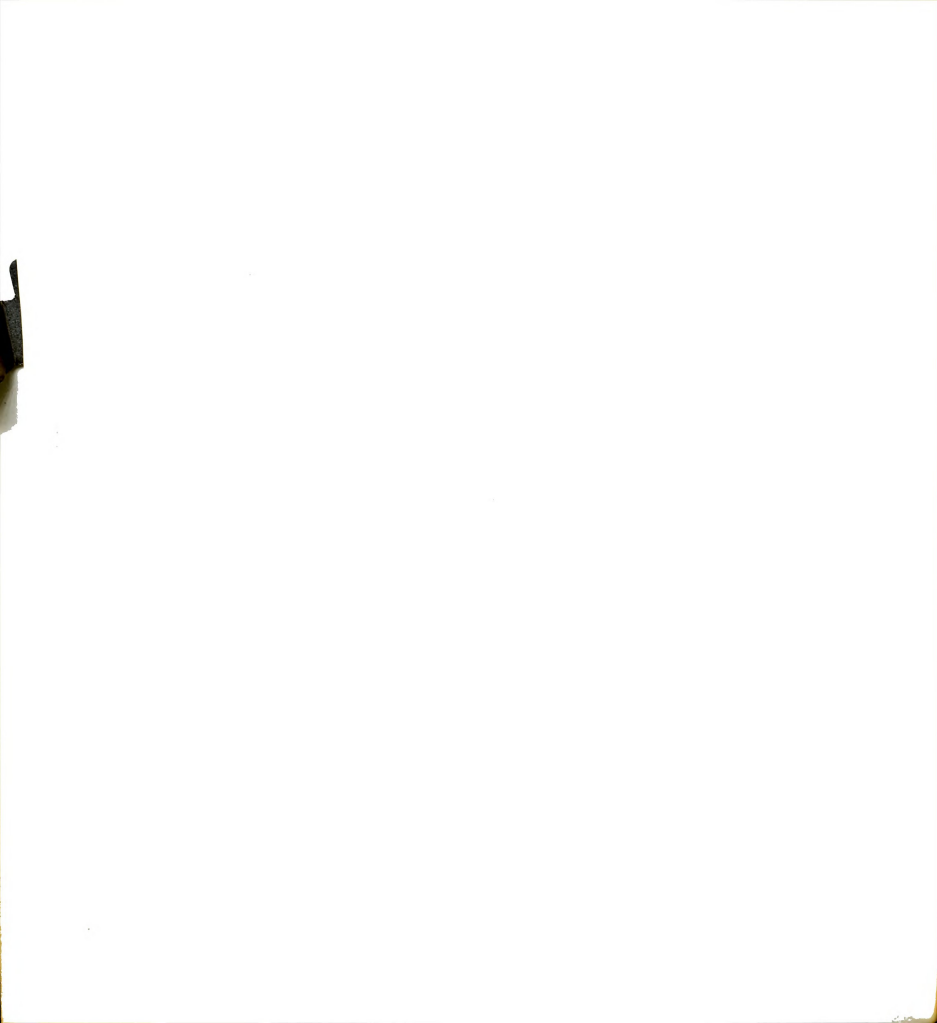
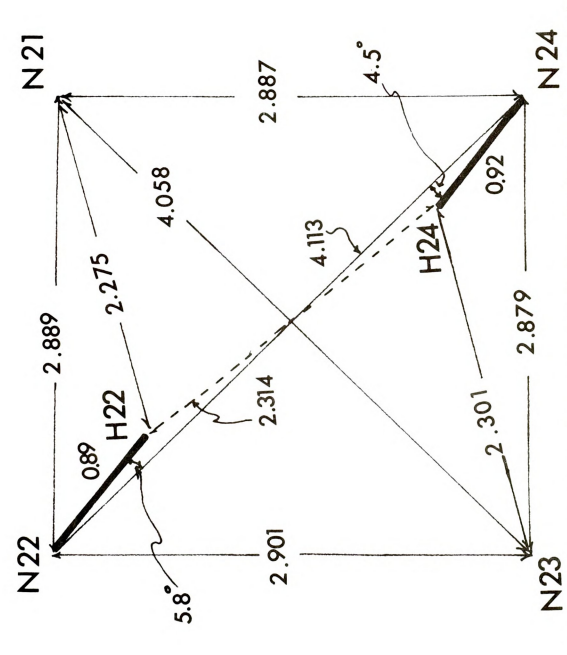
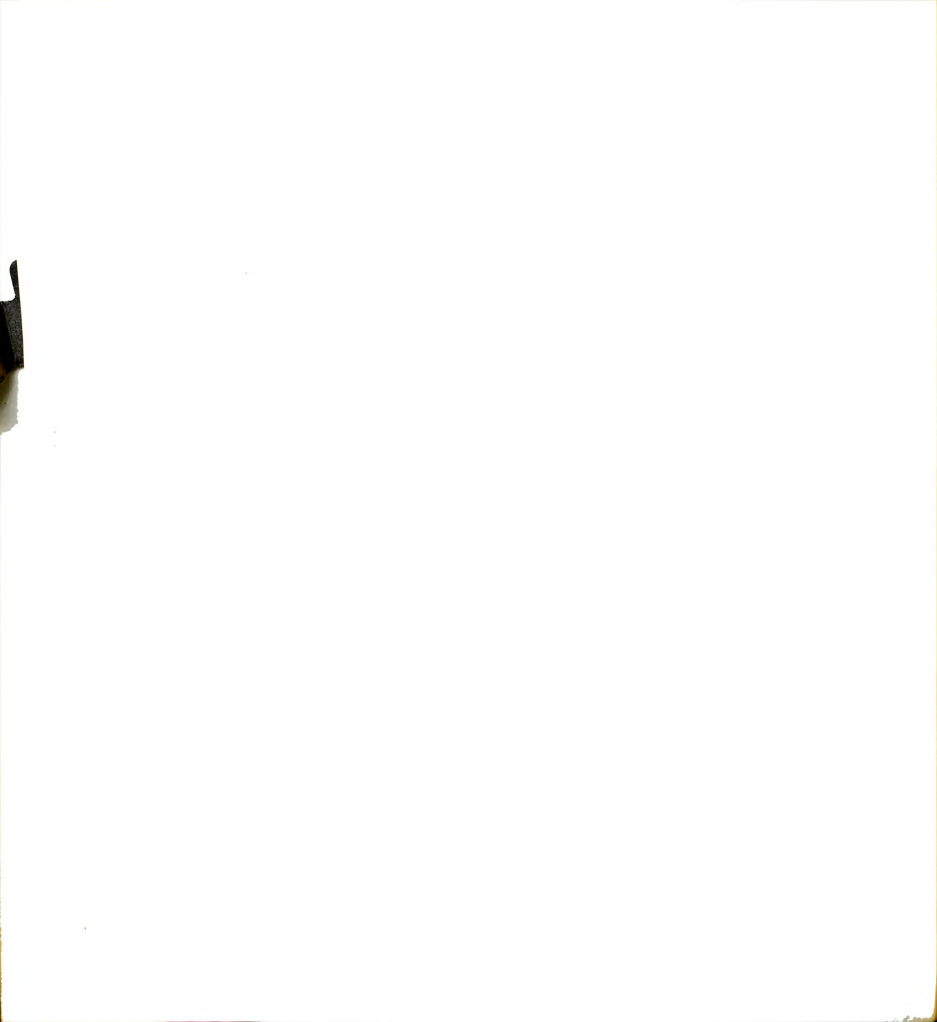


Figure 27. The difference electron density in the vicinity of the four nitrogen atoms. The length of b axis is divided into 60 sections, and the numbers in parenthesis are the section number corresponding to the y-coordinate of the atoms or the residual density (greater than 0.1 e A⁻³) along the b axis.





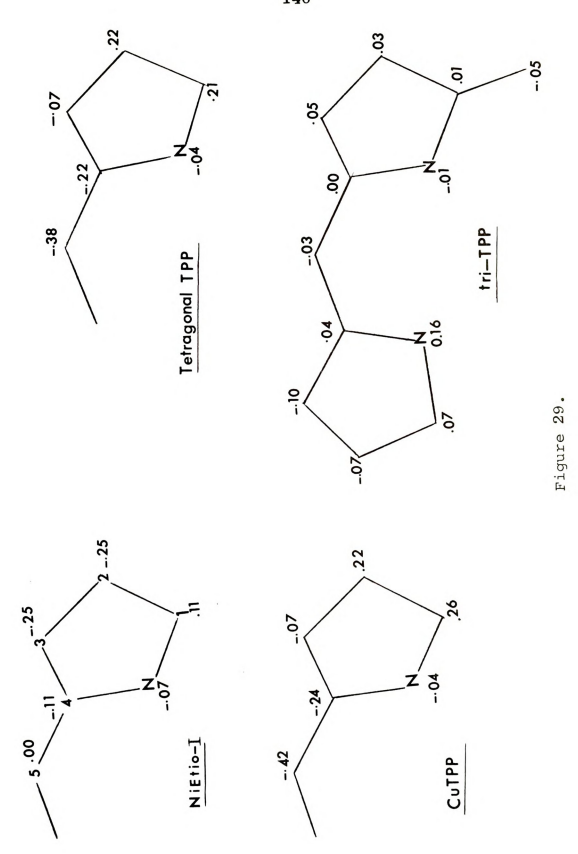
The interatomic distances and angles of the nitrogen and hydrogen atoms. Heavy lines indicate $N-H\ bonds$. Figure 28.



X. DISCUSSION

The deviations of the atoms from the least squares plane of each pyrrole indicate that the individual pyrroles (see Table 21) are essentially planar within the error of the structure determination ($\sim 0.01-0.02$ Å). In addition, from the small atomic deviations from the least squares plane formed by the inner eight atoms, the plane of four nitrogen atoms, and the NLS plane, one can conclude that the porphine molecule is also essentially planar. In contrast to this planarity of the porphine molecule, the porphyrin skeletons of some free base porphyrins and some metalloporphyrins are found to be very ruffled. Factors which might influence the observed departure from planarity could be either metal or side-chain substitution, and/or forces arising from crystal packing. Examples of nonplanar porphyrin skeletons are illustrated in Figure 29. NiEtio-I, CuTPP, and tetragonal TPP crystallize in tetragonal forms and the independent structural parameters determined are restricted to one quarter of the molecule due to the space group symmetry relations. From Figure 29 it can be seen that the nonplanarity of NiEtio-I manifests itself in pronounced deviations of peripheral pyrrole carbon atoms

Deviations of porphyrin skeleton from planarity. Figure 29. In NiEtio-I position 2 and 3, position 1 and 4, and Ni atoms are fixed by symmetry, the atomic deviations indicated are the the perpendicular distances from (008) plane. The atomic deviations of Curpp and tetragonal TPP are the perpendicular distances from (001) plane. The atomic deviations of tri-TPP are with respect to the nuclear least squares plane.



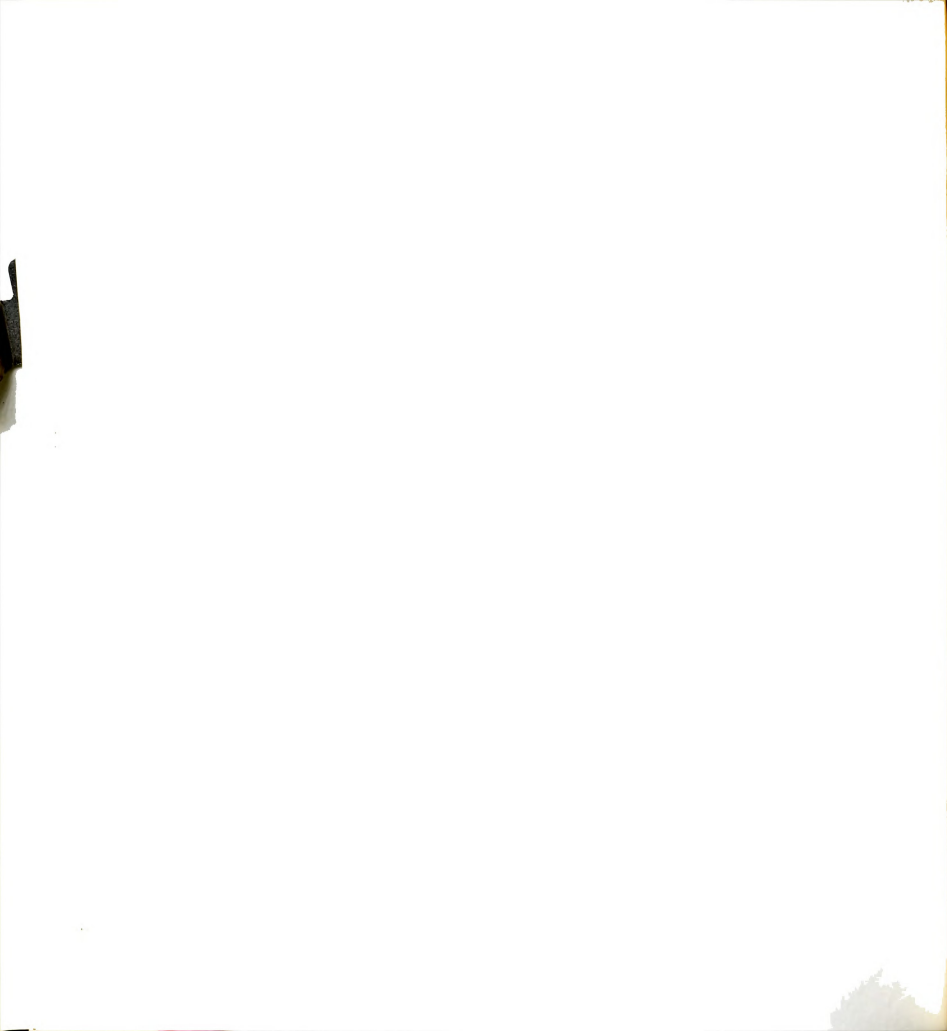
.

($\sim 0.3~\text{\AA}$) from the plane fitting the methine and pyrrole atoms, while CuTPP is nonplanar in a different way: the bridge carbon and some of the pyrrole carbon atoms ($\sim 0.2-0.4~\text{\AA}$) show the largest deviations. In the case of tri-TPP, the maximum deviation is found to be the pyrrole nitrogen atom which carries the central hydrogen atom ($\sim 0.2~\text{\AA}$); in addition, the pyrrole group is inclined with respect to the NLS plane ($\pm 6.6^{\circ}$). The nonplanarity of ClMnTPP is different from all the cases mentioned above. The atomic deviations for ClMnTPP (see Fig. 8, Part I) are found to fall into the following groups of decreasing atomic deviations:

$$d(C_h) > d(C_m) > d(N)$$

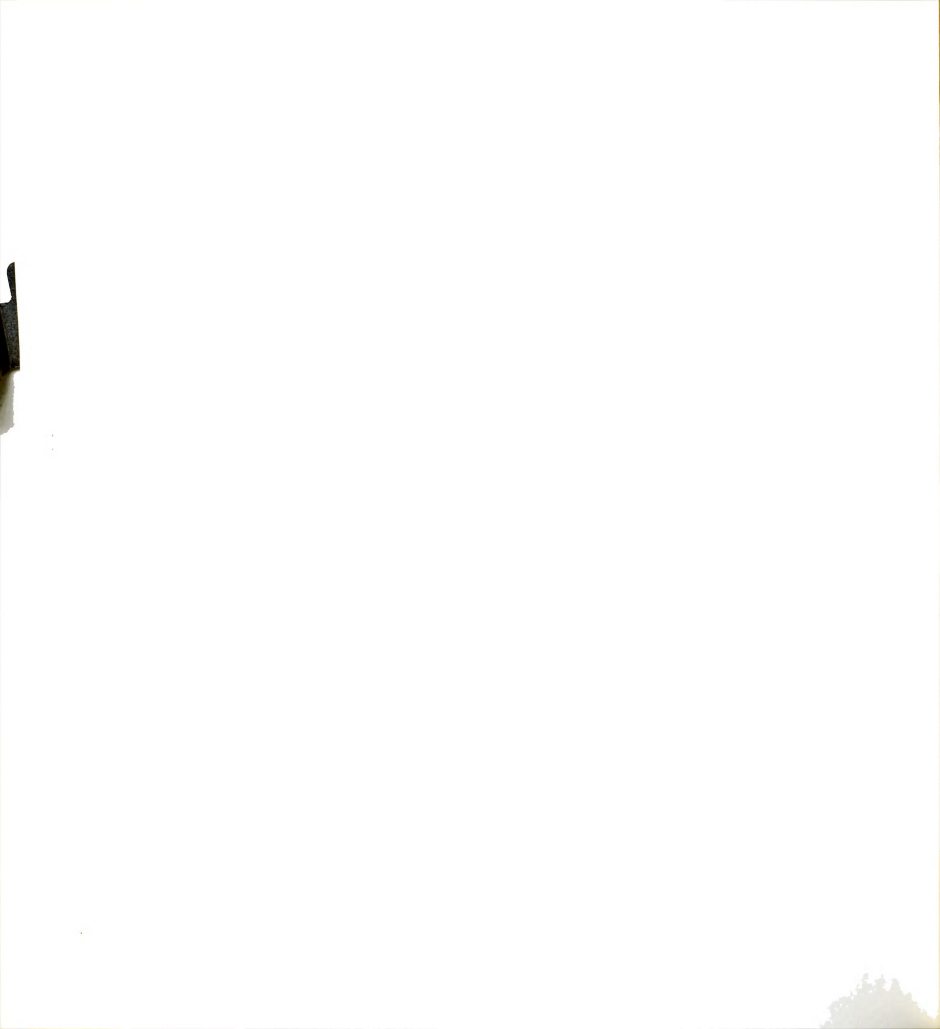
where C_b , C_m , and N denote the peripheral pyrrole carbon, the methine carbon and the nitrogen atoms, respectively. Furthermore, the atomic deviations have approximately $\bar{4}$ symmetry. All these different types of nonplanarity found in porphyrin systems suggest that the porphyrin skeleton is indeed very flexible.

The bond distances shown in Figure 24 have average bond lengths of 1.379 \pm 0.008 $^{\rm A}_{\rm A}$ for C-N, 1.381 \pm 0.008 $^{\rm A}_{\rm A}$ for C $_{\rm a}$ -C $_{\rm m}$, and 1.04 \pm 0.03 $^{\rm A}_{\rm A}$ for C-H. The corresponding bond distances given in Volume III of International Tables for X-ray Crystallography are, C-C of 1.395 \pm 0.003 $^{\rm A}_{\rm A}$ in aromatic systems, and C-H of 1.084 \pm 0.006 $^{\rm A}_{\rm A}$ in benzene. A comparison of the reported values with those of this



determination shows that the bond distances of C-C and C-H are very close to the expected values.

Also of interest are the average distances within the pyrrole rings. The average Ca-N, Ca-Ch and Ch-Ch: distances of tri-TPP, tetragonal TPP, porphine from W&F, and from this structure determination are listed in Table 22; the average of these bond distances on the basis of pyrrole with and without central hydrogen in tri-TPP and porphine are also included. A comparison of the average bond distances of the pyrrole with the hydrogen atom to those of the pyrrole without the hydrogen atom in porphine, indicates the differences: +0.004 Å for N-C_a, -0.021 Å for C_a-C_b, and +0.020 Å for C_{h} - C_{h} . The corresponding values found in tri-TPP are $+0.01~{\rm \mathring{A}}$ for N-C_a, $-0.028~{\rm \mathring{A}}$ for C_a-C_b, and +0.008 $\mbox{$\overset{\mbox{$\sc A}$}{$}$ for $C_{\mbox{$\sc b$}}$-$C_{\mbox{$\sc b$}}$$. Even though the magnitudes of the bond-length$ differences are different in the two cases, the pyrrole with hydrogen attached seems to have larger N-C, and C,-C, bond lengths, and a contracted Ca-Ch bond length. In addition, comparison of the average pyrrole bond angles of the pyrrole with a hydrogen atom to the average pyrrole bond angles of that without a hydrogen atom in the porphine structure is $+2.5^{\circ}$ for \angle C_a,N,C_a, -1.9° for \angle N,C_a,C_b, and 0.7° for $\angle c_a, c_b, c_b$ (see Table 23). The corresponding / N,C_aC_b, and 1.30 for / C_a,C_b,C_b. Such comparisons could not be extended to the tetragonal TPP since its pyrrole rings are similar.



Average Pyrrole Bond Lengths in Some Free Base Porphyrins and Porphine. Table 22.

Av.	1.379	1.442	1,355	
Porphine ^g H Pyrrole	1.381±0.003 1.377±0.012 1.379	1,431±0,006 1,452±0,011 1,442	1.365±0.006 1.345±0.001 1.355	
Porphine Pyrrole N-H Pyrrole (W&F)	1.381 ± 0.003	1,431±0,006	1.365 ± 0.006	
Porphine (W&F)	1,366	1.442	1,342	
Tetrag- onal TPP	1,350	1,455 1,442 1,438	1.347 1.351 1.362 1.342	
Ave	1,369	1,442	1,351	
tri-TPP byrrole Av. N-H	N-C _a 1.374 1.364 1.369 1 _o 350 1 _o 366	1,455	1.347	
t Pyrrole N-H	1,374	c _a -c _b 1.428	c _b -c _b , 1.355	
	N-Ca	Ca-Cb	ر ⁹ -وي	

^aThe pyrrole with central hydrogen.

 $^{\rm b}{\rm The~pyrrole~without~central~hydrogen.}$

 $\ensuremath{\text{d}_{\text{Only}}}$ one set of crystallographically independent pyrrole. $^{\text{C}}_{\text{The}}$ average of pyrrole N-H and pyrrole bond lengths.

enhe structure parameters from W&F porphine. The average is based on four crystallographically indpendent pyrrole groups.

 $^{\rm g}_{\rm The}$ porphine from this work.

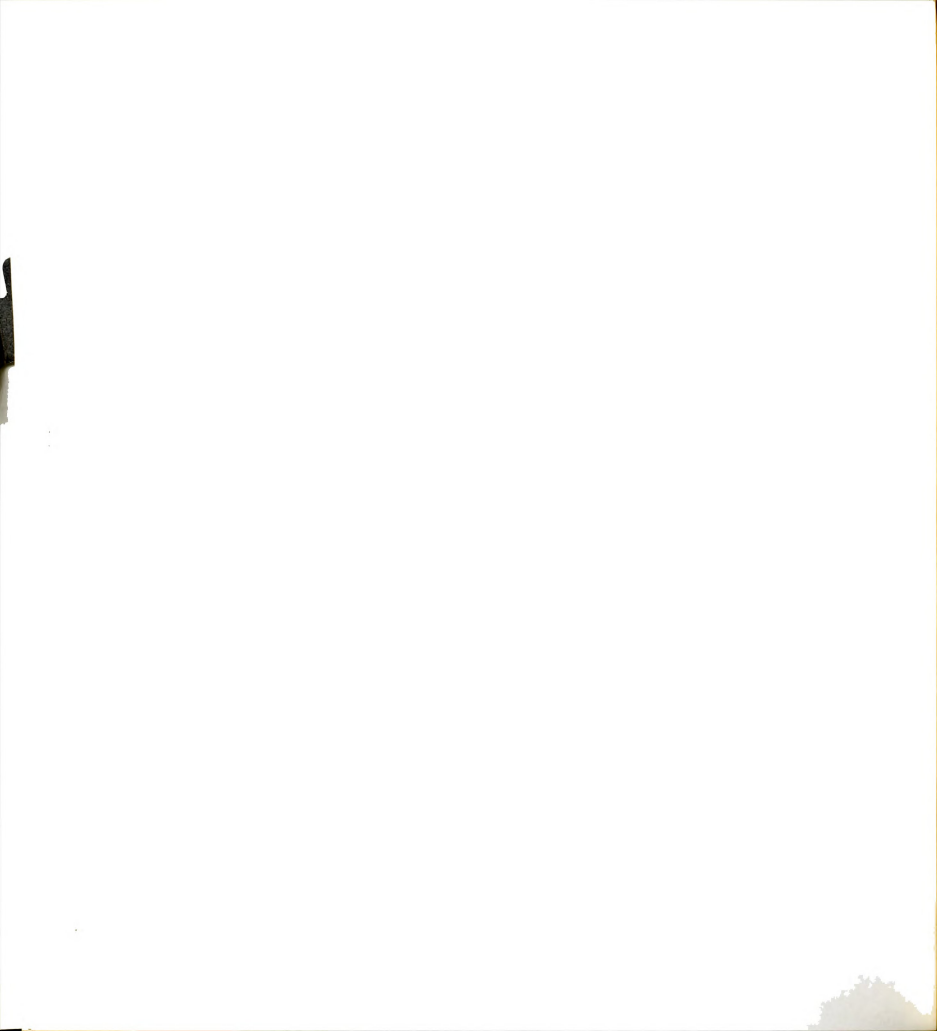
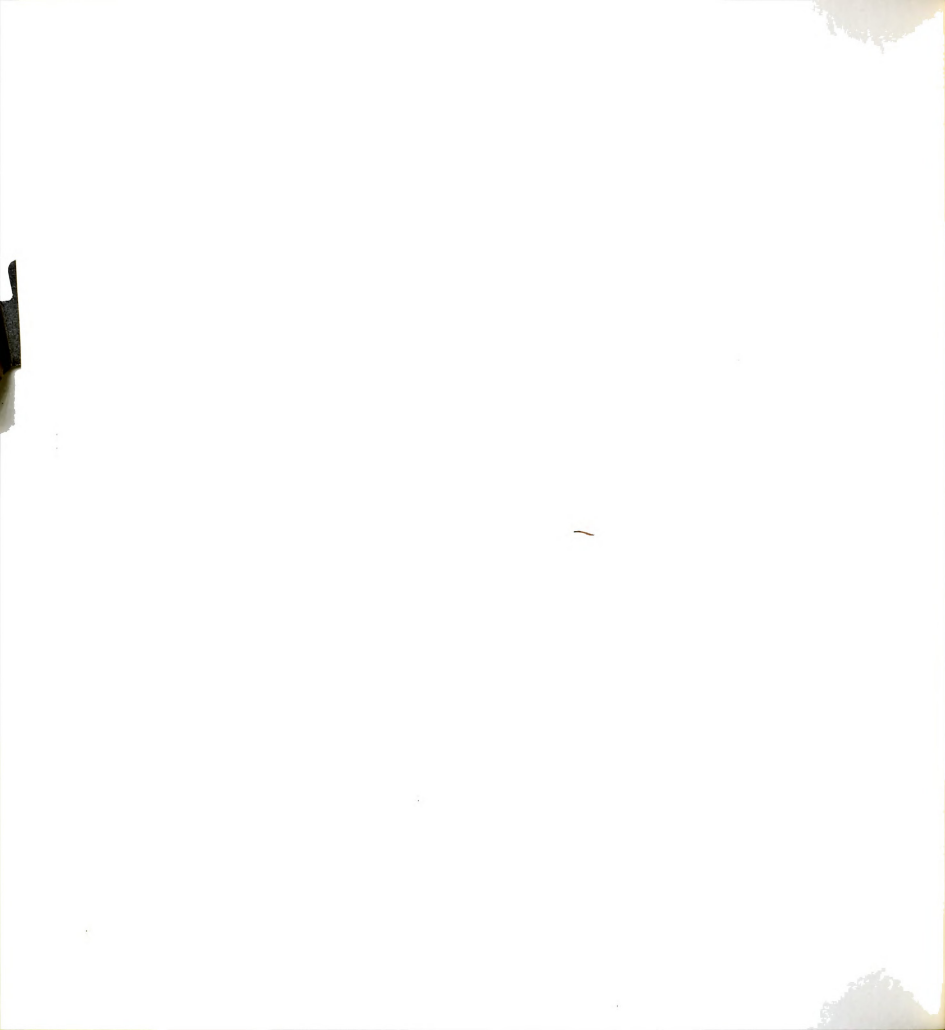


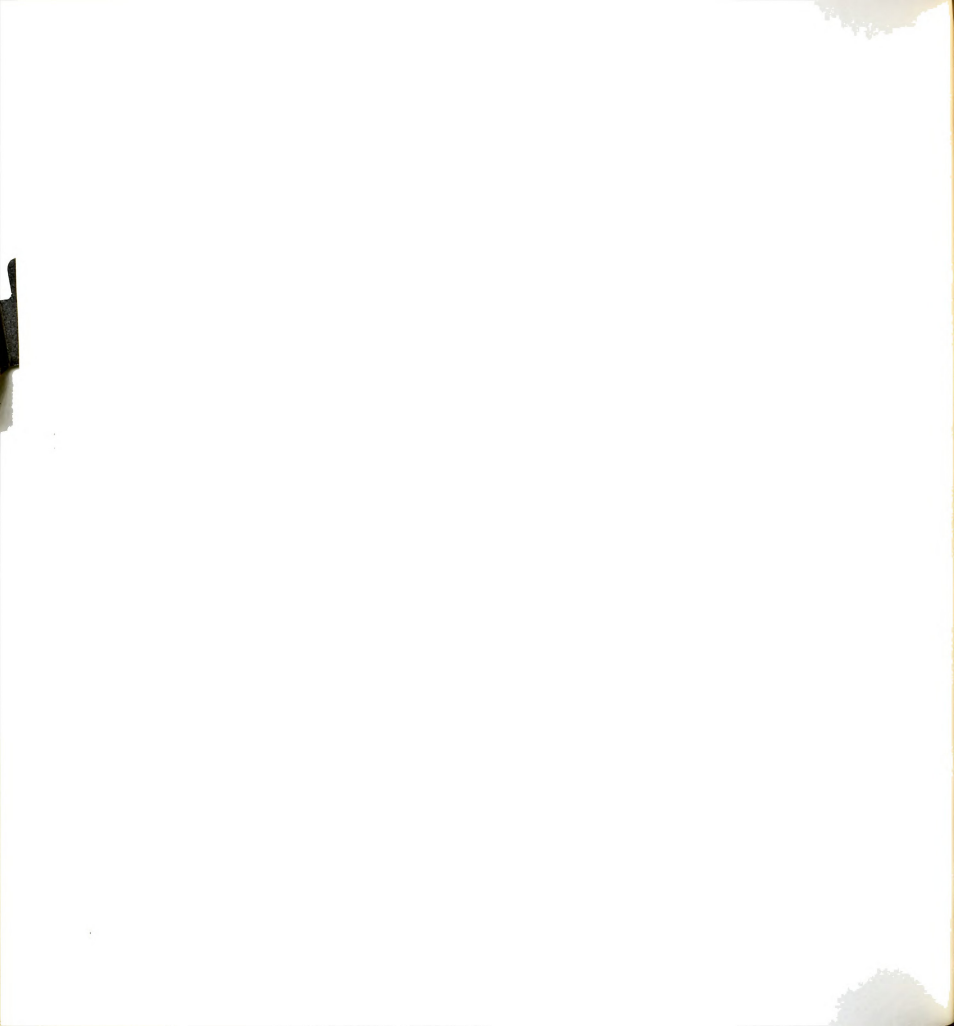
Table 23. Average Pyrrole Bond Angles in tri-TPP and the Porphine of this Work.

	tri	-TPP	Porphine (present work)	
	Pyrrole N-H	Pyrrole	Pyrrole N-H	Pyrrole
$\angle c_a, N, c_a$	109.2	106.2	108.6	106.1
\angle N, c_a , c_b	107.3	110.3	107.9	109.8
$\angle c_a, c_b, c_b$	108.1	106.8	107.9	107.2



It is interesting to note that porphine and the porphyrin nucleus of tri-TPP can be described as corresponding to a structure of hybrids of the two predominant classical resonance forms of the porphine molecule. These two forms are shown in Figure 30(a) and (b); Figure 30(c) is an attempt to represent the expected nature of the hybrid. The average pyrrole bond distances of porphine and tri-TPP are shown; the bond distances of tri-TPP are indicated in parentheses. In the hybrid form, the $\rm C_b-\rm C_b$ distance in pyrrole 1 should show increased double bond character (shorter bond length) compared to the equivalent distance in pyrrole 2. Likewise, the C-N distance in pyrrole 2 should show decreased double bond character compared to that in pyrrole 1. Trends towards these proposed results have been observed in the porphine and tri-TPP structures.

The most striking difference between this structure determination and that of W&F is the existence of two central hydrogen atoms bonded to two opposite pyrrole nitrogen atoms. These hydrogen atoms, H22 and H24, have peak heights of about 0.5 e \aleph^{-3} (background level \sim 0.1 e \aleph^{-3}) as indicated in Figure 27. The N22-H22 and N24-H24 bond distances are 0.89 \aleph and 0.92 \aleph , respectively. The locations of the imino hydrogen atoms are slightly off the line joining their opposite nitrogen atoms; a deviation of 5.8° toward N21 is found for H22 and of 4.5° toward N23 with respect to N22-N24 for H24. These departures make the central hydrogen van der Waals contact (2.31 \aleph) slightly larger (0.01 \aleph)





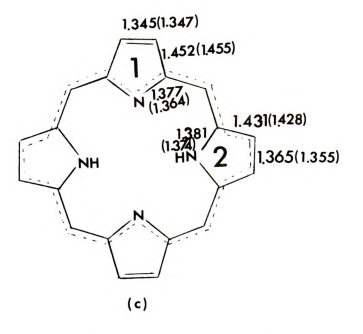
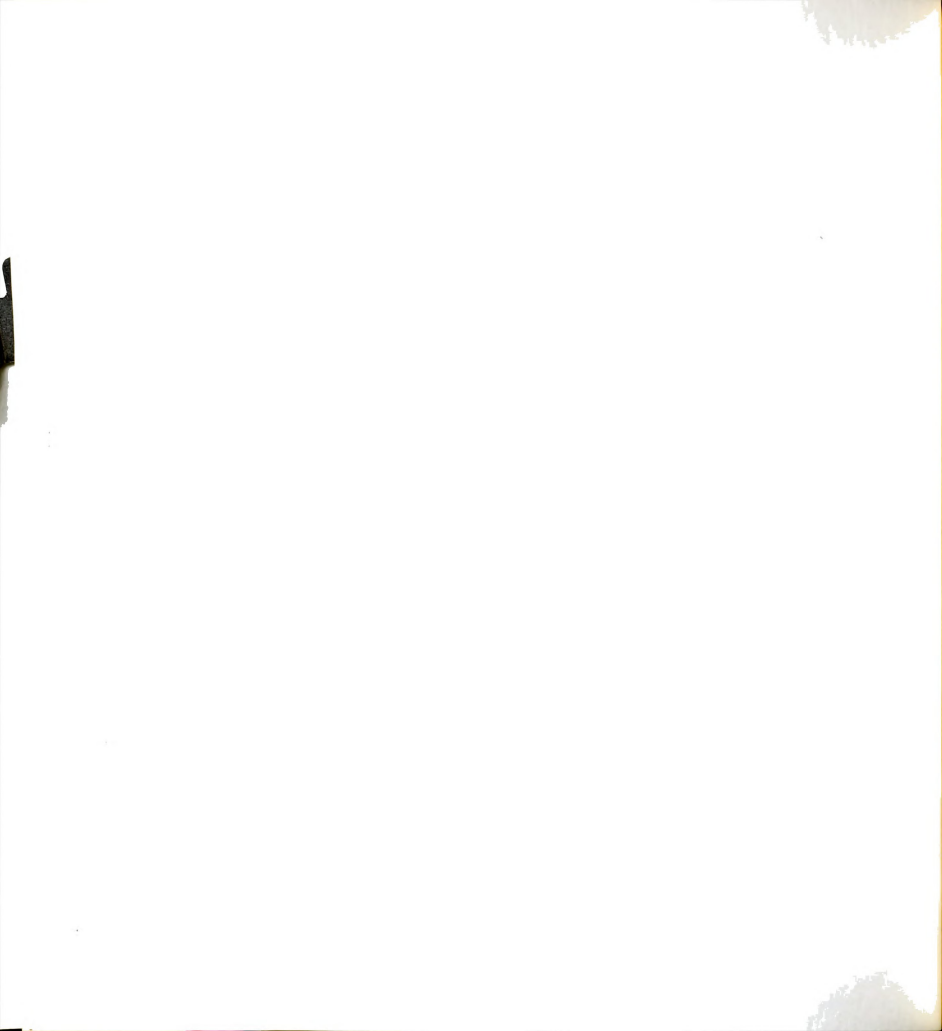


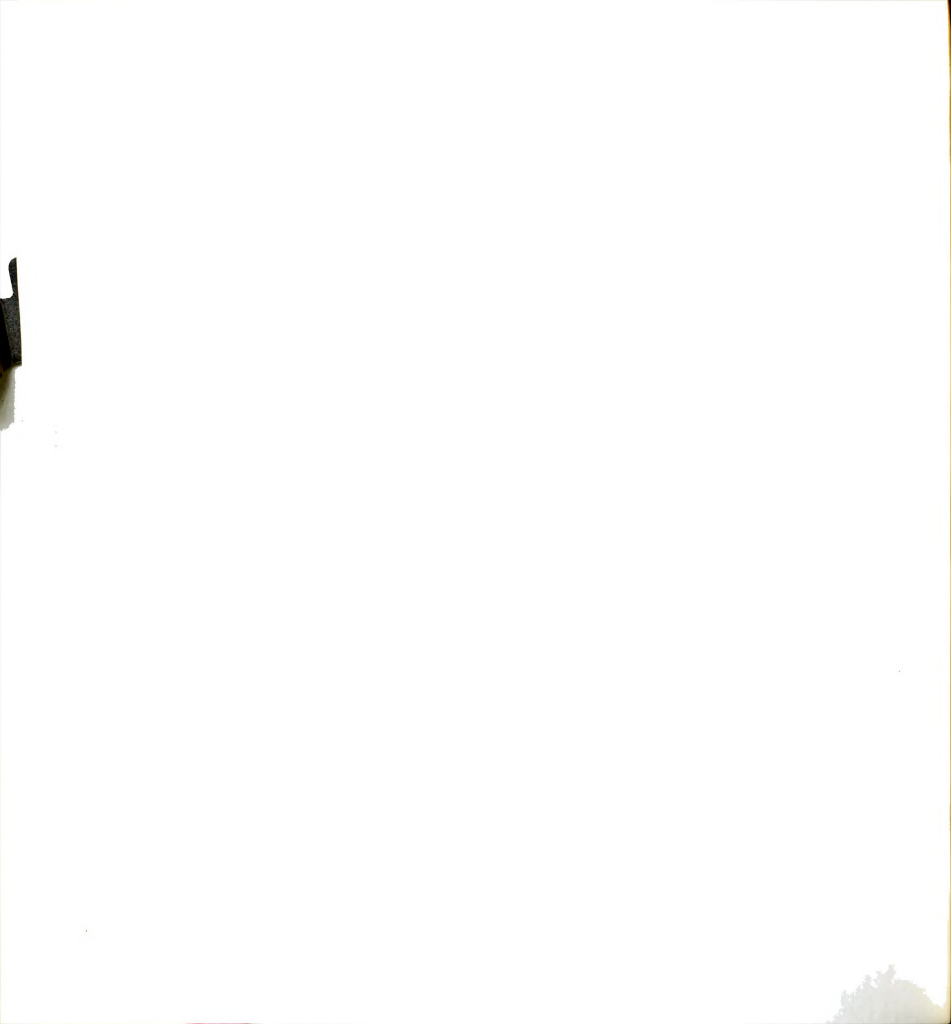
Figure 30. Porphine resonance forms.



than the contact between two hydrogen atoms lying on the line of N22-N24. It is noteworthy that the central hydrogen atoms are essentially coplanar to the porphine molecule, as shown by their small atomic deviations from the NLS plane (see Fig. 23, 0.05 % for H22 and -0.09 % for H24). The central hydrogen structure of the porphine is different from that of tri-TPP. In tri-TPP case the central hydrogen atoms are slightly inclined from the NLS plane, presumably in order to keep a reasonable contact distance.

It is of additional interest that the distance between the pair of pyrrole nitrogen atoms which carry the central hydrogen atoms is $0.06~\text{\AA}$ longer than the corresponding distance of the other pair of nitrogen atoms. A similar value of $0.14~\text{\AA}$ is found in tri-TPP. This slight elongation of the N-N distance tends to increase the distance between the central hydrogens.

A comparison between the central region of the porphine molecule as reported by W&F and this work was made. It can be seen from the difference electron density in the vicinity of the nitrogen atoms projected on the ac plane (see Fig. 27) that only small residual electron densities other than the hydrogen atoms (about $0.1 \ {\rm e}^{\ 3}$) can be found. This observation suggests strongly that: (1) the sample of porphine used for this work does not contain a metal impurity at the center of the porphine molecule, and (2) only one pair of diagonal central hydrogen atoms is bonded to diagonal nitrogen atoms. The coordinates and peak heights of the



central hydrogen atoms of the two structures are listed in Table 24. The pair of alleged "half-hydrogen atoms", H21 and H23 are of peak heights of about 0.3 e $^{-3}$; the corresponding locations are found to lie in negative regions in the present difference electron density. By comparing these peak heights (0.3 e $^{-3}$) with the background level of 0.2 e $^{-3}$ in the structure reported by W&F, one can see that hydrogen atoms, H21 and H23 could be error fluctuations of the background.

Final Remarks

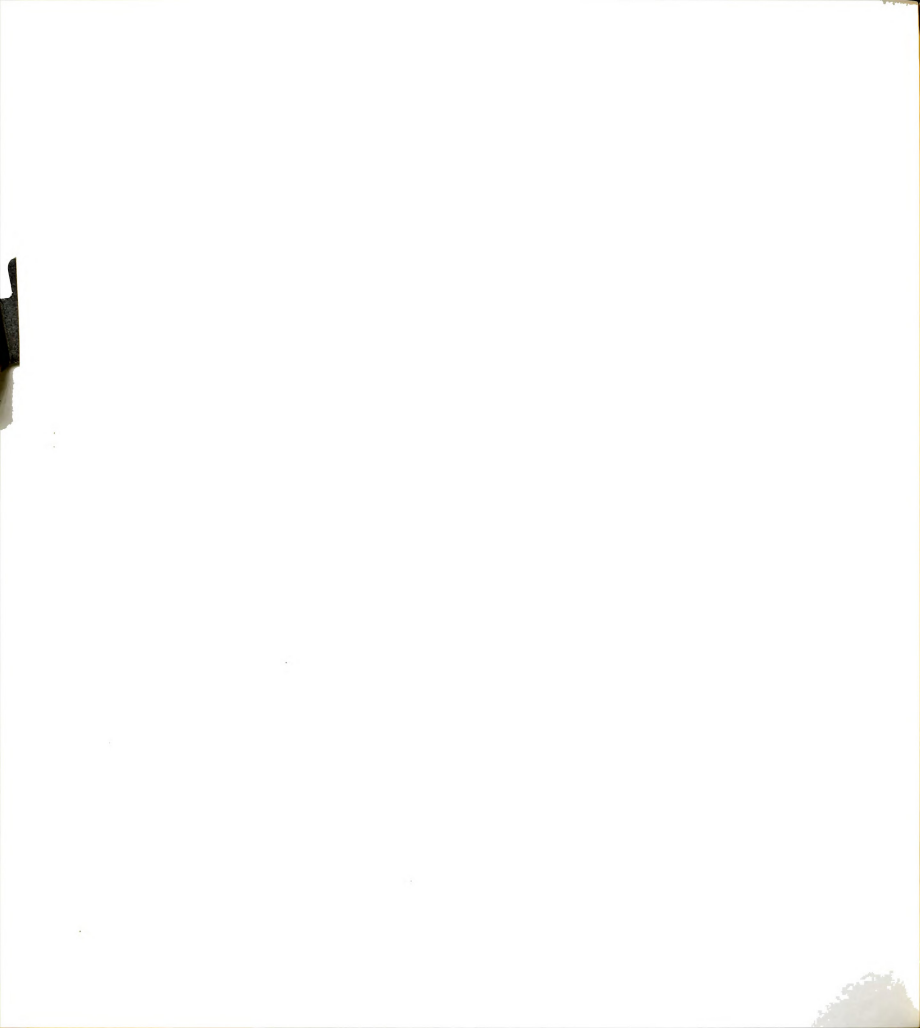
A comparison of the observed structure amplitues of this work with those of W&F gave an R_d -factor, indicating the discrepancy between the two sets of data, which was 0.13, where

$$R_{d} = \sum_{n=1}^{n} \left| |F_{0}| - |F_{0}|_{W \& F} \right| / \sum_{n=1}^{n} |F_{0}|$$

and n is the total number of reflections of the present structure determination (n = 1206). This $R_{\mbox{\scriptsize d}}$ -value indicates a substantial disagreement between the two sets of data. Factors which may have contributed to this disagreement are as follows.

1) Extinction Correction

A secondary extinction correction was made in this work. The crystal used for the main intensity measurement had a size of 0.20 x 0.275 x 0.05 mm, while the crystal



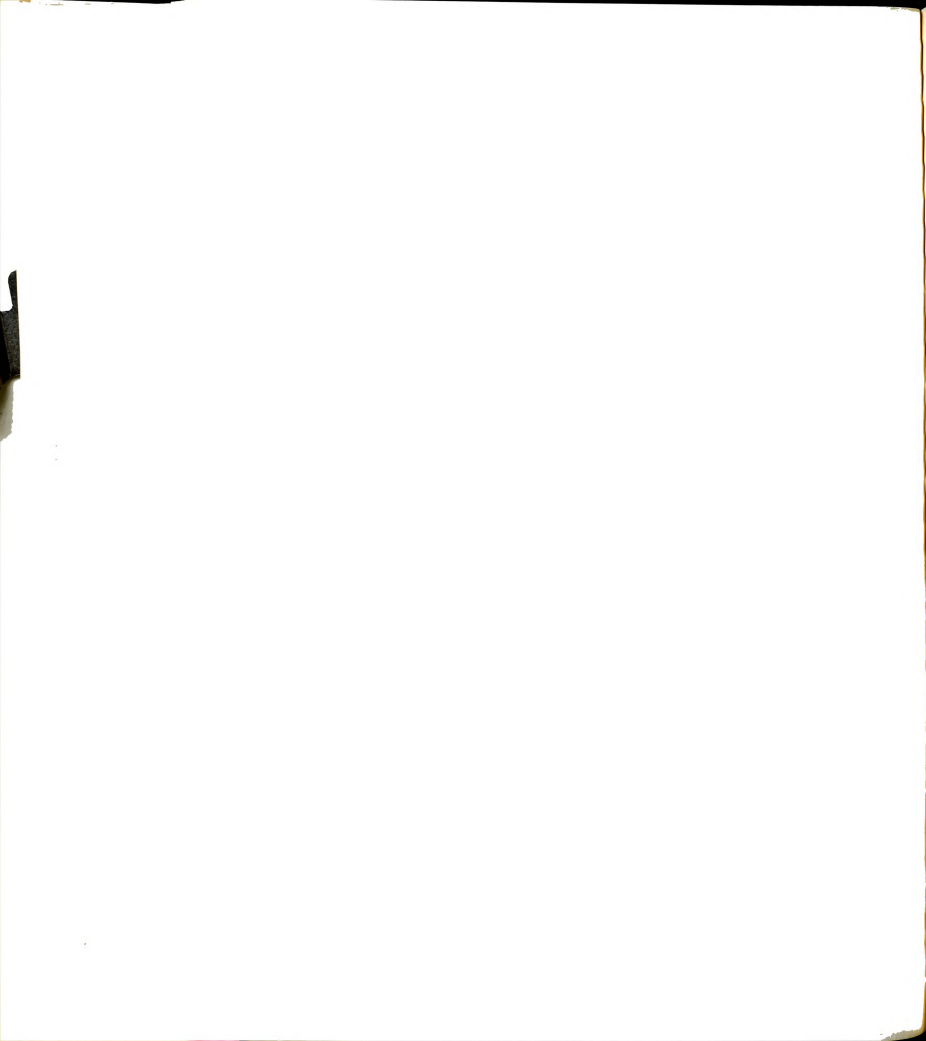
Fractional Coordinates and Peak Heights of Central Hydrogen Atoms from Two Porphine Structure Analyses. Table 24.

Peak

Atom	e _X	Ϋ́	8	Height (e A-3)	Present Work
н21	0.142	0.433	0,125	0.3	(negative)
H22	0.100 (0.118) ^b	0.433 (0.436)	-0.058 (-0.046	16) 0.4	(0.5)
н23	0.033	0.321	-0.058	0.3	(negative)
H24	0.067 (0.063)	0.308 (0.317)	0.108 (0.104)	1) 0.4	(0.5)

z, x of this work. ^aCoordinates x, z from W&F work are equivalent to

 $^{^{\}rm b}_{\rm The~numbers}$ in the parentheses are obtained from this work.

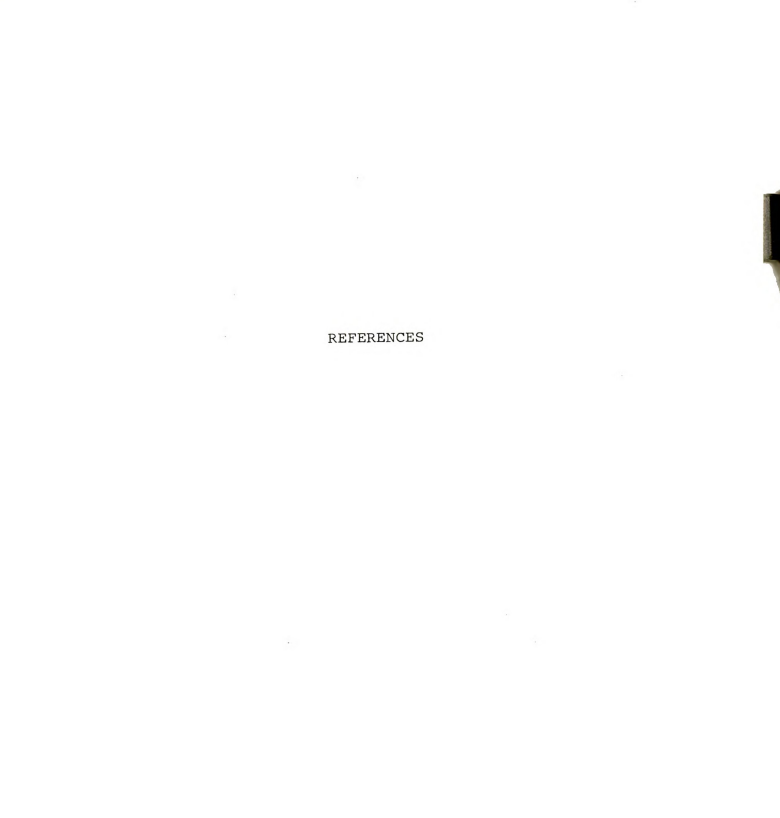


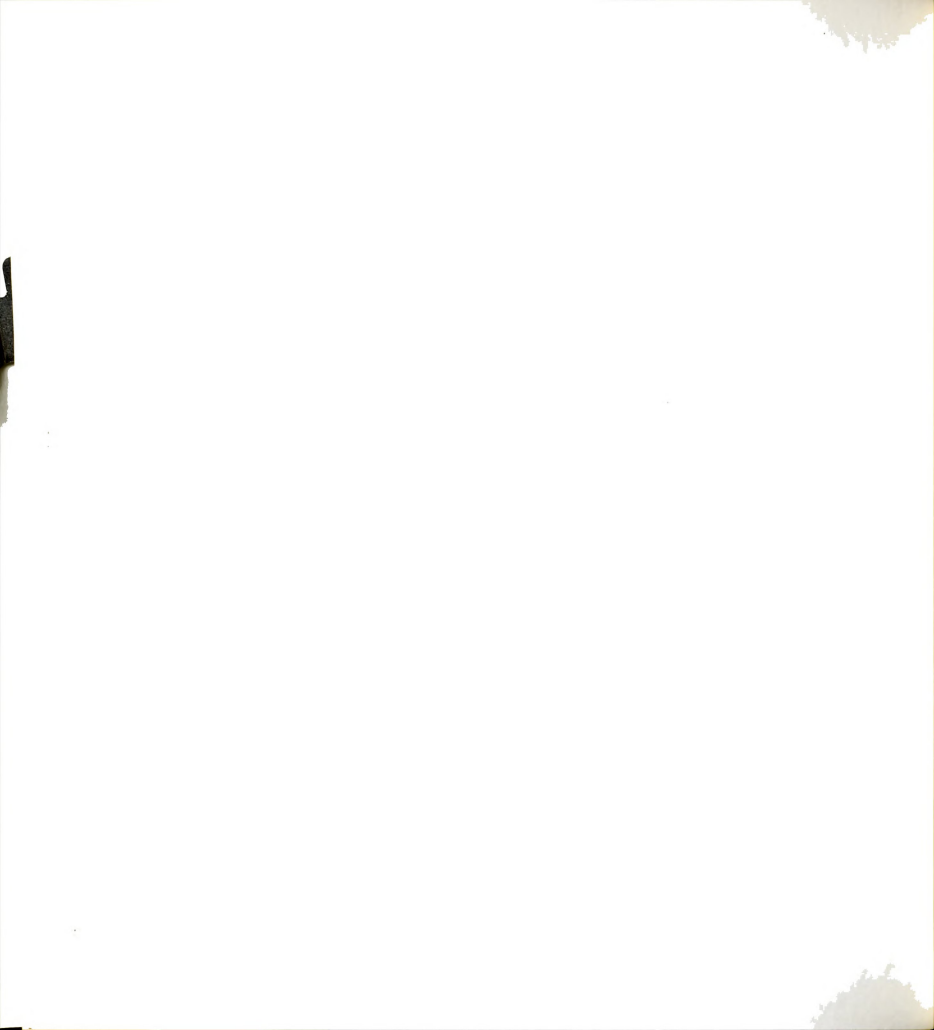
used by W&F work was $0.36 \times 0.36 \times 0.20$ mm (reported as 0.50 mm along the diagonal of one face). The latter is approximately eight times larger than the former. It is well known that secondary extinction effects are much more pronounced for larger crystals. Thus, strong low-order reflections can contribute to the large discrepancy between two sets of data due to extinction.

2) Counting Error

The counting error of 7% of intensity data (80 out of 1206 reflections) from this work was minimized by using ω (omega) step-scan measuring techniques. Thus the set of $|\mathbf{F}_0|^{\mathsf{I}}\mathbf{s}$ of the present data is probably affected by more favorable counting statistics and this could contribute to the discrepancies with W&F data.

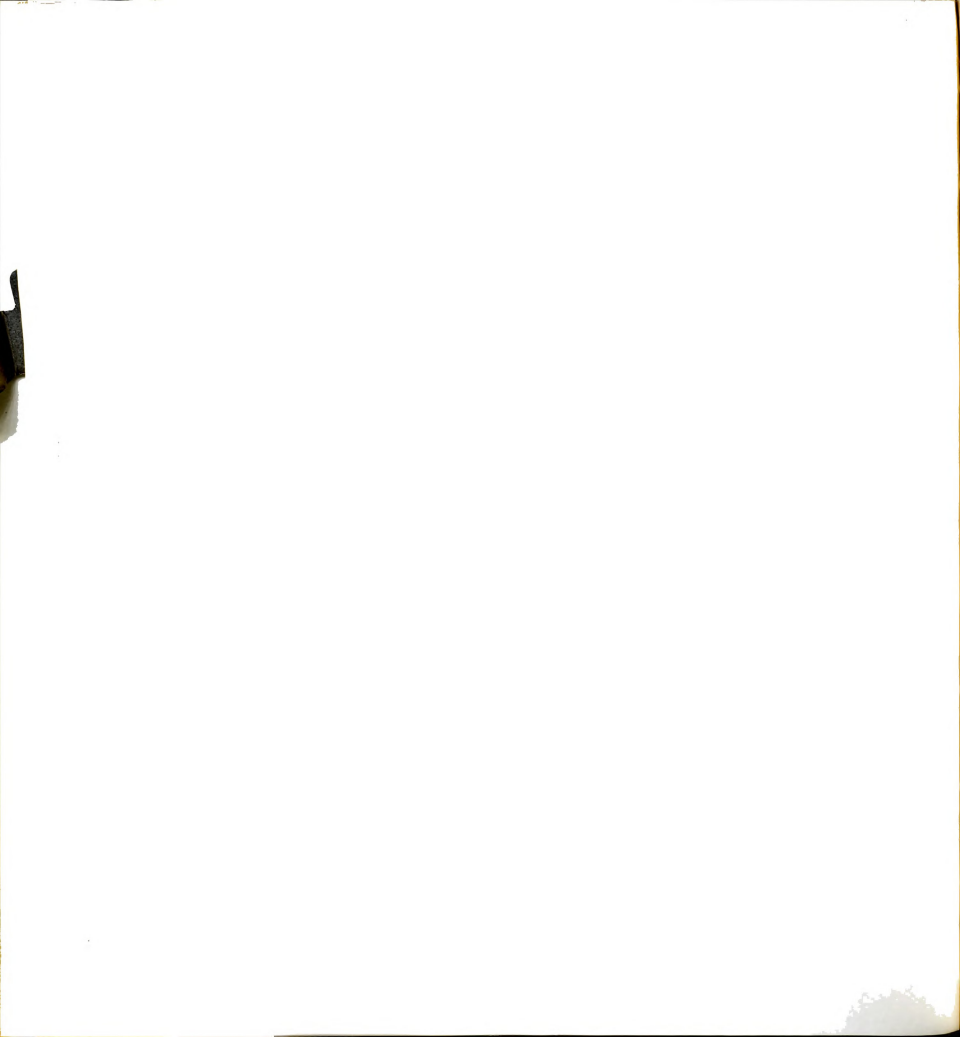




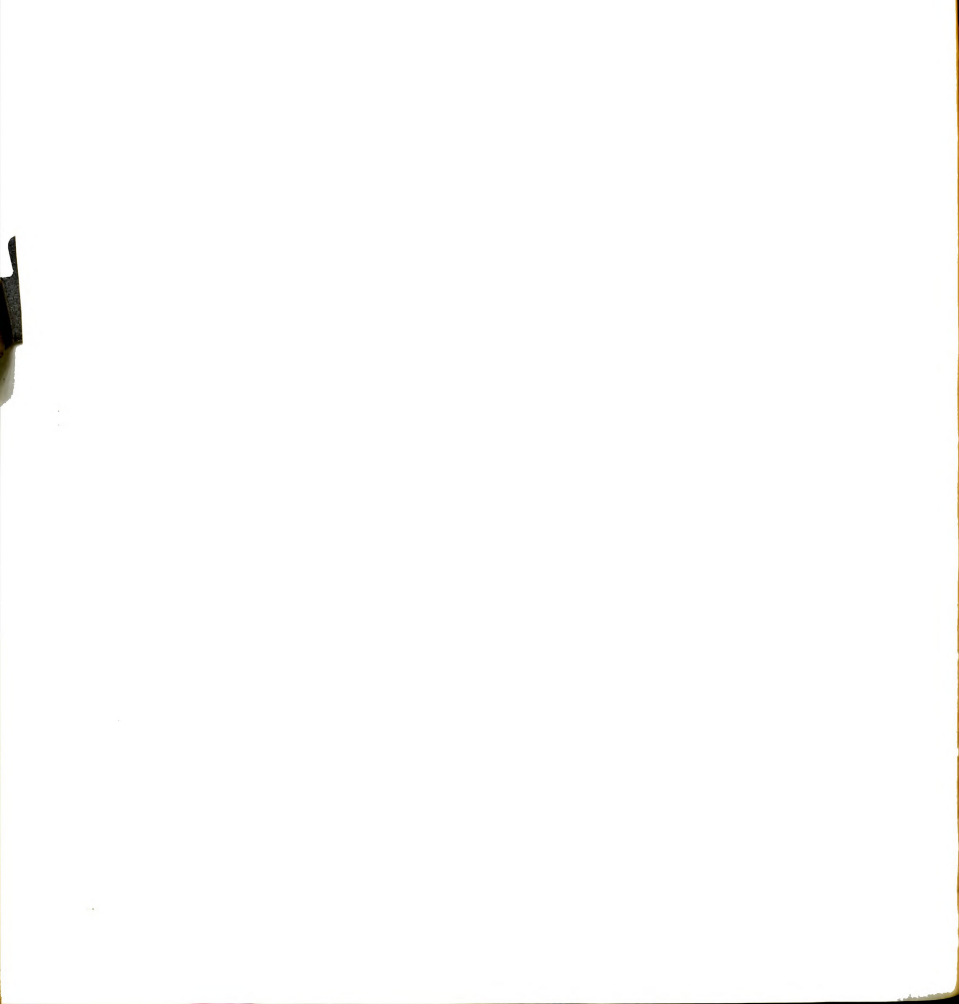


REFERENCES

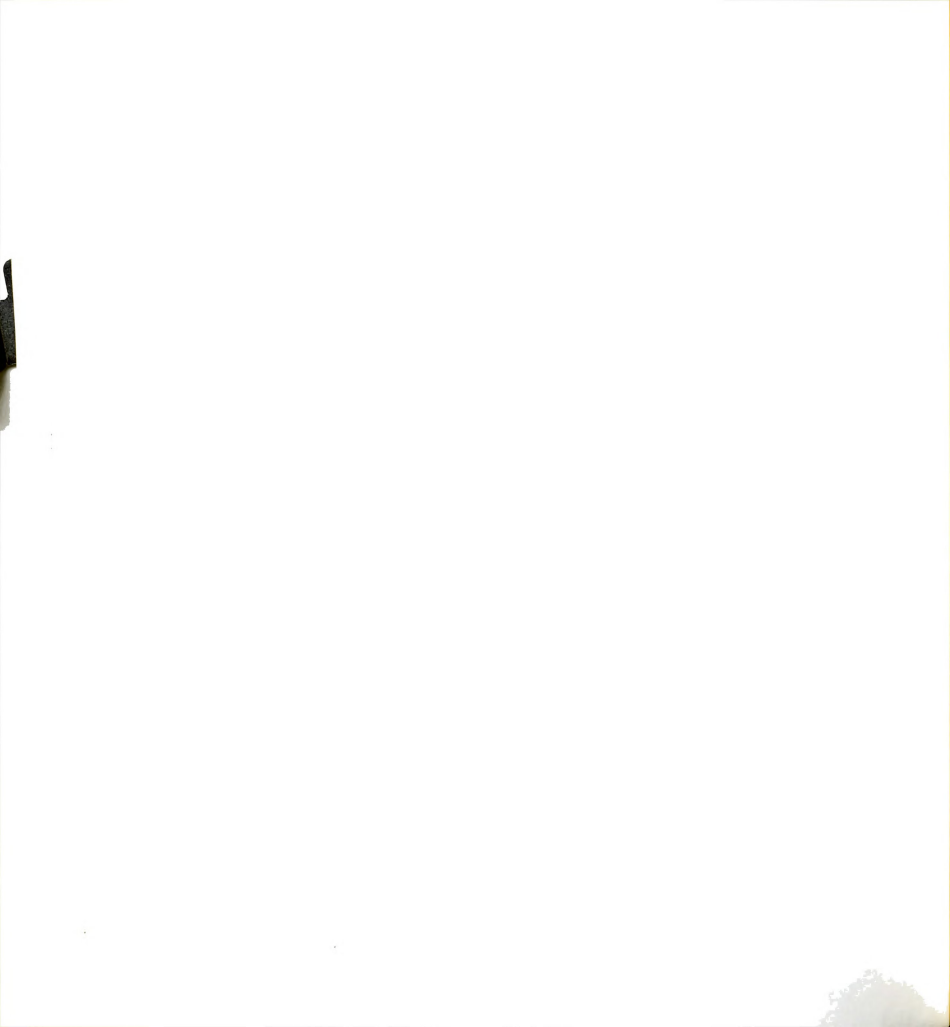
- 1. J. L. Hoard, J. Amer. Chem. Soc., 87, 2305 (1965).
- E. B. Fleischer, <u>Accounts of Chemical Research</u>, 3, 105 (1970).
- E. B. Fleischer, C. Miller, and L. E. Webb, <u>J. Amer.</u> Chem. Soc., 86, 2342 (1964).
- 4. E. B. Fleischer, J. Amer. Chem. Soc., 85, 146 (1963).
- J. L. Hoard, G. H. Cohen, and M. D. Glick, <u>J. Amer. Chem. Soc.</u>, 89, 1992 (1967).
- 6. R. C. Petterson, Acta. Cryst., B25, 2527 (1969).
- R. Timkovich, and A. Tulinsky, <u>J. Amer. Chem. Soc.</u>, 91, 4430 (1969)
- W. E. Bennett, D. E. Broberg, and N. C. Baenziger, <u>Inorg. Chem.</u>, in press.
- E. B. Fleischer, and T. S. Srivastava, <u>J. Amer. Chem.</u> Soc., 91, 2403 (1969).
- J. H. Hoard in "Structural Chemistry and Molecular Biology," A. Rich, and N. Davidson Ed., W. H. Freeman and Company, San Francisco, Calif.. (1968), pp 573-594.
- R. Countryman, D. M. Collins, and J. L. Hoard, <u>J. Amer. Chem. Soc.</u>, <u>91</u>, 5166 (1969).
- 12. P. A. Loach, and M. Calvin, Biochemistry, 2, 361 (1963).
- P. A. Loach, and M. Calvin, <u>Nature</u>, 202, 343 (1964).
- M. Calvin, Rev. Pure Appl. Chem., 15, 1 (1965).
- 15. L. J. Boucher, <u>J. Amer. Chem. Soc.</u>, <u>90</u>, 6640 (1968)
- L. J. Boucher, and J. J. Katz, <u>J. Amer. Chem. Soc.</u>, 89, 134 (1967).



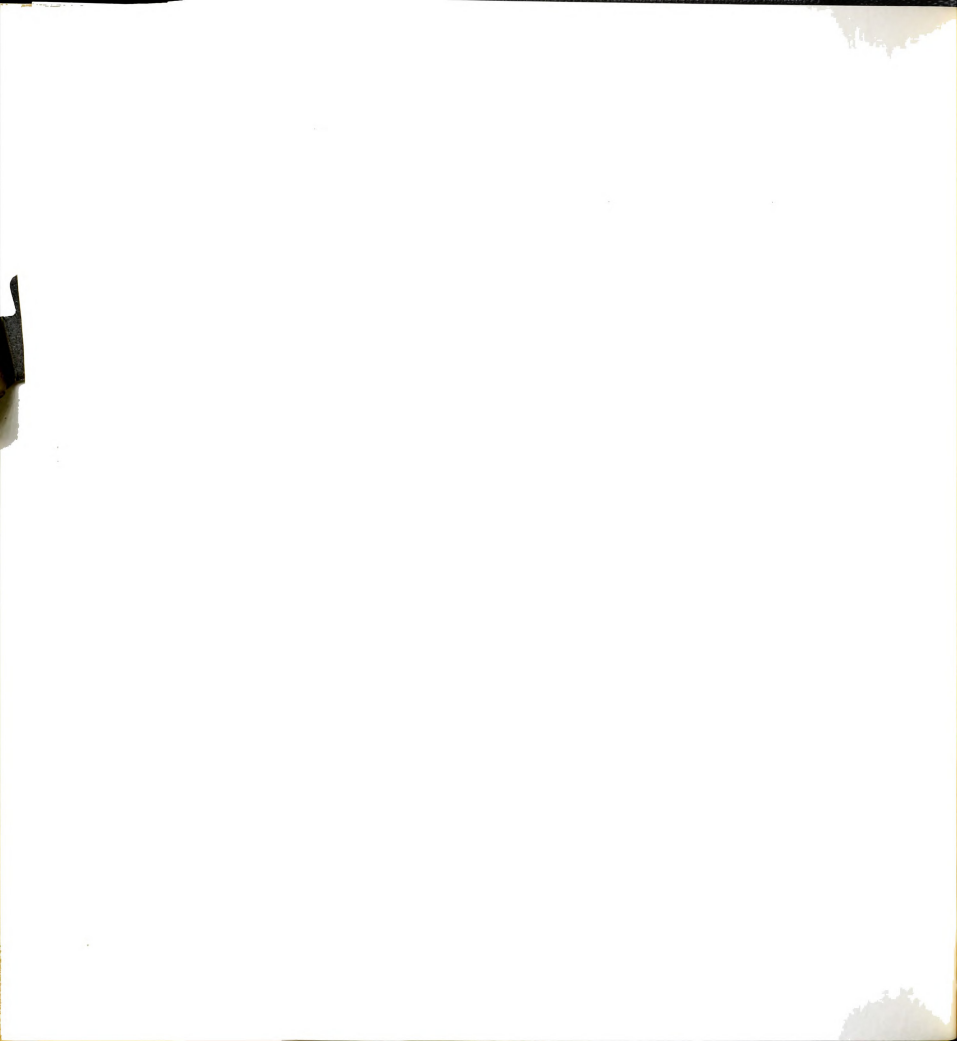
- 17. D. Harker, J. Chem. Phys., 4, 381 (1936).
- 18. R. W. James, "The Optical Principles of the Diffraction of X-rays," Cornell University Press, New York (1965)
- 19. A. D. Adler, J. Inorg. Nucl. Chem., 32, 2443 (1970).
- H. Lipson and W. Cochran, "The Determination of Crystal Structures," Cornell University Press, New York (1966), pp 73-76.
- J. S. Rollett, "Computing Methods in Crystallography," Pergamon Press, Long Island City, New York (1965), pp 133-139.
- G. H. Stout, and L. H. Jensen, "X-ray Structure Determination," The Macmillan Company, New York (1968), pp 242.
- W. R. Bushing, K. O. Martin, and H. A. Levy, "A Fortran Crystallographic Least-squares Program," Report ORNL-TM-305, Oak Ridge, Tennessee (1962).
- C. T. North, D. C. Phillips, and F. S. Mathews, <u>Acta.</u> <u>Cryst.</u>, <u>A24</u>, 351 (1968).
- D. J. Wehe, and W. R. Bushing, "A Fortran Program for Calculating Single Crystal Absorption Correction," Oak Ridge National Laboratory, Report ORNL-TM-229 (1962).
- C. K. Johnson, "ORTEP, a Fortran Thermal-Ellipsoid Plot Program for Crystal Structure Illustrations," ORNL-3794, Oak Ridge National Laboratory, Oak Ridge, Tenn., 1965.
- L. H. Vogt, A. Zalkin, and D. H. Templeton, <u>Inorg. Chem.</u>, 6, 1725 (1967).
- L. E. Sulton, et al., "Tables of Interatomic Distances and Configuration in Molecules and Ions," Burlington House, London (1965), pp 99.
- 29. A. J. C. Wilson, Structure Report, 16, 184 (1952).
- Y. C. Tang, and J. H. Sturdivant, <u>Acta. Cryst.</u>, 5, 74 (1952).
- M. D. Glick, G. H. Cohen, and J. H. Hoard, <u>J. Amer.</u> Chem. Soc., 89, 1966 (1967).
- G. D. Dorough, and K. T. Shen, <u>J. Amer. Chem. Soc.</u>, 72, 3939 (1950).



- J. Erdman, and A. H. Corwin, <u>J. Amer. Chem. Soc.</u>, 68, 1885 (1946).
- 34. M. Gouterman, G. Wagniere, and L. C. Snyder, J. Mol. Spectroscopy, 11, 108 (1963).
- J. Falk, and E. Willis, <u>Austral. J. Sci. Res.</u>, 4, 579 (1951).
- 36. S. F. Mason, J. Chem. Soc., 976 (1958).
- 37. J. M. Robertson, J. Chem. Soc., 1195 (1936).
- G. M. Badger, R. T. Harris, R. A. Jones, and J. Sasses, J. Chem. Soc., 4329 (1962).
- 39. E. D. Becker, R. B. Bradly, and C. J. Watson, <u>J. Amer. Chem. Soc.</u>, <u>83</u>, 3743 (1961).
- 40. S. Silvers, and A. Tulinsky, <u>J. Amer. Chem. Soc.</u>, $\underbrace{89}_{}$, 3331 (1967).
- 41. M. J. Hamor, T. A. Hamor, and J. L. Hoard, <u>J. Amer.</u> <u>Chem. Soc.</u>, 86, 1938 (1964).
- L. Webb, and E. Fleischer, <u>J. Chem. Phys.</u>, <u>43</u>, 3100 (1965).
- 43. T. C. Furnas, "Single Crystal Orienter Instruction Manual," General Electric Company, Milwaukee (1957).
- H. W. Wyckoff, M. Doscher, D. Tsernoglou, T. Inagami, L. N. Johnson, K. D. Hardman, N. M. Allewell, D. M. Kelly, and F. M. Richards, J. Mol. Biol., 27, 563 (1967).
- 45. A. J. C. Wilson, Acta. Cryst., A23, 888 (1967).
- 46. W. Parrish, Phillips Technical Review, 17, 206 (1965).
- 47. E. W. Hughes, J. Amer. Chem. Soc., 63, 1737 (1941).
- U. W. Arndt, and B. T. Willis, "Single Crystal Diffractometry," University Press, Cambridge (1966), pp 15-30, 234-236.
- 49. M. J. Buerger, "Crystal-Structure Analysis," John Wiley & Sons, Inc., New York (1960).
- 50. C. G. Darwin, Phil. Mag., 43, 800 (1922).
- 51. V. Schomaker, J. Waser, R. E. Marsh, and G. Bergman, <u>Acta. Cryst</u>., 12, 600 (1959).



- 52. D. W. J. Cruickshank, Acta. Cryst., 2, 65 (1949).
- 53. D. W. J. Cruickshank, and A. Robertson, <u>Acta. Cryst.</u>, 6, 198 (1953).
- 54. International Tables for X-ray Crystallography (1962), Vol. III, pp 202-207. Birmingham: Kynoch Press.





APPENDIX 1

GENERAL REVIEW OF X-RAY DIFFRACTION48,49

1. Bragg's Law and its Application

Diffraction, considered as the reflection of X-rays from planes $(hk\ell)$ of a crystal lattice, can be expressed in a simple form

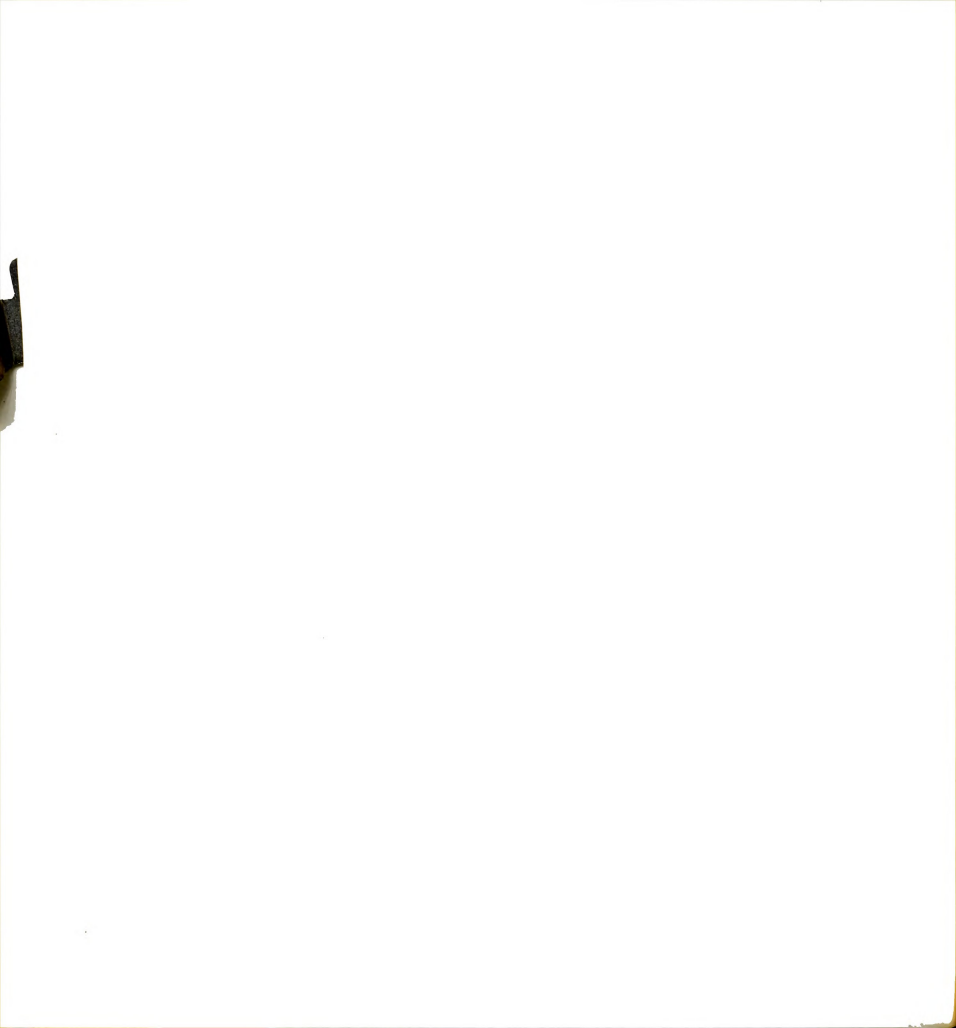
2
$$d(hk\ell) \sin \theta = n\lambda$$

where h, k, ℓ , and n are integers, θ is the angle at which the incident and reflected beam intersect the planes (hk ℓ) and d(hk ℓ) is the spacing of lattice planes which are parallel and intersect the unit cell edges \overline{a}^* , \overline{b}^* , \overline{c}^* , at n(a/h), n(b/k), and n(c/ ℓ). Mathematically, these conditions can lead to equations with different forms. The most common expression is in terms of the reciprocal lattice with corresponding reciprocal cell parameters a^* , b^* , and c^* . The parameters, a^* , b^* , and c^* can be considered as vectors with the following properties

$$\overrightarrow{a}$$
 $\cdot \overrightarrow{a}$ $= \overrightarrow{b}$ $\cdot \overrightarrow{b}$ $= \overrightarrow{c}$ $\cdot \overrightarrow{c}$ $= 1$

and

$$\overrightarrow{a}$$
 $\overrightarrow{*}$ \overrightarrow{b} \overrightarrow{a} $\overrightarrow{*}$ \overrightarrow{c} \overrightarrow{a} \overrightarrow{b} \overrightarrow{c} \overrightarrow{a} \overrightarrow{b} \overrightarrow{a} \overrightarrow{a}



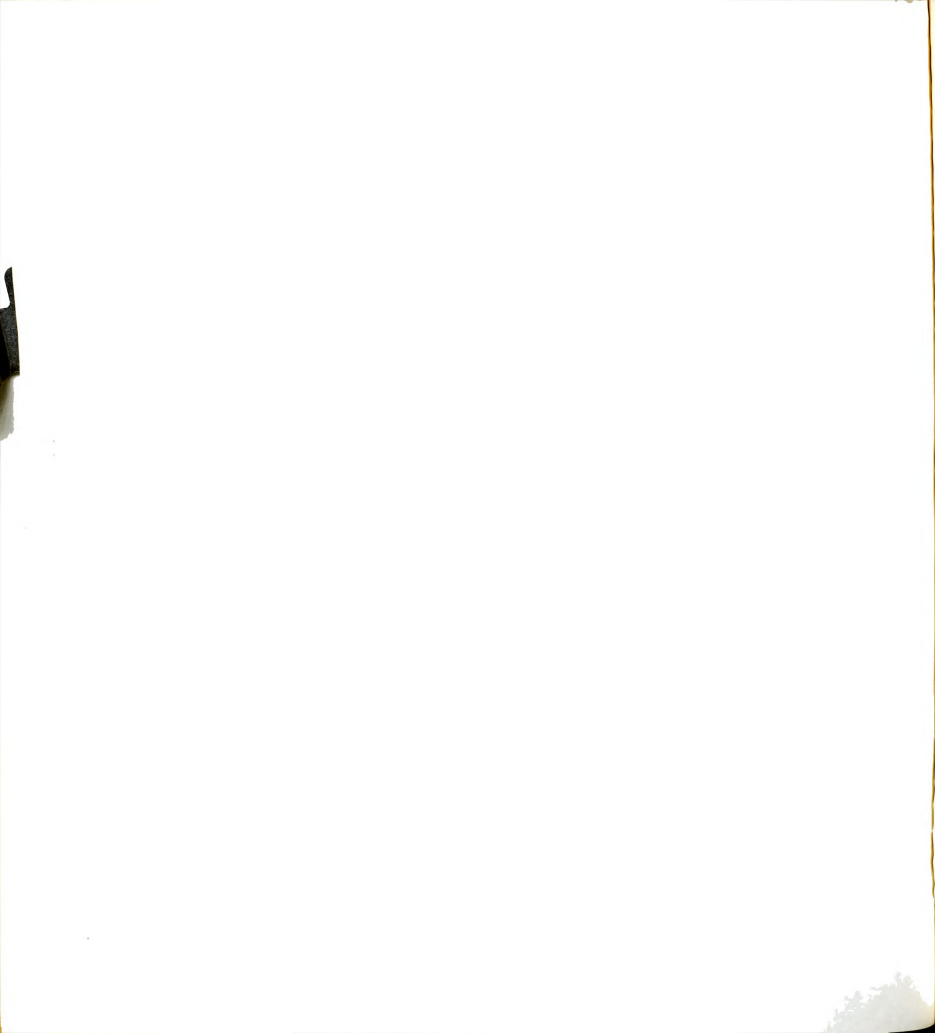
Consider, in the reciprocal lattice, a vector $\vec{r}^* = \vec{h}\vec{a}^* + \vec{k}\vec{b}^* + \vec{k}\vec{c}^*$ constructed between the lattice point hk ℓ and the origin, with a magnitude of $1/d(hk\ell)$, and perpendicular to the lattice plane hk ℓ in direct space. The reciprocal lattice vector \vec{r}^* can then be interpreted in terms of certain angular settings by the use of polar coordinates. An example based on the orthorhombic crystal system is shown in Figure 31.

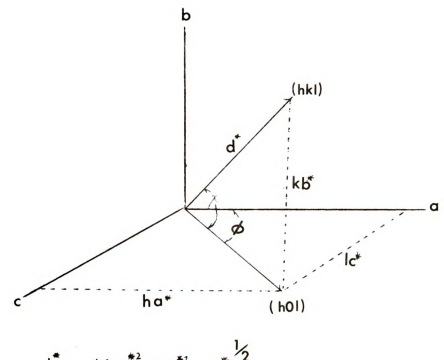
2. Mosaic Crystal

Most crystals possess irregulatities in their atomic arrangement, in the form of dislocations, point defects, and the like. These irregularities tend to destroy the coherence between the components of the incident beam scattered by different parts of the crystal. The crystal can be divided, effectively, into small regions, about 10,000~Å across, which are sufficiently perfect to reflect the X-ray beam coherently, but between which there is loss of coherence. These perfect regions are known as "mosaic block". A crystal possessing mosaic blocks is known as a mosaic crystal.

3. Integrated Intensity

When a crystal is rotated with uniform angular velocity, $\omega_{_{\rm V}}$, through the hk ℓ plane in an incident X-ray beam whose uniform intensity is ${\rm I}_0$, the integrated intensity, I, of the diffracted beam, whose total energy is ${\rm E}_0$, can be





$$d^{*} = ((h a^{*2}_{0}) + (k b^{*2}_{0}) + (l c^{*2}_{0})^{2}$$

$$\sin \chi = k b^{*}_{0} / d^{*}$$

$$2\theta = 2 \sin^{-1} (/ 2d)$$

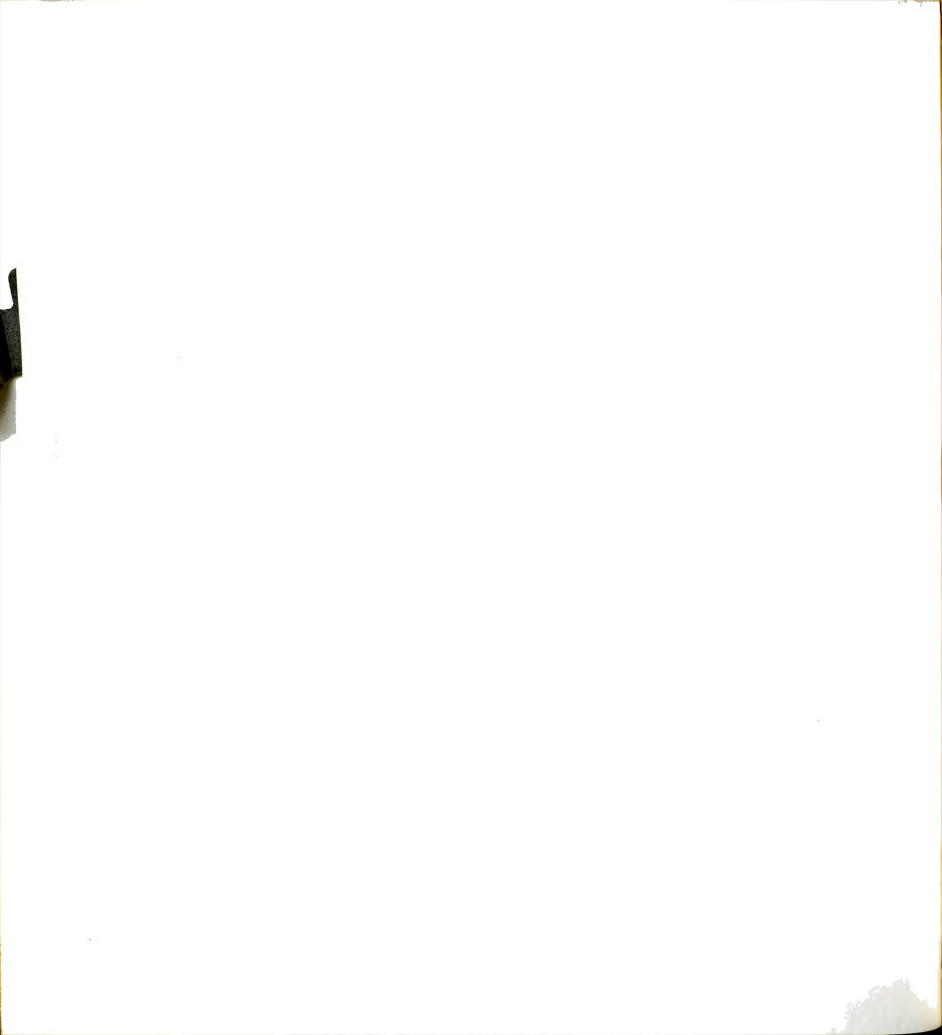
$$\tan \omega = l c^{*} / h a^{*}$$

$$a^{*} = 1 / a$$

$$b^{*} = 1 / b$$

$$c^{*} = 1 / c^{*}$$

Figure 31. Polar coordinates of a reciprocal lattice point $(hk \ell)$ for orthorhombic crystal system.



expressed as

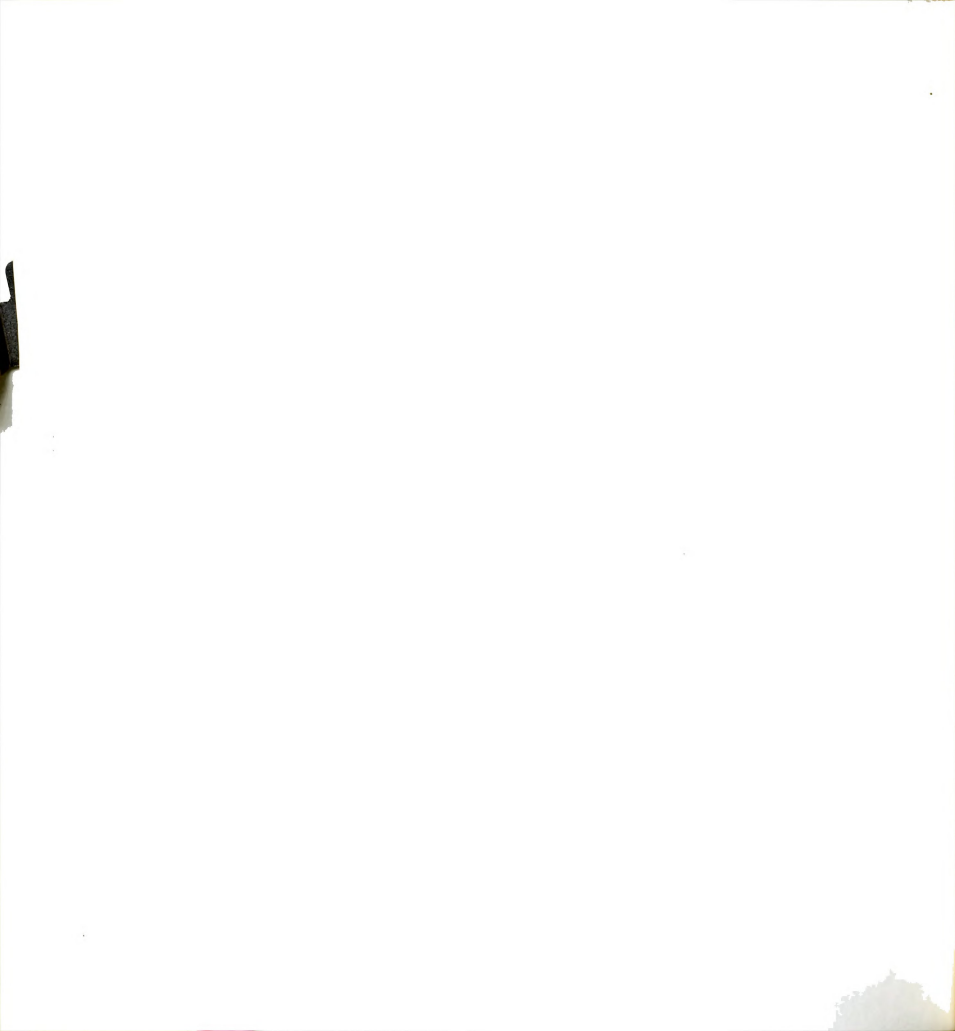
$$I = \frac{E_0 \otimes_{V}}{I_0} .$$

The integrated intensity should be corrected for effects of systematic errors. These types of errors generally arise from absorption and extinction effects and if they are significant, affect the precision of the structure determination.

4. Absorption

The absorption of the incident X-ray beam is dependent on the length of the path of the X-ray beam through the crystal. As a result, in a typical, nonspherical, crystal, the amount of absorption is a function of the angular orientation. The absorption correction procedure for a single crystal may be simplified by grinding the crystal into the shape of a sphere to make the X-ray path through the crystal equal in all directions. However, this grinding process is only applicable for those crystals, which neither fragment nor cleave during shaping.

An absorption correction procedure has been suggested by Furnas $(1957)^{43}$ for the unshaped crystal. The method makes use of the fact that the azimuthal angle, $\,^{\uparrow}$, of some reflection planes can be changed without destroying the Bragg reflecting conditions. To apply this method to the CIMnTPP crystal, whose unique $\,^{\downarrow}$ b axis was at $\,^{\downarrow}$ = 90° ,



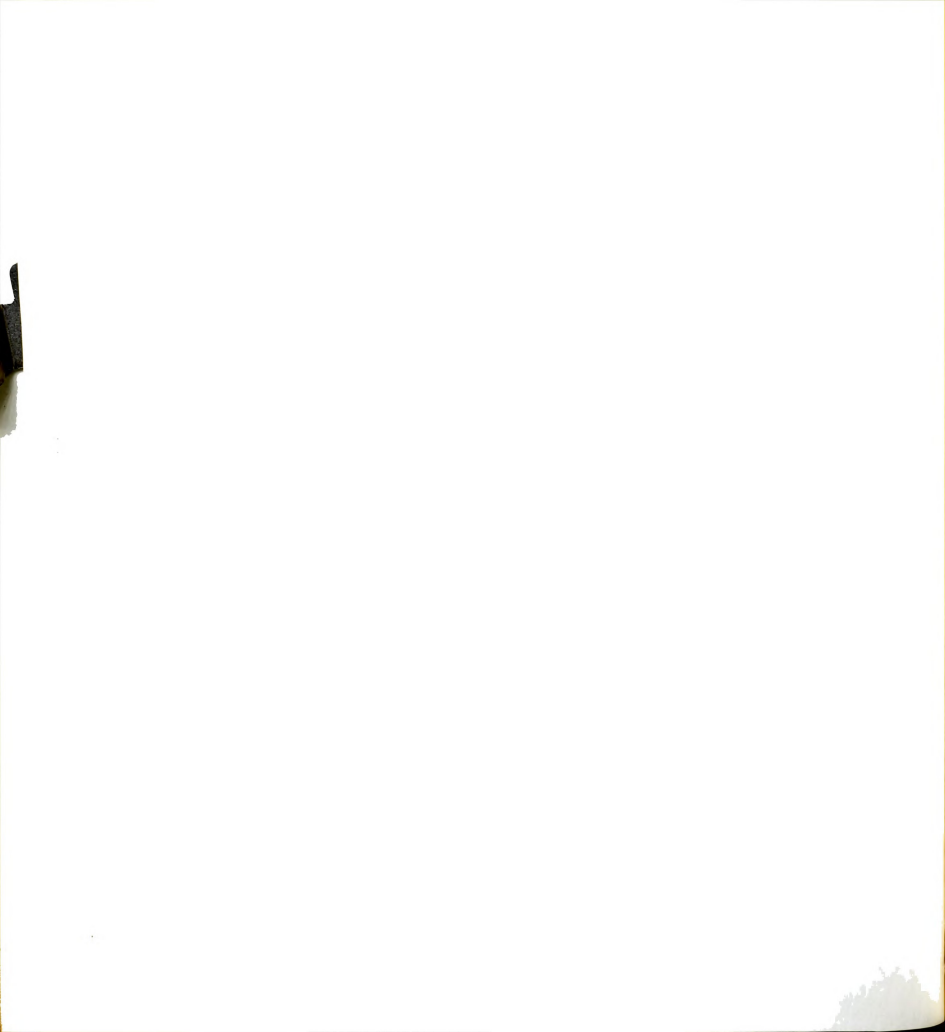
the (0k0) reflections were chosen for the absorption measurement because diffraction from these planes is independent of the azimuthal setting. The variation of the intensity of an axial reflection with respect to $\, \varphi \,$ at $\, \chi = 90^{o} \,$ will be an indication of the absorption of X-rays as a function of crystal orientation.

The intensities of the (0k0) reflections of the ClMnTPP crystal were measured in increments of 10^{0} over the $\,^{\uparrow}$ range in which the X-ray intensity data were taken. The absorption factor, by which each reflection, $hk \, l$, was multiplied depending upon its $\,^{\uparrow}$ value, was

$$A_k(\phi) = I_{max}(\phi_0)/I(\phi)$$

and can be obtained by plotting the quantities $\mathbf{A}_{\mathbf{k}}(\phi)$ as a function of the ϕ angle. For the ClMnTPP crystal the maximum absorption factor from each absorption curve was observed to be linearly dependent on the 2θ angle (Fig. 32). The absorption for each independent reflection was then computed as a function of its ϕ angle and its scattering angle, 2θ .

Other ways to correct for absorption include the method of Bushing and Wehe $(1962)^{25}$ of absorption factor based on the shape of the crystal and the semi-empirical method developed by Phillips <u>et al.</u>, 24 and have been discussed in Part I.



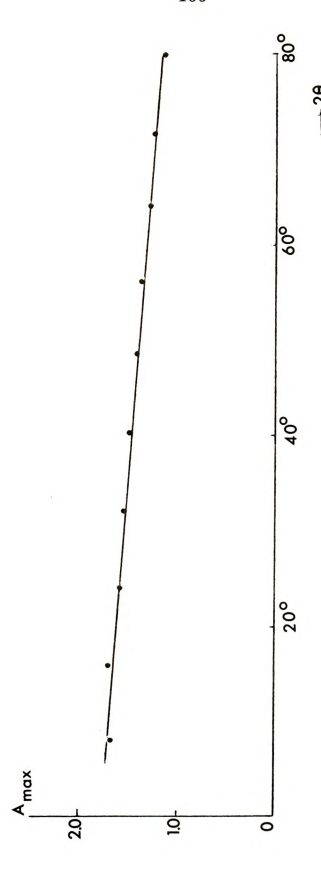
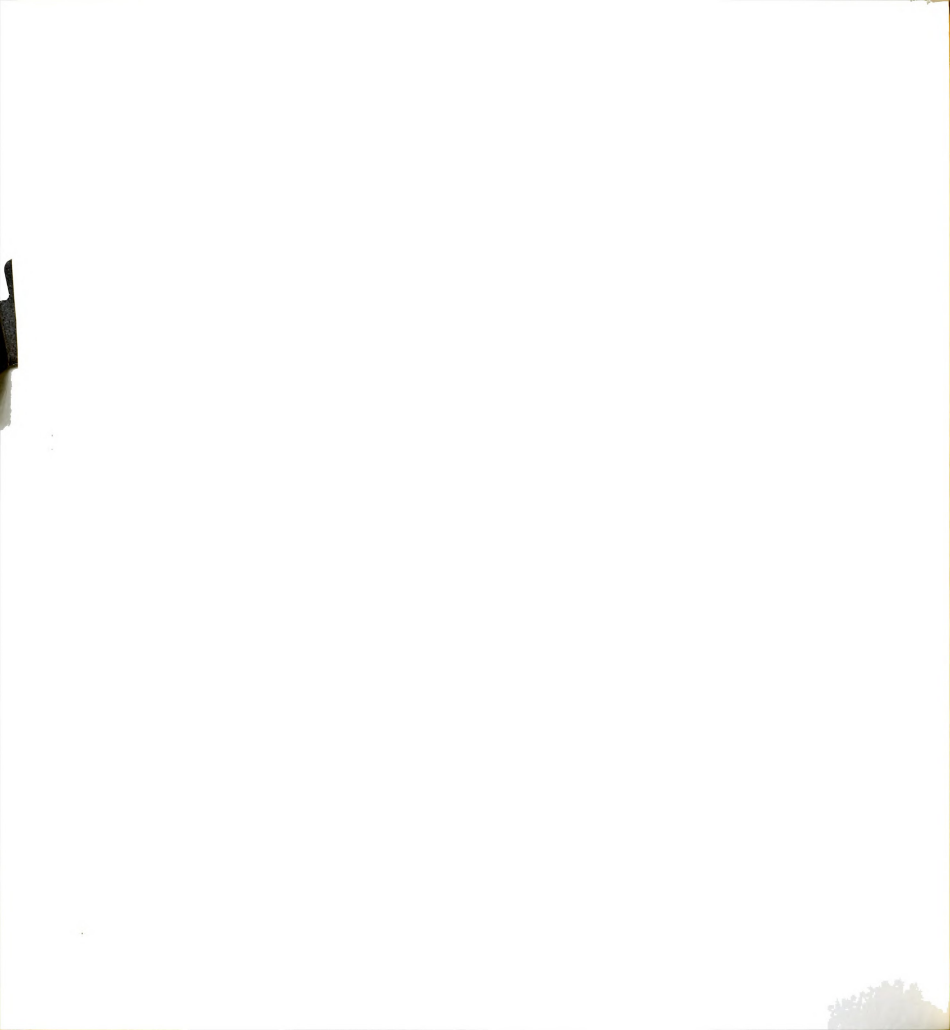


Figure 32. Maximum absorption factors vs 2θ .

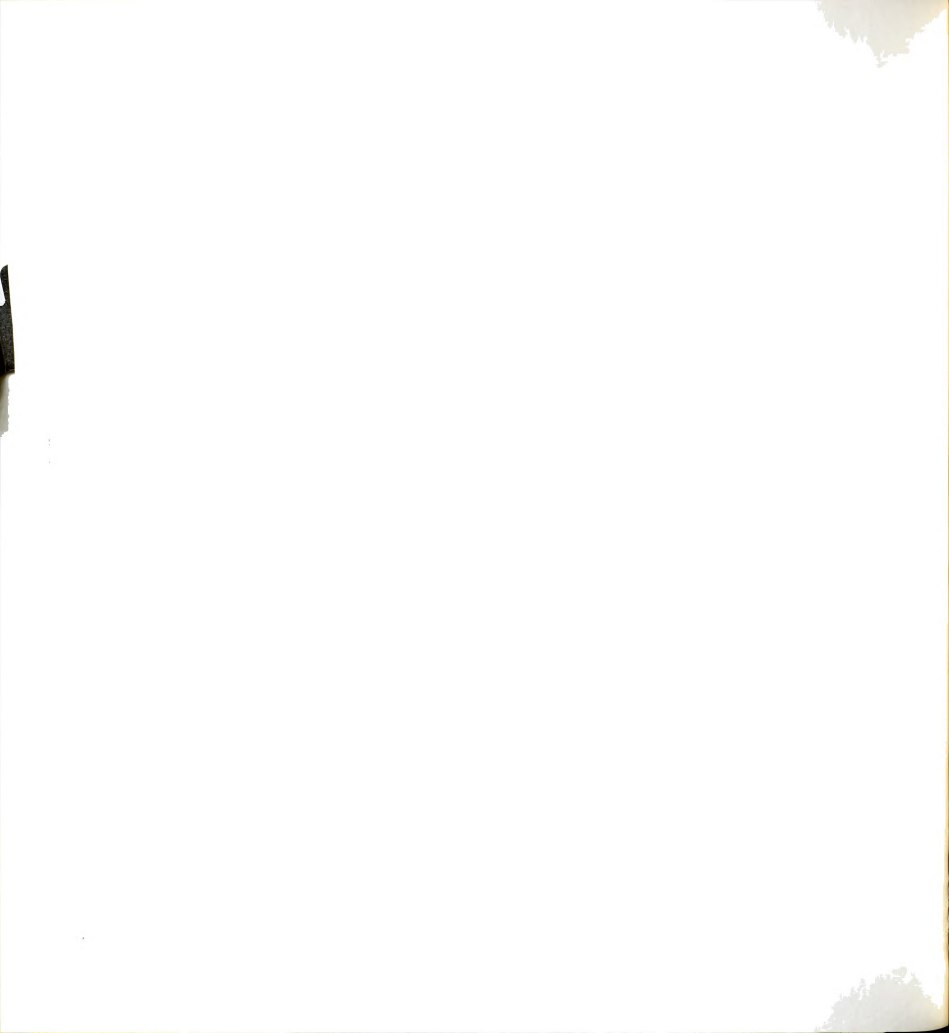


5. Extinction

The effect of absorption is to attenuate the X-ray beam as it passes through the crystal. An additional attenuating effect is extinction which is known to be of two different kinds, classified as primary and secondary extinction.

Primary extinction relates to an interference process which reduces the intensity of a beam as it passes through a crystal. Given a set of planes in the position to reflect the incident beam, the reflected beam can be at the proper angle for further reflection by another set of planes (second time or more). Thus, this interference effect will cause part of reflected beam to be out of phase and decrease its intensity. The primary extinction effects are more serious in perfect crystals than in mosaic crystals. In the latter case, the perfect planes cannot extend over appreciable ranges for multiple reflections with the mosaic blocks.

Secondary extinction is commonly encountered in single crystal work and its effect can be very serious for structure refinement. For a given set of planes at the reflecting position, the deeper planes will receive less incident intensity and therefore reflect less power than the upper planes. This interference effect is usually more pronounced for reflections at low sin θ/λ values and a correction can be made for it. Methods for correcting for



secondary extinction are: (1) an empirical method derived by Darwin (1922),⁵⁰ (2) the use of a small crystal to remeasure those reflections which are most seriously affected by extinction, and (3) quenching the crystal in liquid nitrogen to break up the mosaic blocks into even smaller blocks.

6. Conversion of Intensities to Structure Amplitudes

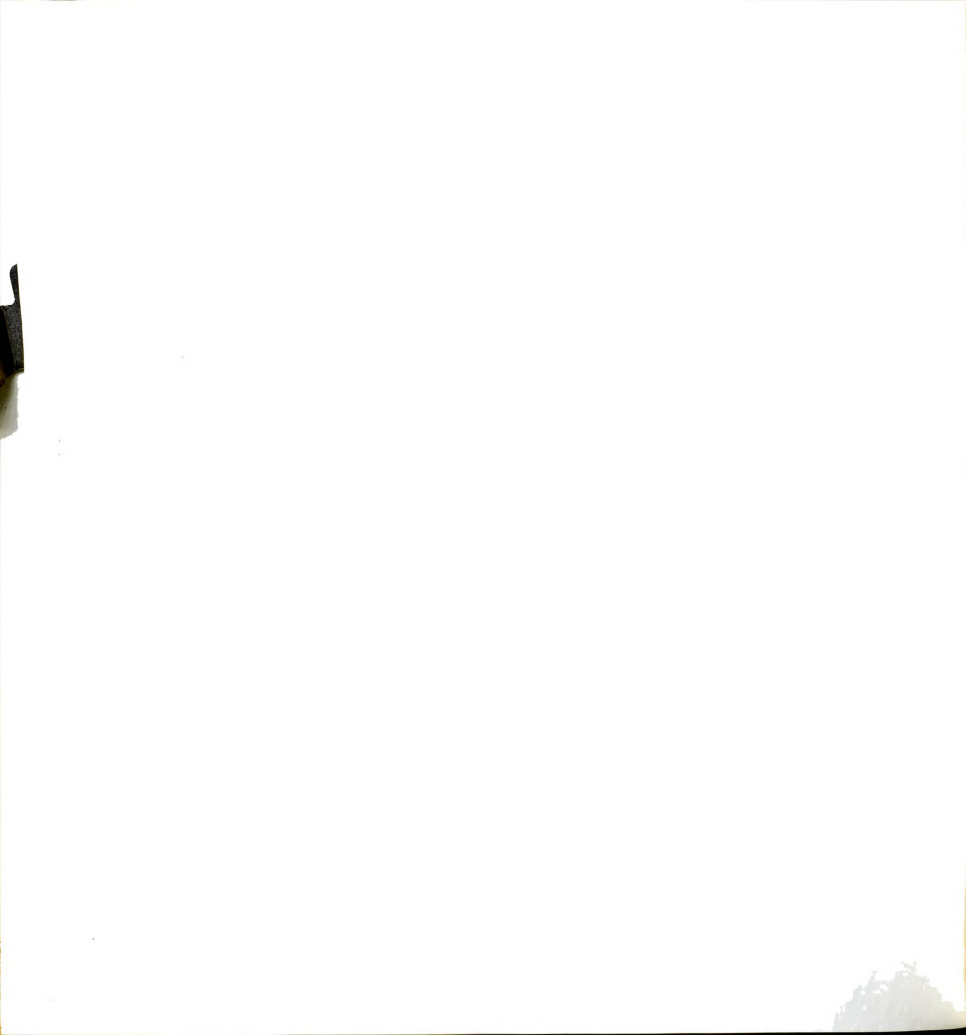
The structure amplitude of a reflection is related to the intensity as

$$\left| F(hk\ell) \right| = \sqrt{\frac{KI(hk\ell)}{LP}} \quad \text{, where} \quad \begin{array}{c} L = 1/\sin 2\theta \,, \\ \\ P = (1 + \cos^2 2\theta)/2 \,, \end{array}$$

and K is a constant which depends on the crystal size, incident beam intensity and a number of other fundamental constants. The polarization factor, P, arises because the degree of polarization of the X-ray beam varies with the reflection angle. The Lorentz factor, L, arises because the time required for a reciprocal lattice point to pass through the sphere of reflection varies both with its position in reciprocal space and the direction in which it approaches the reflecting sphere.

7. Diffractometer

In a four-circle diffractometer the crystal has three rotational degrees of freedom, a number sufficient to give any vector, any arbitrary orientation in space referred to



axes in the crystal. The three circles (see Figure 33) are the ω -circle, the χ -circle which is carried on the ω -circle and whose axis is normal to the ω -axis, and the ϕ -circle which is mounted on the χ -circle and carries the goniometer head supporting the crystal.

The X-ray source is set in a fixed position with respect to the crystal orienter and the detector is mounted on the 2θ circle. The angle between the detector and the direct beam can be set to any desired value within the range of the instrument.

In addition to the four-circle elements described, the diffractometer includes a regulated power supply for the X-ray tube, scalers for counting the pulses produced by the detector, a rate meter for displaying on a chart recorder the rate at which pulses are being received, and a pulse-height analyzer for discriminating against pulses which are either much weaker or much stronger than those expected for the characteristic energy being used.

8. Unwanted X-ray Radiation

The radiation emitted from an X-ray tube is not monochromatic. The desired k_{Ω} radiation is always accompanied by a $K\beta$ component of somewhat shorter wavelength and both K_{Ω} and $K\beta$ are superposed on the background. Unwanted radiation can be removed by use of balanced filters which are made with a pair of metallic foils, one foil of which



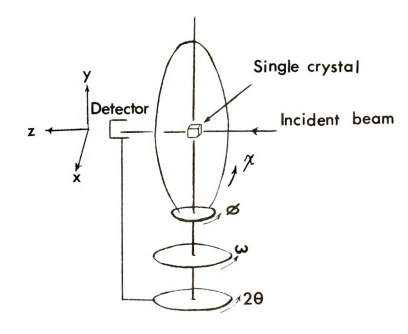
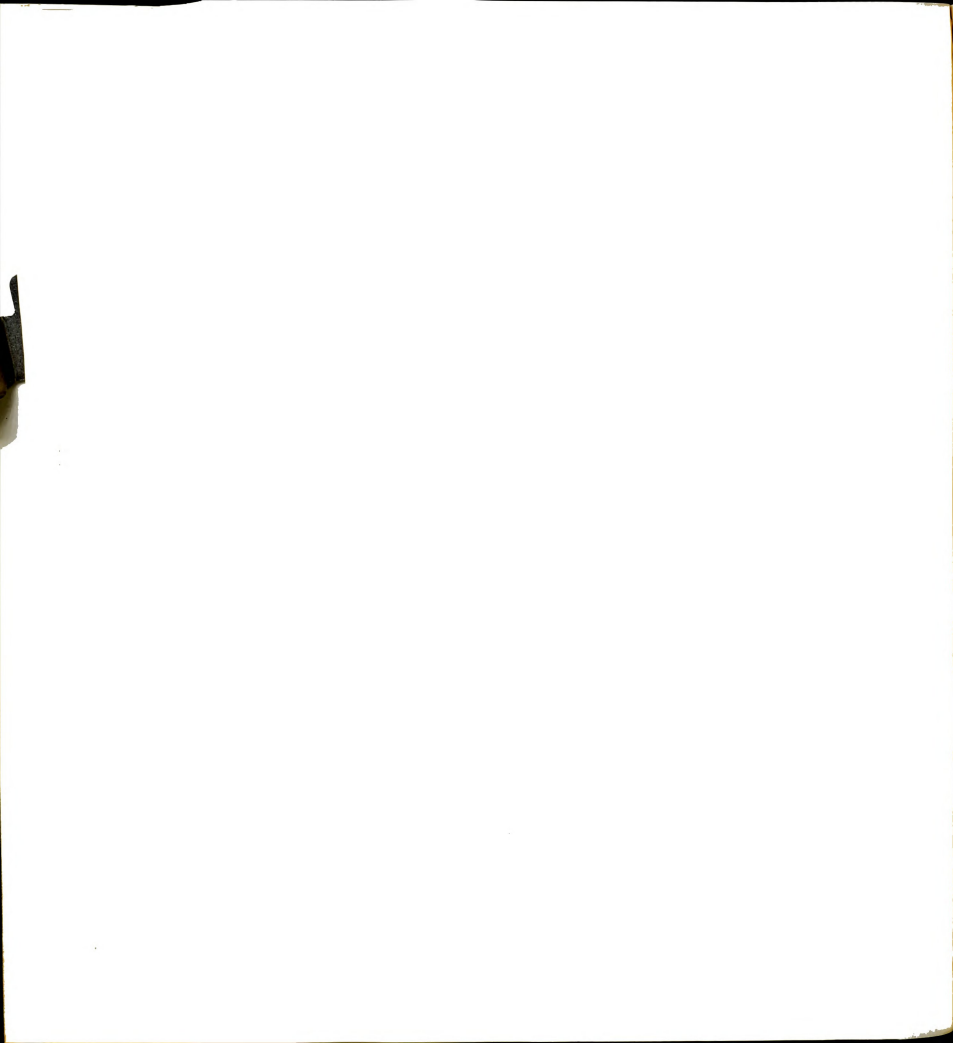


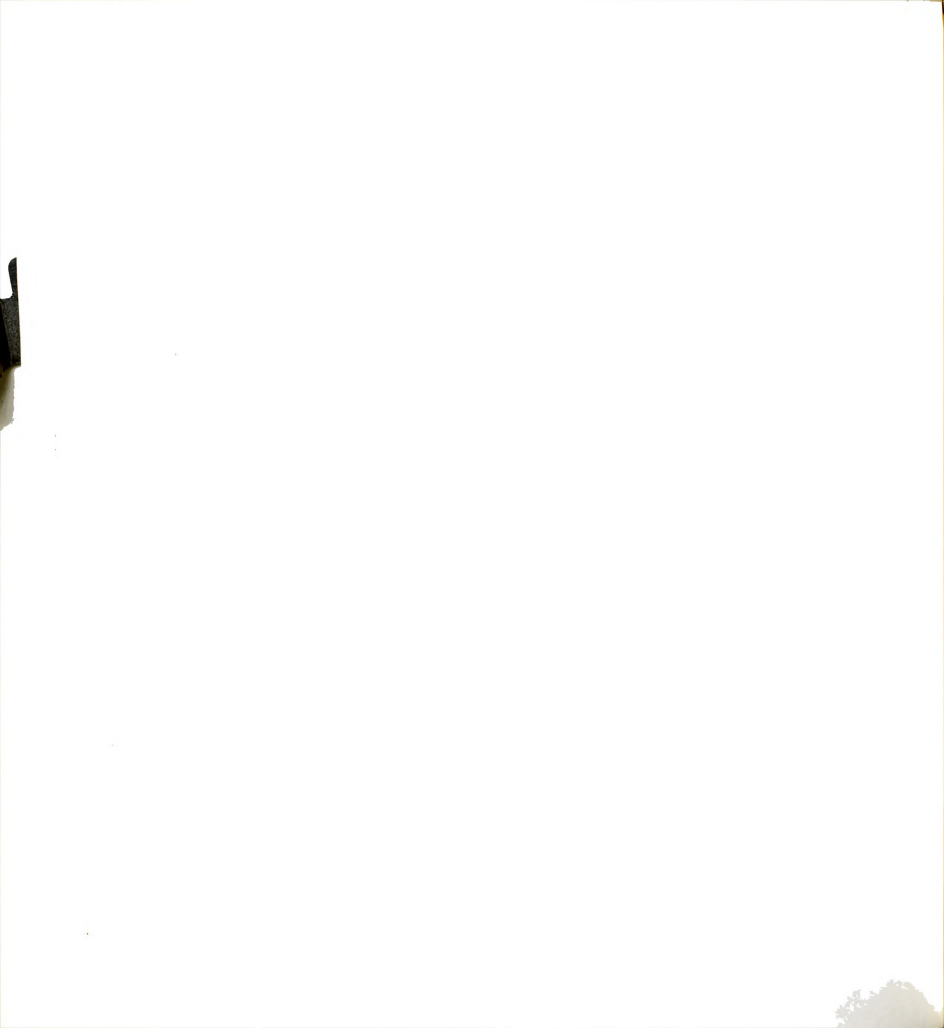
Figure 33. Schematic representation of a four-circle diffractometer.

has an absorption edge just covering the $K\alpha$ radiation and the other an edge covering $K\beta$. The intensity of each reflection is measured once with each filter, and the difference is taken to be the intensity.



APPENDIX 2

- 1. Observed and Calculated Structure Amplitudes of ClMnTPP.
- 2. Observed and Calculated Structure Amplitudes of Porphine.



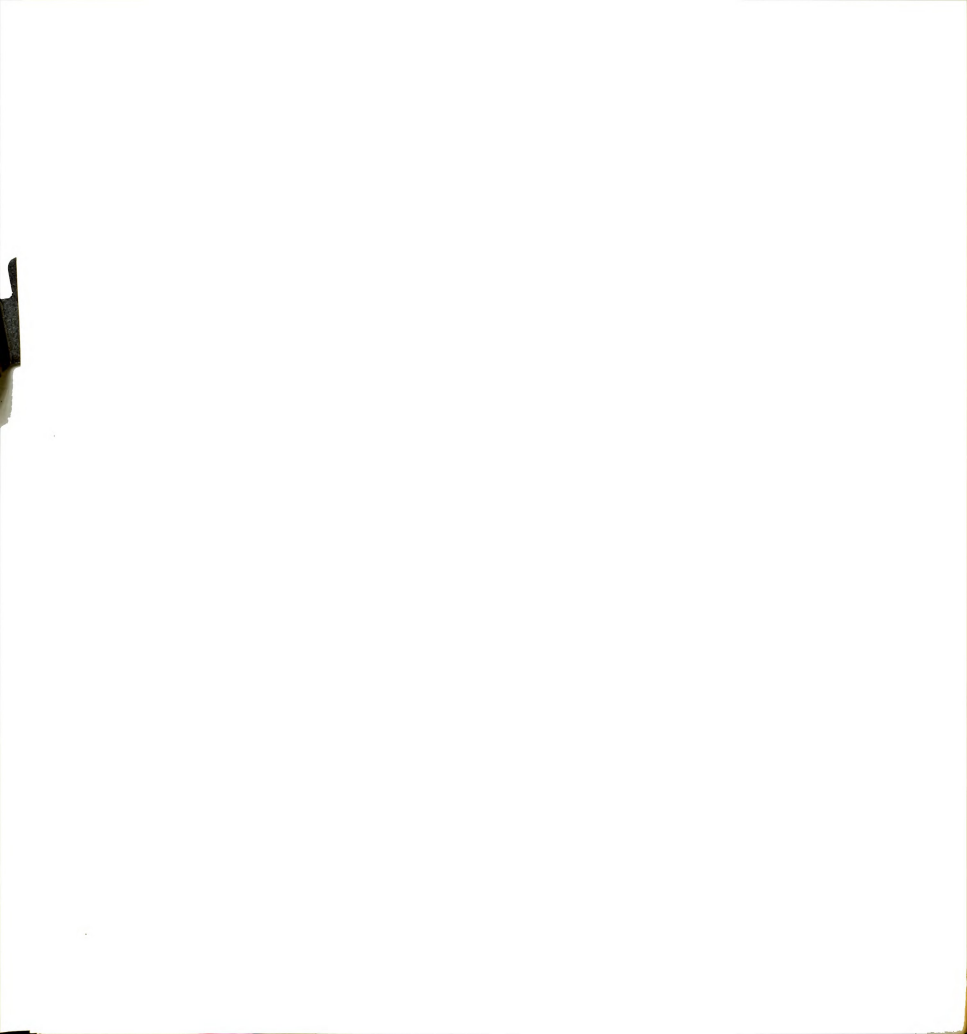
${f 1}$. Observed and Calculated Structure Amplitudes of ClMnTPP

T & C YOURS) TICALC:	H & L 1(6:5) Y(CALC)	H _6 L Y(UPS) Y(LALC)	He K I, T(U-5) T(CALC)
0 2 0 95,2340 96.3110	9 0 0 1v,cren 21.0104	-1 18 1 20,4920 40.5991	- 3
W 4 0 140 1840 120.2495	a 1 0 10.340f 10.7534	1 19 1 1/,2620 19,2/63	-4 10 1 10,9710 11,4/14
0 6 0 31,7365 32.0/17 0 6 0 37,6500 35,7419 0 10 0 16,02/5 17,1264	6 3 0 13,1746 14.0322	-1 19 1 15.5350 18.1259 1 20 1 30.9990 30.7768	-4 17 1 14.1/90 17./570 -4 16 1 0.37/9 4./393
0 10 0 10,02/0 17.1264 0 12 0 /2,4730 43,0773	6 4 0 20,9520 28.3316 0 6 0 0,2990 3,/147	-1 20 1 30,9990 27,4473 -1 20 1 30,0000 27,4473 -1 21 1 19,7470 16,7714	4 19 1 5.4431 4.3385 -4 19 1 6.07/0 5.4011
0 14 0 33,0400 34,1//0	0 7 0 32.0190 33.0020	-1 21 1 51,2440 45.000e	5 1 1 Su.04VA 29.9/51
0 16 0 13.5340 12.8343 0 18 0 9.4790 8.9222	0 9 0 10,9530 19.3240	-2 1 1 102.3018 94.5500 -2 1 1 39.2700 40.0235	3 2 1 10,0700 5.4219
1 0 0 147,0140 17.5346	0 10 0 10,/130 19,2987 0 11 0 30,0870 32./722	-2 2 1 14,0300 27,5/33 -2 2 1 14,0300 2.1021	-5 2 1 3, V3V0 2, 8323.
1 1 1 12.4790 /.8388		Z 1 1 50.5900 44.510V	2 1 1 2.7070 0.1170
1 2 0 41,6110 39.9819	6 13 0 20,/3/6 22.4916 6 14 0 70,/150 20,/575		5 4 1 3.0250 2.3/71 -5 4 1 34.4140 40.0/40
1 4 0 72,0100 71.4900	6 15 0 20,0701 29,2340 6 16 0 0,1590 9,7152	-2 4 1 01.27/0 60.0318 -4 3 1 28.25*0 31.3108	5 5 1 0.03VA 9.6403
1 6 0 /3,0010 78./988	6 17 0 21.2715 23.3972	-2 5 1 43,1010 42,3204	> 6 1 32,3510 33,1159
1 8 0 20,4190 35.8804	7 0 0 00.2120 99.3019	-2 6 1 6//299 00.7049	-3 a 1 4,5420 4,9742 5 7 1 1/,7420 16.5887
1 11 0 3,0350 3,4594	7 2 6 14.4580 11./953	2 7 1 (4510 0.4413	2 1 A,8180 1.3/55 2 8 1 42,0740 42.0694
	7 4 0 29.1290 40.6447		-5 8 1 0.4510 4.0/11
1 14 # Jv 0420 41.2462		"2 8 1 30,3850 29.3147	> 9 1 11,3640 11,3964 -> 9 1 34,8490 38,4150
1 15 0 4,/1/0 4,0267		-2 9 1 18,/95n 18.9153	3 10 1 44.3401 43.8752 3 11 1 12.17/0 12.4113
1 17 0 1v.0con 1v.4436		-2 10 1 4v./710 46.6640	5 12 1 18.4930 21.1902
1 18 0 3/,9410 40,1764 1 19 0 15,0000 14.3133	7 10 0 0,0760 4,3433 7 11 0 10,0940 20.6612	2 12 1 0,8448 9,1919	2 12 1 9,9480 9,4248 2 13 1 9,8310 10,9137 2 13 1 43,8370 44,2427
2 0 0 10/./700 104.4572	7 14 0 10.1940 10.4965 7 15 0 21.2500 22.1430	-2 12 1 8./9/6 8.0993 2 13 1 22.2745 24.3790	-5 13 1 43.v3/0 44.2057
2 1 0 10,8900 ,9933	-0 0 20.43/0 (0.2213	-2 13 1 40.34/4 42.4341 .	-5 14 1 11.2524 13.033A
2 2 0 10,2410 4.7202 2 3 0 20,2300 18.0120	8 2 0 24.0000 23.1037	2 14 1 4,7224 3.0916 -2 14 1 4,9719 3,9969	5 15 1 4.9530 3.4781 -5 15 1 17.1421 17.2491
2 4 9 119,2000 110,4816	8 3 0 33,9940 32,7444 8 5 0 0,1300 7,0021	2 15 1 29.0440 29.4/03	5 16 1 17,0180 18.2167 -5 16 1 14,4410 14.7149
2 6 0 32.4730 37.0495	0 0 0 23,2740 22,0093	2 16 1 24.0340 24.9404	5 17 1 0.990* 5.025/
2 8 J 24,0240 46.5711	8 7 0 4.9290 1.3051 8 9 0 10.5230 0.0022	2 17 1 6,4350 /.3430	-5 19 1 5.1398 5.4911 6 1 1 4.2800 4.0183
		-2 17 1 21.2910 22.9529	-6 1 1 28,0000 25.7424
2 10 0 67,3000 08.8391 2 11 0 10,2000 17,1935	8 11 0 0.0426 3.2/33 8 13 0 18,8436 19.5/71		6 2 1 21.1500 23.0723 -0 2 1 17.3820 15.5022
			0 3 1 22,0100 21.4/33
2 14 0 15,7248 16.1641	9 1 0 22./020 27.9008 9 2 0 19.6390 19.5181	27 24 27 27 27 27 27 27	0 4 1 19,0530 18.5141
2 15 0 15,3500 16,7933 2 16 0 33,2020 31.9172	9 4 9 V.8780 8.4075	-3 1 1 31,7210 32,4492	-a 4 1 27,0680 23,0292 6 5 1 20,1430 19,0889
	9 5 4 23,2840 21,0007	3 2 1 5,5350 2,5424 -3 2 1 22,9020 13,5553	-6 5 1 60 VOAD 39.47AB
2 16 0 12,2690 11.4607 2 19 0 20,1360 20.4308		3 3 1 5, v100 3, 2417	6 6 1 29,3140 29,8831 -0 6 1 31,999 29,8497
2 20 0 12,31/n 12.0302 3 0 0 70,9200 02.09/4	9 7 0 14,5770 15,5723 9 8 0 15,0510 15,9771 9 9 0 17,3720 16,6290	3 1 1 5, V100 3,2017 -3 3 1 00, U5VA 00.5834 3 4 1 19,08/0 19.5120	6 7 1 19, v330 20.0867 -6 7 1 8,5590 7,2165
3 2 0 14.9235 14.5584	10 1 0 1v.9130 19.1000 10 2 0 1/.oran 15.//17	-3 5 1 51,2980 50.0091 -3 5 1 42,9300 46.0205	* \$ 1 0,1530 3,5447
4 0 49,/190 23,8432	10 3 4 10,/5/0 10,4024	-1 A 1 10 +710 12 2409	-A 8 1 30.0(11 30.31/A)
3 6 0 47.2780 40.7468	0 1 1 100,0390 147,2905 0 2 1 03,0900 00.0047 0 3 1 47,0530 00.5157	-3 6 1 11.9418 8.4953 3 7 1 35.5248 39.1562	-0_10_1_34,0500_32.5/42
3 7 0 21./e>n 20.1510 3 8 0 44.6240 47.5247	0 3 1 47,0530 00.5157 -0 4-1-05,0074_03.5224_	-3 7 1 37, Y730 30,4000	0 11 1 10,7500 10,7052
3 10 0 23,/9/0 22,9896	9 5 1 30,2430 20,0000	-3 8 1 26,30/n 28,1140	0 12 1 14.0240 16.3/58
3 12 0 50,4680 58.2027	v 7 1 0.0760 9.7154	-3 9 1 04,440 48,1251 -3 9 1 04,4430 65,4661	-6 13 1 33,0300 31.763/
3 13 0 4.03/0 3.4447 3 14 0 20.5680 19.5104	0 9 1 >>,46/4 >>,4255	J 10 1 10,0090 18,7492	-0 14 1 00.0035 42.7126 -0 14 1 0.1491 9.1494
3 15 0 7.2940 6.4/26	-0 10 1 4v 4910 45 9-67	3 11 1 24./580 22.0747	_ 0 15 1 Y.4410 10.5007
3 16 0 30,1146 30.0087 3 17 0 19,0030 20,4997	0 11 1 5,4100 3.8312 0 12 1 21,0310 18,4947	3 12 1 3/,3300 38.2157 -5 12 1 0./490 0./748	A 1A 1 27.02V0 40.0070
3 18 0 7.4650 0.9100	0 13 1 19,4840 20.5957 0 14 1 0,0210 5,0575	3 13 1 30,50/0 37,5001	-6 le 1 8,0565 8.3171
3 20 0 15,8780 15,4/15	0 15 1 10.0men 9.4441	3 14 1 29,8040 31.1373	-6 16 1 20,1105 20.1510
4 0 0 45,0440 45,7749	9 17 1 18.0305 18.0077	3 15 1 19,24/0 19.6411	1 1 24,-100 26,0358
4 2 0 11.2620 9.9487			7 2 1 64.2780 59.9341 -7 2 1 6.9430 5.9373
4 3 0 25.0950 26.8745 4 4 0 49.8440 47.7999	1 1 1 20.7920 42.4992	3 16 1 11,8550 13.2626 -3 16 1 15,1390 14,2737	7 3 1 22,2/50 21.3834
4 5 0 50,0700 50.8203	-1 1 1 92,0400 88.7701 1 2 1 31./6/0 30./397	3 17 1 5,1370 2.8009	
4 7 0 29,8600 28,8869		-3 18 1 10.9390 10.2288	-7 4 1 4.0650 2.2301
4 9 0 7,9700 5,7344	-1 3 1 6,13/0 10,547y	-3 19 1 12,0280 12,5500 -3 19 1 4,9430 5,2061	-7 5 1 14.4630 14.8546 -7 5 1 22.23/6 22.3342
4 10 0 5.0110 7.2306	1 4 1 94,x2/0 48,2246 -1 4 1 36,58/0 36,0009	3 20 1 25,9460 25,4421	-7 6 1 70.8748 19.1787 -7 6 1 10.4488 10.3973
4 12 0 34,5890 37,8768	1 5 1 47,4010 44,3957	-4 1 1 13,1730 14,1201	
4 13 0 16,/960 1H.V526 4 14 0 29,V016 30,3856	1 6 1 65-68VC 67-4167	4 2 1 18.0420 19.5643	7 6 1 12,8650 13.4150 7 8 1 19,2210 20,4034
4 15 0 12 6/90 11-1569	-1 6 1 35,5890 34,0170 1 7 1 35,16/0 48,3427	-4 3 1 29.1060 23.3439	-7 9 1 45,5100 44.5/74
4 14 0 29 1890 29,5400 4 17 0 4,9437 3,4461 4 18 0 17,0548 18,2089	-1 7 1 52,3260 46,9551	-4 4 1 28.0280 20.0729	-7 10 1 18.29/n 18.6999
3 0 0 3,51/1 7,2658	1 8 1 14.0000 14.1494 -1 8 1 38,5860 40,4014	4 5 1 27./600 21.7489 -4 5 1 25.9920 23.1026	7 11 1 0.9830 7.5776
	1 9 1 47,4790 50,7008		7 12 1 10.4700 10.4687
> 2 0 4,9790 4,5741 > 3 0 17,4410 18,7943 > 4 0 43,0190 45,2498	1 10 1 20,4710 20.3999	4 7 1 29.2450 29.2442	-7 12 1 14,497# 14.5934 -7 13 1 27,999 2#,2041 -7 14 1 14,6640 15.6083
	-1 10 1 13, veen 14.8707 -1 11 1 27, 2140 25,1/20	-4 7 1 4,412n 3.v048	
5 6 0 36,2280 34.6746	1 11 1 20.0485 28.1950	-4 8 1 22,0500 21.3001	-8 1 1 17,8400 17,2324 -8 1 1 44,0000 41,3326
5 8 0 40,5840 39,9252	-1 12 1 0.7345 9.0001 -1 12 1 14,9000 14,4835	-4 9 1 59,5636 62,2216	8 3 1 8,9750 8,9547
> 10 0 13,04/0 12,7200	1 13 1 20.2700 21.7532	4 10 1 40,0370 38,9390	** 4 1 10.11/0 11.15/2 ** 4 1 25,99/0 26.0033
> 11 0 25,5240 25.0025 > 12 0 13,4840 14.0386	1 15 1 14,/600 12,5138	-4 11 1 11,0330 9,0375	
> 13 0 23,0400 23,1011	1 14 1 42 9390 44 9120	12 1 29,9290 31.5075	
	-1 16 1 40,7620 44,4550	-4 13 1 54,1100 57,0271	
5 17 0 V.1740 0.3203	1 17 1 43,3230 14,9625 -1 17 1 23,0750 23,7120	4 14 1 20.0720 20.0613 -4 14 1 14.0120 12.1992 4 15 1 7.1520 8.1628	* 8 1 9,0320 9,7045
3 10 0 0,3440 0,3630	1 16 1 17.2840 17.2976	4 15 1 7.1520 8.1028	-8 1 33.0270 33,7100

TOURST TICALET	n K L Y(Ul-a) Y(CALC)	H "K L YIUPS) TICALC)	H ' K L Y(UHS) Y(CALC)
6 9 1 (.800) 8,4071			-10 0 2 09,98/0 /2.0303
-a 9 1 a.erua 5.7355	-/ 11 / 10.VIV. 13.4VIV.	-> 6 2 43,2020 43,4647 -> 9 2 14,0640 13,4725 -> 9 2 26,1000 27,9344	-10 1 2 16,0170 16,4149
8 10 1 15,0300 14.2510 -8 10 1 0,0000 7.0393	2 11 2 33.070" 33.3261 -2 11 2 13.4136 10.6176	-> 9 2 20.1000 27.9944 -> 10 2 >.1140 4.0406	-10 2 2 12,1300 10.7445 -10 3 2 12,0200 11,4776
8 11 1 2.6020 5.1075	/ 12 / 3.9701 7.7388	5 11 2 11.0550 V.2446	-19 4 2 12,2310 9,1836
-8 12 1 15,4220 15.8202	2 13 2 10.9250 11.6362	-5 11 2 22.9510 24.1741 5 12 2 14.7720 14.4541	
-8 14 1 21,2120 21,5367	-2 13 2 14.092C 13.32C4	-5 12 2 18.1940 17.2242 5 13 2 12.2920 13.4478	-10 7 2 10.1445 V.VV56 -10 8 2 23,8508 24.5937
9 2 1 32,40V0 31,740Z	-2 14 2 43.074C 42.12/3 2 15 2 6.7610 6.4416	-5 14 2 8.67yn 7.07eg -5 14 2 30.94e0 30.654e	-10 9 2 19.27/8 19.8856 -10 10 2 5.0240 2.0245
-9 5 1 20,/120 41,1640		3 15 2 17,3040 14,3339	-11 7 7 (2.3510 23.1164
9 3 1 10,/120 10.2401	2 16 2 22,2945 21.7334	5 16 2 8.6958 V.6919 -2 16 2 14.1845 11.7851	-11 1 2 2,7714 4.9037
9 4 1 20,5280 19.3600	-2 17 2 13.5con 14.1843 -2 14 2 20.7900 27.7361	-5 17 2 6,2130 6,0656	-11 4 2 0,01/0 3.7121
9 5 1 10.0090 10.4/10		-5 18 2 0./170 .8554 -5 19 2 5.1760 4.5926	0 2 3 50,0400 59.7248
-19 6 1 20.0200 23.7412 7 6 1 21.0420 21.2718	-2 19 2 33.1000 34.6036 2 20 2 12.4920 12.3586	* 1 2 28,1910 27,4398	0 3 3 47,1090 /1,8141
-9 9 1 5 5445 4.0585	3 0 2 23,9400 25.5071	A 1 7 34.3940 54.5214	0 5 1 23.0120 23.9900
-9 12 1 4./340 2.0648	-5 0 2 15,8000 11,400J	-6 2 2 7,0660 7.0101 6 3 2 15,5750 14,5196	0 7 3 21.0900 18.5479
-10 1 1 15,3140 15,3146 -10 1 1 15,3140 15,3148	3 1 2 10.2000 13.6976 -3 1 2 01.6870 48.6752	6 3 2 15,5750 14,5196 -6 3 2 44,2490 39,6703 6 4 2 13,5270 13,2428	0 0 1 20 5450 28.9690
-10 2 1 14.0750 12.9429	3 2 2 4.8725 3.7639 -1 2 2 38.9482 49.6425	*6 4 2 28 2010 41.2090	0 10 3 39,5060 42.6868
-10 5 1 2,4760 6,0339	3 3 2 20.0340 48.3187	-6 5 2 16,5370 15.1667	0 12 3 33,06/0 36.0003
0 0 2 60,1150 47.8029	-3 3 2 60,4435 72,8254 3 4 2 10,7300 16,727H	0 6 2 5.0030 5.3245	0 14 J 18,0090 28,6396 0 15 J 6,0390 6,0973
-8 1 2 3,4340 ./990	-5 4 2 62,9230 65,1672		0 16 3 13.0369 14.3948
_ 1 2 c/, y2/5 y0,2832	-4 5 2 AV, 9900 43,0307	-0 7 2 37,7520 37,5006 -0 4 2 4,9740 6,2453	0 19 4 11.2340 13.0357
0 4 2 32,4760 23,4511	3 6 2 4,6650 2.4992 -3 6 2 12,2000 10,3155	-0 8 2 Js.0040 J9.9929	0 20 3 11,89/0 10.3701
9 6 2 22,3201 24,3948	5 7 7 52.92/0 34.7035	6 10 2 6,9830 7.2105	-1 1 5 2,1000 8.44e1
0 8 2 50,1954 50.0316	3 8 2 4,2000 3,5261	* 10 2 10.0048 12.7521 * 11 2 7.6796 4.9853	-1 2 3 14,0040 9.2749 -1 2 3 221,0800 255,0999
0 10 2 12,0250 8.V/12	3 9 2 8,1810 0.0008	6 12 2 7,19/1 20,6274 6 12 2 7,19/1 8,2078	-1 3 3 7. vove 11.3419 -1 3 3 143,0848 150.8564
0 11 2 22,9700 25.6837 0 12 2 19,0350 22,1346	-3 9 2 9.14en 8.2811	-6 12 2 73,1800 23,3014	1 4 3 5,0330 3.5445 -1 4 3 51,2910 54.7631
_0_13_2 7,0020 9,0874	-3 10 2 14.51an 14.1411	0 13 2 0.2590 8.2427 -0 13 2 12,/920 11,7049	
0 15 2 9,1750 9.5218	3 11 2 64,2000 64,3606 -3 11 2 28,4960 29,7030	0 14 2 11,02/0 12,7981 0 14 2 11,02/0 12,7981 -A 14 2 35,4590 45,2245	
0 17 2 9,8940 10.4880	-3 11 2 28,49en 29,703g 3 12 2 10,844n 9.6428 -3 12 2 20,132g 20,1492	-6 15 2 5,6160 5.8680	-1 6 J 11,88/0 4.7405
0 19 2 12.1890 11./603 0 20 2 9.8610 6.7660	3 15 2 4,98/6 4,0472	-0 16 2 18.4930 18.7478 -0 18 2 14.8420 14.7179	-1 7 3 52,0300 50.3924
1 0 2 /4.95/0 06.3902	3 14 2 7,000 5,5087	-7 0 2 25,4550 25,4328	-1 8 3 21,/390 24,7211 -1 8 3 20,8040 26,5010
-1 0 2 103.1690 145.9540 ·	3 15 2 6,7630 6.1230	7 1 2 10.0400 15.2056 -7 1 2 14.0650 16.1609	1 9 3 20,0300 40,2446
	-3 15 2 37,3390 38,6385		1 10 3 49,2140 43.6574
1 2 2 42,67/0 40,7672 -1 2 2 37,7670 38,0113	3 16 2 18,7474 28,5160 3 17 2 10,5790 9,6936	7 2 2 4,3970 4.7569	-1 10 5 7,2990 6.0689 -1 11 3 48,0890 48.1907
1 3 2 37,0339 34,0777	-5 17 2 6,1915 8.0988	-7 3 / 7.6765 5.508/	-1 11 3 19,8130 21.5395
1 4 2 24,777 27.277	-3 16 2 24.09A0 24.2791	7 5 2 0,7727 4,7630	-1 12 5 14,/390 15,7814
-1 4 2 4/,3476 35.269/	-3 19 2 14,0450 12,0366 -3 19 2 25,0360 27,7254	7 6 2 6,54/0 5,9761	-1 13 3 12.>220 14./415 -1 13 3 10.9710 18.991/
-1 - 5 - 7 - 67 H246 V5 (357	-3 20 2 19 0340 15 5541	-7-4-4-24,3932-24,4374-	-1 14 3 23.04V0 28.16V4 -1 14 3 46.07V0 49.7302
-1 4 / 21 4644 39,7240	-4 0 2 Y4,4740 Y7,9732	-7 7 2 33.7495 47.5969	1 15 1 24 4500 /2 4264
1 7 2 31,0014 30,4863	1 2 9.1590 8.7239	-/ 8 2 13.9447 13.2173	-1 15 3 21.4660 21.9383 -1 16 3 8.2090 7.2371
1 8 2 4.5840 5.5079	4 2 2 5,35/6 4,2935	7 9 2 6.2940 4.5807	-1 16 3 10.6500 12.3838
-1 8 2 15.4E/E 14.84b7	4 3 2 34,1980 32,7965	7 10 2 11,/650 11.0319	-1 17 3 10,8148 10,2294 -1 17 3 13,1500 14.0020
1 10 2 10,3660 10,8691	4 4 2 7,7750 6,7761	-7 10 2 23 (240 23.4335 · / 11 2 3.5410 3.9185	-1 18 3 20,1624 28,6177. -1 18 3 11,9760 11.6
-1 10 2 30,3790 25,0354		-7 11 2 12,4340 12,2556	1 20 3 35,3940 33,4265
1 11 2 53,3330 54.10/0 -1 11 2 16,3700 1/,0400	4 5 2 8,4985 8,2331 -4 5 2 34,1748 34,4424	-7 12 2 40.5420 40.3683	-1 24 5 A. VESD 3. YOU
	4 6 2 22,5200 21.1333	-/ 13 2 7,9590 7.5284 -/ 14 2 20,8040 22,0817	2 1 3 4,7200 3.5347
	4 7 2 21./910 V1.A008	-7 16 2 22,/0V0 24,0/56	2 2 3 71,00/0 72,1025
-1 15 2 12,8966 12./016 1 14 2 19,2886 19.4999	-4 8 4 39,45VD 36,7V50	-7 17 2 10.09/g 11.3897 -8 0 2 50.1620 56.4896	2 3 3 23,0000 20,2426
-1 14 2 0.10/0 6.0677 1 15 2 24.0010 25.9915	4 9 2 15,000 16,6353 - -4 9 2 41,4085 37,4663 -	-8 2 2 10,4790 10,9426	2 4 3 26,4520 26.0579
-1 15 2 40,4350 41,5891		8 3 2 16 9920 18 1992	42 4 4 41 HADA 41 2219
1 16 2 10.40/n 18.3593 -1 16 2 10.0100 10./d75	4 11 2 33.0440 40.1175		
-1 17 2 22,2470 21,768V		-6 4 2 32,5100 34,2341 -6 5 2 3,1110 7,0507	-12 A 1 35,4520 AD.120A
-1 18 -2 13,1760 13,1914		* 6 2 11,4450 13.1821 ** 6 2 20,000 27,7401	-2 7 3 7,3890 6.73H1
-1 19 2 19.5780 21.3171	-4 14 2 JZ. YOYO 34.1364	0 7 2 7,3040 6,3447	*2 6 3 35 UTBO 36 3471
2 0 2 70,0040 70.5425	-4 15 2 5.6250 3.6761 -4 15 2 14,7880 13.7044	0 0 2 10.0140 10.11d2	-2 9 3 43,3710 42,3475 -2 9 3 13,5110 13,7896
		-8 A 2 17,0210 17,2000	2 10 5 5,0020 2,9795
2 1 2 35,5420 34,4918 -2 1 2 19,7550 4,2938 2 2 2 24,8100 21,7464		-8 10 2 14.4710 15.0A71	2 11 1 10 /600 12 1414
2 2 2 24,8100 21,7464 -2 2 2 24,8100 21,7464	-4 20 2 14 1404 15 1011		2 12 1 27,0340 29,8252
2 3 2 7,0340 4,0552	-> 0 2 107,0110 114,4044	-8 14 2 17, U320 10, V038	-2 12 3 35,271¢ JH.1147
2 4 2 12,0930 7,7834	5 1 2 27,/750 30.3302 -5 1 2 29,2320 25,7782	-y 1 2 7./160 4.V174	-2 13 3 32.0/80 A1.6537
2 2 13.1550 13.0457	5 2 2 14.9418 13.5166 -5 2 2 9.6648 7.9288	-9 2 2 10.0160 12.2967 -9 3 2 12.14/0 13.2687	2 15 3 4,/6/0 3,8941
2 5 2 3.8890 2.7151 2 6 2 21.0130 19.3047	2 3 2 34,1520 32,3320	-9 4 2 2.7240 .0135	-2 15 3 19.24en 17.1095
	2 4 2 21 2000 19 5545	-9 6 2 4,5710 2,3102	
	-5 4 2 65./616 69.2402		-2 17 3 6,2000 7,4473
2 8 2 3,0030 3,0061		-9 9 2 14,2810 14,7954	-2 16 3 21,1840 22,4049
2 9 2 7,020 7,3239 2 9 2 7,020 7,3392 2 9 2 4,4350 ,5838	5 7 2 43.1730 43.4950 -5 7 2 43.4120 43.3810	-9 11 2 3,2140 4,6122 -9 12 2 11,7540 11,4618	-2 19 3 19,8990 22,1350
-2 9 2 4,4350 .5836	2 4 2 10,0110 12,2271	-9 13 2 22.4400 22.3060	-2 20 3 24.0240 18.1825



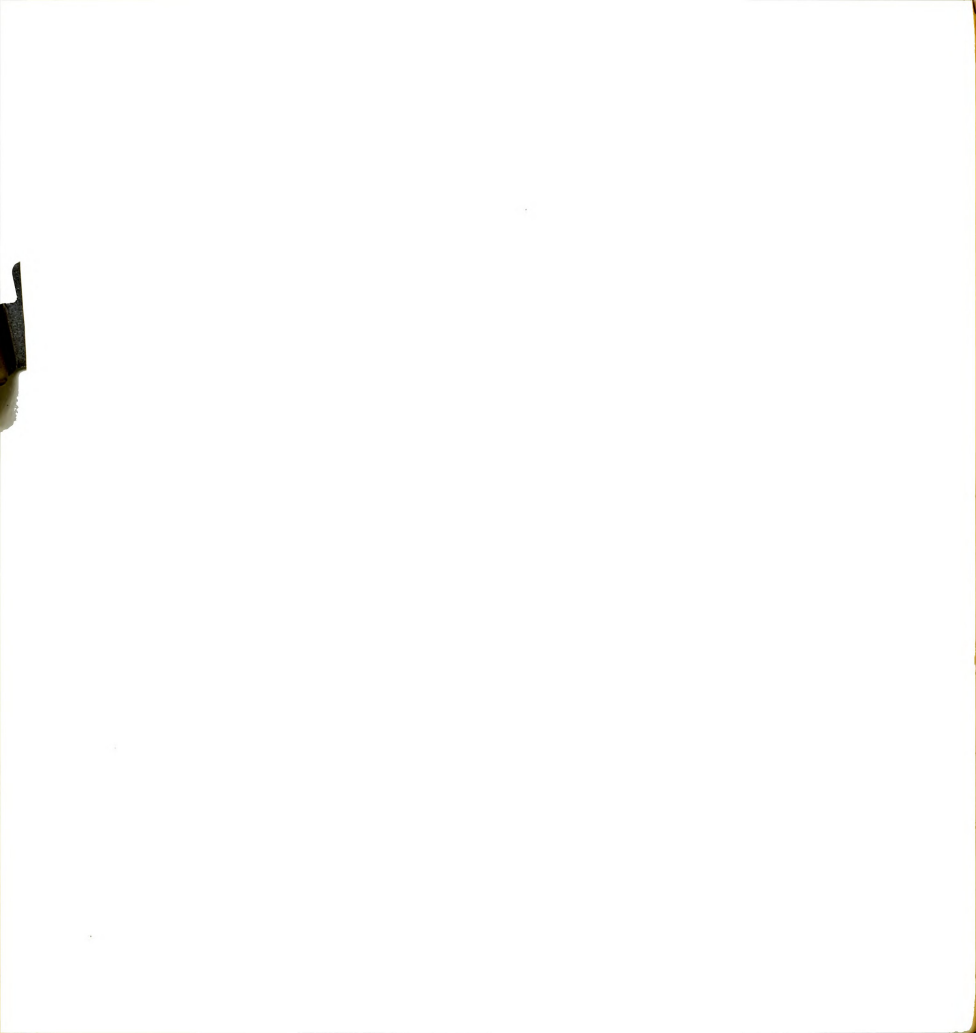
			M A 1 TOURN TIGALCY
H 'K L YIDHS) YICALCI	H IK L Y(UPS) Y(CALC)	m 4 L ffurs) f(C4LC)	H K L TOURS) TOCALCO
3 1 3 21,40/0 21.9750	e 2 3 1/,21en 1/.5013	0 1/ + 11,17/2 12.1535	-3 15 4 45,4710 45.0008
3 2 3 50,0010 4V.1373	-A 2 1 15 00H0 16.4943	0 40 4 20,40/8 21.2544.	-3 16 4 13,6020 14.5971
-3 2 3 151,2220 156,3198	-6 4 4 10.22/0 11.5222	1 0 4 9.4720 1.8478	-3 17 4 12.6090 11.3239
3 3 32,1700 30.2875 -1 3 3 102,9980 102,1320	6 4 3 10,1450 6.5562 -6 4 3 53,/948 46,7384	-1 0 4 10,4810 9.4232 1 1 4 46,3540 30,0881	-3 18 4 33,7420 34.2652
3 4 3 25,29un 24.0007	1A 5 1 A2 /615 39 6165	-1 1 4 56,7110 63.1968	-3 20 4 20,176n 16.8529
3 5 4 4 4910 4 2440	-0 0 3 23,0200 21.7403	-1 2 4 103,1030 1V9.3154	-4 3 4 40.8730 49.788
-4 5 4 10-09/0 10-0101	-0-7-4 10-2000 12-0/44	1 1 4 15 7440 14-4820	-4 1 4 32,0840 45,0090
3 6 3 21.426 22.7402 -1 6 3 15.4780 15.7806	-6 7 3 27,2640 25.8735 6 4 4 4.8070 3.7038	-1 3 4 92,/een 99.3d31	4 2 4 21,445) 20.0413
3 7 3 10,9090 15.9762	-0 6 3 4,/4/8 2.8191	-1 4 4 26.9720 22.3093	
J 8 3 14,3385 12,0006	-6 9 3 9,5780 8.3426	1 5 4 42,0720 44,4577	4 4 4 40,4307 45.7614
-1 8 3 15,/625 18,6612	-6 10 J 23,0590 21,1076	1 6 4 22,0110 19,2587	-4 4 12,3110 12,0693
3 9 3 20,48/0 20.0856	-6 11 3 8.5040 V.4971 6 12 1 21,1548 22,2334	-1 6 4 23.024n 44.7825 -1 7 4 30.5240 40.0578	4 5 4 20,0010 16.1991
3 10 3 21,0500 21.2484	-6 12 3 27,6290 26.0092		4 . 4 4.3227 3.7334
3 11 3 18,6126 19.2094	-6 13 3 15,7486 15.9598	-1 6 4 0,7740 8.0991	
-3 11 3 42 0020 29 1430		1 9 4 14.0030 15.1878	-4 7 4 90.41Y1 Y2.2032
3 12 3 37,0830 38.4539 -3 12 3 54,9520 25,3834	-6 15 3 6,4745 9.6136 -6 16 3 6,2375 6.4973		
	-6 17 3 12,17/0 11,0825	1 11 4 13,0530 14.9494	4 9 4 7,58/0 9.6366 -4 9 4 7,58/0 9.6366
J 14 3 V. 0730 9.1402	-6 19 3 17,6450 16.2773	1 12 4 19./340 19.5954	
-3 14 3 33.0410 31.7143	7 1 1 29.0200 29.0475	-1 12 4 57,9500 59,4951	-4 10 4 11, YEZO 13, 0383
3 15 3 9,9300 8,9367 4 14 3 16,990 14,4620	7 2 3 12,7945 13,1884	-1 13 4 19.5600 20.4962	-4 11 4 10.0140 44.5920
	-7 2 3 36.7690 36.7199	1 14 4 10,1700 10.0962	
3 18 3 4,7480 5.2088	27 4 1 27 8742 27 9144	1 10 4 10,04/0 17,4271	-4 13 4 8,57un 7.0139
	7 5 3 18.9150 19.9280		
-3 19 3 17, V830 17,550V -4 20 3 15,1000 15,6619 -3 21 3 6,14/0 3,V10m		1 17 4 6.4887 5.1683 -1 17 4 10.8618 21.7692	4 15 4 10.0403 11.2190
-5 21 3 6.14/n 3.910m	-7 A 3 39.0794 48.8631	1 18 4 25,0206 20,3074	-4 15 4 26,1200 25.9/76
4 1 3 13,7310 10,8976	-7 7 4 11.0742 11.6758 -7 7 3 6.2440 3.3269	1 19 4 74,3030 23.9896	-4 1A 4 29.8221 30.2/42 -4 17 4 5.8135 A.2197 -4 18 4 11.2382 11.4423
	-7 8 3 17,3640 18,6530	-1 19 4 6.649 6.7675 -1 26 4 6.5376 6.0203	-4 13 4 11.2380 11.4453 -4 19 4 7.6470 7.2332
-4 2 3 125,1000 129,8196 4 3 3 46,7420 42,0262 -4 3 3 27,9400 28,1421	7 9 3 5,7130 4.1747 -7 9 3 5,4837 4.5012 -7 10 3 7,2380 7,4153	-1 20 4 6,53/0 6.0203 2 0 4 20,6690 25,4797	-4 19 4 7,0475 7.2332 -4 20 4 10,1023 12,4412 5 4 10,4200 10,2021
-4 3 3 27,9400 28.1421		2 0 4 20,0690 25,4797	5 4 16,4760 16.2621
-4 4 3 49,/350 49.2236	-7 11 4 10./120 10.499a -/ 12 3 15.6180 10./543	-2 1 4 32.1530 29.7608 -2 1 4 36,8480 41.3908	25 6 4 39.2143 33.9221 2 1 4 9.2743 9.2352
4 5 3 9.0740 7.0163 -4 5 3 14,5800 15.1054		2 2 4 4.4790 4.1841 -2 7 4 113,0400 123,3093	-5 1 4 51,0190 32,9451
4 6 3 4.9200 1.0630		2 3 4 30 4940 28.7166	5 2 4 10,9790 10.7193 -5 2 4 34,5590 28,9322 5 3 4 7,3290 7,930
4 6 3 4,7200 1.0639	-7 16 3 7,5500 6,6014 -7 17 3 27,2400 30.6009	2 3 4 30,4940 28,7166 -2 3 4 79,9880 85,4274	-5 2 4 34.5590 28.9322 5 3 4 7.3290 7.9930 -5 4 57.1340 54.2798
4 7 3 8,8086 6,7943 -4 7 3 19,8486 17,0008	-7 18 4 6,64/0 9,2934 6 1 3 11,1520 10,7101	2 4 4 26.11V0 27.9976	
4 6 3 8,4240 6.3502	-b 1 3 34,0030 34,3018 6 2 3 6,4090 6,7514 -6 2 3 27,7400 29,3907	2 5 4 61,2790 56,6094 -2 5 4 12,9050 10,8044 -2 6 4 5,9360 3.7307	-> 4 4 39,3930 31,4474 -> > 4 95,2120 >>,>474
-4 9 3 47,0020 45,5878	-0 2 3 27.7400 29.3907	-2 6 4 5,5360 3.7307	5 6 4 15,1450 15.5973
4 9 3 13,0120 13,1057	-6 3 3 40.3103 43.347/	/ h + 14.55c) 4,14/9	-> n 4 3,3120 3,7441
-4 10 3 10./710 1 '120	-0 3 3 37,2401 31.1/94	-2 / 4 /u.ers /6.6934	-> / 4 06.1130 85.4498
-4 11 3 10.0000 1 10.017	-d A 3 29,4961 19,7699		5 a 4 33,4340 43,1/5e
4 12 3 21.9590 27.1647		-2 # · 21,2349 41.77/2 ·	-5 4 4 13,1130 12.80/5 -5 4 4 /1090 /.1895 -5 4 6,0040 6.3086
-4 12 3 9,1710 10.723 4 14 3 18,2110 19,7248	-0 9 3 22,9731 41.4132		-5 y 4 6.0040 6.3086
-4 15 5 13.7790 14.1911	-8 11 3 14.9530 13.1758	-2 10 4 20 5/30 ZB.AN42	-5 10 4 18,3490 16,2375
4 14 3 15,0000 15,7418 -4 14 3 29,4400 29,1181	-a 12 1 19.0440 22.2902 -a 13 3 6.4750 3.6114	2 11 4 21,19/2 21,4194	2 11 4 14.0240 12.2023
-4 15 3 11.2500 9.03NO	-4 14 1 70.0070 28.0YZ8	2 12 4 8.3980 18.1776	5 17 4 10.0580 9.5274
4 16 3 20,9600 20.023 - -4 16 3 31,3220 43,1101	-6 15 3 5,2590 4.0562		-> 12 4 14,1730 14,5615 -> 15 4 27,7716 29,4777
		-2 11 4 13.16v1 15./540	-5 16 4 31.1135 31.3400
-4 17 1 19.7040 21.6/21 -4 18 3 16.5550 17.8703	-9 5 3 6.1570 J.0942 -V 4 3 14,0670 14.2727		-5 17 4 13.90vn 14.3035 -5 18 4 23.7040 24.7992
		2 15 4 9.5954 10.5993	
-4 20 3 7.5917 4.4376	-9 6 3 8.5050 8.1028		-> 20 4 15,4490 15,4633 6 0 4 14,7671 15,8543
-5 1 3 /,0001 4.0/08	aw to 1 17 2040 16.3280	2 17 4 12,4426 11.1158	
5 2 3 13,5981 13,8207 -5 2 3 77,2981 77,4356	-9 12 3 5.4385 4.2678 -9 13 3 16.2195 16.7256	2 16 4 29,3130 31.1467	0 1 4 5,5320 4,3421 -6 1 4 43,3280 45.7781
2 3 42.0710 10.4752			A 2 4 22.9410 23.1569
-> 3 3 10,9340 16,7046	-10 1 3 38,2790 39.4588 -10 2 4 14.5680 14.8316		-6 2 4 15, V320 14.4507
> 5 5 5,3540 2,4152	-10 4 3 10.2620 10.7165		-A 5 A 44 9410 41.5553
-5 5 3 34,1490 40,0046 5 6 3 7,4750 6.3520	-10 5 3 25.0730 24.0469 -10 6 3 8.1710 5.5914	-3 3 4 41.2460 44.2029 -3 3 4 81.24/3 84.4629	-0 4 4 20,0; VA 20.0076
		4 1 4 29 21/0 40.1134	A 5 4 7.4216 6.2114
5 7 3 23,92/0 23.0446	-10 9 3 37,0500 36.7902 -10 10 4 18,9930 18,1953	-3 1 4 13,4757 16.3148	-6 5 4 53,9737 56.5736
5 8 3 6,1080 5,7612	#10 11 4 16 A6/6 15-6967	-5 7 4 41 VANA 45-5480 -	-6 6 4 13.3446 11.4627
-5 A 3 33,7076 32,8232 5 9 3 5,4710 2,4575	-11 1 3 24,7400 20,5332 -11 2 3 6,0410 6.9468	3 1 4 40 0AV1 40.04V1 -3 1 4 25.0711 20.1207	-a 7 4 43,4150 40,1952 a 6 4 14,5090 12.0154
-5 0 1 21 9415 94 4391	-11 4 3 12.4246 12.5328	3 4 4 42.2340 41.0490	-A A 4 28.Je10 27.4343
-5 10 3 4,07/0 3.2501 5 11 3 4,8460 3.3830	-11 5 3 5,9500 6.2879 -11 6 3 11,2690 11,1774 -11 8 3 10,7720 10.2748	-3 4 4 11.0200 12.0457 3 5 4 10.3103 15.4202	-6 9 4 7,3797 6,4933 6 10 4 19,7116 20,3812
-5 11 3 20.7980 20.3049	-11 6 3 11.7690 11.1774 -11 8 3 10.7720 10.2748		-A 10 4 B.Veet 6.0334
-5 12 3 20./640 20.7698 -5 12 3 7.3650 7.5631	0 0 4 59.8000 09.1615	3 6 4 14./245 16.3138	-6 12 4 11.02/0 12.3955
D 13 3 18.9790 19.4960	0 2 4 23.8610 25.5621	-3 7 4 /3./410 /2.0014	0 13 4 7.4290 8.1160
-> 13 3 11,00Vn 13.0876	0 4 4 8.2880 5.9072	-3 A 4 24 MOAD 23.7192	-6 15 4 15.8030 14.9671
3 14 1 6.8920 6.3428 -5 14 3 9.2770 10.2566 5 15 3 10.4566 8.9784 -5 15 3 10.2080 9.3618	0 5 4 4,0090 2,0231	-5 9 4 10.14/h 10.8672	-0 16 4 34.54Z0 35.8062
-5 15 3 10,3500 8,9/84 -5 15 3 10,2000 9,3618	0 7 4 17,47/0 19,0565	3 10 4 12,0320 12,4174	-6 17 4 8,9240 9,1628 -6 18 4 18,3640 17,9558
		-3 10 4 8.0500 7.8523	-6 10 4 26.64/0 28.0203
-5 18 4 27,4600 29,5118	0 9 4 51,4990 52,6240 0 10 4 30,0790 29,6293 0 11 4 19,5620 20,4631	-3 11 4 84.4422 82.2115	-/ 0 4 4.7240 2.7130
-5 19 3 13.0600 13.8922	0 10 4 30.0790 29.6593 0 11 4 19.5620 20.4631 0 12 4 30.8850 33.3407	3 12 4 19.1146 17.4336	
6 1 3 12.8940 11.4868	0 13 4 4.2500 4.7980	3 14 4 10,4580 10.8403	-7 1 4 9.6780 2.5982 7 2 4 21.8550 22.3627 -7 2 4 23.9330 23.4117
-6_ 1 3 13,3800 15.7283	0 15 4 8.2920 0.4072	-3 14 4 10.3140_11.0700_	-7 2 4 23,9330 23,4117



TO A L TEUPS) TELALOT	A 4 L YIURN) YICALCI	H & L TIDES) TICALCI	H & L TIONS) TICALUI
/ 3 4 9,5547 10.4325	1 11 > 5,6611 4.3297		-11 6 > 12,10/6 12.7436
		45 1 2 14 124" 17-1771	-11 7 3 4.VE45 9.8291
-7 4 4 13,1310 12,4793		5 5 24,0200 20,0820	-11 6 3 0.1730 7.3905 -11 9 3 0.4530 0.0204
7 5 4 6.5F4* 9.1511 -7 5 4 30.2610 31.0699	-1 14 > 35,2150 38,2043	-5 5 5 19,96/0 16.3568 5 5 10,6320 9,0000	-11 10 > 22,3240 1V.0050 -11 11 5 10,4950 16,7774
-/ A 4 35.2510 33.9576	-1 14 2 7.3680 7.356/	15 6 2 22.0091 20.0229	0 0 0 16,2100 21.0018
-/ A 4 21.0444 20.5672	-1 15 5 13.6183 17.0008 -1 15 5 11.2080 10.5318	5 4 3 8 /990 8.8108	0 2 A 4A.4610 45.7280
-7 9 4 9.1595 11.9478 -7 11 4 38,2530 40.2511	1 17 5 47,0021 50.4162	-5 6 5 73.3749 /4.2228 5 9 3 36.07/9 36.1634	0 4 6 52,0950 55,1338
-7 12 4 6. Y730 7.4931		.5 0 5 19.0994 21.6123	0 6 6 20,7740 20.2056
-7 14 4 21.4245 19.5054		-5 16 2 14.0216 11.0/27	
-7 15 4 12./140 13.4920 -7 16 4 26.8870 28.6934	-1 20 5 14,32/0 12.38V6 2 1 5 42,02V0 45.08U7	-5 11 7 5,/550 3,2065 -5 12 5 22,1320 22,0138	0 6 6 11,/620 12.1/66
-/ 10 4 26,8870 26,8934 -/ 17 4 4,6926 2,239/ -7 18 4 8,2036 2,9224	-2 1 5 57.4940 5H.5981	-> 13 9 19,2130 18,1078 -> 14 9 20,5180 21,1101	0 10 6 10,4960 4.6300 0 11 6 13,6980 14,4934
-6 0 4 52,3500 53.5151	-2 2 > 71.0540 /0.5474	-5 15 5 21,/160 21.15/e	
-8 2 4 13,43e0 13.6390	-2 3 5 40,5290 35.2227	-5 1/ 5 8.0241 0.1008	0 14 0 10.3940 14.1462
-8 1 4 33,21en 42,0675	2 4 5 6,/660 8,8945		0 14 0 14 0421 11.1274
-4 5 4 11,0410 9,3273	-2 5 5 100.00/c 100.1073	-0 1 5 5.4143 0.3205	0 10 0 J1,9920 J2.6049
-4 7 4 45, 1200 46, 6193	-2 A 5 42,5110 42,6509	A 1 5 14 6740 18-1404	1 4 4 41.1421 01.2945
	2 7 5 12,9020 14,7077	-6 3 5 53.6824 51.1259 6 4 5 19.1841 10.0925	-1 0 6 26,3220 33,3844 1 1 6 30,4290 2/,9300
-0 10 4 4.94¢0 5.6397	2 6 5 5,0730 6.3273	-6 4 5 46,9505 49,9904 6 5 5 15,7180 15,2074	-1 1 0 12.000 /.0892 1 2 0 19.2000 19.0291
*# 12 # 9.75/0 9.7465	2 9 5 40.0710 40.6275		-1 2 A 7.99/A 9.8057
	2 10 2 10.0020 10.1327	-A A 5 29 48A3 31.975B	
-8 16 1 15.4720 19.6612	-2 14 5 13.0190 14.5600 7 11 5 4.0360 3.1340	-4 7 5 4.545 1.0114 -6 8 5 25,950 25.0016	1 4 4 41,3120 35,7835
		-6 9 5 5.0400 0.0001	1 5 6 27.2500 27.7891 -1 9 6 31.9490 33.7952
-9 2 4 22, V830 21.0189 -9 3 4 45, 3120 43, 9809 -9 4 4 20, 0090 24, 4845			
-9 4 4 20.00un 24.4445 -9 5 4 0.6390 /.0894	2 14 7 22,99en 23.6736	-6 14 5 5.27/6 2.1830 -6 15 5 24,33/6 22.8920	
	2 15 5 16,5550 17,8094	-6 16 > 14,4100 15.9018	
-9 7 4 26,3810 24,7357 -9 8 4 5,4590 1,9399	-2 15 > 24,4020 23,2563 -2 16 5 20,0550 26,4663	-6 18 5 14.J2YA 12.6828	-1 8 0 10.0920 9.8017 1 9 0 0.0490 5.5770 -1 9 0 13.5080 14.3904
-9 7 4 20,810 24,7357 -9 8 4 5,690 1,939 -9 9 4 17,8410 18,1958 -9 10 4 14,9230 14,7498	-2 17 3 31.3436 33.0241	-7 1 5 13./£40 11.0131	1 10 0 14.4890 15.1102
-9 11 4 /.2240 5./Jep -9 12 4 22.6920 25.1080	-2 16 5 0.0000 6.0463 -2 20 5 14,9120 12,3154	-7 3 5 68.9110 e2.vene	-1 1s 6 4.1780 3.0739 1 11 6 5.0050 6.2077
-9 13 4 16 4710 17-1985	3 1 9 34,4evo 35,1540	-/ A 5 28.4640 29.0484	-1 11 6 V.3030 0.0206
-9 14 4 14,0600 11.9413 -9 15 4 16,3020 16,2771 -10 0 4 36,7493 38,4262	3 1 3 41,2900 30,0710 3 2 3 21,7930 22,0939 -3 2 3 37,1200 36,9855	-7 7 5 20,1230 20.1481 -7 8 5 18,9730 15,9579 -7 9 5 10,3370 9,4381	1 12 6 6,8980 7.2868 1 13 6 26,7710 27,7110 -1 13 6 4,6490 4.9778
-9 15 4 10.3020 10.2771 -10 0 4 30.7490 38.4262	-3 2 5 37,1200 36,9855 3 3 5 28,3600 29,0944	-7 10 5 32.0000 32.4992	-1 13 6 4,0400 4.9778
-10 1 4 /,6399 8,6018 -10 2 4 24,4420 25.2571 -10 3 4 17,4630 18,7574	-3 3 5 4,4548 8.4145		1 14 6 12,8480 11.9548 -1 14 6 20,2676 20.7507
-10 4 6 14,6737 14.2462	-4 4 2 14 2545 14 1429	-7 14 9 4.0610 .3028	1 15 0 10,0500 15,0540 -1 15 0 5,2(10 6.50)2 1 14 4 7,007 6,2272
-10 6 4 12 3940 11.8655 -10 7 4 12,0840 11.2084	-3 3 17,4201 17,4119	-7 15 5 20 /140 20.4169 -7 16 5 1/,/550 20.6266 -/ 17 5 9.9610 9.2249	1 14 4 7.007 6.4472
-10 A 4 Ja. Vata 41.4844 -10 0 4 6.0810 5.1210	-3 a 7 12,711 13,3308	-7 17 3 9.9410 9.2249 -7 18 3 7.9126 9.1354	-1 18 6 24.010: 24.1171. -1 19 6 10.036* 10.3001
-10 10 4 13,5000 14.0000	-1 / 2 0.0110 5.9414	-6 1 5 V-4146 8-6235	_2 0 A 32 3615 34.6201
-10 11 4 1-,8320 14.7109	-1 / 2 6.6110 8.9234 -3 1 7 7,060 3.7694 -4 2 7,1745 41-6017	-8 2 5 76,7360 75,4161 -8 1 5 6,1480 5,4232	2 1 4 4/,6545 48,5598
-10 13 4 4.9790 5.9265 -11 0 4 24.46/0 21.4706	-3 4 5 33,5950 33.2010 4 11 5 15,3881 15,3312	-6 4 > >.08/0 7.3235 -8 5 > 12.4540 15.1176	-2 1 4 35.2654 41.//29 -2 2 4 44.9696 45.4634
411 1 4 4.4890 .4943	-3 11 > 33,2744 32.1969	-6 6 > 24,2600 24.9035	2 3 6 4,3740 3.8087
-11 3 4 12.2310 14.0314	3 12 2 27.3700 31.0764	** 4 5 10 5028 10 AAST	7 4 4 9.44/4 10.4185
-11 4 4 A.20/0 3.7147 -11 5 4 0.3336 0.7363	4 14 9 5.0190 3.5/78	-8 9 5 4.2600 2.9815 -6 10 5 4.7030 2.1104	2 4 4 12 2380 12 2314
-11 A 1 12.63/8 12.4957 -11 7 4 29.6798 29.9339	-3 11 5 45,88/0 44,2/13 3 14 5 20,8660 21,/517	-8 11 3 8.2472 9.1400 -8 12 5 32.7040 33.2962	-2 5 6 85,1300 87,0404 2 5 0 8,1910 8.9161
	-3 14 5 13.2430 12.4065		
0 1 > 29,2750 29,9570 0 2 > 5,8350 7,5776 0 3 > 39,0740 41,0132	*1 15 > 21.0526 23.2008		2 4 4 20.4550 42.4137
	-3 16 > 27.4848 30.7781 -3 1/ > 30.7848 31.3473	-0 17 5 11,0000 14.0039 -9 2 5 49,9490 21.0720	-2 8 6 11,/990 8.2894 2 10 6 33,38/0 33,9092
0 5 5 36./040 37.0411 0 6 5 5.8750 4.8265		-9 3 5 38,0820 32.0/24 -9 4 5 7.2980 7./041	2 10 0 33,30/0 33,9092 -2 10 0 0,2000 7.0230 -2 11 0 9,0420 11,7280
0 7 5 4,8900 6.1377	4 2 5 24,0300 24.4021	-9 5 5 5,/000 4,0009	2 12 4 12,0220 12.5200
0 10 5 4,2210 2.5060	4 3 5 14,2710 13,/829	-9 7 5 11,5740 13.4942	2 13 4 36,/190 37.5325
0 11 5 7 9550 A.VA76 0 13 5 19 4530 21.2880	4 4 5 18,010F 17,9460	-9 a 5 5,1800 5,3949 -9 9 5 6,8900 7,4277	-2 11 4 26,/120 25,2316 2 14 6 7,00/0 5,0174
0 14 5 15.8480 14./489	4 5 5 20,/048 28.3827		2 13 4 11,1000 9.0049
0 14 5 15 0760 14-1434		-19 12 h 6.9860 8.2170	-2 15 A 12,1050 11,6090
0 17 5 23,9970 26.0701 0 18 5 5,4330 4,3777	4 6 5 6,1050 5,5457	-9 13 > 14,1016 13,9706 -9 14 > 5,5516 5,3362	-2 16 0 15.7520 14.9170 -2 17 8 15.2010 14.7284
0 19 5 15,0100 16.1787	4 7 5 22,0450 23.6515	-9 15 5 0,8600 6.V639	-2 18 6 14,6869 15.2438 -2 19 6 12,5898 12,3363
-1 1 5 19.8900 20.3826	4 8 5 15.4500 17.0700	-10 1 5 4./798 5.2288	3 0 6 21,0100 21.3839
1 2 5 14.4200 10.7109	4 0 > 30,5490 30,9931	-10 2 5 40.5020 41.2308 - -10 3 5 35,4630 35.1230 -	
1 3 > 64,8120 93,9460	-4 0 5 49./300 48.4978 -4 10 5 57,1810 59.3054	-10 5 5 5.3140 3.5601 -10 6 7 8.8350 8.3/16	3 2 6 12,3410 11,3236
1 4 > >,0620 6.2408	-4 11 5 10.9490 13.5/22 4 12 5 /,4990 4.1805	-10 7 5 25,3900 24,1479 -10 8 5 4,8720 ,7434	-3 2 6 06.5210 02.2101
	*4 12 4 24 2340 24 0089	-10 9 5 16,0720 16,9166 -	*3 3 A 7 A2/A 5 020A
-1 5 5 77,4480 /9.8072 -1 6 5 5.2621 4.6678	4 13 5 16,2260 17,1470 -4 13 5 29,7380 28,7040	-10 10 5 7,5230 4.4093 -10 11 5 13,0150 12,8874	-3 4 6 44,0488 45,8495 -4 5 6 17,0440 17,7497
1 7 > >2.0301 >3.3832	-4 14 > 30,0300 30.9755	-10 12 5 17.5556 17.5228 a	-3 5 6 38,1628 38.2544 4 6 21,8018 21,2888
1 6 > >,0851 4.9026	-4 18 5 10.9740 11.1610	-10 14 5 10.9905 V.HANS	
1 9 2 23,3200 20,0090	-4 19 5 6.2240 5.7002 -4 20 5 14,2320 10.1282	-11 1 5 /.85/6 7,V933 -11 2 5 26,5126 28.4003	3 7 6 15.7650 15.33V0 -3 7 6 66.9370 61.5414
	5 1 5 11.8320 12.8754	-11 1 9 34.6228 33.2261 -11 4 5 15.5186 15.7664 -11 5 5 7.4156 6.1044	3 7 6 15,7620 15,3370 -3 7 6 46,8370 61,5414 3 6 6 14,1110 13,5106 -3 8 6 8,9170 6,5934 3 9 6 8,4220 7,7292
1 10 2 9,0040 9,2005 -1 10 5 3,9400 4,9800	3 2 3 11.4650 12.6252	-11 5 7 7.4130 6.1044	3 9 6 8,4220 7,7393

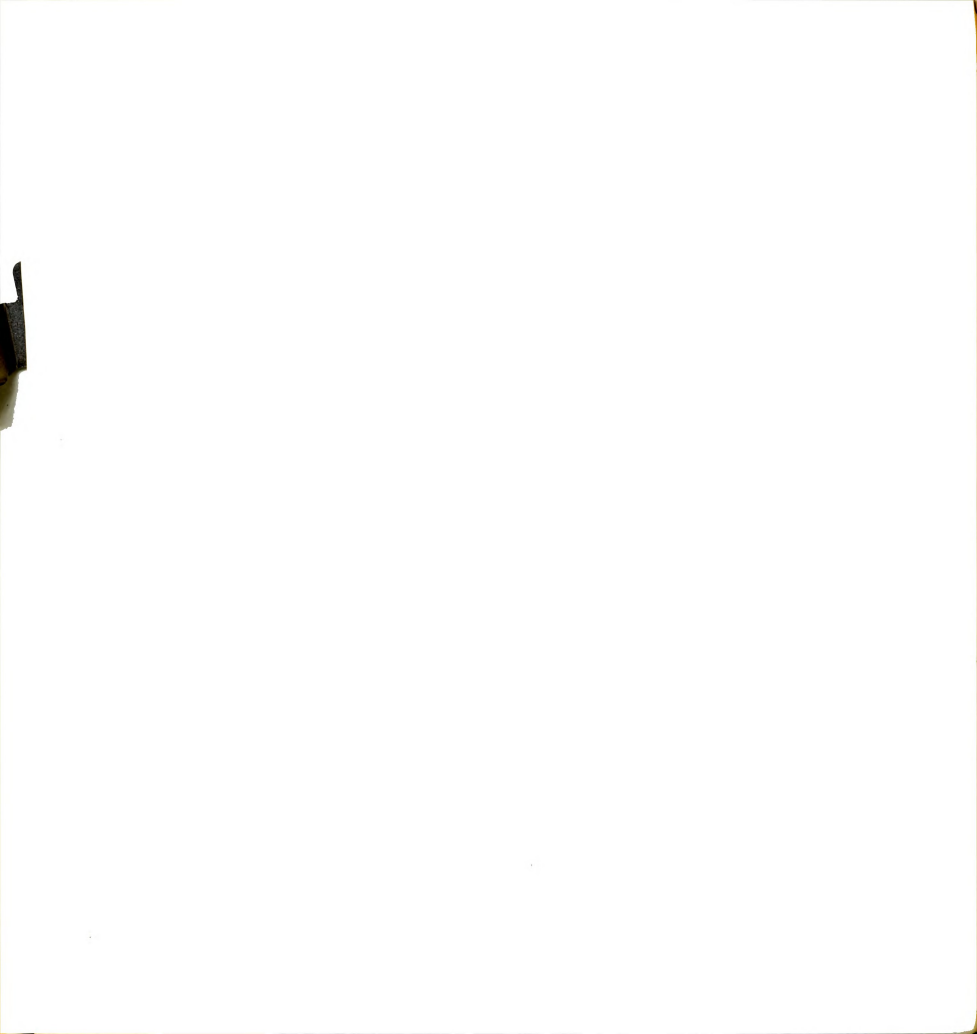
	H & L YIUFS) TECAUCT	mild to Tra-by MILALES	M 4 4 ffu-b) FECALCI
H "K L Y(UHS) Y(CALC)		-2 5 7 50,4917 51.04FV	-7 4 7 10,4710 15.3775
3 10 4 3 272 30 VATZ	-8 1 6 24,4500 23.5135	2 4 7 31,2405 30,2950	-/ 1 / 22,2120 43,35/4
-3 10 6 45,3600 46.3053	-6 3 6 20.0160 29./967 -8 4 6 /9.2300 2/.2/24	-2 / / 21.9300 /3.6561	-7 / / 10.4030 17.3534 7 0.9110 11.1039
3 11 6 21,3898 23,2807 -3 11 6 0,1278 4,1/27	-6 6 6 10,0010 10.1397	-2 8 7 17.e934 18.0080 2 9 7 29.1284 30.0794	
3 12 6 11.4516 10.8621	-8 7 0 38,9508 19.5091 -8 8 0 21,2480 19.9930	-2 9 / 27.1280 30.0/94 -2 9 / 5.8980 3.5851 -2 10 / 27.0000 23.0/55	-7 10 7 19.0020 19.3223 -7 11 7 24.2120 22.1891
1 13 6 12.2040 10.27/3	-8 8 0 21,2480 10,9930 -8 9 6 10,6146 10,2421 -9 10 0 8,7430 7,6805	-2 10 / 19,6924 19,9743	-/ 11 / 24.2120 22.1801 -/ 12 / 17.5250 18.0352 -/ 11 / 21.3410 21.0396
-3 13 0 24.391n 23.14m1 -3 14 6 38.0230 37.1358		-2 11 7 10,2000 9,7320 -2 11 7 7,1300 0.5101	-7 14 7 32,2200 30.2500
	-8 13 8 10,0150 9.5214 -8 14 8 20,0710 20,1/14	-2 12 / 14.4042 14.944B 2 15 7 9.1627 9.4363	-/ 15 7 6.4205 4.7324 -7 16 7 8.0506 9.2064
-3 17 6 40,4900 41.766/		.2 11 / 12,8910 13,1472	-7 17 7 18.3210 19.0200 -0 1 7 24.07/0 26.2987
-3 14 6 27.0000 27.0041 -3 19 6 14.3550 13.9633	-9 1 0 27,1590 26.9108	2 14 7 0.9490 0.4540 -2 14 / /.4690 7.4455	0_2 / 10.0240 10.0005
-4 0 0 43.0051 20.7014	-9 2 6 4.3188 2.2714 -9 3 6 27.8508 28.4239	-2 15 / 5,5210 5.0000	-6 4 7 5,2340 5,4282 -8 5 7 23,5550 24.3677
- 1 6 10,3150 9.3656 - 1 6 15,9882 14,9838	-9 A A 21.8548 22.2103 -9 5 6 30.1528 30.6892	-2 1/ 7 7,9000 7,9209	
-4 1 6 15,9883 14,8838 4 2 6 14,8476 14,8527 -4 2 6 4,8576 2,1478	-9 A A 15,4080 14,2035	-1 1 7 88.3230 /0.8970	
4 3 6 7,7265 7.0700	-9 8 6 20.6290 26.43/b.	3 2 7 25.4450 25.1165	-6 9 7 41,5778 43.9152 -6 10 7 12,7198 12.2398
	-9 9 6 11.46Jn 12.5588	3 1 / 6,4340 6.5144	-0 11 / 11./598 12.9688 -0 12 / 20.4408 19.2772
4 5 6 13,9710 15,120B	-9 11 0 0./0/0 5.2003		-4 13 7 9.9130 8.2745 -8 14 / 40,2180 41.1336
-4 6 6 21,0743 20.7588		-3 4 7 24,7310 23.3185 3 5 7 5,0030 4,4685	-8 17 7 Ju. 0000 32. 3858
4 8 6 10,0130 17,5/46	-y 15 6 10.6450 8.0185 -y 16 6 5,/990 4.4276	-3 5 7 06.08V0 6V.C7NO	-9 1 7 45,2020 44,4402 -9 2 7 6,1600 5,6063
4 9 6 13.2320 15.4861	-10 0 0 29,2660 48,4274 -10 1 6 46,9210 49,7799	-1 A / 49.5450 51.3609	-9 3 7 32,4310 30.7692
-4 9 6 32,0510 29.4131 4 10 6 16.7580 16.5471		-J / 7 45,0500 40,7435	-9 5 7 32.6210 29.7750
-4 10 6 52,/8/6 49./345	-10 3 6 40,1200 42,4692 -10 4 6 10,1958 5,1864 -10 5 6 13,6790 12,9201	-3 8 7 5,2217 4,1310 -3 8 7 13,5990 11,1306	-9 6 7 26.8496 23.1414 -9 7 7 20.4436 18.3308
-4 11 6 29.0110 26./058	-10 5 6 13,0790 12,9201 -10 7 6 5,3420 1,1697		-y 6 7 23,9780 24,1916 -y 9 7 29,6020 28,5044
-4 12 6 36.8950 36.9912 -4 13 6 11.9990 11.6412	-10 8 6 7,940f 5,0548	-3 9 7 0.0070 5.2420 -3 9 7 0.0090 5.2430 3 10 7 24.0700 24.5303	
-4 14 6 24.2000 (3.2294 -4 15 6 14.1500 14.0970	-10 9 6 7.49a0 6.0244 -10 10 0 0.1580 0.4807		-V 11 7 15,3726 14.2717 -V 12 7 7,2066 5.4849
-4 16 6 27.08en 26.6776	-10 11 6 7.9780 6.8/mg	*A 12 / 22 1380 20.6947	
-4 17 6 11,5790 10.8707 -4 18 6 14,3980 14.0013	-10 13 o 18,4910 18.8017	-3 13 7 37 4920 38.1729 -3 14 7 29.3990 31.1999	-9 14 7 20,3476 20.1534 -9 15 / 17,7568 19.5909
-4 19 6 9.0120 7./304	-10 15 6 15./5/0 15.0159 -11 0 4 4.0600 2.1136	-3 16 7 26.6980 25.3885 -3 16 7 15.5480 16.7797	-9 16 / 13.2210 16.8952 -10 1 / 40,0360 38.0263
	-11 0 0 4.0600 2.1136 -11 1 0 23,7290 22.0905 -11 2 0 32,1490 44,9332	-3 17 7 24 4500 24-0384	-10 A / 19 13en 18,9149
5 1 6 5,2000 4,1593		4 1 7 8,1590 6,2439 -4 1 7 38,1310 34,3345 4 2 7 9,8770 7,0849	-10 4 7 20,249n 20,240e -10 5 7 25,128n 23,8708
5 2 6 4,6690 3.9062	-11 5 6 15,4200 14,78H0 -11 6 6 10,2610 10.3002	4 2 7 9.87/n 7.0849 -4 2 / 10.5110 6.6686	-10 A 7 18.3020 17.9440 -10 7 7 24.3560 24.8687
-5 2 6 22.2620 22.6274 -5 3 6 17.4460 17.6508	-11 7 6 13.2740 13.2124 -11 8 6 19./610 11.1034	-4 3 7 92./320 93.0911	-10 7 7 24,3560 24.8687 -10 8 7 22,5660 24.6389 -10 9 7 10,9290 11.3589
5 4 6 8.6220 6.5456	-11 9 6 24.67an 23.2436		-10 9 7 10,9290 11.3589 -10 11 7 7,1220 6.6506
-5 4 6 33,6620 35,3047 5 6 6,8440 7.0332	-11 11 A 20 8990 19.4672	4 5 7 4,9970 9,2427	*10 12 / 24,34,5 (4.5/m)
-> 4 0 75.714" 24.3023	0 1 7 (7,570° (0.7745	-4 4 / 12,1545 42,1115	-10 14 / 10,491 17,444
5 7 6 22.6vir 21.3648	0 3 / 42,11-07 21,1000	4 7 / 4 0647 4,3101	-14_15_/_ 2.6532_ 4.0335. -11 1 / 42.777* 42.4484
5 7 6 72,6017 21.3848 -2 7 6 22,9412 34.1238 -3 8 67,1216 67,6763	0 5 / 25,/200 25.0003	-4 7 / 23, Vno: 23, /700	
	-0 9 / 35.2946 32.0013	-4 8 7 12,7431 11,0366 -4 8 7 12,7491 13,4477	
-3 11 0 JC-0110 J4-7340	U a / 19,4045 28,1248	-4 14 / 24 2180 24-8211	-11 5 / 0.0335 4.0160 -11 6 7 7.27/0 11.4029
-> 12 6 26.00/A 29.1634 -> 13 6 7.9392 7.5279	0 10 / 22.0P40 20.4174	-4 12 / 21,/5/0 19.//98	
	4 12 7 10,0010 17,3005	-4 11 / 45./8u0 45./551 -4 14 / 21,0140 20.6268	
	0 13 / 17,20/0 16,99/2	-4 15 / 12.59V0 12.01/5	
-> 16 0 >,6590 1.0138		-4 17 7 38, V440 39, 4074	-11 13 7 22,0900 21,0445 0 0 0 1,5000 5,3007
-5 19 6 5,9410 5,3958 -6 0 6 10,1240 3,4259	1 1 / 19,2960 19.3786	-4 19 7 6.4230 3.9973 -5 1 7 52,6380 57,7132	0 1 3 10 2630 21.2201
-0 1 0 24,9200 24,0540		-5 1 7 52,0360 57,7132 -5 2 7 17,4160 17,9296 -5 1 7 36 5880 41,4932	0 3 4 3 9030 2.0396
-a 1 a 34.5900 42.0005	-1 2 / 71.84us /2.6439 -1 3 / 68.7304 69.5413	-5 4 7 14.9490 16.0228	3 4 d 5.024n 3.4234
-6 4 6 23,9858 25,5458 -6 5 6 32,43/8 38,0879	1 4 7 7,9549 7,7344	-5 5 / 67,3520 91,7722 - -5 6 7 23,6110 23.4613	0 6 8 6,3860 5.3435 4 7 4 33,0410 53,2387
-A A A 6./010 4,9178	4 7 19 8495 20,4002	-5 7 7 4.04/1 5.0511	
-6 7 6 50.3890 50.0358 -6 8 6 10.2130 9.4721 -6 9 6 17.5890 18.0319	1 5 7 61.4056 63.3702		0 10 4 10,67/0 9.9130
-6 10 6 37,4200 37.8056	-1 4 7 8.3980 2.9419	-5 12 7 15.0010 14.4/85	0 11 # 13.7030 15.4288 0 12 # 20.7140 20.7490
-0 11 0 32,2930 32,5925 -0 12 0 15,2390 14,8035	1 7 7 20.5720 19.7440 -1 7 7 13.2190 10.1536	-5 13 7 12,7601 13.0824 -5 14 7 6,4040 4,7598	0 13 4 0.1500 5.7539
44 13 A 18 8950 19,1270	-1 a / 12,3140 12,9125 1 0 / 33,3850 14.5599	-5 15 7 10,2394 10.1928 -5 16 7 12,6291 13,3279	
-6 15 6 13,4340 14,3450	-1 0 7 7,4410 8,4188		1 1 d d.95/4 8.3690 -1 1 d 23./640 23.2871
-6 15 6 13.4340 14.3450 -6 16 6 19.4000 20.0665		-> 18 7 16.7700 16.6473 -6 1 7 43.5090 45.3045	1 2 0 4,0140 4.0114
-6 17 6 5.5690 4.3101 -6 18 6 13,4820 14.5328	1 11 7 5.1270 6.2994	-6 2 7 6.2740 3.7973 -6 3 7 19.6030 18.7219	1 3 5 7./490 5.5098
-/ a a re.berg rv.6384 -/ 1 a 52,1420 49.3212	-1 12 7 7,4310 5.9244 1 13 7 11,7180 12,3263	-6 4 7 18.8520 16.3739	1 4 9 9,45/9 9,6797
-7 2 6 66.1310 61.7961 -7 3 6 40.5410 37.6051	1 14 7 5.9950 4.6308	-6 5 7 81,2500 84.1645 -6 6 / 12,/350 12,5892	1 5 8 5.3998 4.3325
-7 4 6 41,3930 43,0090 -7 5 6 41,1030 39,7975	-1 14 7 7./280 /.5008 1 15 7 5./490 4.3965		-1 5 4 21,4034 21,4433 -1 6 6 23,7436 24.6630
-7 5 6 41,1030 39.7975 -7 6 6 32,4690 32.8477 -7 7 6 10,6650 20,7349	-1 15 / 9,2090 8.3818		
-7 7 6 10,6650 20,7349 -7 8 6 9,2210 5,0347	-1 14 7 13 0230 12,2015	-6 10 7 17./520 17.4395 - -6 11 7 4,3470 3.3520	-1 7 6 V.2746 7.7166 -1 8 6 1V.10/0 1V.0064
-7 9 6 18,7700 19,3435		-6 12 7 12.3340 11.0124 -6 11 7 27 (000 29.0129	1 9 8 9.0300 10.0342
	2 1 / 8,/01* 7.8303	-0 14 7 3.3600 3.9293	
-7 12 6 30,8948 31,0690 -7 13 6 19,1828 19,9187	2 2 7 16,/350 14.2066	-6 15 7 13,42/4 13,/798 -6 17 7 14,7260 12,4002	-1 10 # 15./220 15.8441 1 11 # 11.0500 11.1922
-7 14 6 1m. 3F36 18.7705	-2 7 7 22.6360 23.7954 -2 3 7 80.7280 82.6363	-6 19 7 6,4599 6.2537 -7 1 7 20,2650 27,4644	
-7 15 6 22,03/6 24,5567 -7 17 6 14,4785 14,5136 -7 18 6 32,1326 36,0666	2 4 7 5,0500 1,7231	-7 1 7 20,2020 27,4044 -7 2 7 8,7210 7.9785 -7 1 7 48,4420 47.6030	1 12 8 21,5500 21.8803
-7 17 6 14,3785 14,5136 -7 18 6 32,1326 36,0666 -8 0 6 41,3466 48,6872	2 5 7 5./340 2.9000	-, 1 / 10.1170 17.8030	

	M & L FRUITS) TECALCY	H & L TINESS SICALOS	- 4 L TILEST TICALCI	H K L Y(UHS) YELALCE
	1 13 4 5,4132 7,5004			
		-7 4 8 71.0338 24.0394 -7 5 8 4.4470 3.0173	-2 7 V 13.4150 13.3050	19 A 9 A /9.45 1.61.47
	-20	-/_ 6_ 6 _10,1724 _15,0330_		-9 7 9 /,3316 7,6389
	-2 1 8 27,>240 40,1307	-7 8 0 44./7/0 45.43×2	2 . 10 9 12. Yey0 16.0552	-9 9 V 43.3420 43.0741
	-2 2 N 10.3400 10.3/69	-7 10 8 20,4000 45,4384	-2 12 V 5.0040 3.524h	-9 12 9 11.81/0 12.0169
1	-2 3 4 49.13/0 52.14/0	-7 12 A 22 4580 21.0078	-2 14 9 15./500 15.JJ4H	-9 14 9 11.3e30 9.0348
			-2 14 V 3.2810 4.5779	
	2 6 8 10,0500 9,4822	-7 17 6 15, VO40 17.6324	3 1 9 9,0530 A.0130	
	2 7 8 21,4590 22.4810	-6 0 8 3.2830 1.0702		
	2 8 8 5.4936 5.4963	-6 2 6 23.0100 23.1512	-3 3 9 J0,1210 J1.2418	-10 7 9 4.6330 5.8048
		-d 1 8 3,9521 3,2072 -d 4 8 7,4750 8.0921	-3 5 9 34, Ueen 32, byny	
		-8 6 8 20.Y010 23.1780	-3 7 9 2V. 9700 30.0739	-10 10 9 21,2450 20,2450
	-2 11 8 15.3330 17.3339 -2 12 8 21.8820 23.3881	-6 7 6 78.7788 20.4559 -6 8 8 44.4488 45.1352	-3 8 9 14.6636 14.7360 -3 9 9 27.3286 23.2472	-10 12 9 14.8980 15.1898 -10 13 9 12.8720 10.2850
	-2 13 8 20.43/0 20.4307			-10 14 9 15./250 14.3200
		*# 12 # 29.5540 27.5271		
	-2 17 8 10,0730 15.5375	-6 15 4 4.9200 9.0020	-3 1a 9 19.4320 18.4492	-11 2 0 11,4890 11.63V2 -11 4 9 27,1160 30,2343
	A 1 8 16 5465 10 2001	v 0 8 29.54V0 34.1100	-4 1 9 6.9290 5.9921	
		-9 2 8 12 3636 14-9146	-4 3 9 31 8990 28.2019	
	3 3 8 15,4830 14,8627	-9 3 8 4.1190 6.50e3		-11 9 9 21.2250 14.05/3
	-3 4 6 59,4420 63,0285	-9 5 8 6,7774 5.0500	-4 6 9 25,5440 25,4013	
	-3 5 8 14,9140 11,9112	-9 7 d 13, V3/0 11.0008	-4 8 9 5,0360 2,7698	-11 12 9 7.7348 0.7810 -11 13 9 35,0140 34.4055
	-3 6 6 14,0700 13,9451 -3 6 6 17,9610 17,5762	-Y 10 H ZH. U785 28./269		-11 14 9 22.Jevs 22.J036
			-4 12 9 21,9450 21,2970 -4 13 9 20 4140 28 5280	_ 9 1 10 18.0610 21.0217
1	3 8 8 10.4100 10.7580	-9 13 4 29, vo40 28.3219	-4 14 9 31,5586 31,9092	9 4 10 15.2000 11.8496
	-3 9 8 19,4200 18,4033	-9 14 8 20.37/0 19.4772		- 1 10 5./5/0 5.0903
		-10 0 8 11.4626 12.3456 -10 2 8 12.4926 12.4977	-> 1 9 15.7100 14.3>32	
		-10 3 8 1/.51/6 1/.6219	-5 2 9 51,024n 51.4624 -5 3 9 14,080n 14,1405	1 0 10 4,0000 1,2000
		-10 6 8 23,1916 21.0691		1 1 10 15,1980 15.3478
	-3 1/ 8 10,3130 15.4656	-10 8 8 40,4300 41.5811	-> 6 y 13,2130 14,3644	1 2 10 9,0000 9,7053
		-10 12 8 1v.4650 8.3168		-1 3 10 4,/400 8,/569
1	-4 1 0 30,0130 49,6024	-10 15 6 6,4120 7,4645	-5 10 9 11,4447 11.14h7	-1 4 10 21,0040 15.0479
1	-4 5 H 4.YF30 6.6034	-11 0 d 14.0//0 15.40// -11 1 8 /.5100 7.6463	-5 12 9 47.71 vs 41.21es	
	-4 4 8 9.7630 9.1006.	-11 3 8 10.6846 17.1056 -11 4 6 10.7246 20.5308		-1 6 10 71.>100 XZ.4/11
	-4 A N /A-18VA /4-/595	-11 5 0 27,0400 28,3011		-1 7 10 20.4780 23.0303
	** * * 11-4610 10-6679	-11 A A 9-4120 8-9168	-12 17 9 7 /440 0-991	
1	-4 10 8 12.3950 12.8V42		*0 2 9 27 1346 A1.0482	-1 12 10 24.4740 30.4212
1	-4 12 # 22.91/0 22.01UP			
1	-4 13 8 12,/29A 12.0986	-11 13 8 11,0036 10.5057 0 1 9 13,0000 11,1418	-6 6 V 41.3240 40.0890	-2 0 10 8,/841 6,4411
	-4 15 # 2A 4150 2A.4285	0 2 V 12,7510 12.0334	-6 9 w 17 6550 17,1555	-2 1 10 4.9420 4.2928
1	-4 17 8 3,1470 5.0514	0 5 V 7.9080 9.2780	-0 10 9 20.0670 27.2374	-2 3 10 V.4955 11.0676
3 1 3400 3500 3 4 1 1 1 1 1 1 1 1 1	-5 0 8 75,54/0 76.6855	0 8 9 27,2890 28,1554	-6 12 9 14,9405 13.6208	-2 5 10 15,3900 15,2307
1	-5 2 8 5,4840 1.5510	9 10 9 10,0010 10,1008	-6 17 9 15,1720 15.2782	-2 7 10 A/ 2515 Ad /978
1	-5 3 8 15,71/6 15,3972		-7 1 9 50,9540 55.0324 -7 2 9 19,0010 17.4312	-2 8 10 5,1100 3,0395 -2 9 10 22,5555 22,2658
	-5 5 8 25.0210 26.1248	0 14 9 22,4140 22,1859	-7 4 9 8.0420 7.0926	
1			-7 A 9 11-0100 12-0164	-2 12 14 22,02/5 22,207A
1	-> 10 8 10.2000 10.2/71	1 3 9 9.95/0 9.1100	-7 8 9 12,0000 11,4914	-3 0 10 21,4385 20,5447
	-> 12 A A.43V0 0.4174	1 4 9 14,8410 15,7425	-7 10 9 12.3346 11.4398	-3 1 10 5,1300 2.0406 -3 2 10 5,4950 2,9647
3 1 1 1 1 1 1 1 1 1 1 1 1 1 1 1 1 1 1 1	-> 13 8 5,1140 5.8547	1 5 9 9,9945 9,4575		
1	-> 16 8 11,813n 12,1311	1 6 9 16./190 17.6920	-7 15 9 7,4740 0.0112	-3 5 10 23.4330 24.3763 -3 6 10 24.0490 28.7556
		-1 6 9 37,4740 40.6273	-7 16 9 8,2050 8.5087	-3 7 10 4y.2930 49.6/59
$ \begin{array}{c ccccccccccccccccccccccccccccccccccc$	-6 1 8 6,6240 /.1300	-1 7 9 11./940 13.0076		-J 9 10 14,4300 15,948A
To the control of the	-6 2 8 6,09/0 10.0100	-1 8 9 24,7500 24,5900		
	-6 4 6 41,0130 39,3221		-8 5 9 15,2450 13.9111	-3 15 10 3,1240 4,7411
	-6 6 14,1505 13,1/35	-1 11 9 12,9920 13,8812 -1 11 9 14,0540 15,4802		-4 1 10 20,5300 21,1168
$\begin{array}{cccccccccccccccccccccccccccccccccccc$	-A A A 40 /730 44.5561	-1 12 9 18.2050 9.6128 -1 13 9 25 8440 27 5219	-8 10 9 34.3760 44.4741	-4 2 10 10,0360 10.4295 -4 3 10 12,4100 11.0450
1	-6 11 8 20.8FV9 21.2546	-1 14 9 24,5200 24,2400	-8 11 9 8,0170 V.4183	-4 4 10 19,1240 14,2403
** 1		-2 1 9 14,9720 13,7579		
** 1 ** 1 ** 1 ** 1 ** 1 ** 1 ** 1 **	-6 14 d 10,1440 14.5983 -6 15 0 0,4410 7,7390		-8 15 9 18,1490 18,7461	
-7 0 0 31,917 35,576 2 6 7 11,076 17,103 49 2 7 15,100 15,407 41 10 10 10 10 10 10 10 10 10 10 10 10 10		-2 4 9 42,40V0 42,6840	-9 1 9 13,>000 12,4003	*4 10 10 22.4650 22.22A0
The second secon	-7 U 6 51, V176 55.3706	2 6 9 11,3710 10.1435		-4 11 10 32,48/0 32.1222 -4 12 10 /,6370 A.V.43

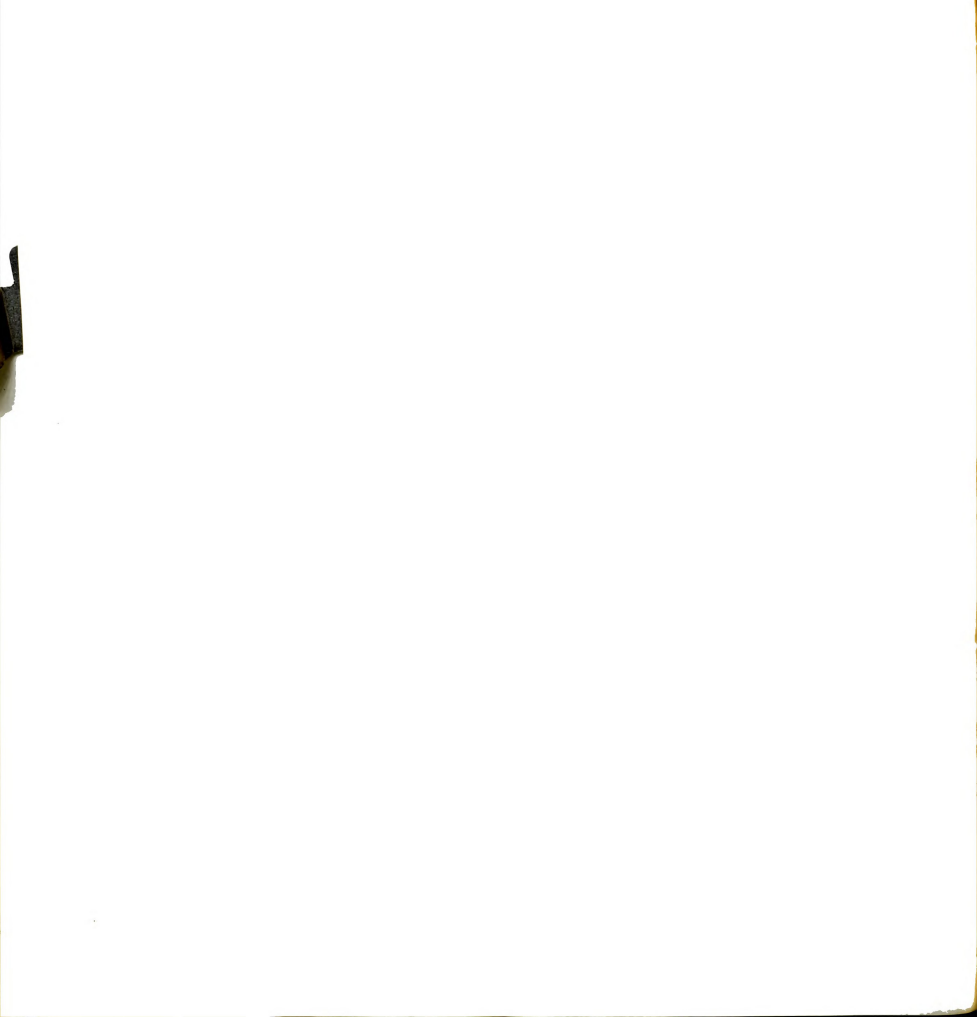


H & L TIUFS) YELALD	H K L T(UFS) T(CALC)	m & L Y(US) Y(CALC)
-4 13 10 5,1993 6,2914	-11 12 10 8,0700 9,7/52 -11 13 10 77,4500 63,0450	-6 9 11 17,475° 17,4434
-4 14 10 12.1101 14.0334 -4 15 10 11 2215 42.0030	0 1 11 10 0140 11.4995	-8 10 11 3.9260 3.1834 -8 11 11 23.0560 20.3598
-5 0 10 50.9497 61./298 -5 1 10 40.9030 42.0103	0 2 11 11.9250 9.6729	-8 11 11 23,050 27.3598 -8 12 31 13,0200 11.48(1 -8 13 11 5.7630 4.0542
-5 1 10 40, VO36 42, 0163 -5 2 10 6,0340 8,2225 -9 3 10 7,1466 4,022	0 5 11 15.0510 14.5343	
	0 6 11 7,3710 7,7637 0 7 11 10,2630 17,1228	
	-1 1 11 15,/924 15,#837 -1 2 11 23,0000 28,0436	-9 6 11 3v,/440 41.2645 -v 7 11 22.62/6 25,7532
-5 4 10 10.32/2 6.8052 -5 10 10 22,4314 22.1565	-1 3 11 10,2710 9,4700	.v 4 11 /.8445 /.5532
-5 11 10 20.0121 19.3525		-9 10 11 13.0297 10.1088 -9 10 11 5,1130 2.3230
-5 11 10 20.0154 19.3525. -5 17 10 10.7594 7.2664 -5 13 10 27.5246 20.4527	-1 6 11 7,3400 8,1966 -1 7 11 13,9000 14,8202	
	41 A 11 14.4850 14.8788	-9 12 11 0,9550 9.0873 -9 14 11 17,2600 17,2986 -9 15 11 14,3250 13.5417
-5 14 10 5.9980 7.0227		-9 14 11 17,2000 17,0986 -9 15 11 14,3250 13.5417 -10 1 11 0,9574 6,2187
-6 0 10 4.49/5 8.0977 -6 1 10 52,2720 51.0929	-1 11 11 A.Z410 A.YYZZ -2 1 11 7,UZ40 5.5971	
-6 2 10 10.9510 10.9998	-2 3 11 9.4740 7.7193 -2 4 11 29.0520 25.8677	-10 1 11 10,0000 19,2147 -10 4 11 12,4650 12,7/49
-6 5 10 36,0830 35.8517 -6 4 10 9,3820 10,4062 -6 5 10 47,6850 47,0046	-2 4 11 22,0520 25.8677 -2 5 11 22,0450 23,7145	-10 5 11 6.9730 6.29/6
-6 5 10 47.6850 47.0046	-2 a 11 27,0a90 28.1301 ·	
-n 7 10 20.59/0 16.9230	-2 9 11 11,8100 11,5803 -2 9 11 16,2240 17.0618	-10 8 11 30,5330 30.7500 -10 9 11 5,4370 5,5814
-6 8 10 22,/0/0 23,5351 -6 10 10 15,5785 17.0614	-2 9 11 16,2240 17.0018 -2 10 11 5,9750 5,9440 -2 11 11 12,9470 13.2728	-10 10 11 9.9390 7.1893
-6 11 10 12.2975 12.2762		-10 11 11 9 0285 V.8619
	-3 1 11 10,0120 9.3854	
	-) 1 11 9.9424 2.8593	-11 3 11 13,4300 13,8675
-6 15 13 /.1526 4.9950 -6 16 16 9.6396 9.5/14 -6 17 16 9.9286 11.3959 -7 8 16 13.9326 15.6045	-3 4 11 18,0438 19,3028 -3 5 11 33,2340 32.0247	-11 4 11 6,7190 8.7932 -11 5 11 9,2540 11,3036 -11 6 11 24,6840 27.7221
-6 17 10 9.920 11.3929 -7 0 10 14.9320 15.0045	-3 A 11 21,8230 21,9306 -3 7 11 5,1770 4.1576	-11 5 11 9,2542 11,3036 -11 6 11 54,6640 57,7221 -11 7 11 13,4967 15,6918
	-3 A 11 30.0P40 31.9391 -3 9 11 27,4109 20.2345	-11 8 11 9.0226 10.5609
-7 3 10 37.6910 37.4713	-3 10 11 15.4310 15.6457	
-7 4 10 5./220 3.8393 -7 5 10 34,1764 36.3636 -7 7 10 6./988 6.7430	-3 12 11 8.0003 9.3437 -3 13 11 17.0034 17.5092 -4 1 11 12./400 11.0003	-11 10 11 42,1700 42,7038 -11 11 11 9,0510 1.7746 -11 13 11 10,0970 17.1202
	-4 1 11 12,/400 11.0803 -4 2 11 10,0800 10,3593	-1 1 12 10.0070 17.1202 -1 1 12 27.7030 32.0272
-7 8 10 12,4450 11,7588 -7 9 10 7,60/0 6.2466	-4 2 11 10.6850 10.3393 -4 3 11 7.4730 4.6675	-1 0 12 29 903 20 222 -1 1 12 0,1540 4.067 -1 2 12 8,8150 9.0966 -1 4 12 22,0260 20.9726
-7 9 10 7,60/8 6.2466 -/ 11 10 9,05/8 9,1070 -7 12 10 7,4960 9.2930	-4 3 11 7,4736 4.6675 -4 4 11 24,3470 24,8922 -4 5 11 4,9367 1.9020	-1 1 12 0,1540 4.000/ -1 2 12 0,0150 9,0966 -1 4 12 22,0200 20,9720 -1 1 12 15,0540 15,1107
-7 13 10 10 2790 10 1011	-4 6 11 75.V050 25.Vd63	-1 5 12 17.0540 15.1167 -1 6 12 5,0120 4.3329
-7 15 10 25.2580 25.8935 -7 17 10 16.5510 14.9789	-4 A 11 74.0720 24.7470 -4 9 11 30.0200 29.7010	-1 5 12 12,8540 15,1167 -1 6 12 5,0120 4,3329 -1 7 12 6,2920 7,8233 -2 0 12 33,6300 36.5514
-7 17 10 16,5510 14,9789 -8 0 10 49,1790 48,2859 -8 1 10 50,3270 54,5558 -8 2 10 8,2560 8,6638		
-8 1 10 50,3270 54.5558 -8 2 10 8.2560 8.6630	-4 11 11 31,7630 31.6357 -4 12 11 13,7420 13.6606	-2 4 12 20,9340 20,4560 -2 5 12 8,8830 8,8805 -2 6 12 6,2090 5,1198
· 6 3 10 20,1830 26.9329		-2 6 12 0,20VA 5.11V6
-8 5 10 25.0520 24.3695	-4 14 11 19.2640 18.0109 -2 1 11 20.0000 29.2929	-2 8 12 18,1730 19,0478 -2 9 12 7,9220 6,8838
-a a 10 30.1500 27.0791 -6 7 10 10.0920 15.7101	-5 1 11 24.0791 26.9577	
	-5 5 11 23, Yess Z4, Jan	-3 0 12 12 9754 12.6506 -3 2 12 16.6550 16.7672
	-> 6 11 /,6684 H.5566 -> 7 11 6,8056 7,2541	
	-> 8 11 30,8945 31.8245 -> 9 11 35,2532 34,7426	-3 4 12 17,0740 15.8000 -3 5 12 22,1400 21,0400
-p 14 10 15,2440 16.1485	-9 10 11 27.0000 20.1/02 -9 11 11 0.1092 5.3/37	-3 6 12 24,004 27.3630 -3 7 12 24,0042 7.0366 -3 8 12 6,0140 7.5862
	-5 12 11 20.1020 4/.5254	
-9 0 10 17.14V8 30.4037 -9 1 10 28.1746 29.9795 -9 2 10 28.5788 29.0329	-5 13 11 15 8385 15 8839 -5 14 11 30,7506 30.7531 -5 15 11 14.5790 13.0017	-3 10 12 14,4520 16.0219
-9 0 10 37,1492 30,4037 -9 1 10 28,1726 29,9795 -9 2 10 28,2766 29,0329 -9 3 10 3,6136 29,0329 -9 3 10 3,6136 2,4134		-5 12 12 5.2130 1.5701
	*A 2 11 A7 V9A0 A/-7A3A	-4 0 12 4.7840 1.7203 -4 1 12 5.2450 6.6496
	-6 3 11 29,8240 31.8415 -6 4 11 13,/168 13,86/7	
-v 7 10 20,2756 29.3675 -v 4 10 18,4306 18.0679		-4 4 12 6 1976 4.6744
-v 9 10 17.6760 19.2572		
-9 10 10 10.1990 10./925	-6 # 11 19.4140 19.5405 -6 # 11 5.8840 5.4313	-4 7 12 19,8950 19,2407
-9 14 10 14,9270 14.5/59	-6 10 11 24 1600 22.5/45 -6 11 11 8,8330 9.0442	-4 9 12 24,4430 25,2976
-9 15 10 22.2000 21.0001		-4 10 12 9.3256 10.2235 -4 12 12 41,4926 41.2223
-10 0 10 14.5700 15.6879		
-10 1 10 25,5830 24,9947	-6 15 11 16.6724 16.9970 -6 16 11 3.2090 6.6175	-5 2 12 10,1540 9,0240
		-5 3 12 12.0850 13.9979
-10 4 10 31./548 31.5558 -10 5 10 5.6378 4.9983 -10 6 10 14.5018 14.5159	-7 3 11 3m.110n 40.de74	-5 5 12 21.15en 21.3009
-10 6 10 14.2010 14.2129		-5 4 12 28.02/0 27.4357 -5 7 12 18.7940 19.6530
-10 7 10 45,6940 44.2898 -10 6 10 12.9050 11./182 -10 10 10 6,6730 3.8094		-5 7 12 18,7940 19.6530 -5 8 12 48,4640 49,1230 -5 9 12 9,7360 9.3692
-10 10 10 0.0736 3.0094 -10 11 10 17./698 10.8841 -10 12 10 4.9436 3.3314	-7 7 11 19,000n 19,9312 -7 8 11 8,2020 7,5589 -7 10 11 24,7190 24,2300	
-10 11 10 17./898 16.8841 -10 12 10 4.9436 3.3314	-7 10 11 24,/190 24.2300	
-10 13 10 15.7476 14.7799 -10 15 10 13.1516 12.2946	-7 11 11 25,3430 23.9768 -7 12 11 15,1410 15.0894	
-11 0 10 0.014f 0.0424 -11 1 10 9.3610 9.0262	-7 14 11 10.4410 9.7182 -7 15 11 19.4350 17.7976 -7 16 11 12.0710 12.1505	
	-/ 16 11 12,0210 12,1505 -8 1 11 11,2500 10,3405	-6 4 12 15,2A9A 15,9001 -6 5 12 20,031A 20,45A6 -6 6 12 21,463A 21,9590
-11 4 10 15.7400 14.9865	-8 2 11 48,JA8* 49,91/4	
	-8 3 11 21,3200 21.1151 -8 4 11 6.3940 6.3501 -8 5 11 11,8490 12.7135	
-11 8 10 11,7418 10.1183 -11 9 10 24,3450 24,8804	-8 4 11 6.3940 0.3501 -8 5 11 11.8490 12.7135 -8 6 11 31.9350 33.3501	-6 12 12 26.1090 23.0496 -6 13 12 2.5770 4.7548
-11 9 10 24.3490 24.8804 -11 10 10 27.4420 28.4376 -11 11 10 33.1560 34.2911	-0 6 11 31, 9320 33, 3301 -8 7 11 25, 1690 25, 3684 -8 8 11 5, 3630 2,7226	-0 12 12 20.1290 23.0496 -6 12 12 20.1290 23.0496 -6 13 12 2.27/0 4.7548 -6 14 12 0.8300 7.1176
-11 11 10 00.1900 34.2911		

	4		114-51	TICALC)
/	- 0	14	34,0940	36./380
/-	ů	12		
-/	2	14	7.0710	A. V>82
1_	i_	14_	23.5420	23.4725
-7	•	12	24.2740	0.0204
-:/-		12	14,2200	
-2	á	14	21./222	20.7211
-/		12	6.0600	7.9112
1_	_10_	12_	14,/1/0	13.0002
-7_	11	12	9.7743	0.0450
	13	12	14.3014	15.9003
-1	14	12	17.1245	10.0/44
- 0		12	44.6850	33.4208
	1	12	15,6909	15.3594
::	5	12		22.6561
	-	12	0.3698	5.5227
		12	12.6885	11.1005
	7	12	12./300	15.0040
		12	19,2800	20.2147
:	10	12		10.1/50
	12	12		4.0411
	-13	12		13.1540
-8	14	12	26,3160	26.7073
	15	12	21,/680	23.7551
-9	0	12	27.2960	29.2120
	2	12	5.2850	4.0550
- 0	1_	12	6./640	5.5924
- 9	4	12	21,4690	7.2369
-9	-5-	12	25.0010	26.1475
		12	8.2320	8.1210
-9		12	27,1240	26.3694
-2	-11	12	13.4422	13.7497
-9	12	12	3,5580	9.2000
-10	14	12	10,8375	12.2307
-10	1	12	42.2690	45.4177
-10	3	12		5.4482
-10	_	_12_	28.1720	27.8973
-10	5	12	19.0195	22.8546
-10		12	7,1200	7.3675
-10	10	12	8.8680	7.8674
*10	11	12	12.3960	13.4900
-10	-12	12	10.5420	10.1215
-10	13	12	11,1500	11.0723
-10	14	12	28,8200	29.8051
-11	- 3	12	43,1760	43.4615
-11	,	12	14.0830	18.1034
-11		12	10.4290	8.7409
-11	7	12	34,2310	33.4808
-11	10	12	>.0100	3.6154
-11	11	12	10,2380	10.0157
-11	12	12	29,2010	27.1671



2. Observed and Calculated Structure Amplitudes of Porphine



H K	L Y(CBS) Y(CALC)	H K L Y(085) Y(CALC)	H K L Y(OR5) Y(CALC)	H K L Y(OBS) Y(CALC)
-5 3 -5 4 -5 5 -5 7 -5 7 -5 9 -5 9 -5 10	3 4.0000 3.1124 3 7.0001 7.9828 3 7.0001 7.9828 17.5001 10.7594 9 7.5000 4.4926 9 7.0000 4.4926 1 8.0000 5.4027 1 8.0000 3.7014 1 8.0000 3.7014 1 8.0000 7.4027 1 8.0000 7.402			

	×	L	Y(095)	Y(CALC)	н		L	Y(GRS)	Y(CALC)	н	K	L Y(095)	Y(CALC)	
• •	4	6	4,2000	4,38/3	-4 -		7	6,8000	8,7497	-7	5	8 3,2000	2,7733	
:	:		3,3000	3,4674 5,5875 5,4285 13,4209	-4	1	7	10,6000 3,9000 7,5000 3,2000	10,8331	-8		6 10,1000	12,2595 5,9046 13,1384	
-4	6		4.2000	5.4285	;		ź	7.5020	7.1857	-8	ě.	6 13,0000	15,1384	
-:	*	:	. 13,0000	13,1209	-5	3	7	3.2000	2,9628	0	;	8 0.5000 8 13.0000 9 4.0000 9 10.1000		
		٠	10 8000	11 1645	5	3	,	4.2000	8,7497 10,8331 6,3149 7,1857 2,9628 2,4248 3,4612		i		24,4193	
.;		:	5,4000	3,9511	-5	•	2	3,1000 4,2000 10,9000 6,0000 4,3000	10,4680		1 2 2 3 3 4	9 6,2000	10,3446 24,4193 7,0056	
-;	0	•	33,4000	34,4666	-:	3	7	4.0000	4,9435	-1	1	9 11.0000	11,4594	
.,			5,4000	>,3516	-;	,	,	14.9000 4.7000 7.0000 19.2000	14,4285	-1	2	9,2000	6,7244	
	1		3,1000	2,6919	-3	?	?	4.7000	4,6028	1	3	9 >,5000	5,4724	
.;	ž	6	5,7000	5,2933		ż	ź	19.2000	19,9900	-i	3	4,7000	4.1029	
-;	2 2 3 4 4		17,9000	17,4274	-6	2	777777777777777777777777777777777777777	24,2000	24,4292	-1	;	4,3000	2,7803	
-;	i		3.5000	2 0917	-:	,	ź	5.9000	7.4112	-1	,	26 1000	25 8225	
?	:	6	3,2000	2,4996			7	24,2000 12,4000 5,9000 3,2000	4,1498	-1	7 1	5,4000	4,7774	
• 5	3		4.6000	1.1140	-6	. 6	,	4.7000	5 5930	-2	2 1	12.9000	12.9942	
-5	5	6	9,1000	10,2754	-7	3 -	?	7,9000	- 0.8590	-2	2 1	15,6000	14,8917	
- 6	é		4.3000	11,7605 2,9511 34,4606 4,4606 4,4606 2,3518 2,4919 9,8742 5,2933 17,4274 10,4322 2,0917 2,4996 7,1563 10,2754 4,1429 10,2754 4,1429 13,2251 2,4249	-7	6	7777777777778	3,2000 3,2000 7,7000 7,9000 7,4000 7,4000 6,6000 8,9000 10,4000 12,2000 6,0000	14,4285 4,6028 6,9438 19,9900 24,8292 13,6680 7,4112 4,1498 3,8896 5,5930 6,8590 2,4670 8,0332	-2	2 1	9 6.200 9 11.000 9 11.700 9 7.500 9 7.500 9 17.300 9 6.700 9 6.700 9 6.700 9 7.000 1 7.400 1 2.400 1 2	7,0056 11,4594 11,4594 8,7244 10,5211 10,5212 2,7803 2,7803 2,7803 2,7803 2,7803 2,7803 2,7803 1,774 10,841 10,891 11,891	
-6	0	6	13,1000	13,2251	-0	1	ż	7,0000	7,0218	-2	; ;	5,1000	5,1727	
	i	0	15 8000	10 2005	-:	3	7	0,6000	7,2149	- 2		49 9000	48 5010	
-6	2	6	5,3000	10,2005			7	-10,4000	9,4538	2 .	6 9	4,0000	3,4584	
	3	. 6	6 2000	17,1993		5	7	9,0000	8,4144			3,2000	2,9746	
- 6	4	6	4,3000	6,9365 5,4430	-9	2	7	12,2000	11,7411	-2		3.2000	3.0257 2.9216 14.0499	
	:		3,6000	2,6641	-0	3 .	?	6.0000	- 0.5448	-3		14.1000	14,0499	
	5		12,6000	12,9728	- 0 -	2 .	8	6.0000 7.7000 6.5000	6,1648	3	,	4.0000-	2.8737	
-6	6 7	6	8,9000	11,2048	0	5	8 8	12,6000	12,5185	-3		8.7000	9,2915	
6		6	1.100 1.200 1.3,000 1.400 5,400 3.400 3.400 3.400 3.100 1.5,000 1	9.2058	0	,	8	7,1000	5,8690	3	,	10,6000	10.0675	
.7	0		6,000 4,000 3,300 9,700 3,500 3,500 5,700 5,700 6,700 1,300 1,300 6,300 1,200	2,4430 10,4097 11,4097 11,2048 11,2048 9,3058 9,3058 9,3058 9,3058 9,7459 1,781 2,7752 2,3247 10,0604 6,5903 21,0434 12,9444 12,9444 12,9444 12,9444 12,9444 12,9444 12,9444 12,9444 11,9444 1	-1	1 .		0,5000 12,6000 5,9000 7,1000 19,7000 22,5000 3,5000 5,9000	8, 0332 7, 2149 9, 7805 9, 7805 9, 8734 6, 9745 1, 7445 1, 7445 1, 7446 1, 7434 1, 743	-3 -3 -3	9 9 9	3.2000 14.1000 5.0000 4.0000 8.7000 3.9000 15.2000 4.1000 3.2000 8.2000	14,0499 4,2014 2,8737 9,2915 4,3389 10,0675 15,5762 3,4945 3,2584 6,8418 8,2640 3,0572 3,9203	
-,	1 2	ô	4,0000	4.4020	-1 1	2	8	3,5000	1.4455	-3-		3,2000	3,4945	
7	3 4 5	6	3,3000	2,8981	1	2	8	5,9000	5,6758	-4	. 9	8,2000	6,9418	
.,	3	- 6	9,7000	9,1781	-1	3	:	3.2000	13,9386	-:-		4 7000	3 0572	
7	5	6	3,5000	2, 3247	-1	;	٠	13,0000-	11,5821	-: :		4,4000	3,9203	
.,	7	6	9 5000	5,5681	1	.; .	:	34,2000	32,5893	:;	9	5.7000	12,1818	
8 8	0	6	5,2000	6,6696			٠	3,4000	3,4338	-5		7,4000	7,1003	
	2	6	20 5000	6,5903	1-	6 -	8 8 8 8	14,1000 3,2000 13,0000 5,7000 3,4000 7,0000 4,2000 3,2000 10,6000 20,1000 5,7000 10,6000 16,5000	3,4729		,	8,2000 8,0000 4,7000 12,7000 5,7000 7,4000 8,9000 9,3000 3,7000 14,3000 11,2000 12,000 12,000 15,600 16,000 8,7000	3,0572 3,0203 12,1818 5,4831 7,1083 9,9601 8,8886	
- 8	3		11,3000	12,9464	-1		0 -	3,2000	3,4168		9	3,7000	3,1114 14,9506 11,4550 11,4707 16,2547 11,7462	
	6	6	7,2000	8,9763	-1	1 1 2 3	:	10,6000	10,7152	:		14.3000	14,9506	
	1	6	6,3000	7,3450	2	i	8	5,7000	4,0678	-6		11.2000	11,4707	
	1	9	3,2000	2,2134	- 2	3	:	10,8000	15,4413	-:	:	15.6000	16,2547	
			15.7000	15.7825	2	3	8		2.7627			6.7000	9.4451	
0	3	7	15,7000 10,2000 14,9000 14,4000 4,0000 4,0000 4,9000 0,2000 21,1000 32,5000 17,1000 9,5000 5,6000	19,7875 9,4140 19,1598 14,0415 6,1320 5,5022 5,6075 3,298 20,0053 37,0116 8,0304 5,4981 37,7932 24,0981	-2	1	8	21,0000	20, n657	-7 -7 -8	9	6,7000 5,7000 4,2000 8,4000	9.8451 6.3757 3.4698	
0	:	7	14,9000	15,1508	2	;		6.2000	7,6167	-	10	8,4000	0.1449	
0	6	7	6,3000	6,1320	-2	,	٠	8,2000 17,0000 9,1000	16,9711		10	4.5000 4.6000	4,3385	
0		7	4,6000	5,5022	2 -	,		0,9000	0.1042		10	- 4.6000	3,9043 4,9958	
1	1	7	4.2000	5,3298	-2	•		6,9000	10,9711 9,3084 6,1042 8,3555 5,3145 2,4182 7,0218 5,0998 11,9937 4,1746 5,0342 7,0188 23,2987 4,3538 4,7575	-1	10	18,9000	19,2179 17,7927 5,9864 8,4444 2,5769	
1	2	7	21.1000	20.9093	-2	:	:	3 2000	5,3145	-1	10	17.8000	17,7927	
1	ź	ź	17,1000	17.9116	-3 -	1 2	ě	7,9000	7,0858	-1	10	6.7000 8.6000 3.7000	8,4444	
1	3		9.5000	6,9304	-3	2	:	7 9000	2,4495	-1	10	3.7000	4,4995	
1 .	4	7	39.3000 22.3000 5.7000 14.4000 7.5000	37.2932	-3	3 -	:	5,5000	5.0998	-1	10	13,6000	7,5648	
1 -	5	7	22,3000	24,4961	-3	4 .	:	12.0000	11,9937	1 - 1	10	8,7303	7.5648	
i -	3	7 7 7 7 7 7	5,7000	2,4295		4 -	:	0.5000-	5.9342	-2	10	13.6000	3,1625 14,4908 22,7945 2,3806 11,0717	
	÷	7	7,5000	6,1585	-3	5		8.7000	7,7188	2	10	23,5000	22,7945	
1	?	7	10,5000	9,8469	-3	,	8	4.5000	4.3030	-2	10	11.4000	11.0717	
	:	ź	5,9000	5,1886	- 3	7-		5,9000	4,7575	-2	10	13,1000	12,9280	
2 -	9	7 7 7 7	10.5000 13.6000 5.9000 3.5000 13.9000 4.2000 19.4000 4.1000 5.0000	3,3090	-3	:	8	24,6000	24.9288	2 2 2	10	11.7000	10,5518	
2	1	7	4,2000	2.1170	-:-	0	8	9,9000	10,3301	·2 ·2 ·3	10	16,7000	11.3772 15.5763 3.0209	
2 .	2 2	7	19,4000	19,2278	-	1	8 -	5.7000	10,7924	-2	10	19 4000	3.0209	
ž	3	7	5.0000	4,5944	4	2	8 -	5,3000 -	5.0373	3	10	7,3000	7,7739	
2 2	3	7 7 7 7 7		5,3903	1-	3 -	8	3.5000	4,7975 4,2859 24,9288 19,3391 18,7924 5,7569 5,0373 9,0885 2,6535 11,7224 8,53/9 9,3572 4,6889 5,9277	2 2 2 2 2 2 2 2 2 2 2 2 2 2 2 2 2 2 2 2	10	4,900 13,600 8,738 3,500 23,500 13,600 13,100 11,700 11,700 11,700 11,700 11,700 11,700 10,700 10,700 10,000 7,300 8,800 10,000 3,900 4,000 4,000	9,8194	
2		'	23.8000	23.3728	-4	4	٠	11.4000	11,7224	-3	10	3,9000	3,7298	
2 -	;	7	10,6000	10,2156			٠	6.9000 -	8,5379	-3	10	3,9000	4,1899	
2	9	7	23,8000 10,6000 11,0000 14,4000 3,5000	9,7860	-;	å	8	3,6000 -	4.8889	-3	10	4.0000	4.2516	
2	9	7	3,5000	1,9882			8	5,5000	3,9277	-3	10	16,5000	16,7282	
2 2 3	9	7	3,5000 6,0000 5,1000 30,1000 2,8000 9,4000 11,3000 14,2000 21,7000 5,5000 8,000 5,4000 31,7000	0 1595 0 1595 13,4286 5 1886 5 1886 5 1886 13,9276 2 1170 19,2278 3 3098 4 5994 5 3993 32,3327 23,3278 10,2196 9,7860 14,2116 1,982 4,127 1,982 4,127 1,982 4,127 1,982 4,127 1,982 4,127 1,982 4,127 1,982 4,127 1,982 4,127 1,982 4,127 1,982 4,127 1,982 4,127 1,982 4,127 1,982 4,127 1,982 4,127 1,982 4,127 1,982 4,127 1,982 4,127 1,982 4,127 1,982 4,127 1,982	-5	1 2 3	8 8 8 8	6.9806 6.2806 7.2806 7.2806 7.2806 7.2806 6.4080 6.5080 8.7080 8.7080 8.7080 9.8080 9.8080 8.7080 9.8080 16.3080 16.3080 11.4080 8.7080	3,9277 15,7635 6,0092 6,0791 5,0057 3,3486	4	10	4.0000 16.5000 6.2000 15.8000 10.5000 4.9000 10.1000	3,0209 20,1700 7,7739 5,8194 -8,1188 3,7298 4,1899 11,0383 4,2516 16,7282 5,5310 15,3062 9,6888 5,4717	
3	1 2	7	30,1000	28,9794	-5 -	2 .	٠	5,9000	0,0701	::	10	10,5000	9,6868	
3	2	7	2,8000	1,5667	-;			2,4000	3.3486		10	4.9000	4,2840	
3	3	7	11,3000	10,4345		;	8	9,1000	8,8285		10	10.1000	9,5671	
3	3	7	14,2000	10,4345 13,7880 20,7776	-3	6 1	:	9,1000 13,4000 6,4000 3,2000 7,6000 17,9000	6.4011	-;	10	5 7000	9.5671 9.7053 5.8347	
		7	5,5000	5,4407		7	i	3,2000	6,4611 3,5811 16,7227 7,9814	-5 2		5,2000		
3	5	7	8.5000	5,44u7 9,1034 7,4843	:		å	7.4000	16,7227	-6	10	5.2000 4.2000 5.4000	4.6373	
3		'	31,7000		6	0 1	8	17,9000	19,6261 17,1630 12,7351 6,6227	-7 :	1.0	6,2000	4,6373 6,2935 8,1826	
3	?	?	8.2000	9.0897 10.1569 19.6754	-6-	3 1	6	17.5000	17,1630	1	11	6.2000 6.0000 10.0000	5,3982 8,9483	
4	8	7	18.5000	19.1569	-6 -	4 . (7,3000	0.6227		. 11	7.0000	7.1044	
4	2 2	7	31.7000 8.2000 8.8000 18.5000 2.9000	19,4754 3,1114 11,4987	-6	5 6				-1	11	3.2000	2,6663	
•	3	7		11,4987		1 4			10,4723	-1 -	11	5,5000	3,9393	
	5	7	9.6000 6.5000 10.1000	9,1597 4,2045 10,8025	•?	3		3,2000 -	8,8561 2,1943 5,7265		11	4,5000	5,5193 3,1678 6,9502	
		7	10,1000	10,8025	-/	•	•	-,0000	9,7205	-2 2	11	•.1000	0,9502	

* * \$ \ \(\text{Y}(08) \)

-2 3 11 11,300

-2 4 13 5,000

-3 5 11 13,000

-3 1 13 5,000

-4 1 13 5,000

-4 1 13 5,000

-4 1 13 1,000

-4 1 13 1,000

-4 1 13 1,000

-4 1 13 1,000

-4 1 13 1,000

-4 1 13 1,000

-4 1 13 1,000

-4 1 13 1,000

-4 1 13 1,000

-4 1 13 1,000

-4 1 13 1,000

-4 1 13 1,000

-4 1 13 1,000

-4 1 13 1,000

-4 1 13 1,000

-4 1 13 1,000

-4 1 13 1,000

-4 1 13 1,000

-4 1 13 1,000

-4 1 13 1,000

-4 1 13 1,000

-4 1 13 1,000

-4 1 13 1,000

-4 1 13 1,000

-4 1 13 1,000

-4 1 13 1,000

-4 1 13 1,000

-4 1 13 1,000

-4 1 13 1,000

-4 1 13 1,000

-4 1 13 1,000

-4 1 13 1,000

-4 1 13 1,000

-4 1 13 1,000

-4 1 13 1,000

-4 1 13 1,000

-4 1 13 1,000

-4 1 13 1,000

-4 1 13 1,000

-4 1 13 1,000

-4 1 13 1,000

-4 1 13 1,000

-4 1 13 1,000

-4 1 13 1,000

-4 1 13 1,000

-4 1 13 1,000

-4 1 13 1,000

-4 1 13 1,000

-4 1 13 1,000

-4 1 13 1,000

-4 1 13 1,000

-4 1 13 1,000

-4 1 13 1,000

-4 1 13 1,000

-4 1 13 1,000

-4 1 13 1,000

-4 1 13 1,000

-4 1 13 1,000

-4 1 13 1,000

-4 1 13 1,000

-4 1 13 1,000

-4 1 13 1,000

-4 1 13 1,000

-4 1 13 1,000

-4 1 13 1,000

-4 1 13 1,000

-4 1 13 1,000

-4 1 13 1,000

-4 1 13 1,000

-4 1 13 1,000

-4 1 13 1,000

-4 1 13 1,000

-4 1 13 1,000

-4 1 13 1,000

-4 1 13 1,000

-4 1 13 1,000

-4 1 13 1,000

-4 1 13 1,000

-4 1 13 1,000

-4 1 13 1,000

-4 1 13 1,000

-4 1 13 1,000

-4 1 13 1,000

-4 1 13 1,000

-4 1 13 1,000

-4 1 13 1,000

-4 1 13 1,000

-4 1 13 1,000

-4 1 13 1,000

-4 1 13 1,000

-4 1 13 1,000

-4 1 13 1,000

-4 1 13 1,000

-4 1 13 1,000

-4 1 13 1,000

-4 1 13 1,000

-4 1 13 1,000

-4 1 13 1,000

-4 1 13 1,000

-4 1 13 1,000

-4 1 13 1,000

-4 1 13 1,000

-4 1 13 1,000

-4 1 13 1,000

-4 1 13 1,000

-4 1 13 1,000

-4 1 13 1,000

-4 1 13 1,000

-4 1 13 1,000

-4 1 13 1,000

-4 1 13 1,000

-4 1 13 1,000

-4 1 13 1,000

-4 1 13 1,000

-4 1 13 1,000

-4 1 13 1,000

-4 1 13 1,000

-4 1 13 1,000

-4 1 13 1,000

-4 1 13 1,000

-4 1 13 1,000

-4 1 13 1,000

-4 1 13 1,000

-4 1 13 1,000

-4 1 13 1,000

-4 1 13 1,000

-4 1 13 1,000

-4 1 13 1,000

-4 1 1

YCCALCI

10.7157 25.6864 -8.4934 5.4934 5.7935 5.7036 6.4227 6.6879 6.4523 6.2458 14.9823 3.4988 6.2063 12.1988 14.8255 8.3558

